

SANDIA REPORT

SAND2000-1751

Unlimited Release

Printed July 2000

CaveMan Version 3.0: A Software System for SPR Cavern Pressure Analysis

Sanford Ballard and Brian L. Ehgartner

Prepared by

Sandia National Laboratories

Albuquerque, New Mexico 87185 and Livermore, California 94550

Sandia is a multiprogram laboratory operated by Sandia Corporation,
a Lockheed Martin Company, for the United States Department of
Energy under Contract DE-AC04-94AL85000.

Approved for public release; further dissemination unlimited.

RECEIVED
AUG 22 2000
OSTI



Sandia National Laboratories

Issued by Sandia National Laboratories, operated for the United States Department of Energy by Sandia Corporation.

NOTICE: This report was prepared as an account of work sponsored by an agency of the United States Government. Neither the United States Government, nor any agency thereof, nor any of their employees, nor any of their contractors, subcontractors, or their employees, make any warranty, express or implied, or assume any legal liability or responsibility for the accuracy, completeness, or usefulness of any information, apparatus, product, or process disclosed, or represent that its use would not infringe privately owned rights. Reference herein to any specific commercial product, process, or service by trade name, trademark, manufacturer, or otherwise, does not necessarily constitute or imply its endorsement, recommendation, or favoring by the United States Government, any agency thereof, or any of their contractors or subcontractors. The views and opinions expressed herein do not necessarily state or reflect those of the United States Government, any agency thereof, or any of their contractors.

Printed in the United States of America. This report has been reproduced directly from the best available copy.

Available to DOE and DOE contractors from
U.S. Department of Energy
Office of Scientific and Technical Information
P.O. Box 62
Oak Ridge, TN 37831

Telephone: (865)576-8401
Facsimile: (865)576-5728
E-Mail: reports@adonis.osti.gov
Online ordering: <http://www.doe.gov/bridge>

Available to the public from
U.S. Department of Commerce
National Technical Information Service
5285 Port Royal Rd
Springfield, VA 22161

Telephone: (800)553-6847
Facsimile: (703)605-6900
E-Mail: orders@ntis.fedworld.gov
Online order: <http://www.ntis.gov/ordering.htm>



DISCLAIMER

**Portions of this document may be illegible
in electronic image products. Images are
produced from the best available original
document.**

CAVEMAN VERSION 3.0: A SOFTWARE SYSTEM FOR SPR CAVERN PRESSURE ANALYSIS

Sanford Ballard
Geophysical Technology Department

Brian L. Ehgartner
Underground Storage Technology Department

Sandia National Laboratories
P. O. Box 5800
Albuquerque, NM 87185-0750

ABSTRACT

The U. S. Department of Energy Strategic Petroleum Reserve currently has approximately 500 million barrels of crude oil stored in 62 caverns solution-mined in salt domes along the Gulf Coast of Louisiana and Texas. One of the challenges of operating these caverns is ensuring that none of the fluids in the caverns are leaking into the environment. The current approach is to test the mechanical integrity of all the wells entering each cavern approximately once every five years. An alternative approach to detecting cavern leaks is to monitor the cavern pressure, since leaking fluid would act to reduce cavern pressure. Leak detection by pressure monitoring is complicated by other factors that influence cavern pressure, the most important of which are thermal expansion and contraction of the fluids in the cavern as they come into thermal equilibrium with the host salt, and cavern volume reduction due to salt creep. Cavern pressure is also influenced by cavern enlargement resulting from salt dissolution following introduction of raw water or unsaturated brine into the cavern. However, this effect only lasts for a month or two following a fluid injection.

In order to implement a cavern pressure monitoring program, a software program called CaveMan has been developed. It includes thermal, creep and salt dissolution models and is able to predict the cavern pressurization rate based on the operational history of the cavern. Many of the numerous thermal and mechanical parameters in the model have been optimized to produce the best match between the historical data and the model predictions. Future measurements of cavern pressure are compared to the model predictions, and significant differences in cavern pressure set program flags that notify cavern operators of a potential problem. Measured cavern pressures that are significantly less than those predicted by the model may indicate the existence of a leak.

CONTENTS

INTRODUCTION	1
THERMAL MODEL	2
THE NEW THERMAL MODEL	3
THERMAL MODEL INPUTS	5
THERMAL PRESSURIZATION RATE.....	7
SALT CREEP MODEL.....	8
MODEL PARAMETER OPTIMIZATION AND STATISTICS.....	11
SALT DISSOLUTION MODEL.....	13
MAGNITUDE OF THE PRESSURE DROP DUE TO RAW WATER INJECTION.....	13
TEMPORAL DISTRIBUTION OF A DISSOLUTION-INDUCED PRESSURE DROP.....	17
SUMMARY.....	20
REFERENCES	21
APPENDIX A	A-1
APPENDIX B.....	B-1

FIGURES

Figure 1 Volume Reduction Factor as a function of temperature for the special case where raw water is isothermally transformed to saturated brine.....	16
Figure 2 Pressure drop per 1000 barrels of raw water injected into a typical 10 MMB SPR cavern.....	17
Figure 3. Brine Specific Gravity vs. Time for 10 MB Injection of Raw Water into a Cavern at Various Oil/Brine Interface Heights.....	18
Figure 4. Saturation Fraction vs. Time for 10 MB Injection of Raw Water into a Cavern at Various Oil/Brine Interface Heights.....	18
Figure 5. Saturation Fraction vs. Time for all Cases. Curves are based on various starting times within the individual analyses.....	19

TABLES

Table 1 – Thermal properties	6
Table 2 – Mechanical Properties of Low Impurity Salt.....	9
Table 3a – Density of sodium chloride brine solutions, in g/cm ³ , as a function of temperature and weight % sodium chloride in solution.....	14
Table 3b – Weight % sodium chloride in solution and density of saturated sodium chloride solutions as a function of temperature.....	14

INTRODUCTION

The United States Department of Energy Strategic Petroleum Reserve (SPR) is currently storing over 500 million barrels of crude oil in 62 caverns that were solution mined in salt domes along the Gulf Coast. These caverns were primarily constructed in the early 1980's, although some were already in existence at the time the SPR was created. One of the concerns in operating such a large number of aging caverns is the possibility of a leak developing in one or more of the caverns.

To certify cavern integrity, the current operational practice involves performing a pressure test approximately every five years. In these tests, the cavern wellbores are pressurized with nitrogen. The nitrogen level is forced to slightly below the casing seat and the nitrogen temperature and pressure, along with its interface level, are used to calculate any leakage over the duration of the test. This procedure has several disadvantages. First, the cavern wells are only tested for leaks every five years. In the interim, a leak could go undetected. Another disadvantage is the risk of damaging the well during the test. Nitrogen test pressures are significantly higher than operating pressures at the well head and can approach lithostatic pressure at the casing seat. The SPR caverns have a total of approximately 120 wells, therefore the program constitutes a considerable expense. The advantage to nitrogen tests is the ability to detect very small well leaks.

An alternative or complementary approach to leak detection is to use a model for cavern pressurization which could predict daily cavern pressures. Significant departure of the predicted and measured pressures may be cause for concern. Unexplained pressure decreases, measured over periods of weeks or months, might be an indication of a leak somewhere in the system. This would prompt the cavern engineer to check for sources of possible leakage. Conversely, a cavern that pressurizes faster than expected could result from tertiary creep or the onset of failure. This alternative approach to assuring cavern integrity would likely detect leaks much sooner than periodic nitrogen testing.

Cavern leaks are often difficult to detect by monitoring well head pressures because cavern pressure changes occur as a result of salt creep, changes in temperature of the contents of the cavern, and any dissolution of salt following injection of unsaturated brine. In the absence of a model to predict cavern pressurization, the effects of a leak may not be discernible from the other mechanisms that influence cavern pressure.

To implement a monitoring program based on cavern pressures, all of the factors that influence cavern pressure must be accounted for in a model. The most important factors are the known oil and brine movements into and out of the cavern, the steady state and transient creep closure of the cavern, and the thermal expansion and contraction of the oil and brine in the cavern as their temperatures equilibrate with the surrounding salt. Salt dissolution effects are also important, but occur only after raw water injections and are of limited duration.

To investigate the possibility of implementing a cavern leak-detection procedure based on monitoring of the well head pressure, a model for cavern pressure has been developed which

accounts for the above factors. There are a number of parameters in the model that can vary from cavern to cavern and are known with varying degrees of certainty. The approach that has been adopted is to develop a set of model parameters for each cavern. For the parameters in the model that are reasonably well known, the value is specified. Other parameters were determined by a nonlinear, least-squares optimization procedure that selects the set of values for the parameters that results in the best match between the predicted and historical cavern pressure data.

To make it possible for site cavern engineers to easily run the model, the historical pressure data, model parameters and the ability to calculate predicted cavern pressures are all contained in a Microsoft Excel workbook and the coding was done using Visual Basic. The cavern engineer enters the daily cavern pressure readings, fluid movements, and associated comments, and then runs the model. The cavern pressures predicted by the model are compared to measured data and atypical cavern pressures are flagged by CaveMan based on statistical analyses. An operating procedure defines subsequent steps. Large anomalies require immediate site attention, whereas subtle changes are investigated using software tools developed to evaluate anomalous cavern responses. The outcome of an investigation may require nitrogen testing of the cavern wells or, in an emergency, the withdrawal of oil from a cavern.

In the remainder of this report, the thermal, creep, and dissolution models at the heart of CaveMan, and the optimization scheme that was used to determine the model parameters for each cavern, are described. Model parameters and statistics are presented for all 62 caverns in the SPR system. Finally, thermal, fluid, and pressure data from the caverns are presented and compared to model predictions.

THERMAL MODEL

A significant component of SPR cavern pressurization is due to the thermal expansion and contraction of the fluids in the caverns.

In CaveMan versions 1 and 2 (Ehgartner, et al, 1995; Ballard, et al, 1997) it was assumed that the temperatures of the oil and brine in the caverns increased monotonically. The basis for this assumption was that the caverns were originally leached at temperatures of around 60 to 80 °F and were initially filled with fluids at similar temperatures. The salt surrounding the caverns was substantially warmer than that, typically about 130° F. After initial filling, only very minor fluid transfers into or out of the caverns occurred and the cavern fluids slowly warmed as they came into thermal equilibrium with the salt surrounding the caverns. In versions 1 and 2 of CaveMan, these slow monotonic fluid temperature increases were modeled with simplified analytic expressions (Ostensen, 1995).

Since deployment of the early versions of CaveMan, the assumption of a very simple cavern thermal history was violated for a significant number of caverns due to degasification operations (Henderson, 1994) and due to the transfer of SPR Weeks Island oil to other sites (Molecke, 2000). During degasification operations, oil was removed from the caverns and heated to remove dissolved gasses in the oil. After degasification, the oil was reinjected into the caverns at

temperatures that were substantially higher than the temperature of the fluids that they replaced. This abruptly raised the temperature of the fluids in the cavern to temperatures higher than the temperature of the salt at the cavern wall. This caused the cavern fluids to cool and hence contract for a few months after degas and then to expand at a reduced rate for a considerable period of time afterwards.

Starting in late 1995, approximately 70 million barrels of oil were transferred from the Weeks Island SPR site to other sites when it was determined that Weeks Island was no longer a suitable storage facility. Because the storage facility at Weeks Island was located relatively close to the surface, the temperature of the Weeks Island oil was only about 80 °F. It was injected into caverns at the other sites where it replaced cavern fluids that had been at much higher temperatures, typically around 100 to 120 °F. This significantly reduced the temperature of the fluids in the caverns into which the Weeks Island oil was injected, causing the fluids in those caverns to warm more quickly after injection of the cool oil than they had before.

The thermal effects of the degas operations and the transfer of the relatively cool Weeks Island oil into warmer caverns caused significant changes in the pressurization rates of the affected caverns, which CaveMan version 2 was unable to adequately predict due to the limitations of the simple analytical model employed.

THE NEW THERMAL MODEL

In order to predict the effect on cavern pressurization rates of a sudden injection of a fluid with a temperature significantly different than the current cavern temperature, a numerical approach is required. The new thermal model that has been developed actually consists of two linked thermal conduction submodels, one for the oil and one for the brine. Each model is a one dimensional, radial, axisymmetric finite element heat conduction model that predicts the temperature in the salt surrounding the cavern as a function of time and radial distance from the cavern wall. Each model requires solution of the partial differential equation

$$\frac{\partial T}{\partial t} = \frac{K}{\rho c} \left(\frac{\partial^2 T}{\partial r^2} + \frac{1}{r} \frac{\partial T}{\partial r} \right), \quad r_0 < r < r_\infty, \quad (1)$$

with appropriate initial and boundary conditions. In Equation (1), T is temperature, t is time, K , ρ and c are the thermal conductivity, density and specific heat of salt, respectively, r is radial distance from the center of the assumed infinitely long cavern, r_0 is the radius of the cavern, and r_∞ is a point in the salt far from the cavern. For the numerical solution of Equation (1), a finite element solution scheme described in Kikuchi (1986) was implemented in Visual Basic.

A constant temperature boundary condition is applied at r_∞ , which is chosen to be sufficiently large such that there is zero heat flux from the model at this boundary. At r_0 , a temperature boundary condition is applied which reflects the current fluid temperature adjacent to the cavern wall. At each time step in each submodel, the temperature of the cavern wall is calculated. The calculation takes into account changes in cavern fluid temperature that result from 1) heat

transfer from the salt across the cavern wall, 2) heat transfer across the oil/brine interface, and 3) transfer of fluids of different temperatures and fluid properties into the cavern.

The calculations proceed as follows: At time zero, the salt temperatures in the oil and brine submodels are each uniform and independent of each other. The temperatures at the cavern walls in both submodels are set to a specified initial temperature that reflects the temperature of the brine used to leach the cavern. Then, the salt temperatures in the two submodels begin to evolve. The time step in the model is one day. At first, the cavern wall boundary condition is considered to be isothermal in time in order to simulate leaching of the cavern.

After the initial isothermal period is over, the cavern wall boundary conditions in the two submodels are calculated at each time step. This calculation is performed as follows: first, the amount of heat conducted into each fluid from the salt during the previous time interval is calculated from the salt temperature at the two inner nodes of each submodel and the surface area of the cavern wall in contact with the fluid.

$$Q_{salt,oil} = -K_{salt} \frac{(T_{oil,0,prev} - T_{oil,1,prev})}{(r_0 - r_1)} \Delta t \ 2\pi r_0 h f_{oil} \quad (2a)$$

$$Q_{salt,brine} = -K_{salt} \frac{(T_{brine,0,prev} - T_{brine,1,prev})}{(r_0 - r_1)} \Delta t \ 2\pi r_0 h f_{brine} \quad (2b)$$

$Q_{salt,oil}$ and $Q_{salt,brine}$ are the total amounts of energy conducted across the cavern wall from the salt into the cavern in each submodel during the preceding time step, K_{salt} is the thermal conductivity of the salt, $T_{oil,0,prev}$ and $T_{brine,0,prev}$ are the temperatures at the cavern wall in the oil and brine submodels, respectively, at the preceding time step, $T_{oil,1,prev}$ and $T_{brine,1,prev}$ are the temperatures at the first model node in the salt in the oil and brine submodels, respectively, at the preceding time step, r_1 is the radial distances from the axis of the cavern to the first model node in the salt, Δt is the time increment between time steps (one day), h is the height of the cavern and f_{oil} and f_{brine} are the fraction of the cavern containing oil and brine, respectively.

Next, the amount of heat transferred from the brine to the oil is calculated:

$$Q_{interface} = -H \pi r_0^2 (T_{oil,0,prev} - T_{brine,0,prev}) \Delta t \quad (3)$$

H is a heat transfer coefficient.

Just prior to the new time step, the fluid temperatures are given by:

$$T'_{oil,0,new} = T_{oil,0,prev} + \frac{(Q_{salt,oil} + Q_{interface})}{V_{oil} \rho_{oil} c_{oil}} \quad (4a)$$

$$T'_{brine,0,new} = T_{brine,0,prev} + \frac{(Q_{salt,brine} - Q_{interface})}{V_{brine} \rho_{brine} c_{brine}} \quad (4b)$$

$T'_{oil,0,new}$ and $T'_{brine,0,new}$ are the oil and brine temperatures at the cavern walls just prior to the new time step, V_{oil} and V_{brine} are the oil and brine volumes in the cavern at the previous time step, respectively, ρ_{oil} and ρ_{brine} are the constant oil and brine densities, respectively, and c_{oil} and c_{brine} are the constant oil and brine specific heats, respectively.

If any fluid transfers occurred at the beginning of the new time step, then it is necessary to incorporate their thermal effects on the cavern fluid temperatures. The oil and brine temperatures at the start of the new time step are given by:

$$T_{oil,0,new} = T'_{oil,0,new} + \frac{(T_{oil,in} - T'_{oil,0,new}) V_{oil,in}}{V_{oil} + V_{oil,in} - V_{oil,out}} \quad (5a)$$

$$T_{brine,0,new} = T'_{brine,0,new} + \frac{(T_{brine,in} - T'_{brine,0,new}) V_{brine,in}}{V_{brine} + V_{brine,in} - V_{brine,out}} \quad (5b)$$

$T_{oil,in}$ and $T_{brine,in}$ are the temperatures of any injected oil and/or brine, respectively, and $V_{oil,in}$, $V_{oil,out}$, $V_{brine,in}$ and $V_{brine,out}$ are the oil and brine volumes transferred into and/or out of the cavern at the start of the new time step.

After the fluid temperatures at the start of the new time step are calculated, they are applied as boundary conditions on the salt thermal submodels and new salt temperatures at the end of the new time step are calculated according to Equation (1). The results of a model calculation are the oil and brine fluid temperatures as a function of time since the beginning of leaching.

THERMAL MODEL INPUTS

There are a substantial number of parameters needed to run the thermal model. These include:

- Information about the cavern geometry (height and effective diameter).
- Material properties of salt, oil and brine.
- The heat transfer coefficient that regulates the heat transfer across the oil/brine interface in each cavern.
- The initial temperature of the salt surrounding the cavern.
- The time, duration and temperature of cavern leaching.
- A complete history of fluid transfers into and out of the cavern, including the volume and date of all fluids extracted from the cavern and the volume, date, and temperature of all fluids injected into the cavern.

The overall objective of the thermal model is to accurately predict the evolution of the temperatures of the fluids in the caverns, so that they can be used to calculate cavern pressurization rates that result from thermal expansion of the fluids. In order to achieve this goal, a subset of the important input parameters was selected and values of those parameters were sought which resulted in the best match between the predicted cavern fluid temperatures

and actual measured temperatures of those same fluids. The SIMPLEX optimization algorithm described by Cececi and Cacheris (1984) was used to determine the values of the optimized input parameters. The optimization process was implemented on a cavern-by-cavern basis, yielding separate parameter values for each of the 62 caverns in the SPR system. Results are presented in Appendix A.

Caverns were assumed to be right circular cylinders. Available cavern height and cavern volume information were used to calculate an effective radius for each cavern. None of these parameters were optimized. Values of these parameters are listed for each cavern in Table A-1 in Appendix A.

The material properties of the salt, oil and brine were also not optimized. These were assumed independent of temperature and pressure and their constant values are listed in Table 1.

Table 1 – Thermal properties

Property	Value
Salt Thermal Conductivity	77.61 BTU/ft/°F/day
Salt Specific Heat × Density	28.48 BTU/ft ³ /°F
Oil Specific Heat × Density	22.95 BTU/ft ³ /°F
Brine Specific Heat × Density	58.09 BTU/ft ³ /°F

The oil/brine interface heat transfer coefficients for each cavern were unknown and these were, therefore, one of the parameters determined in the optimization process.

The undisturbed temperatures of the salt adjacent to the oil and brine portions of the caverns have a very profound effect on the shape of the model temperature vs time curves and, therefore, these parameters were optimized.

The temperature and timing of leaching also have a profound influence on the shape of the temperature vs time curves and, therefore, elements of the leaching process were also optimized. For the older Phase I caverns, which have unknown but very complex pre-SPR operational histories, leaching was assumed to have lasted for two years, but the date of the end of the leaching process was optimized. The temperature of leaching was also optimized, but was constrained to be greater than 60 °F. For Phase II and III caverns, which were all created by the SPR and hence have much better known operational histories, the date of the end of leaching was specified, but the duration of leaching was optimized. The temperature of leaching of Phase II and III caverns was optimized but was constrained to be between 60 and 70 °C.

The thermal model also requires information about all fluid transfers into and out of the caverns. While information about the date and amounts of fluid transfers could be deduced from historical monthly oil inventory data, the temperature of injected fluids was unfortunately not available. Due to limitations on the number of parameters that could be optimized, it was assumed that for all historical oil and brine injections, the fluids were injected at the same temperature, yielding a single brine injection temperature and a single oil injection temperature for each cavern. These injection temperatures were overridden in cases where the injection temperature was known, such as was the case for the degasified oil injection temperatures and the Weeks Island oil transfers.

THERMAL PRESSURIZATION RATE

Once the rates of change of temperature of the oil and brine have been calculated, the cavern pressurization rate that results from the thermal expansion of the two fluids must be determined. Calculation of the pressurization rate is complicated by the fact that the two fluids have different rates of change of temperature, thermal expansion coefficients, and compressibilities. This implies that, while the total fluid volume in the cavern will not change, the oil/brine interface may move up or down very slightly, resulting in equal but opposite changes in the oil and brine volumes.

In the derivation of an expression for the thermal pressurization rate it is assumed that the oil and brine change temperatures at rates $\frac{\partial T_{oil}}{\partial t}$ and $\frac{\partial T_{brine}}{\partial t}$, have thermal expansion coefficients β_{oil} and β_{brine} , and compressibilities κ_{oil} and κ_{brine} , respectively. It is further assumed that as a result of thermal expansion of the fluids, the oil/brine interface moves upward, resulting in rates of increase in the oil and brine volumes of $-\frac{\partial V_i}{\partial t}$ and $\frac{\partial V_i}{\partial t}$, respectively. The rate of change of pressure in the oil and brine due to thermal expansion of the fluids will be:

$$\frac{\partial P_{oil}}{\partial t} = \left(\beta_{oil} V_{oil} \frac{\partial T_{oil}}{\partial t} - \frac{\partial V_i}{\partial t} \right) \frac{\kappa_{oil}}{V_{oil}} \quad (6)$$

and

$$\frac{\partial P_{brine}}{\partial t} = \left(\beta_{brine} V_{brine} \frac{\partial T_{brine}}{\partial t} + \frac{\partial V_i}{\partial t} \right) \frac{\kappa_{brine}}{V_{brine}} \quad (7)$$

respectively.

Since the two fluids coexist in the same cavern, the rate of change of pressure with time must be the same in each fluid and must be the same as the rate of change of pressure in the entire cavern

$$\frac{\partial P_{cavern}}{\partial t} = \frac{\partial P_{oil}}{\partial t} = \frac{\partial P_{brine}}{\partial t} \quad (8)$$

Solving Equations (6), (7) and (8) for $\frac{\partial V_i}{\partial t}$, and substituting the result into Equation (7) yields the cavern thermal pressurization rate:

$$\frac{\partial P_{cavern}}{\partial t} = \left(\beta_{brine} V_{brine} \frac{\partial T_{brine}}{\partial t} + \frac{\beta_{oil} V_{oil} \frac{\partial T_{oil}}{\partial t} - \beta_{brine} V_{brine} \frac{\partial T_{brine}}{\partial t}}{\frac{\kappa_{oil}}{V_{oil}} + \frac{\kappa_{brine}}{V_{brine}}} \right) \frac{\kappa_{brine}}{V_{brine}} \quad (9)$$

SALT CREEP MODEL

The creep of salt was represented by the multi-mechanism deformation (M-D) model (Munson, Fossum, and Senseny, 1989a,b). The model is state-of-art in predicting time-dependent salt deformation and is based on a first principles approach. The model was originally developed by Munson and Dawson (1979, 1982) and later modified to provide a more descriptive transient strain function (Munson, Fossum, and Senseny, 1989a,b). Transient creep is incorporated through both workhardening and recovery branches that reflect the internal structure in the salt (Munson and Dawson, 1982). When salt is developing internal structure, it is workhardening and hence developing a resistance to creep. As a result, the strain rates decelerate over time. Conversely, a recovery mode in salt is manifested by accelerating strain rates. At equilibrium, the salt is in steady state creep.

The M-D model has several steady state creep mechanisms, of which only one (mechanism 2) was selected for use in the cavern model, based on its dominant influence over the other mechanisms for SPR caverns. The dominance of a mechanism is determined by the stress and temperature regime for the cavern. For this mechanism, the steady state creep rate is:

$$\varepsilon_s = A e^{-Q/RT} (\sigma / \mu)^n \quad (10)$$

The above mechanism relates the steady state strain rate to temperature, T, and stress, σ . The constants A, n, Q can be determined from laboratory creep tests, where Q is the activation energy and n is the stress exponent. R is the universal gas constant and μ is the shear modulus of salt.

Transient creep is included in the model through a function, F, where the total strain rate (transient and steady state) is the product of F times the steady state strain rate:

$$\varepsilon = F \varepsilon_s \quad (11)$$

The transient function, F, is composed of a workhardening, equilibrium, and recovery branches. F is greater than 1 when the salt is workhardening, and F is less than 1 when the salt is in a recovery mode. When F is equal to one, there is no transient effect.

$$F = \begin{cases} e^{\Delta(1-\zeta/\epsilon_t)^2} & , \zeta < \epsilon_t \text{ Workhardening} \\ 1 & , \zeta = \epsilon_t \text{ Equilibrium} \\ e^{-\delta(1-\zeta/\epsilon_t)^2} & , \zeta > \epsilon_t \text{ Recovery} \end{cases} \quad (12)$$

Δ and δ are workhardening and recovery parameters, and ϵ_t is the transient strain limit. The internal state variable, ζ , is compared to the transient strain limit to determine whether the salt is in equilibrium, or is workhardening or recovering. The equation governing the evolution or rate of change of the internal variable, is:

$$\zeta = (F - 1) \varepsilon_s \quad (13)$$

The transient strain limit is related to stress and temperature through the following function where K_0 , c , and m are constants.

$$e_t = K_0 e^{cT} (\sigma / \mu)^m \quad (14)$$

The workhardening and recovery parameters are defined as a function of stress through:

$$\begin{aligned} \Delta &= \alpha_w + \beta_w \log(\sigma / \mu) \\ \delta &= \alpha_r + \beta_r \log(\sigma / \mu) \end{aligned} \quad (15)$$

The α 's and β 's are constants, with the subscripts denoting either the workhardening or recovery branches.

The relevant creep parameters are only partially known for SPR salts. Significant variability is known to exist among measured laboratory creep of salts from the same dome and from dome to dome (Wawersik and Zeuch, 1984), as evidenced by significant differences in cavern closure rates (Ehgartner, 1997). A complete set of creep properties has been measured for low impurity (clean) salt from the Waste Isolation Pilot Plant (WIPP) site (Munson, Fossum, and Senseny, 1989a,b). This salt (Table 2) is assumed to represent the relatively pure quality found in SPR domal salts.

Table 2 - Mechanical Properties of Low Impurity Salt

Steady State Creep	Transient Creep
A	9.672 E12 /s
Q	12000 cal/mol
n	5.0
μ	1.8×10^6 psi
R	1.987 cal/mol-deg

M	3.0
K_0	6.275 E5
C	0.009198 /T
α_w	-17.37
β_w	-7.738
α_r	-3.0
β_r	-1.1

The creep equations can describe the time-dependent strain rate of salt subject to a given stress state. The stress state around a cavern varies both spatially and temporally. Typically, the finite element method which traces the spatial and time variation of stress is used to predict cavern volume changes, and hence pressurization over time. However, this approach is computationally intensive. In the absence of these analyses, the following engineering approach was adopted.

An approximation of the stress state and the amount of salt being stressed was used to calculate a representative cavern closure rate. Here, the deviatoric stress or differences in the principal stress magnitudes control creep. The deviatoric stress is assumed to be proportional to the difference in lithostatic and fluid pressure acting against the cavern wall. The fluid pressure was calculated by summing the oil pressure at the wellhead and weight of the downhole oil and/or brine column to a depth at three quarters between the roof and floor of the cavern. Finite

element analyses have shown that volumetric closure rates are approximately equal for cavern volumes above and below this depth (Ehgartner, 1992). Thus, creep at this depth is believed to represent an overall average for purposes of calculating volumetric closure and hence pressurization rates. The salt temperature for the creep model is based on thermal logs which were taken in some of the wells prior to cavern development. Unlike cavern fluid pressures, the deviatoric stress state in salt, that controls creep, is unknown. To account for this, a factor, f , was incorporated into the following equation. This factor reflects the triaxial stress state of the salt. The deviatoric stress used in predicting cavern pressurization is defined as:

$$\sigma = (1 - f)(P_L - P_d) \quad (16)$$

P_d is defined as the fluid pressure at depth acting against the cavern wall and P_L is the lithostatic pressure. Lithostatic pressure is influenced by depth, the caverns in a field, and other factors, therefore it is also considered an unknown and is optimized to find a value that best fits the data. Similarly, the true triaxial stress state of the salt surrounding a cavern is unknown and f is also optimized to best fit measured cavern pressures.

The amount of salt subject to creep was defined as length parameter, L , in the model. It represents the distance from the cavern wall into the salt that is stressed. The characteristic length parameter was also treated as an unknown and optimized to best fit previous cavern pressure data. From the strain rate calculated using the above equations and stress state, and the characteristic length of salt, the change in cavern diameter can be calculated as:

$$\Delta D = \varepsilon L \Delta t \quad (17)$$

Δt represents a time step in the model. The volumetric change for a cylindrical cavern follows as:

$$\Delta V = (\pi / 4) \Delta D (2D_o - \Delta D) H \quad (18)$$

D_o is the initial cavern diameter and H is the cavern height. The pressurization due to creep is then calculated as:

$$\Delta P = K \frac{\Delta V}{V} \quad (19)$$

K is the compressibility of the fluid in the cavern and V is the volume of the cavern.

In addition to the stress state and volume of salt stressed, an initial value is needed for the internal variable used to calculate transient creep. This variable reflects the internal microstructure in the salt that has accumulated over time since the beginning of leaching. Since this parameter evolves with time and complete cavern pressure histories are not available, it is impossible to simulate its development to date. Therefore, the initial value of the state parameter for a given data set is an unknown variable in the model that also can be optimized to best fit the historic pressure data.

In summary, four creep related parameters were considered as unknown and therefore selected for optimization. The lithostatic stress, the triaxial stress factor, the characteristic length, and the initial internal variable were varied to predict results that best fit the historic pressure data.

MODEL PARAMETER OPTIMIZATION AND STATISTICS

To obtain estimates of all the model parameters, the thermal model was optimized first to select the set of model thermal parameters which resulted in the best fit between the measured oil and brine cavern temperatures and temperatures predicted by the thermal model. The parameters that resulted from the optimization process are presented in Table A-2 in Appendix A. The measured oil and brine temperatures used in the optimization process, and the oil and brine temperatures predicted by the thermal model using the optimized thermal parameter sets, are presented for each cavern in Appendix B.

After the temperatures as a function of time were determined for each cavern, the cavern pressurization rate that resulted from thermal processes in each cavern was calculated according to Equation (9). These thermal pressurization rates were subtracted from the measured pressures and the salt creep model was optimized to obtain the creep parameters that resulted in the best match between the residual measured pressures and predicted pressures. At that point, it was noted that for some caverns, the thermal model seemed to be having either too much, or in some cases, insufficient influence on the pressurization rates. To correct for this, an additional optimized parameter was introduced. This parameter, called the Thermal-Creep Ratio, is a multiplier on the thermal pressurization rate. It was constrained to be within the range of 0.5 to 2, meaning that it could either enhance or diminish the influence of the thermal pressurization rate by a factor of 2. Inclusion of this additional parameter is justified by the fact that the primary goal of the optimization procedure is the achievement of good agreement between the measured and predicted pressures so that future pressure values can be accurately predicted.

The creep optimization procedure was implemented both with and without the Thermal-Creep Ratio. If inclusion of the parameter improved the match between the measurements and the predictions by more than 10%, it was retained. Otherwise, the Thermal-Creep Ratio was set to 1. Values of the Thermal-Creep Ratio for each cavern are presented in Table A-2 in Appendix A.

The creep parameters used in the creep model are presented for each cavern in Table A-3 in Appendix A. Plots of measured and predicted pressures for each cavern are presented in Appendix B.

Note that the salt dissolution model, which is discussed in the next section, was not applied to the historical data during the optimization process. This was due to the fact that information about the salinity of historical brine/raw water injections into SPR caverns was not available.

Once all the model parameters are determined, we want to predict cavern pressures at times after the time range of the data used in the optimization process, and compare the predictions to

measured pressures. Significant differences between measured and predicted pressures will cause CaveMan to raise a flag, alerting the cavern operators to potential problems.

Since measured and predicted pressures are highly unlikely to agree perfectly, we need criteria that indicate whether or not the measured and predicted pressures differ significantly. These criteria should be based on the historical performance of the cavern. The statistical measure chosen for this purpose is the Root Mean Square Difference:

$$D_{rms} = \sqrt{\frac{\sum_{i=1}^{i=N} (P_{m,i} - P_{p,i})^2}{N}} \quad (20)$$

$P_{m,i}$ and $P_{p,i}$ are the i^{th} measured and predicted pressures, respectively, N is the number of observations, and i is an integer that ranges from 1 to N . Only observations obtained when the cavern pressure was not being manipulated and which fall within the normal operating pressure range of the cavern are included in the calculation of D_{rms} . All the historical data from a cavern that were used in the optimization process were included in the calculation of D_{rms} . It is assumed that the caverns were not leaking during this time. A separate D_{rms} value was calculated for each cavern. These values are included in Table A-3 in Appendix A. In Appendix B, the difference between the measured and predicted pressures are plotted for each cavern. The horizontal lines are $\pm 3 \times D_{rms}$.

D_{rms} is in many ways analogous to the standard deviation of the difference between the historical measured and predicted pressures. If it is assumed that the historical differences between the measured and predicted pressures are normally distributed, then 63% of all the historical differences between the measured and predicted pressures would be less than D_{rms} .

We define the Status Variable as:

$$SV = \frac{P_m - P_p}{3D_{rms}} \quad (21)$$

If it is again assumed that the historical differences between the measured and predicted pressures are normally distributed, then 99% of all the historical Status Variables would fall in the range of -1 to 1. For new measured pressures, Status Variables less than -1 indicate that the cavern is pressurizing at a rate that is significantly less than expected. Status Variables greater than 1 indicate that the cavern is pressurizing significantly more rapidly than expected, as compared to the historical trends. These conditions may indicate that some unmodelled phenomenon, such as a cavern leak, exists and further investigation by cavern operators is warranted.

SALT DISSOLUTION MODEL

From time to time during the operation of SPR caverns, raw water is injected into the caverns; this can have a significant influence on the cavern pressure for some months after the injection occurs. To accurately predict cavern pressures after these injections, it is necessary to predict both the magnitude and the temporal distribution of the changes in cavern and fluid volumes that result from the injections.

When raw water is injected into a cavern, it mixes with the brine already present in the cavern, reducing its salinity below saturation. As the unsaturated brine contacts the cavern walls, salt is dissolved, thereby enlarging the cavern. The brine volume increases as well, due to the addition of dissolved salt to the fluid, but the fluid does not increase in volume by quite as much as the volume of the solid salt that was dissolved. Given a volume of raw water, and a volume of solid salt such that the salt will completely dissolve in the water yielding fully saturated brine, the volume of the resulting brine will be slightly less than the sum of the initial volume of the water and the initial volume of the solid salt. Hence, when raw water is injected into a cavern, an additional volume equal to about 3% of the volume of water injected is generated. Since the caverns are closed systems, this volume generation results in a calculable decrease in cavern pressure.

While the magnitude of the total pressure drop is straightforward to calculate with reasonable accuracy, the temporal distribution of the pressure drop is more problematic. If the salt dissolution and resulting pressure drop occurred instantly, the whole issue of salt dissolution would not be of interest as far as cavern pressure monitoring is concerned since cavern pressures are always flagged in CaveMan during fluid transfers and for a day or two following a transfer. Unfortunately, when raw water is injected into a cavern, it generally takes several months for the water to completely mix with the brine and find its way to the walls of the cavern where it can dissolve salt. This process is highly dependent on the dynamics of fluid flow patterns in the cavern.

The problem of how the cavern pressurization rate is affected by raw water injections is considered in two steps below. First, an expression for the total pressure drop that results from an injection of raw water or unsaturated brine will be derived. Secondly, how that pressure drop is distributed in time will be considered.

MAGNITUDE OF THE PRESSURE DROP DUE TO RAW WATER INJECTION

First, we must determine the amount of volume that is generated following an injection of unsaturated brine into a cavern. Then the pressure drop will be the volume generated divided by the volume of the cavern, further divided by the effective compressibility of the fluids in the cavern.

A very general statement of the problem to be solved is: we start with a volume of unsaturated brine V_1 , at condition 1 where it has a density ρ_1 and temperature T_1 . This fluid is altered to condition 2 by having rock salt dissolved in it and by having its temperature changed. In

condition 2 it has a density of ρ_2 and temperature T_2 . We must determine how much salt was dissolved, V_S , what the volume of the new brine is at condition 2, V_2 , and the change in volume per unit volume of injected brine, V_{RF} . This latter quantity will be referred to as the *Volume Reduction Factor*.

To accomplish our objective we need to know the mass fraction of sodium chloride in the brine as a function of density and temperature. Tables 3a and 3b specify the relationship between temperature, brine density and mass fraction NaCl in sodium chloride brine solutions (reproduced from Kaufmann, 1960; density of fresh water as a function of temperature obtained from CRC Handbook). The mass fraction of sodium chloride in brine with an arbitrary density and temperature can be obtained from Tables 3a and 3b by interpolation.

Table 3a – Density of sodium chloride brine solutions, in g/cm^3 , as a function of temperature and weight % sodium chloride in solution.

Weight % NaCl	0 °C	10 °C	20 °C	25 °C	30 °C	40 °C	50 °C	60 °C	80 °C	100 °C
0	0.99987	0.99973	0.99823	0.99707	0.99567	0.99224	0.98807	0.98324	0.97183	0.95838
1	1.00747	1.00707	1.00534	1.00409	1.00261	0.99908	0.99482	0.9900	0.9785	0.9651
2	1.01509	1.01442	1.01246	1.01112	1.00957	1.00593	1.00161	0.9967	0.9852	0.9719
4	1.03038	1.02920	1.02680	1.02530	1.02361	1.01977	1.01531	1.0103	0.9988	0.9855
6	1.04575	1.04408	1.04127	1.03963	1.03781	1.03378	1.02919	1.0241	1.0125	0.9994
8	1.06121	1.05907	1.05589	1.05412	1.05219	1.04798	1.04326	1.0381	1.0264	1.0134
10	1.07677	1.07419	1.07068	1.06879	1.06676	1.06238	1.05753	1.0523	1.0405	1.0276
12	1.09244	1.08946	1.08566	1.08365	1.08153	1.07699	1.07202	1.0667	1.0549	1.0420
14	1.10824	1.10491	1.10085	1.09872	1.09651	1.09182	1.08674	1.0813	1.0694	1.0565
16	1.12419	1.12056	1.11621	1.11401	1.11171	1.10688	1.10170	1.0962	1.0842	1.0713
18	1.14031	1.13643	1.13190	1.12954	1.12715	1.12218	1.11691	1.1113	1.0993	1.0864
20	1.15663	1.15254	1.14779	1.14533	1.14285	1.13774	1.13238	1.1268	1.1146	1.1017
22	1.17318	1.16891	1.16395	1.16140	1.15883	1.15358	1.14812	1.1425	1.1303	1.1172
24	1.18999	1.18557	1.18040	1.17776	1.17511	1.16971	1.16414	1.1584	1.1463	1.1331
26	1.20709	1.20254	1.19717	1.19443	1.19170	1.18614	1.18045	1.1747	1.1626	1.1492

Table 3b – Weight % sodium chloride in solution and density of saturated sodium chloride solutions as a function of temperature.

T, °C	Weight % NaCl at Saturation	Density at Saturation (g/cm^3)
0	26.34	1.2093
10	26.35	1.2044
20	26.43	1.1999
25	26.48	1.1978
30	26.56	1.1957
40	26.71	1.1914
50	26.89	1.1872
60	27.09	1.1830
80	27.53	1.1745
100	28.12	1.1660

At condition 1 we have:

$$V_1 \rho_1 = M_{S,1} + M_w \quad (22)$$

and

$$F_1 = \frac{M_{S,1}}{M_{S,1} + M_w} \quad (23)$$

V_1 , ρ_1 and F_1 are the volume, density and mass fraction NaCl of the brine solution at condition 1, respectively. $M_{S,1}$ and M_w are the masses of NaCl and water in the brine solution at condition 1, respectively.

At condition 2 we have:

$$F_2 = \frac{M_{S,2}}{M_{S,2} + M_w} \quad (24)$$

$M_{S,2}$ and F_2 are the mass and mass fraction of NaCl in the brine at condition 2. Note that the mass of water in the solution has not changed relative to condition 1. Combining Equations (22), (23) and (24) yields:

$$\Delta M_S = M_{S,2} - M_{S,1} = V_1 \rho_1 \left[\frac{(1-F_1)}{(1-F_2)} F_2 - F_1 \right] \quad (25)$$

ΔM_S is the mass of salt that was dissolved in the brine in going from condition 1 to condition 2. The volume of salt dissolved in this process is:

$$V_s = \frac{\Delta M_S}{\rho_s} \quad (26)$$

ρ_s is the density of rock salt. The volume of the brine at condition 2 is:

$$V_2 = \frac{(V_1 \rho_1 + \Delta M_S)}{\rho_2} \quad (27)$$

Finally, the Volume Reduction Factor is:

$$V_{RF} = \frac{(V_1 + V_s - V_2)}{V_1} \quad (28)$$

which can also be expressed:

$$V_{RF} = 1 - \frac{\rho_1}{\rho_2} + \left[\frac{(1-F_1)}{(1-F_2)} F_2 - F_1 \right] \left(\frac{\rho_1}{\rho_5} - \frac{\rho_1}{\rho_2} \right) \quad (29)$$

In the special situation where pure water is isothermally converted to saturated brine by salt dissolution, the Volume Reduction Factor as a function of temperature is well approximated by a cubic polynomial of the form:

$$V_{RF} = 5.30 \times 10^{-2} - 3.81 \times 10^{-4} T + 1.91 \times 10^{-6} T^2 - 2.96 \times 10^{-9} T^3 \quad (30)$$

T is temperature in °F. The Volume Reduction Factor as a function of temperature for this special case is illustrated in Figure 1.

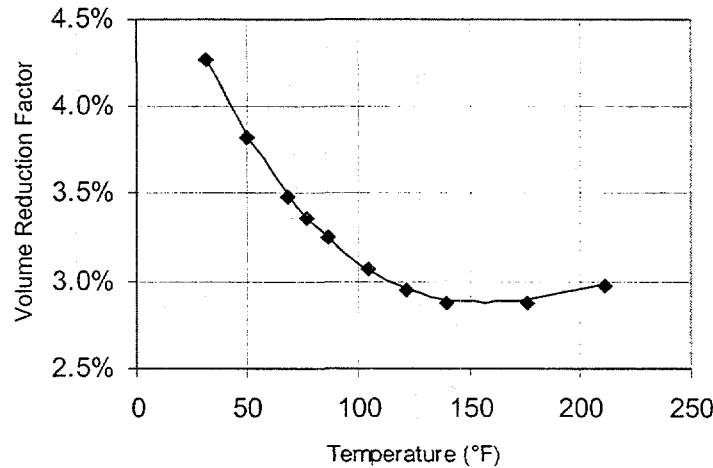


Figure 1 Volume Reduction Factor as a function of temperature for the special case where raw water is isothermally transformed to saturated brine. Symbols represent values calculated from data tabulated in Tables 3a and b. The curve represents the third order polynomial approximation presented in the text.

The total pressure drop resulting from the injection of unsaturated brine is:

$$\Delta P = \frac{V_1 \cdot V_{RF}}{V_{cav} \cdot k_{eff}} \quad (31)$$

V_{cav} and k_{eff} are the cavern volume and the effective compressibility of the fluids in the cavern, respectively.

Typical compressibility values for oil and brine are 3.85×10^{-6} and 2.90×10^{-6} psi⁻¹, respectively. Figure 2 illustrates the pressure drops per 1000 barrels of raw water injected into typical 10 MMB SPR caverns full of oil and brine.

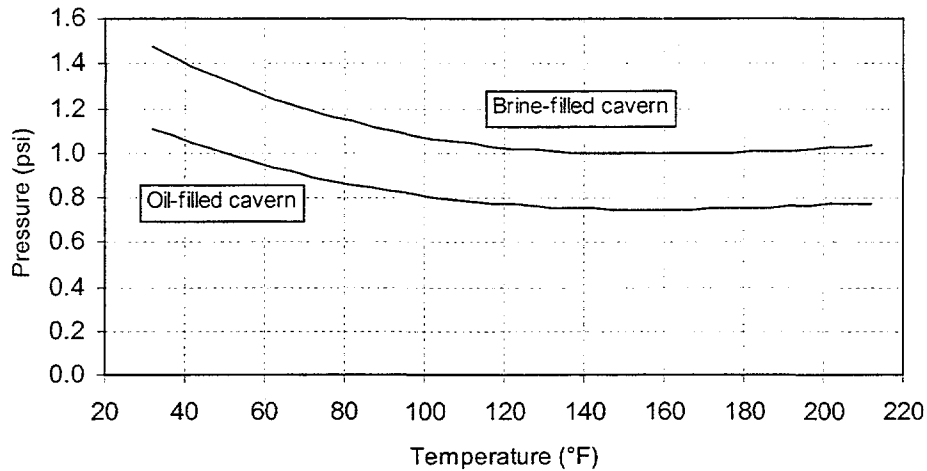


Figure 2 Pressure drop per 1000 barrels of raw water injected into a typical 10 MMB SPR cavern.

TEMPORAL DISTRIBUTION OF A DISSOLUTION-INDUCED PRESSURE DROP

Cavern leaching analyses were performed using SANSMIC (Russo, 1983) to provide simplified equations to incorporate into the CaveMan program. SANSMIC results were used to characterize cavern depressurization due to salt dissolution after the injection of raw water.

The SANSMIC analysis considered a typical SPR cavern with a height of 2000 ft and a diameter of 200 ft. The cavern shape was idealized as a cylinder resulting in a volume of 11.2 MMB. Raw water was injected at 45 ft above the cavern floor. The analyses varied the amount of raw water injected (5, 10, 20, 40, 80, & 160 MB) and the height of the initial oil/brine interface above the floor of the cavern (50, 100, 150, 200, 400, 800, 1400, 1990 ft). The majority of caverns in the SPR may be approximated using the above geometry, but the acquired or Phase I caverns may have atypical geometries.

Figure 3 is a plot of the predicted brine specific gravities for the 10 MB injection. Similar plots were obtained for the other injection quantities simulated.

Figure 4 plots the saturation fraction for the 10 MB injection for the various oil/brine interface heights. The saturation fraction reflects the change in specific gravity since the injection and varies from 0 to 1. It is interesting that the results trend with one another with the exception of the 50 ft interface height. The 50 ft interface placed the injection string only 5 ft below the oil/brine interface which may have introduced some error into the model predictions since the cavern's vertical domain was discretized in 20 ft increments. Therefore the 50 ft interface results are suspect and are probably a numerical or modeling artifact.

A time dependent saturation function was developed to approximate all of the analysis results. The initial saturation content used in developing the function was based not only on the initial specific gravities of brine in the analyses (immediately following injection), but also used

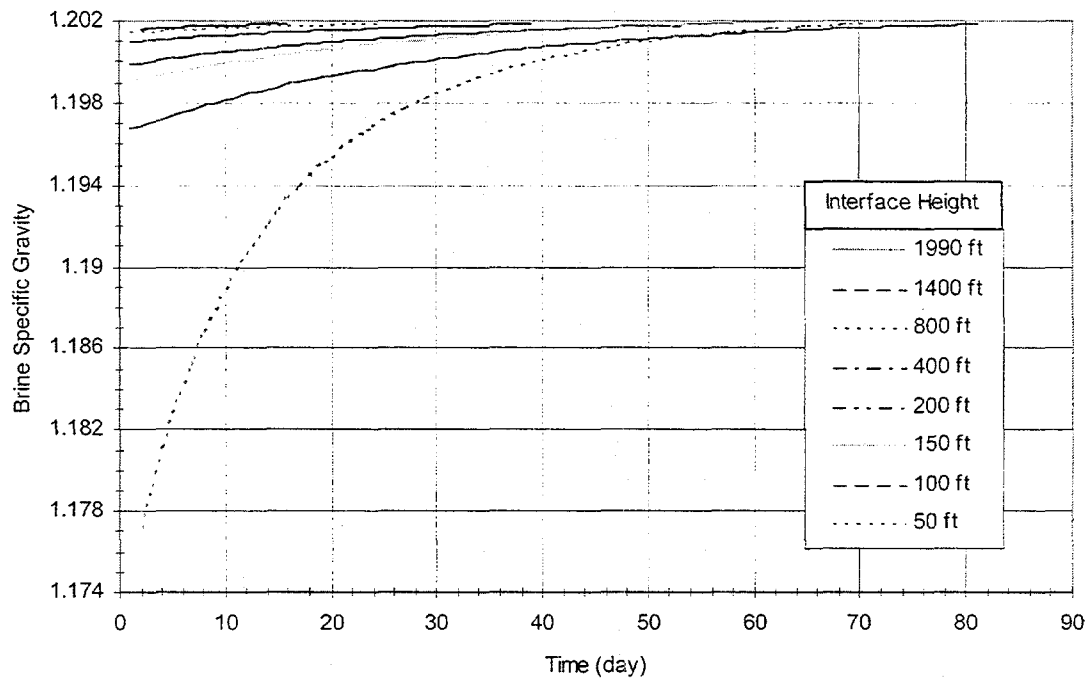


Figure 3. Brine Specific Gravity vs. Time for 10 MB Injection of Raw Water into a Cavern at Various Oil/Brine Interface Heights.

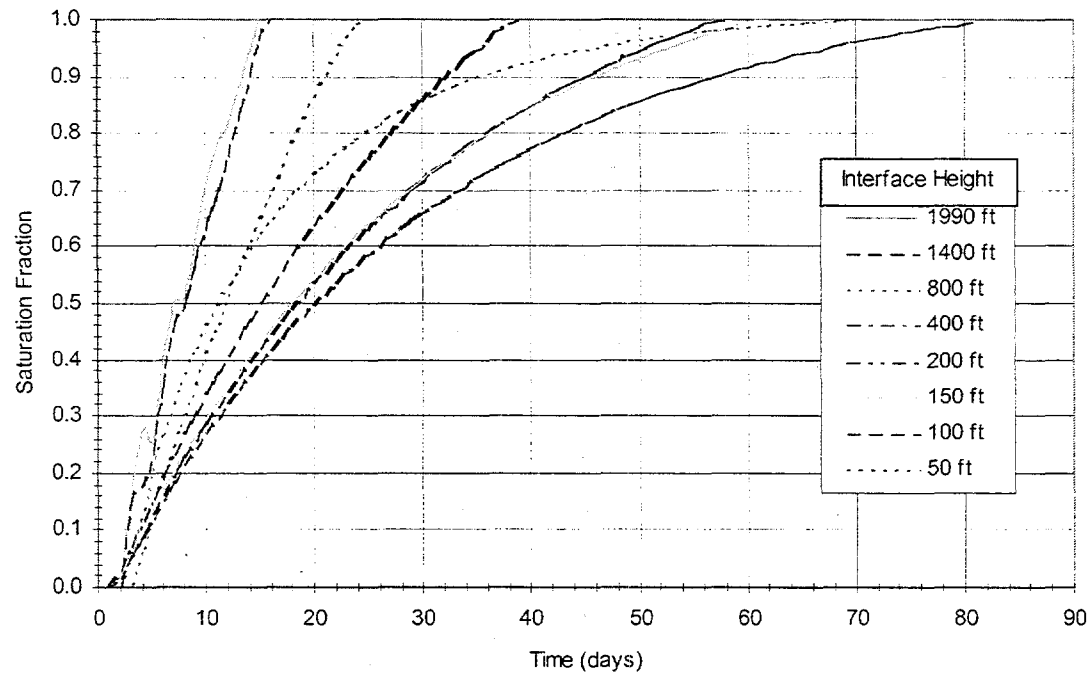


Figure 4. Saturation Fraction vs. Time for 10 MB Injection of Raw Water into a Cavern at Various Oil/Brine Interface Heights.

subsequent predictions as a starting point. As a result, the initial brine specific gravity ranged from 1.08 to 1.202 (full saturation). The relationship expressing saturation fraction (F_s) as a function of time in days (t) after an injection can be expressed as an exponential function:

$$F_s = 1 - e^{-0.0368t} \quad (32)$$

The function provides a good approximation from 1 to 112 days, when the brine reaches full saturation ($F_s=1$). Figure 5 compares the exponential relationship to the range of saturation fractions calculated at a regular interval from the analyses.

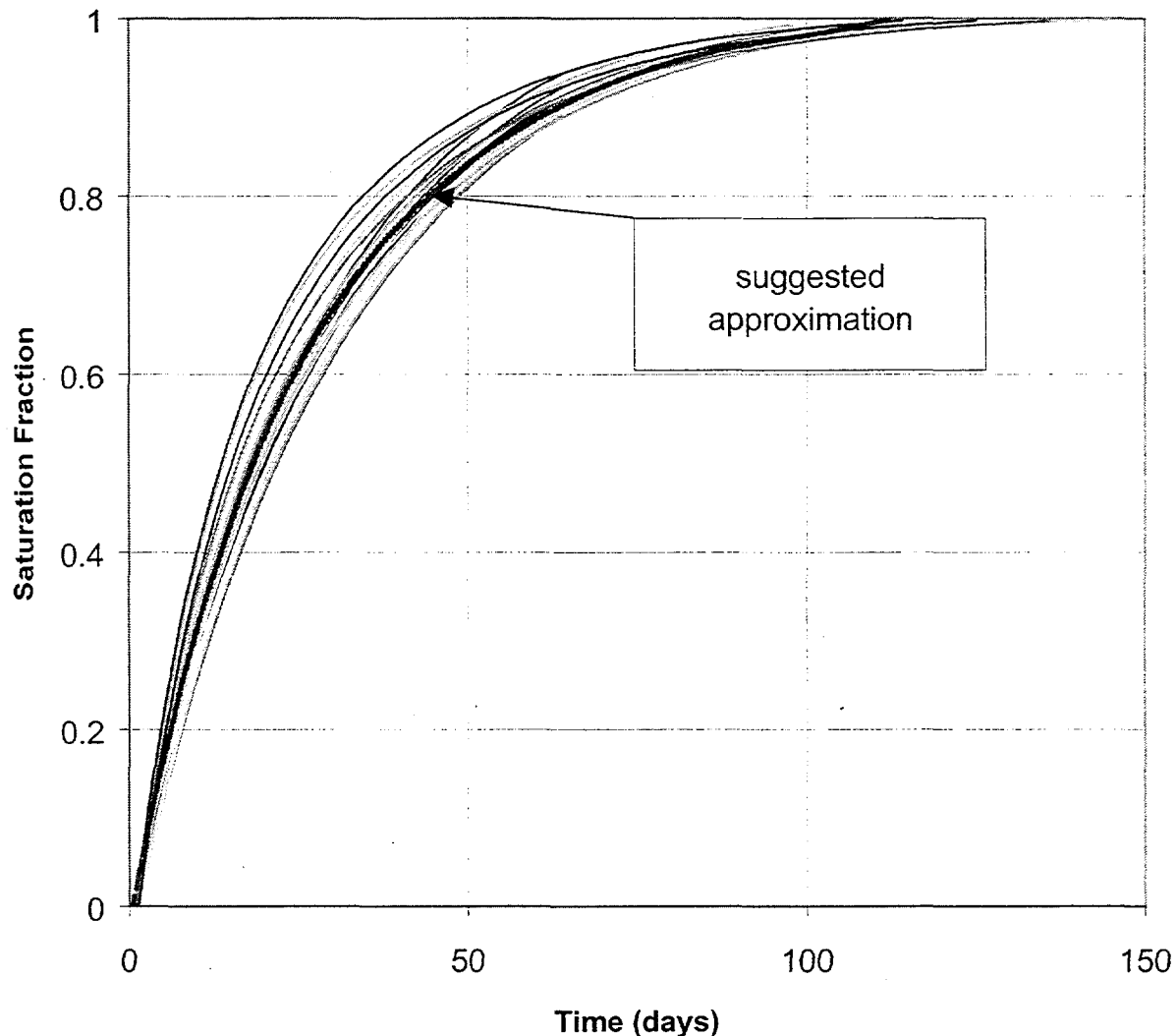


Figure 5. Saturation Fraction vs. Time for all Cases. Curves are based on various starting times within the individual analyses.

If it is assumed that saturation fraction is directly proportional to the change in cavern pressure, the following relationship results for use in CaveMan:

$$P(t) = pF_s \quad (33)$$

where $P(t)$ is the change in cavern pressure due to leaching, p is the pressure drop due to dissolution as defined in the above section, and F_s is defined above.

The above relationship for the pressure drop as a function of time can be used in CaveMan to approximate the effects of raw water injections. If multiple injections of raw water occur within 112 days or an injection of partially saturated brine occurs, then the raw water quantity needs to be calculated based on the salinity of the brine in the cavern after the injection.

The above results should be used to approximate cavern behavior. No attempt has been made to model each individual cavern within the SPR system. Detailed modeling of specific cavern parameters and injection histories may be considered if a cavern exhibits anomalous pressure conditions in the future that may be attributed to leaching. However, model predictions using SANSMIC for the conditions considered in this report have not been validated in the field and some caution is advised in the use of the model predictions (Russo, 1983).

SUMMARY

A software-based cavern pressure analysis system called CaveMan has been developed that can be used as one component of a larger program to monitor the integrity of SPR oil storage caverns. The software implements models for cavern pressurization resulting from thermal expansion of the cavern fluids, creep closure of the caverns, and cavern enlargement due to salt dissolution resulting from injection of raw water or unsaturated brine into the caverns. Parameters in the thermal and creep models were optimized to obtain the best match between historical measured cavern pressures and predicted values. Statistical tests have been derived which assess the significance of differences between measured and predicted cavern pressures. Measured pressures obtained after the time range encompassing the data used in the optimization process are compared to predicted values and significant differences are flagged by the program. Caverns that are pressurizing at rates significantly below predicted rates require further investigation to determine if the anomalous pressurization rates are due to a leak of cavern fluids.

REFERENCES

Ballard, S., B. L. Ehgartner, J. Berndsen, R. Myers, and J. McHenry, 1997, The CAVEMAN cavern pressurization model, SAND97-2952C, Sandia National Laboratories, Albuquerque, NM.

Caceci, M. S., and W. P. Cacheris, 1984, Fitting Curves to Data, Byte, v. 9, no. 5.

Ehgartner, B.L., 1992, Effects of Cavern Spacing and Pressure on Subsidence and Storage Losses for the US Strategic Petroleum Reserve, SAND91-2575, Sandia National Laboratories, Albuquerque, NM.

Ehgartner, B.L., 1997, SPR Ullage Study, Report to R.E. Myers from J.K. Linn, Sandia National Laboratories, Albuquerque, NM.

Ehgartner, B, S. Ballard, M. Tavares, S. Yeh, T. Hinkebein, and R. Ostensen, 1995, A Predictive Model for Pressurization of SPR Caverns, Fall Meeting paper, Solution Mining Research Institute, San Antonio, TX, October 23-24.

Henderson, J. K., 1994, Strategic Petroleum Reserve Gas and Geothermal Effects on Crude Oil Vapor Pressure, Dept. of Energy Strategic Petroleum Reserve Report MP 94W000031, New Orleans, LA.

Kaufman, D., 1960, Sodium Chloride: The Production and Properties of Salt and Brine, American Chemical Society Monograph Series, Reinhold Publishing Corporation, NY.

Kikuchi, N., 1986, Finite Element Methods in Mechanics, Cambridge University Press, Cambridge, UK.

Molecke, M. A., 2000, Final State of the Strategic Petroleum Reserve (SPR) Weeks Island Mine, SAND2000-0400, Sandia National Laboratories, Albuquerque, NM.

Munson, D. E., 1979, Preliminary Deformation-Mechanism Map for Salt (with Application to WIPP), SAND79-0076, Sandia National Laboratories, Albuquerque, NM.

Munson, D. E., and P. R. Dawson, 1982, A Transient Creep Model for Salt During Stress Loading and Unloading, SAND82-0962, Sandia National Laboratories, Albuquerque, NM.

Munson, D. E., A. F. Fossum, and P. D. Senseny, 1989a, Advances in Resolution of Discrepancies Between Predicted and Measured In Situ WIPP Room Closures, SAND89-2498, Sandia National Laboratories, Albuquerque, NM.

Munson, D. E., A. F. Fossum, and P. D. Senseny, 1989b. Approach to First Principles Model Prediction of Measured WIPP In Situ Room Closure in Salt, SAND89-2535, Sandia National Laboratories, Albuquerque, NM.

Ostensen, R.W., 1995, "Approximate Thermal Model for Cavern Heating", Internal memo dated July 19, Sandia National Laboratories, Albuquerque, NM.

Russo, A.J., 1983, A User's Manual for the Salt Solution Mining Code, SANSMIC, SAND83-1150, Sandia National Laboratories, Albuquerque, NM.

Wawersik, W.R., and D. H. Zeuch, 1984, Creep and Creep Modeling of Three Domal Salts- A Comprehensive Update, SAND89-2535, Sandia National Laboratories, Albquerque, NM.

(this page intentionally left blank)

APPENDIX A

In this Appendix, tables containing the various model parameters for each cavern are presented.

In Table A-1, a number of parameters that were not optimized in the models are tabulated. These include the oil API, the depths of the top and bottom of the caverns, and the undisturbed salt temperature at the depth of the top and bottom of the cavern.

In Table A-2, thermal parameters that were optimized in the thermal model are presented. The date of the end of leaching was only optimized for Phase I caverns; for Phase II and III caverns this parameter was fixed. The duration of leaching was only optimized for Phase II and III caverns; it was fixed at two years for Phase I caverns. For historical cavern data (prior to 1999), oil and brine injection temperature data was not available and hence this parameter was optimized. The assumption being made here is that all oil injections prior to 1999 were made at the same temperature and that all brine injections occurred at the same temperature (the brine temperature could be different from the oil injection temperature). While this assumption is highly unrealistic, there was no choice since historical data was unavailable. If oil or brine injection temperatures were known for individual injections, the known values were specified. The oil and brine salt temperatures are the undisturbed salt temperatures adjacent to the oil and brine in the thermal model. They are the temperatures applied at the constant temperature boundaries in the oil and brine submodels of the thermal model. The Thermal/Creep Ratio is the multiplier on the thermal pressurization rate. See the main text for additional discussion of these parameters.

In Table A-3, the parameters used in the salt creep model are presented. L is the characteristic length parameter, which describes the distance into the salt from the cavern wall that is being stressed. The salt lithostatic stress parameter is self-explanatory and f is the triaxial stress parameter described in the text. ζ_0 is the starting value for the internal variable that reflects the internal microstructure in the salt. Date is the date when ζ_0 is valid. It is usually the date of the first available pressure measurement from a cavern. D_{rms} is the Root Mean Square Difference parameter that characterizes the mismatch between the measured and predicted pressures during the time when the data used in the optimization operation was collected.

Table A-1 – Cavern Geometry Parameters

	API	Top of Cavern (ft)	Bottom of Cavern (ft)	Salt Temperature at Top of Cavern (°F)	Salt Temperature at Bottom of Cavern (°F)
Big Hill					
BH101	33.0	2266	4176	108.6	135.5
BH102	33.0	2300	4087	109.1	134.3
BH103	33.0	2200	4054	107.7	133.8
BH104	32.0	2278	4247	108.8	136.5
BH105	34.6	2280	4232	108.8	136.3
BH106	34.6	2284	4108	108.9	134.6
BH107	32.8	2265	4118	108.6	134.7
BH108	34.6	2334	4148	109.6	135.1
BH109	34.6	2300	4273	109.1	136.9
BH110	34.6	2300	4219	109.1	136.1
BH111	34.6	2300	4243	109.1	136.5
BH112	34.6	2300	4228	109.1	136.3
BH113	34.6	2300	4166	109.1	135.4
BH114	34.6	2300	4160	109.1	135.3
Bryan Mound					
BM101	34.1	1998	4162	116.5	152.2
BM102	33.5	2225	4249	120.3	153.7
BM103	34.7	2110	4138	118.4	151.8
BM104	33.0	2220	4175	120.2	152.4
BM105	33.2	2100	4206	118.2	152.9
BM106	22.5	2097	4031	118.2	150.1
BM107	32.9	2225	4106	120.3	151.3
BM108	33.7	2165	4138	119.3	151.8
BM109	33.3	2170	4185	119.4	152.6
BM110	32.8	2150	4118	119.0	151.5
BM111	33.8	2125	4162	118.6	152.2
BM112	33.4	2065	4152	117.6	152.1
BM113	36.2	2159	4219	119.2	153.2
BM114	36.2	2150	4180	119.0	152.5
BM115	36.2	2185	4137	119.6	151.8
BM116	36.2	2100	4266	118.2	153.9
BM1	36.3	2345	2768	122.2	129.2
BM2	36.6	1450	1672	107.5	111.1
BM4	35.8	2495	3081	124.7	134.4
BM5	33.6	2102	3275	118.2	137.6
Bayou Choctaw					
BC15	32.9	2597	3304	108.9	118.8
BC17	33.8	2590	4029	121.9	141.7
BC18	33.8	2100	4232	115.2	144.5
BC19	32.7	2980	4231	127.3	144.5
BC20	36.1	3825	4233	138.9	144.5
BC101	34.6	2550	4824	121.4	152.7
West Hackberry					
WH101	36.6	2555	4446	125.9	146.1
WH102	37.6	2628	4502	126.7	146.7
WH103	36.6	2700	4424	127.4	145.9

	API	Top of Cavern (ft)	Bottom of Cavern (ft)	Salt Temperature at Top of Cavern (°F)	Salt Temperature at Bottom of Cavern (°F)
WH104	36.6	2625	4555	126.6	147.3
WH105	37.5	2648	4612	126.9	147.9
WH106	34.3	2760	4361	128.1	145.2
WH107	37.3	2600	4547	126.4	147.2
WH108	37.3	2600	4427	126.4	145.9
WH109	33.8	2485	4648	125.1	148.3
WH110	37.6	2650	4571	126.9	147.5
WH111	33.5	2630	4600	126.7	147.8
WH112	34.6	2575	4532	126.1	147.0
WH113	36.8	2925	4684	129.8	148.7
WH114	34.1	2600	4548	126.4	147.2
WH115	34.2	2550	4631	125.8	148.1
WH116	37.2	2680	4719	127.2	149.0
WH117	33.8	2570	4616	126.0	147.9
WH6	33.1	3225	3385	133.1	134.8
WH7	37.0	2540	3495	125.7	135.9
WH8	33.2	2440	3452	124.7	135.5
WH9	32.9	3210	3572	132.9	136.8
WH11	33.2	2945	3743	130.1	138.6

Table A-2 – Thermal Model Parameters

	End of Leaching	Duration of Leaching (days)	Temperature of Leaching (°F)	Oil Injection Temperature (°F)	Brine Injection Temperature (°F)	Interface Heat Transfer Coefficient (BTU/day /ft ² /°F)	Oil Salt Temperature (°F)	Brine Salt Temperature (°F)	Thermal / Creep Ratio
Big Hill									
BH101	09/18/1990	2	64.5	84.5	64.5	10.52	109.05	128.79	1
BH102	10/20/1990	15	69.1	74.2	58.8	27.95	109.12	129.89	1
BH103	11/28/1990	1	69.4	63.5	90.0	28.25	122.88	121.40	1
BH104	10/21/1990	0	70.0	59.2	68.0	19.68	119.55	128.54	1
BH105	05/14/1990	89	61.4	84.2	90.0	11.29	128.94	130.21	1
BH106	10/16/1990	40	70.0	72.9	70.0	7.71	130.94	134.60	1
BH107	04/24/1990	5	67.8	58.5	90.0	1.00	128.83	125.23	1
BH108	06/14/1990	7	69.9	66.5	67.8	24.28	120.64	135.10	1
BH109	07/24/1990	217	70.0	68.3	66.7	139.39	129.36	136.88	1.9384
BH110	04/19/1990	251	65.3	63.1	86.4	55.34	111.27	136.02	1.6551
BH111	07/15/1991	2	68.4	84.3	68.4	17.70	114.29	121.88	1
BH112	06/18/1991	0	70.0	87.2	73.7	24.20	113.02	119.88	1
BH113	05/01/1991	54	61.0	74.8	72.6	1.00	119.99	128.76	1
BH114	08/27/1991	0	70.0	66.8	70.0	18.17	118.94	126.80	0.5048
Bryan Mound									
BM101	09/03/1984	2	68.7	76.9	77.2	20.10	135.65	146.47	1
BM102	07/26/1984	20	70.0	71.3	69.6	13.98	139.55	133.43	1
BM103	04/30/1984	28	66.0	70.9	50.0	26.75	138.50	151.80	1
BM104	01/01/1983	0	64.0	59.9	88.2	38.31	131.89	151.41	1
BM105	07/25/1983	0	70.0	73.9	89.9	6.78	131.90	145.15	1
BM106	12/16/1982	15	60.1	78.7	50.3	14.97	133.30	150.10	1
BM107	01/04/1983	309	68.9	74.2	50.0	26.05	144.83	151.29	1
BM108	08/20/1985	0	60.0	77.2	77.1	15.57	133.51	139.24	1
BM109	07/28/1983	124	60.5	81.0	62.6	36.70	140.01	152.59	1
BM110	12/23/1982	40	60.2	65.1	90.0	48.71	133.71	151.50	1
BM111	02/14/1984	1213	62.2	105.4	78.2	31.38	151.43	152.20	1
BM112	11/30/1984	81	68.4	68.7	67.9	76.98	142.14	152.10	0.5000
BM113	10/08/1985	36	70.0	87.2	64.7	19.00	132.42	153.20	1
BM114	08/26/1987	2	70.0	75.3	50.0	23.50	133.47	137.55	1
BM115	08/11/1986	0	67.8	88.0	70.5	11.78	131.87	148.71	1
BM116	07/28/1986	37	69.6	80.7	84.9	25.29	134.83	153.89	0.5000
BM1	05/03/1983	729	77.9	124.7	51.8	50.75	127.94	128.08	1
BM2	06/03/1984	729	125.1	99.8	85.0	195.31	107.50	103.30	0.5000
BM4	12/10/1983	729	123.0	79.9	50.0	7.61	136.16	125.63	1
BM5	06/06/1967	729	60.0	89.2	89.4	23.33	118.24	129.40	1
Bayou Choctaw									
BC15	12/15/1977	351	70.0	71.7	90.0	12.97	111.38	113.03	1
BC17	06/05/1976	729	60.0	52.9	90.0	25.74	122.69	136.70	0.6298
BC18	07/13/1979	729	60.0	81.4	57.9	12.89	124.69	133.56	1
BC19	07/04/1981	729	61.7	63.4	73.0	26.38	130.73	144.47	0.8523
BC20	09/04/1981	729	67.6	82.1	58.7	2.50	147.24	132.33	1
BC101	03/30/1989	2220	70.0	124.4	67.8	16.17	124.51	150.67	1
West Hackberry									
WH101	12/28/1983	20	67.3	69.4	90.0	8.46	134.77	132.35	0.5000

	End of Leaching	Duration of Leaching (days)	Temperature of Leaching (°F)	Oil Injection Temperature (°F)	Brine Injection Temperature (°F)	Interface Heat Transfer Coefficient (BTU/day /ft ² /°F)	Oil Salt Temperature (°F)	Brine Salt Temperature (°F)	Thermal / Creep Ratio
WH102	11/08/1984	51	70.0	72.1	69.6	8.96	135.08	142.40	0.5000
WH103	01/14/1984	74	70.0	70.4	85.8	5.34	134.00	139.78	1
WH104	02/27/1984	118	60.0	80.4	80.6	4.02	134.94	142.07	1
WH105	01/18/1984	91	64.3	79.1	88.5	1.00	134.04	134.73	1
WH106	05/01/1986	13	70.0	76.6	89.8	12.73	135.20	130.25	1
WH107	07/06/1984	177	69.9	78.3	72.3	14.06	138.29	137.55	1
WH108	12/07/1984	42	66.6	81.7	90.0	17.15	135.40	139.25	0.5000
WH109	04/06/1988	2	69.1	72.9	76.2	15.25	130.37	148.30	1
WH110	03/15/1985	10	60.2	78.3	76.1	2.34	129.94	147.45	1
WH111	04/01/1988	364	68.0	106.2	64.4	38.05	126.70	140.11	1
WH112	01/03/1987	106	61.7	71.4	50.0	35.04	144.91	126.10	0.5000
WH113	06/10/1985	0	63.6	71.7	77.5	15.24	145.87	129.80	1
WH114	09/05/1985	20	68.6	70.3	67.5	30.29	138.80	126.40	0.5000
WH115	06/01/1987	60	70.0	59.5	75.1	30.90	135.73	148.10	1
WH116	09/04/1985	1	70.0	69.0	71.1	10.04	135.39	134.52	1
WH117	10/30/1988	33	70.0	83.7	82.8	23.74	130.82	140.38	1
WH6	10/12/1982	731	65.5	70.5	70.5	20.50	134.45	134.45	1
WH7	08/07/1965	729	64.7	50.0	50.1	18.60	134.44	130.52	1
WH8	04/02/1974	729	60.0	72.3	90.0	2.78	131.15	124.70	1
WH9	07/29/1965	729	72.3	70.9	89.7	2.07	135.95	136.66	1
WH11	12/06/1977	729	86.5	98.3	66.5	30.41	131.09	138.50	1

Table A-3 – Creep Model Parameters

	Characteristic Length, L (ft)	Lithostatic Pressure, P_L (psi)	Triaxial Stress Factor, f	Internal Variable, ζ_0	Date	D_{rms}
Big Hill						
BH101	20.00	4089.59	0.241040	0.010164	09/19/1990	9.62
BH102	1000.00	4026.40	0.637258	0.000233	03/23/1991	9.87
BH103	105.00	4002.07	0.386402	0.001506	11/29/1990	9.90
BH104	34.51	3903.48	0.200000	0.002852	06/01/1991	8.21
BH105	59.94	7000.00	0.798919	0.001327	05/14/1990	6.42
BH106	20.00	3499.28	0.200000	0.000722	10/17/1990	8.58
BH107	182.81	3406.34	0.200000	0.014687	04/25/1990	7.19
BH108	76.46	3547.46	0.200000	0.000854	06/14/1991	6.48
BH109	20.00	6242.88	0.804448	0.001380	07/25/1990	10.00
BH110	20.02	7000.00	0.860846	0.000577	04/20/1990	10.41
BH111	20.00	7000.00	0.774020	0.000820	07/15/1991	9.02
BH112	159.27	7000.00	0.828766	0.000401	06/19/1991	9.18
BH113	494.40	7000.00	0.872159	0.000655	05/02/1991	7.29
BH114	38.77	4682.98	0.468026	0.000690	08/29/1991	8.84
Bryan Mound						
BM101	1000.00	5933.85	0.903182	0.000279	01/01/1990	6.52
BM102	307.72	3533.82	0.771932	0.001087	01/01/1990	7.56
BM103	989.06	6472.67	0.896264	0.000559	01/01/1990	7.43
BM104	647.65	4437.33	0.780589	0.002306	01/01/1990	5.94
BM105	383.76	7000.00	0.883833	0.003191	01/01/1990	20.39
BM106	1000.00	4544.23	0.809393	0.000606	01/01/1990	7.21
BM107	25.05	3232.46	0.200000	0.043466	01/01/1990	6.35
BM108	20.09	4261.14	0.680143	0.002502	01/01/1990	8.58
BM109	24.05	3218.25	0.200002	0.003915	01/01/1990	4.54
BM110	265.05	2264.79	0.228983	0.000377	01/01/1990	11.94
BM111	758.45	7000.00	0.905723	0.001078	01/01/1990	15.24
BM112	606.98	3655.32	0.673512	0.001200	01/01/1990	10.86
BM113	1000.00	5197.42	0.850465	0.000323	01/09/1990	9.58
BM114	1000.00	4155.79	0.756845	0.000561	01/01/1990	9.14
BM115	369.56	3940.83	0.675820	0.000775	01/01/1990	6.73
BM116	52.16	3770.40	0.519232	0.000806	01/01/1990	6.61
BM1	325.67	2723.58	0.858133	0.001238	01/01/1990	13.29
BM2	442.53	2869.07	0.860335	0.001150	01/01/1990	6.13
BM4	53.72	7000.00	0.866638	0.002399	01/01/1990	12.50
BM5	26.18	7000.00	0.824679	0.001408	01/01/1990	13.31
Bayou Choctaw						
BC15	1000.00	3256.47	0.607975	0.001108	01/01/1990	5.67
BC17	306.72	3313.15	0.784502	0.001090	01/01/1990	9.04
BC18	30.32	7000.00	0.848271	0.007251	01/01/1990	8.91
BC19	305.53	3618.75	0.750314	0.001031	01/01/1990	9.37
BC20	253.32	6999.97	0.876111	0.000436	01/01/1990	8.10
BC101	227.36	6196.08	0.833512	0.000177	01/01/1990	19.23
West Hackberry						
WH101	263.59	4856.79	0.726436	0.000861	01/01/1990	7.35
WH102	371.61	4630.95	0.724639	0.000517	01/01/1990	7.34
WH103	24.10	6524.00	0.755739	0.002047	01/01/1990	9.57
WH104	1000.00	5157.98	0.817191	0.000337	01/01/1990	6.92

	Characteristic Length, L (ft)	Lithostatic Pressure, P_L (psi)	Triaxial Stress Factor, f	Internal Variable, ζ_0	Date	D_{rms}
WH105	20.00	6961.26	0.756113	0.003010	01/01/1991	9.47
WH106	836.80	7000.00	0.891681	0.000168	01/01/1991	6.43
WH107	1000.00	5209.70	0.820763	0.000209	01/01/1991	9.37
WH108	410.93	4251.74	0.658519	0.001115	01/01/1991	10.46
WH109	999.98	5243.18	0.808075	0.000499	01/01/1991	9.21
WH110	662.40	5113.16	0.795814	0.000107	01/01/1991	7.83
WH111	451.80	4563.51	0.703030	0.000801	01/01/1990	8.38
WH112	373.03	5669.85	0.812911	0.000561	01/01/1990	9.64
WH113	1000.00	6022.64	0.851699	0.000235	01/01/1990	7.76
WH114	259.19	4792.13	0.712114	0.000932	01/01/1990	10.27
WH115	153.12	4131.64	0.524007	0.004237	01/01/1990	8.01
WH116	20.00	4717.48	0.492035	0.007203	01/01/1990	8.78
WH117	370.83	7000.00	0.864550	0.000264	01/08/1990	8.99
WH6	20.00	6753.26	0.711233	0.003497	01/01/1990	10.14
WH7	20.00	4923.65	0.627556	0.005152	03/13/1990	19.36
WH8	50.51	3750.83	0.482219	0.001399	01/01/1990	11.26
WH9	1000.00	5650.11	0.839984	0.000133	01/01/1991	6.50
WH11	747.43	4056.34	0.713179	0.000894	01/01/1990	6.22

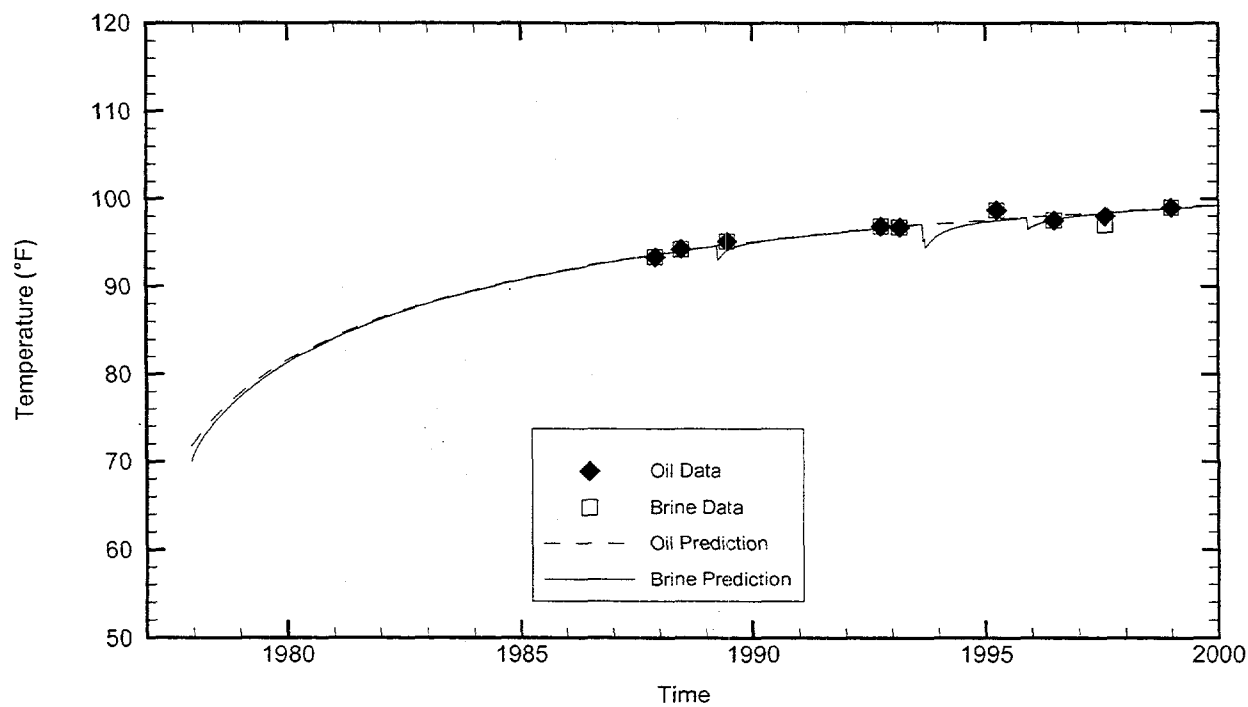
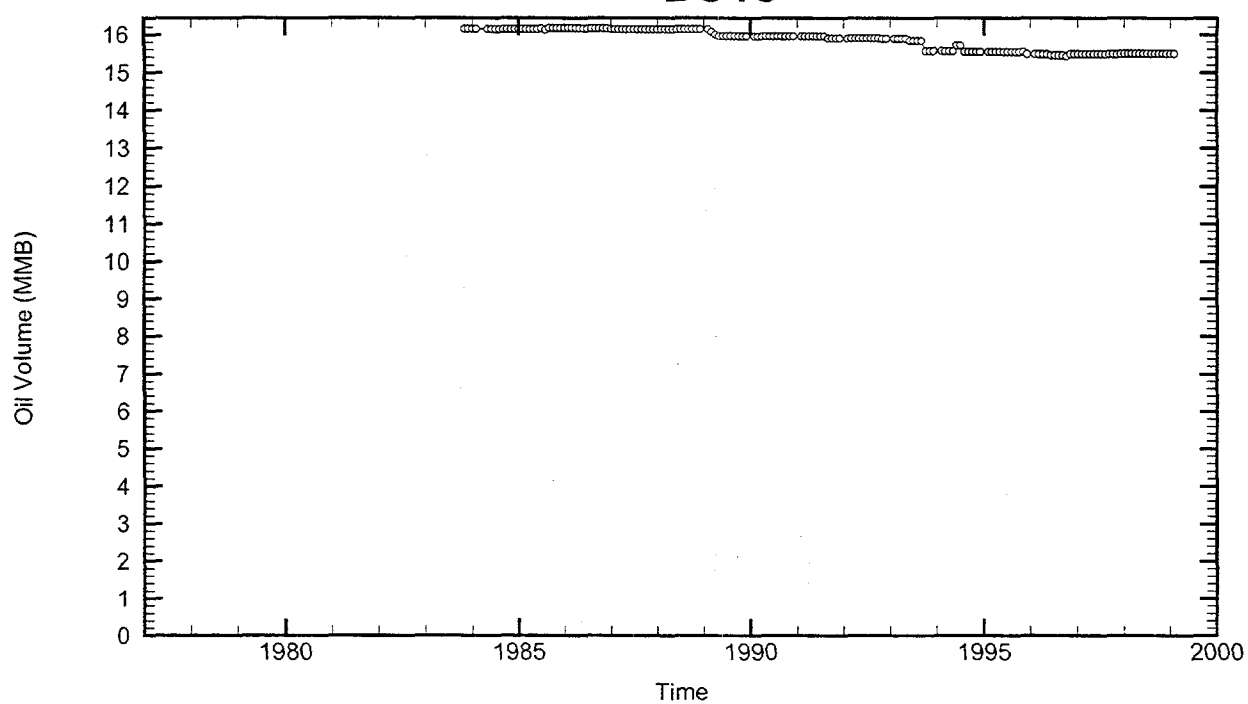
APPENDIX B

In this appendix, four plots are presented for each cavern. The first plot illustrates the monthly oil inventory in each cavern. The upper limit of the vertical axis in each plot is the cavern volume in January 1999. These data were used to deduce oil and brine transfer histories from each cavern. It was assumed that if oil volume increased, then an oil injection and a brine extraction must have occurred, and vice versa.

The second plot shows the evolution of the oil and brine temperatures in the cavern since the time of leaching. Symbols are the measured oil and brine temperatures that were used in the optimization phase of the development of the thermal model. The curves are the oil and brine temperatures predicted by the thermal model.

The third plot presents the measured and predicted pressures from each cavern and the fourth plot illustrates their difference. Also shown on the fourth plot are two horizontal lines that correspond to plus and minus three times the Drms value for the cavern. Pressure differences that fall outside the pressure range bounded by these two lines would cause flags to be raised in CaveMan.

BC15



Cavern: BC15

End of Leaching: 12/15/1977

Duration of Leaching: 11.5318 months

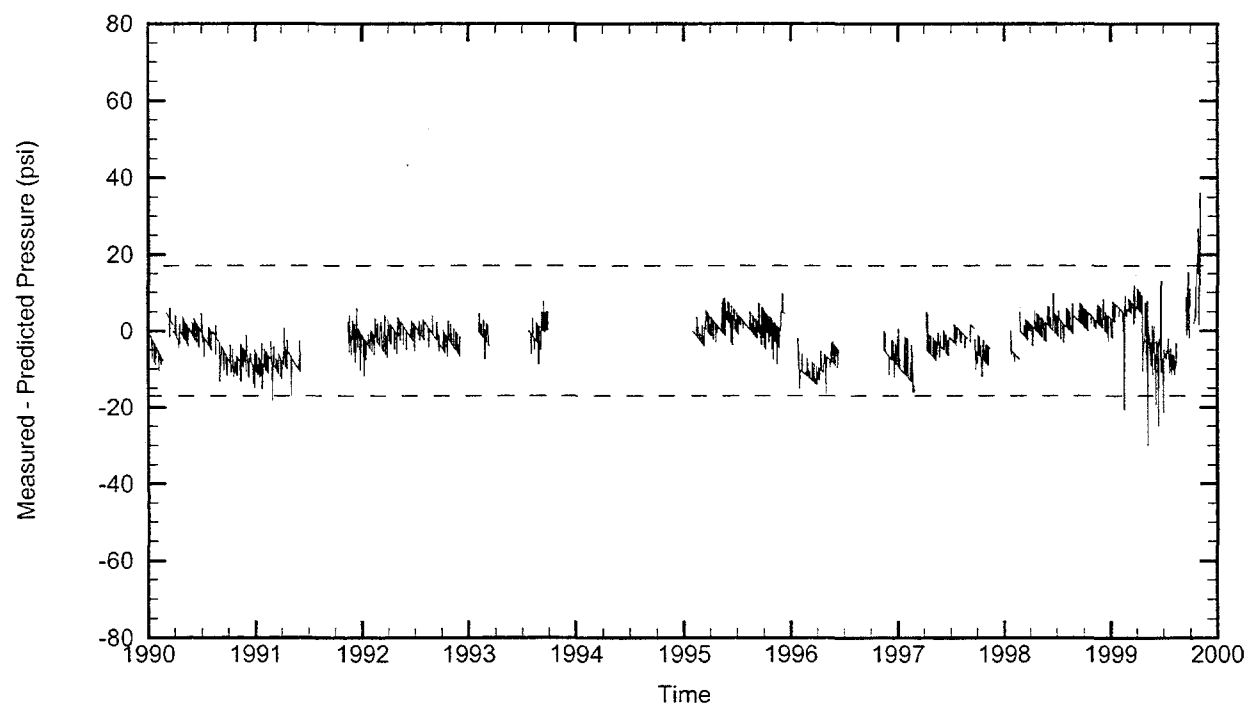
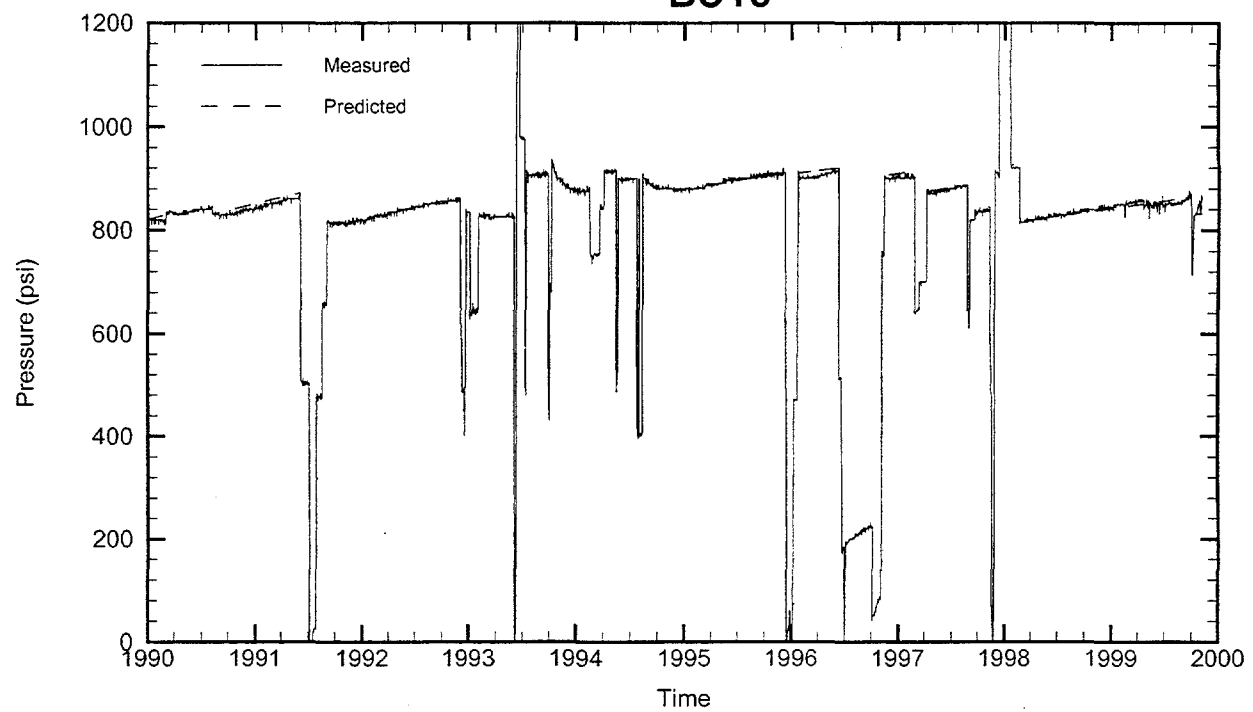
Leaching Temperature: 70.00 °F

Oil Injection Temperature: 71.71 °F

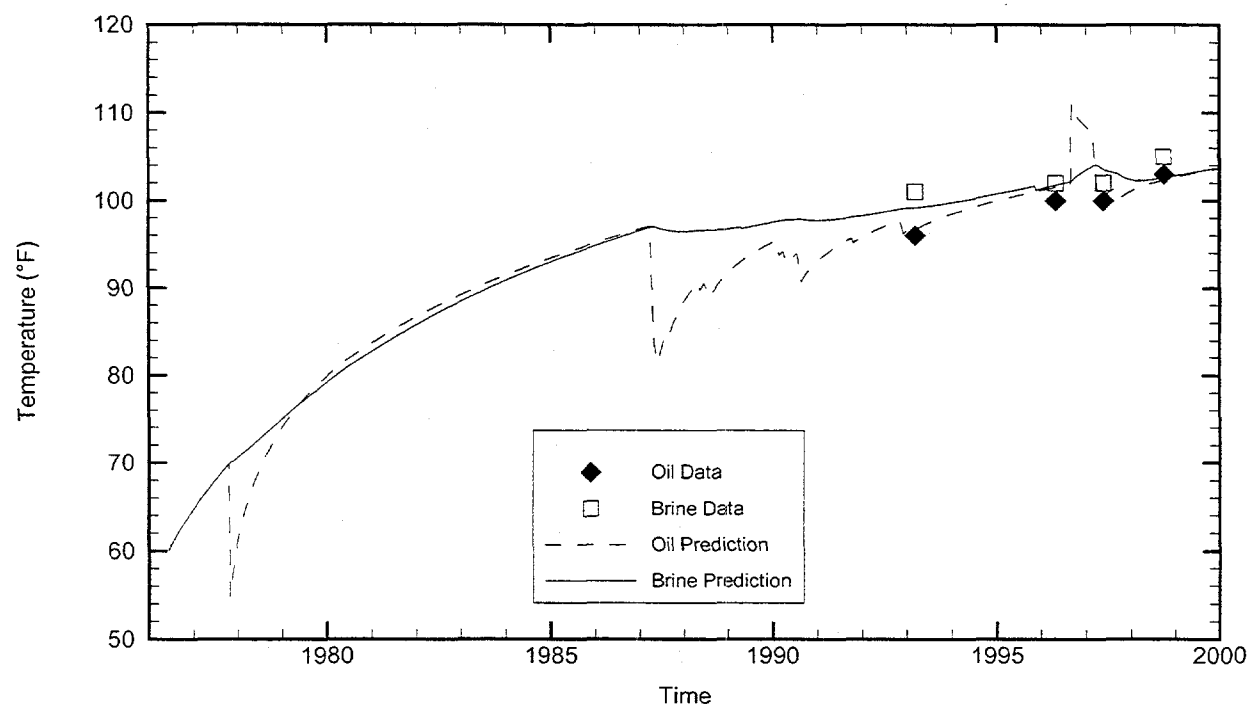
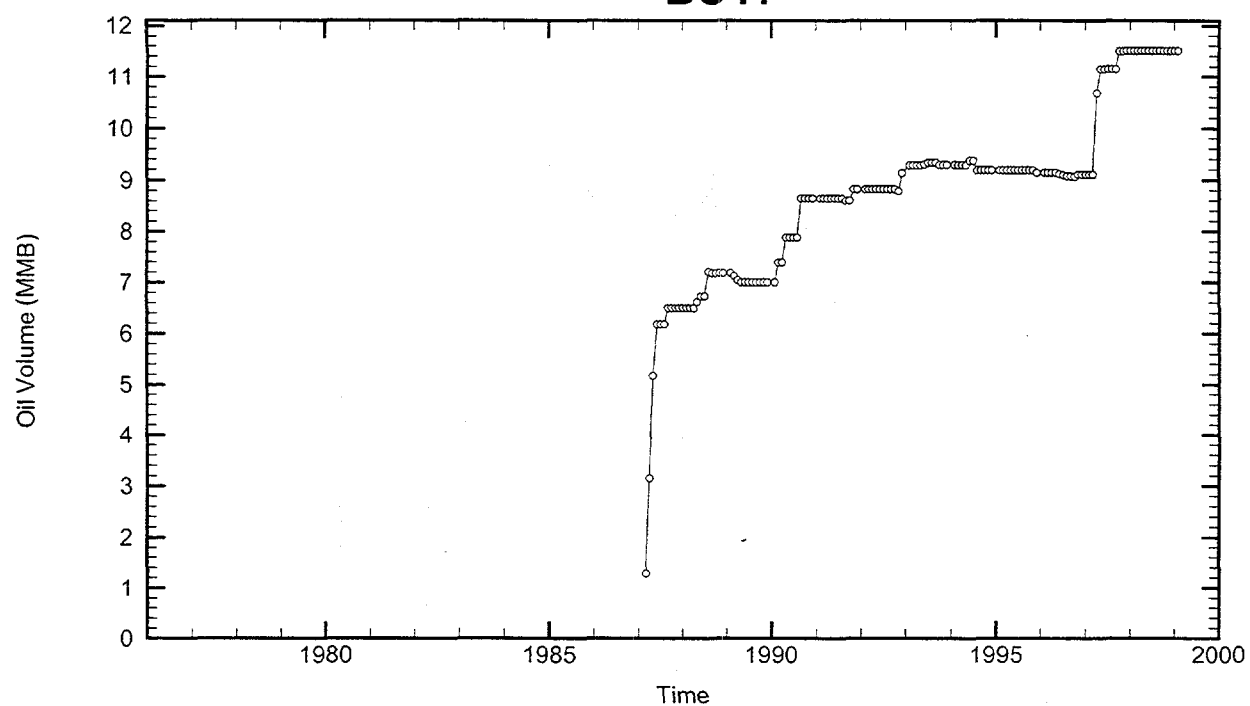
Brine Injection Temperature: 89.98 °F

Number of iterations: 442

BC15



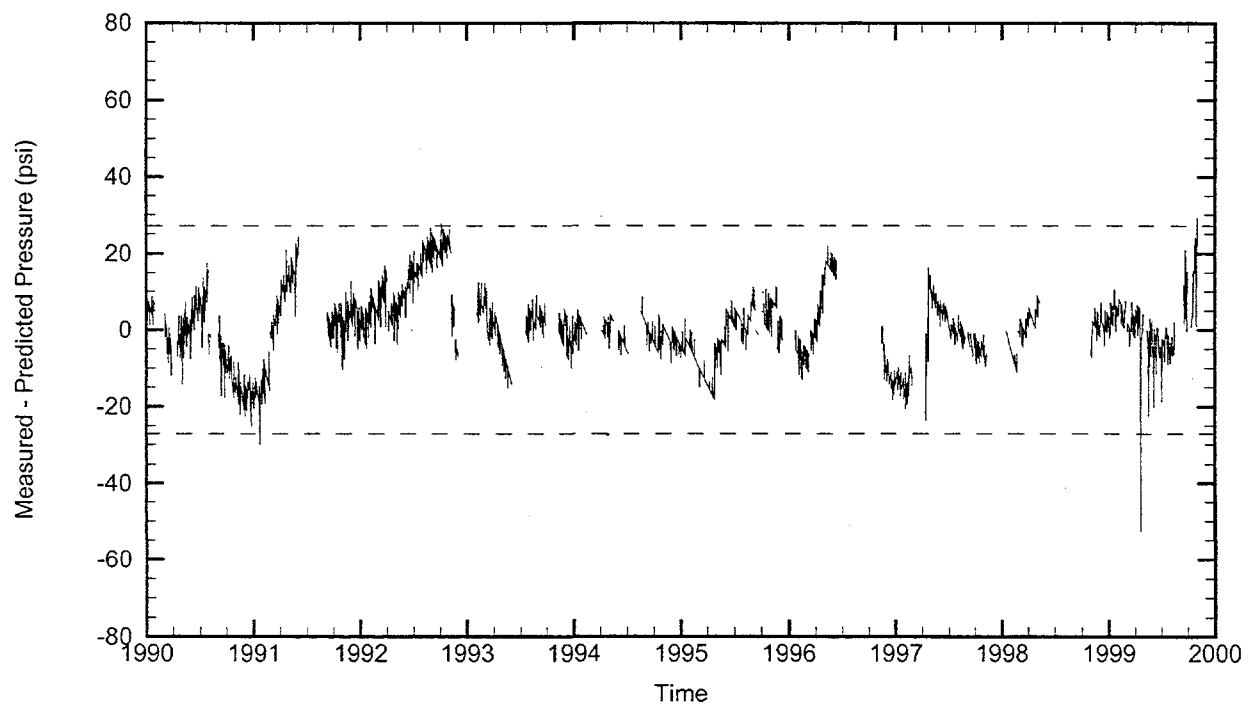
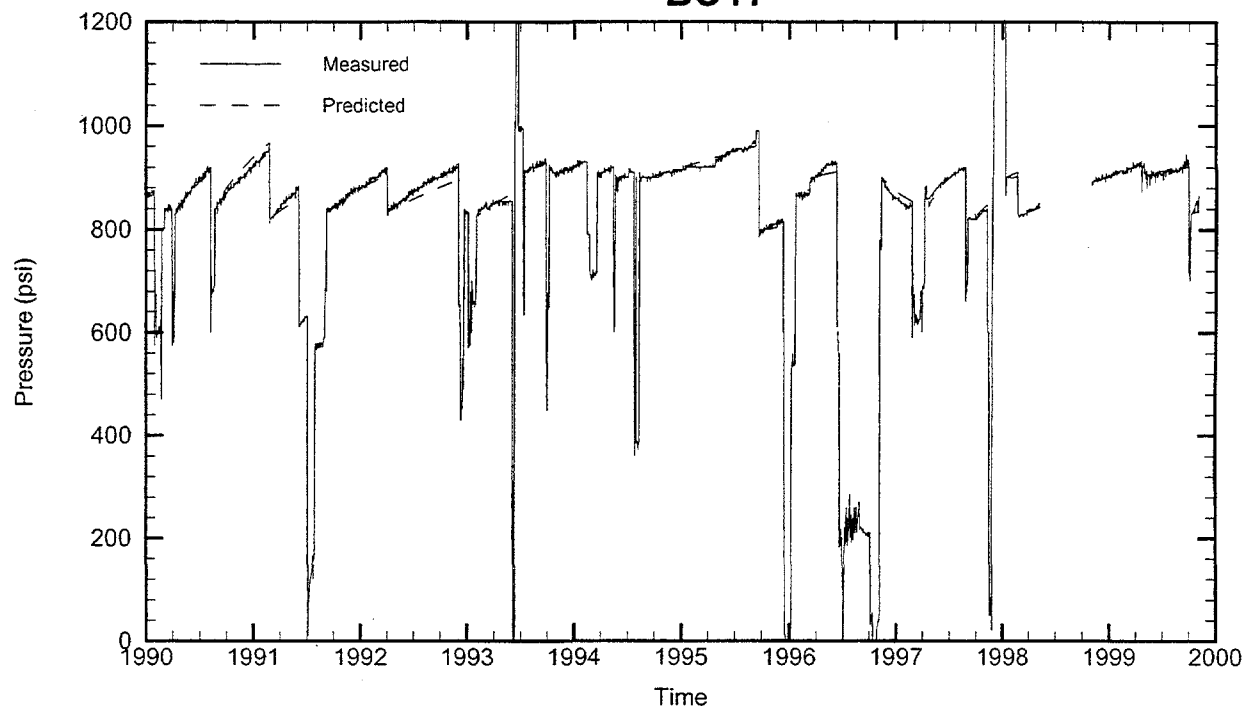
BC17



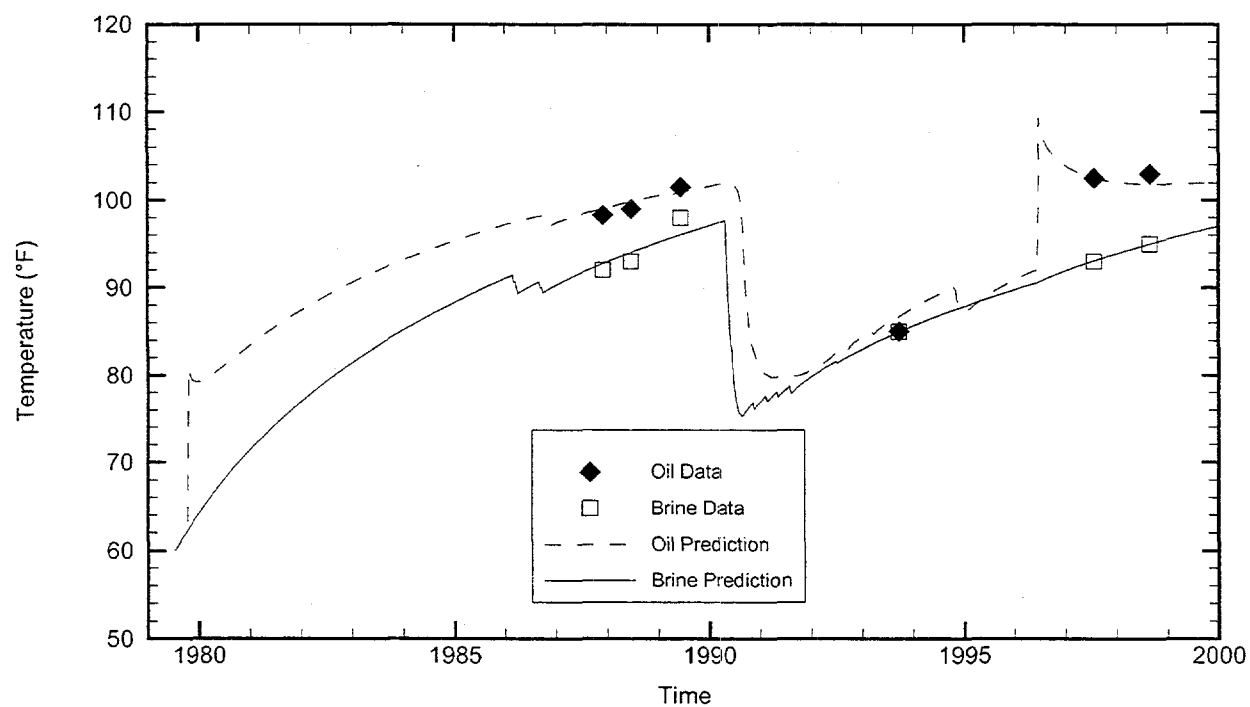
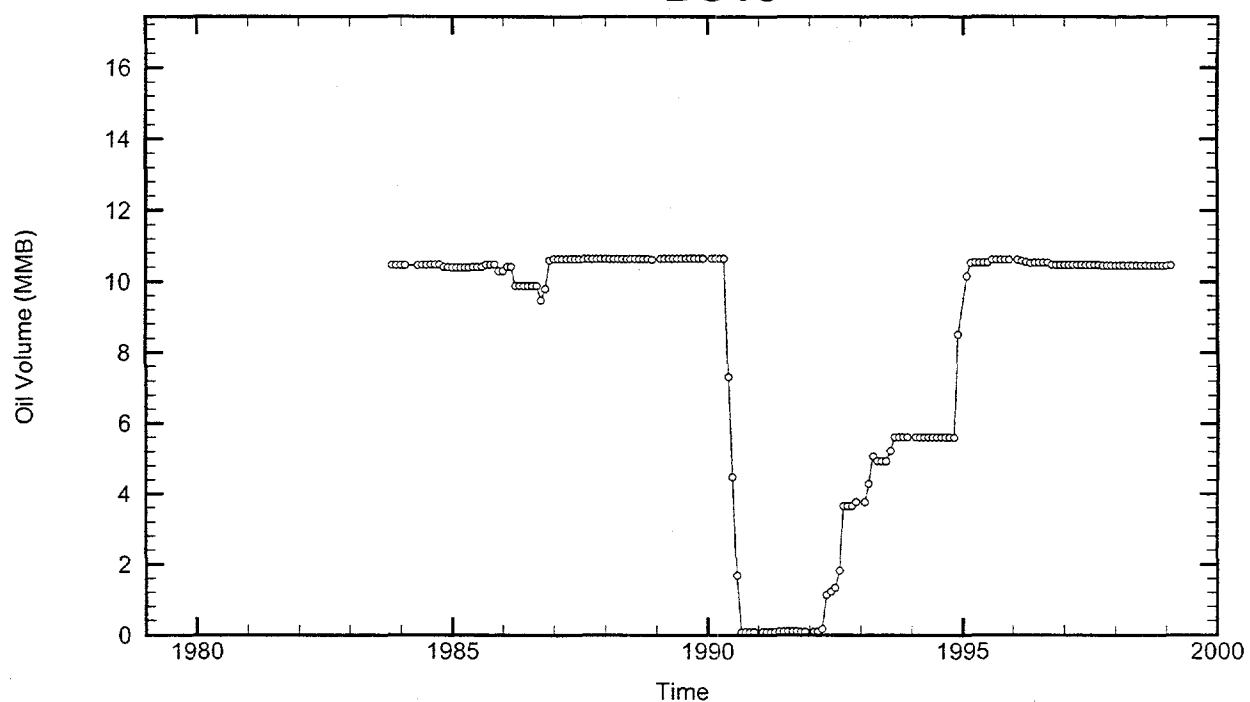
Cavern: BC17
End of Leaching: 06/05/1976
Duration of Leaching: 1.9959 years
Leaching Temperature: 60.00 °F

Degas: 08/30/1996, 112.13 °F, 9.03 MMB
Oil Injection Temperature: 52.86 °F
Brine Injection Temperature: 90.00 °F
Number of iterations: 520

BC17



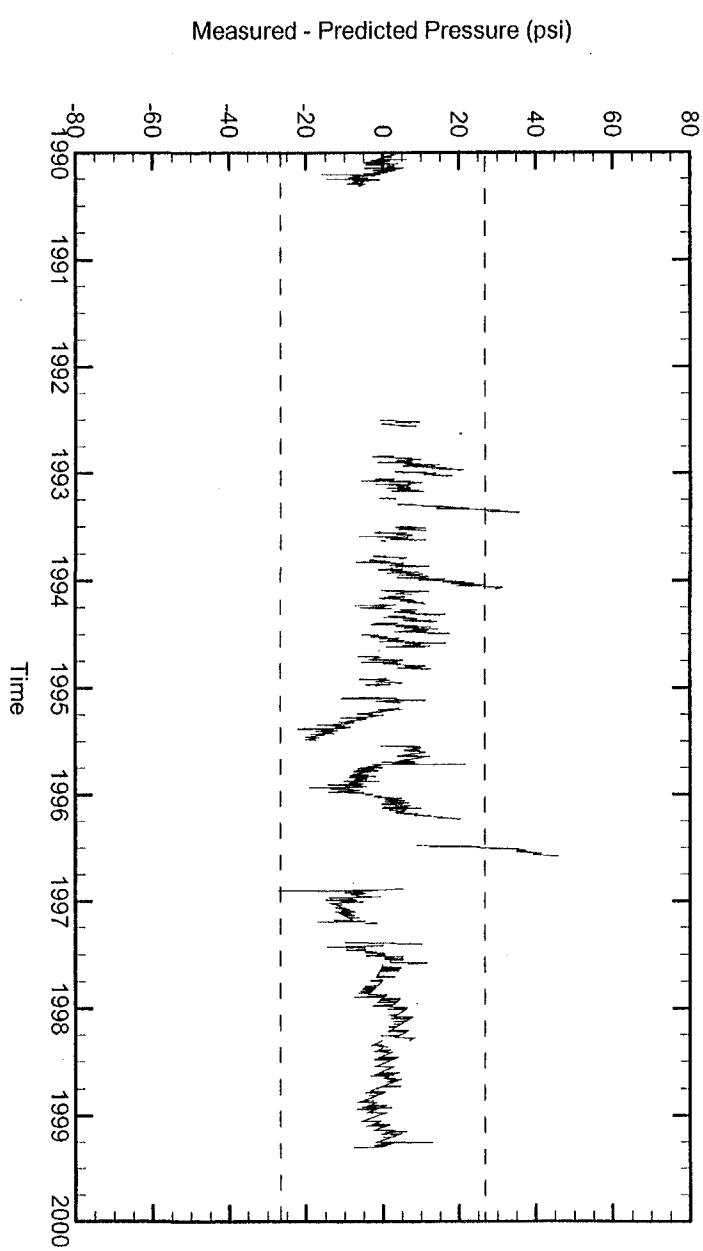
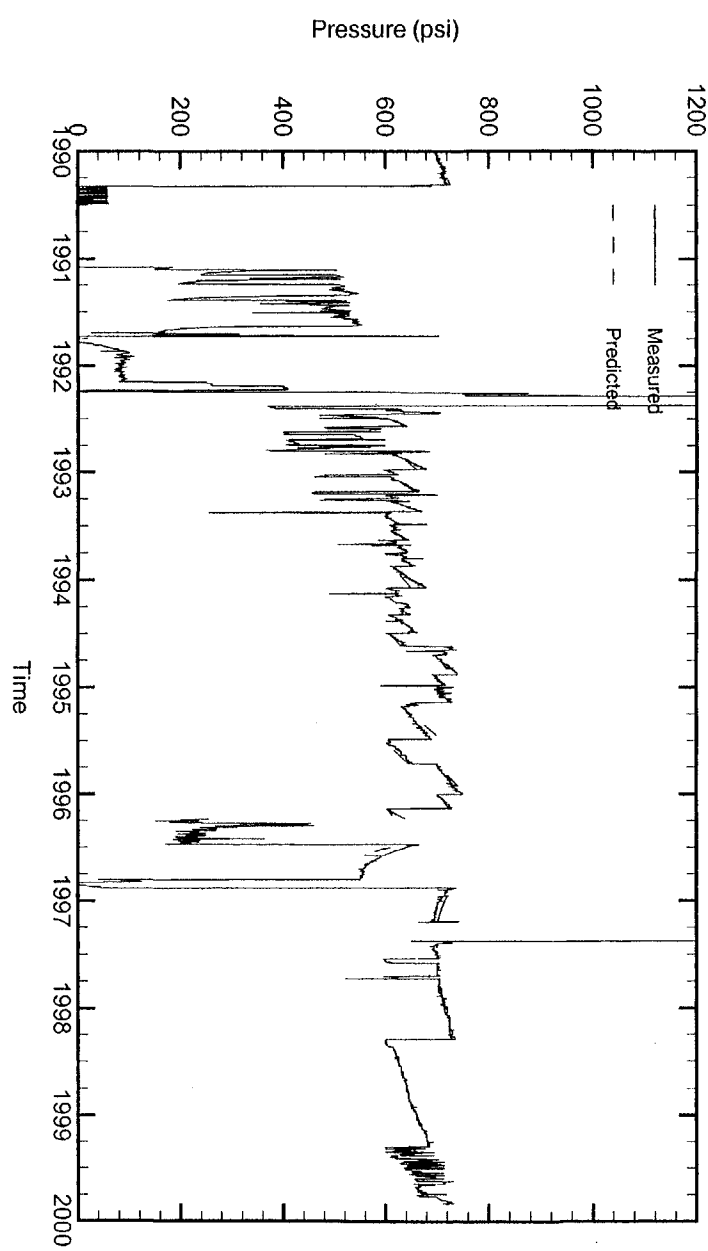
BC18



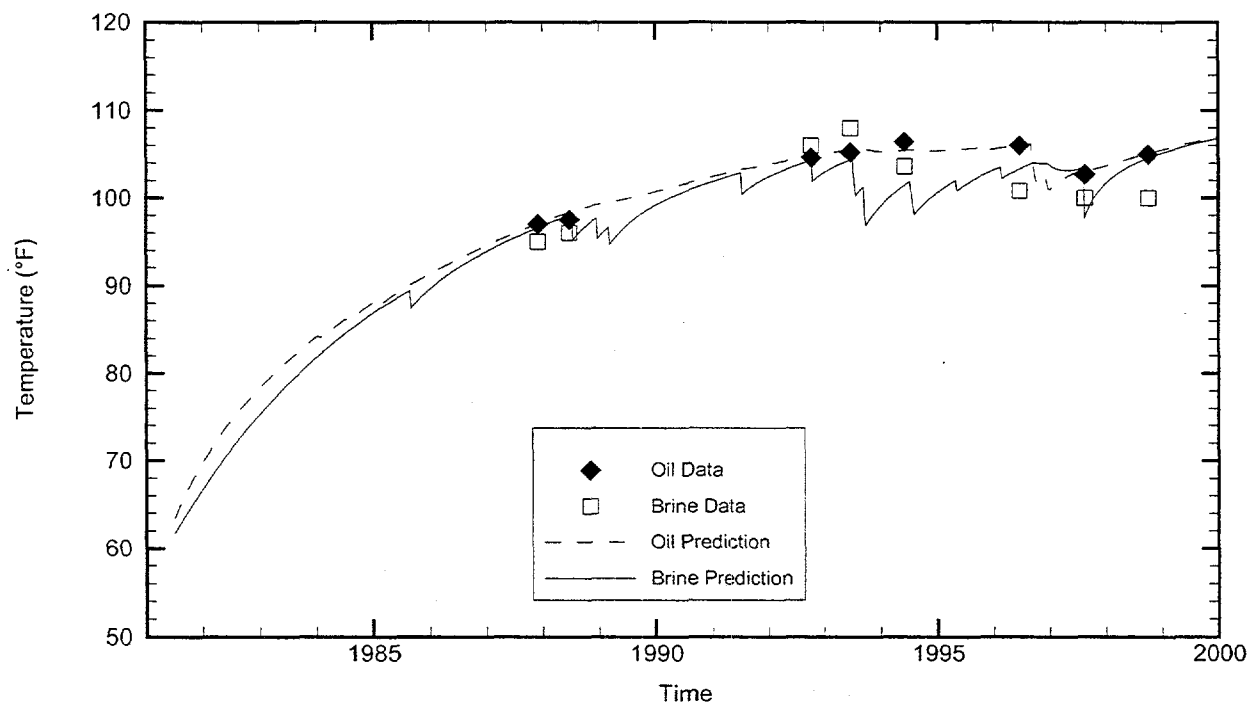
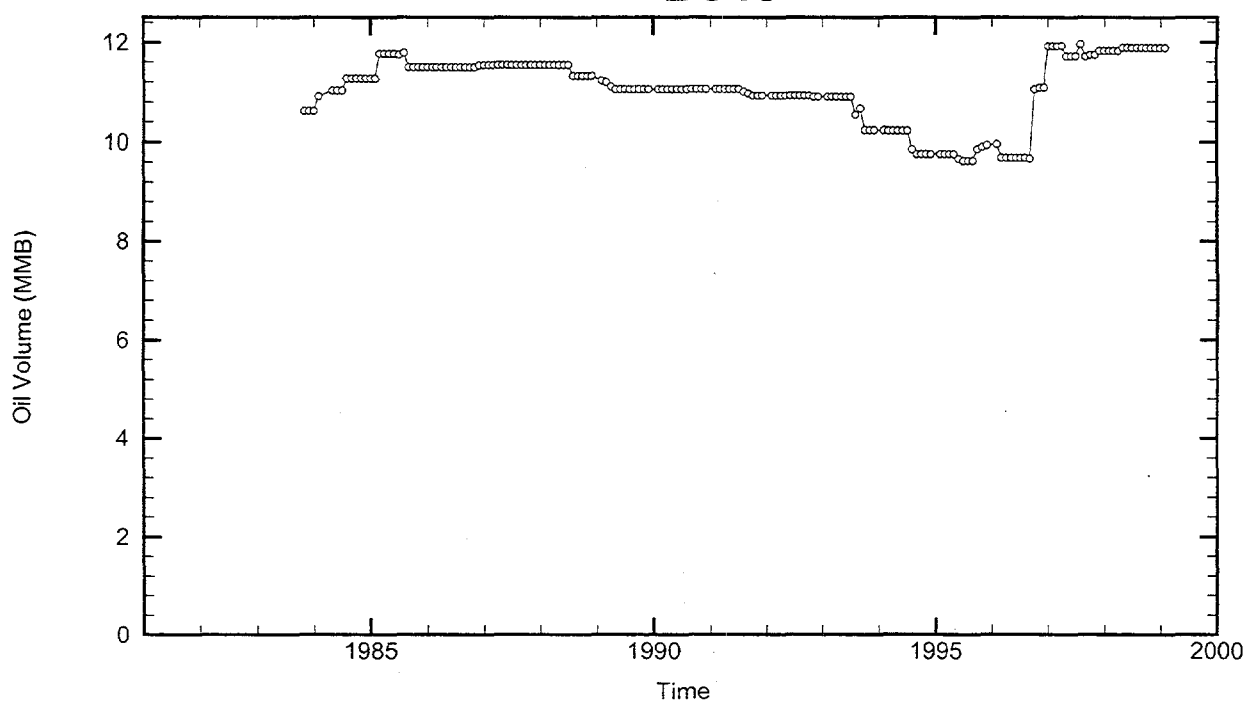
Cavern: BC18
End of Leaching: 07/13/1979
Duration of Leaching: 1.9959 years
Leaching Temperature: 60.00 °F

Degas: 06/21/1996, 112.53 °F, 9.04 MMB
Oil Injection Temperature: 81.43 °F
Brine Injection Temperature: 57.87 °F
Number of iterations: 354

BC18



BC19



Cavern: BC19

End of Leaching: 07/04/1981

Duration of Leaching: 1.9986 years

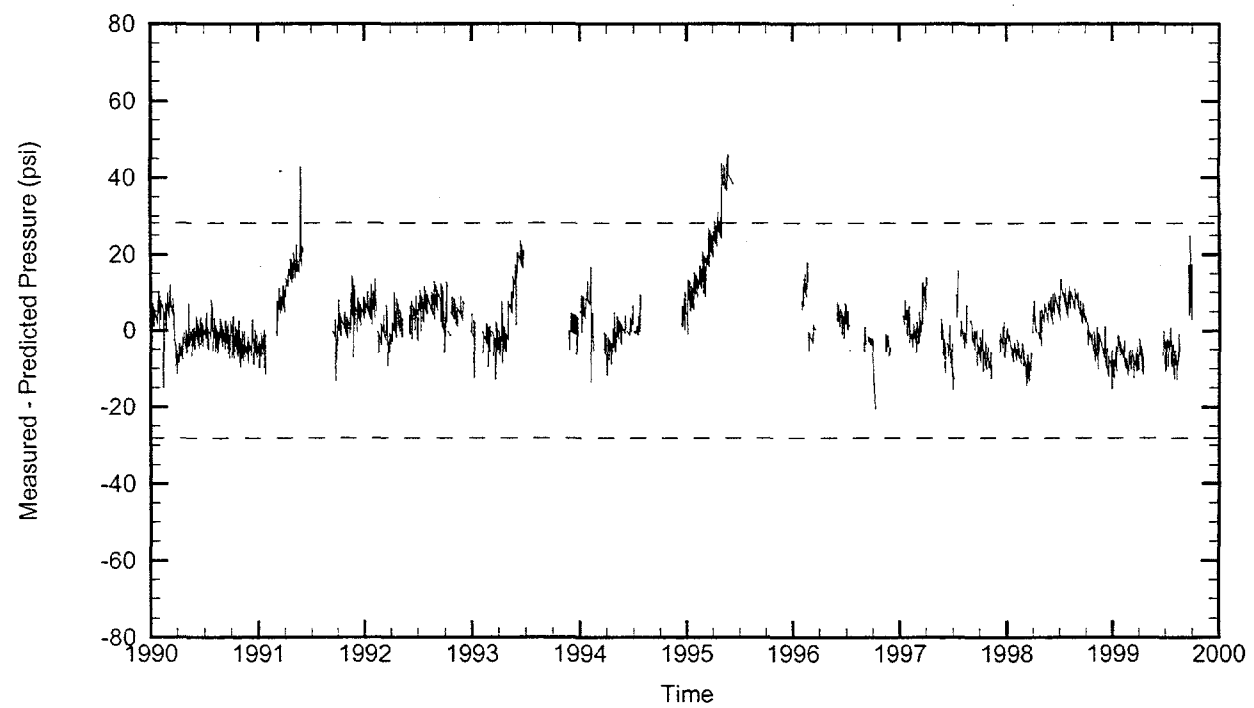
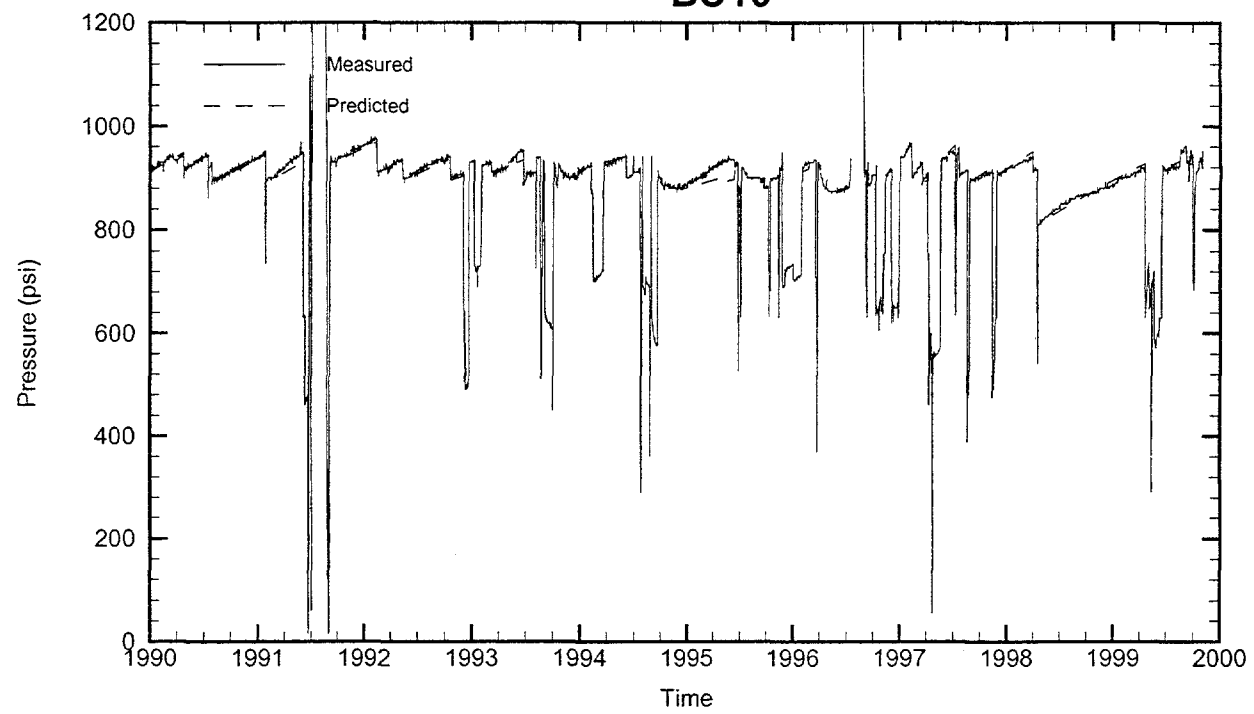
Leaching Temperature: 61.68 °F

Oil Injection Temperature: 63.42 °F

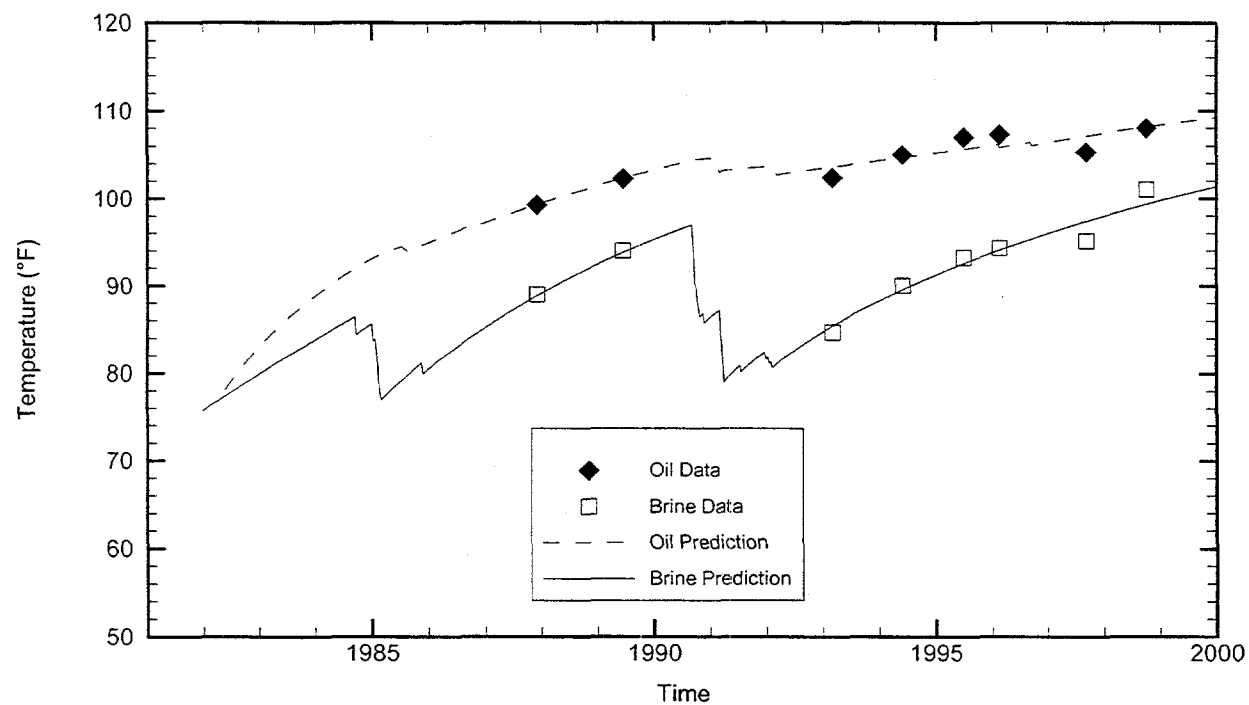
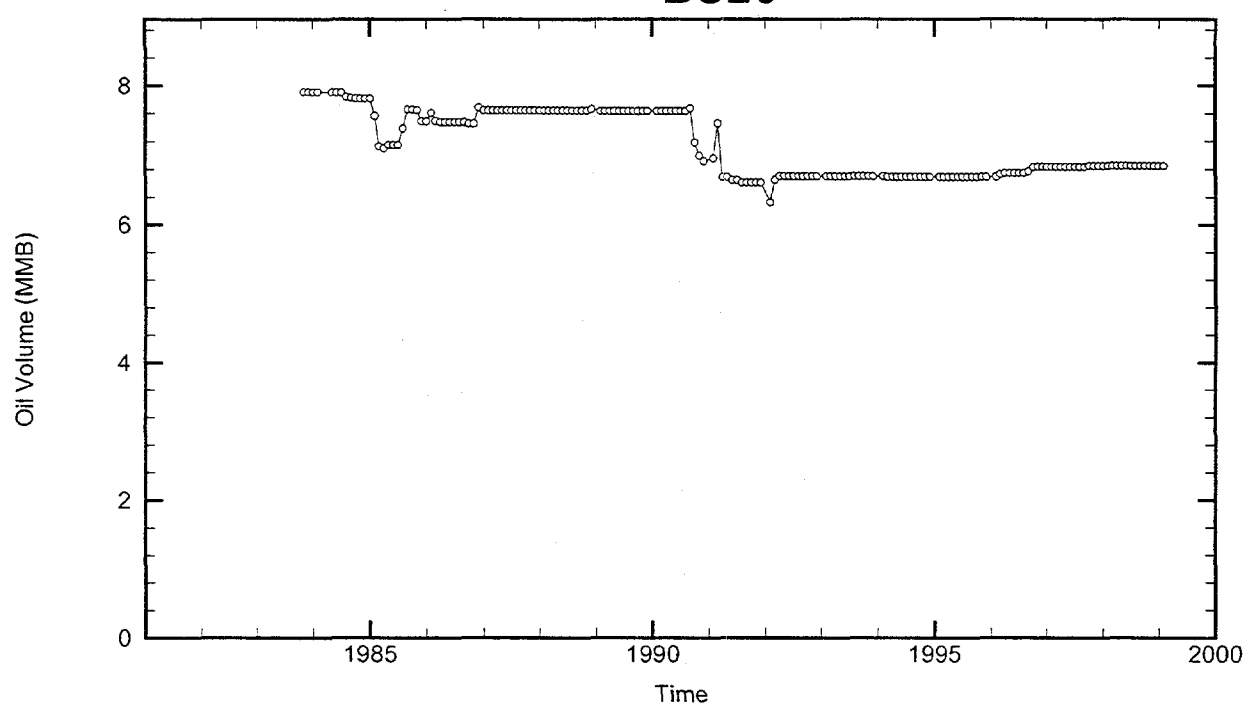
Brine Injection Temperature: 72.97 °F

Number of iterations: 322

BC19



BC20



Cavern: BC20

End of Leaching: 12/28/1981

Duration of Leaching: 1.9959 years

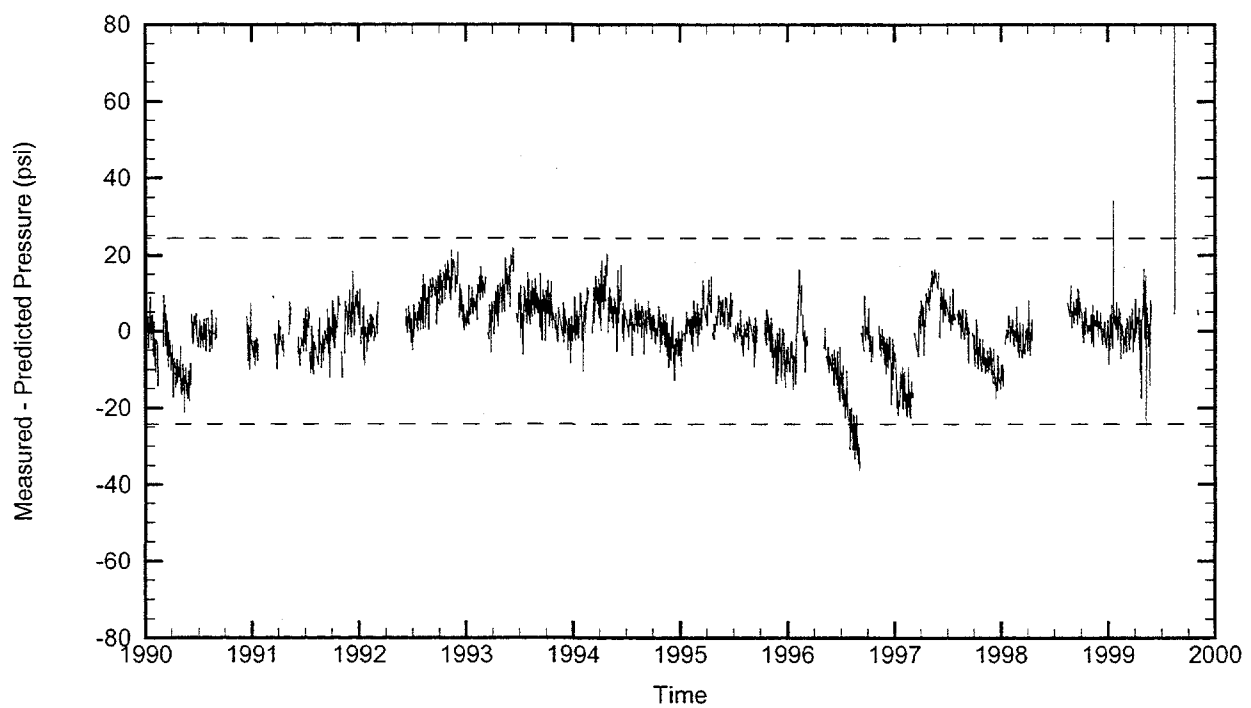
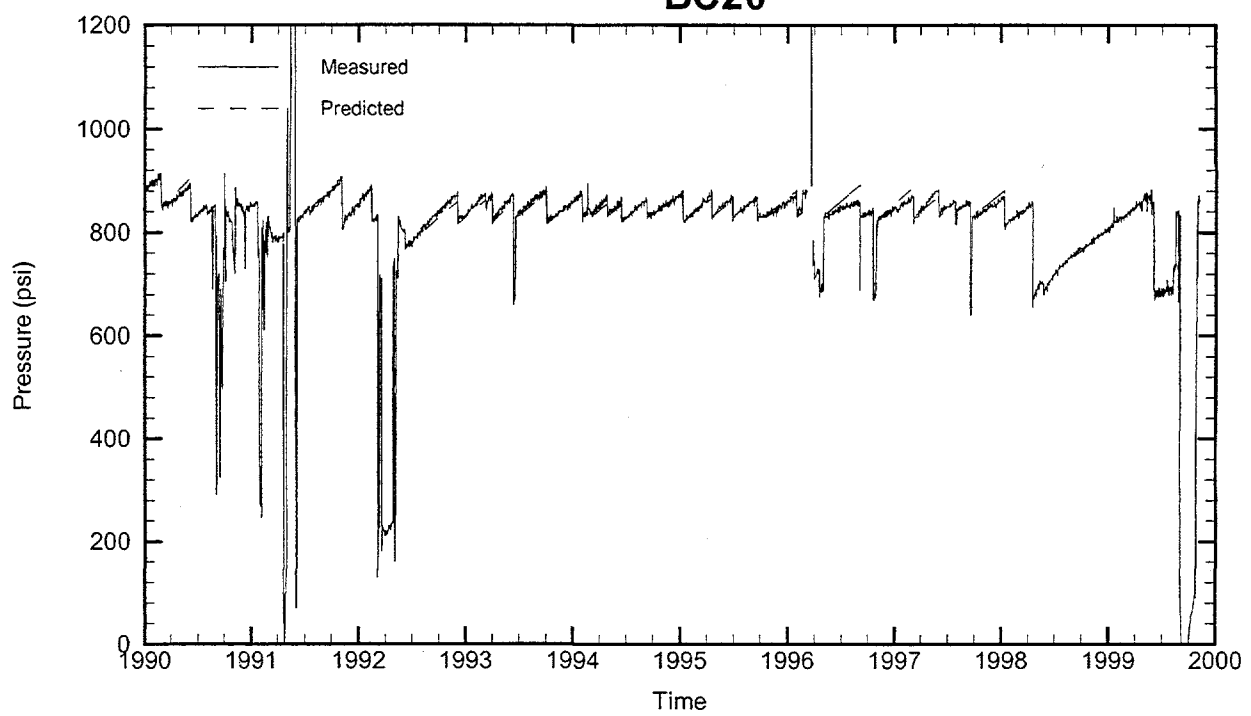
Leaching Temperature: 75.68 °F

Oil Injection Temperature: 76.59 °F

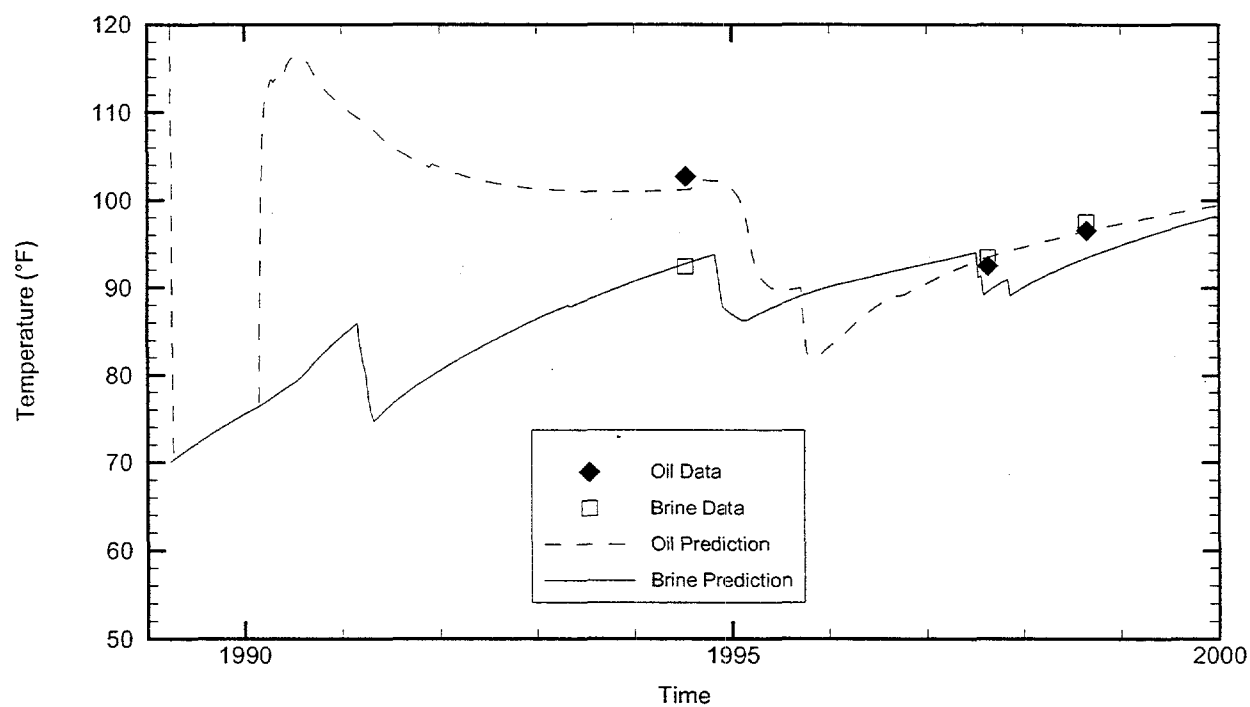
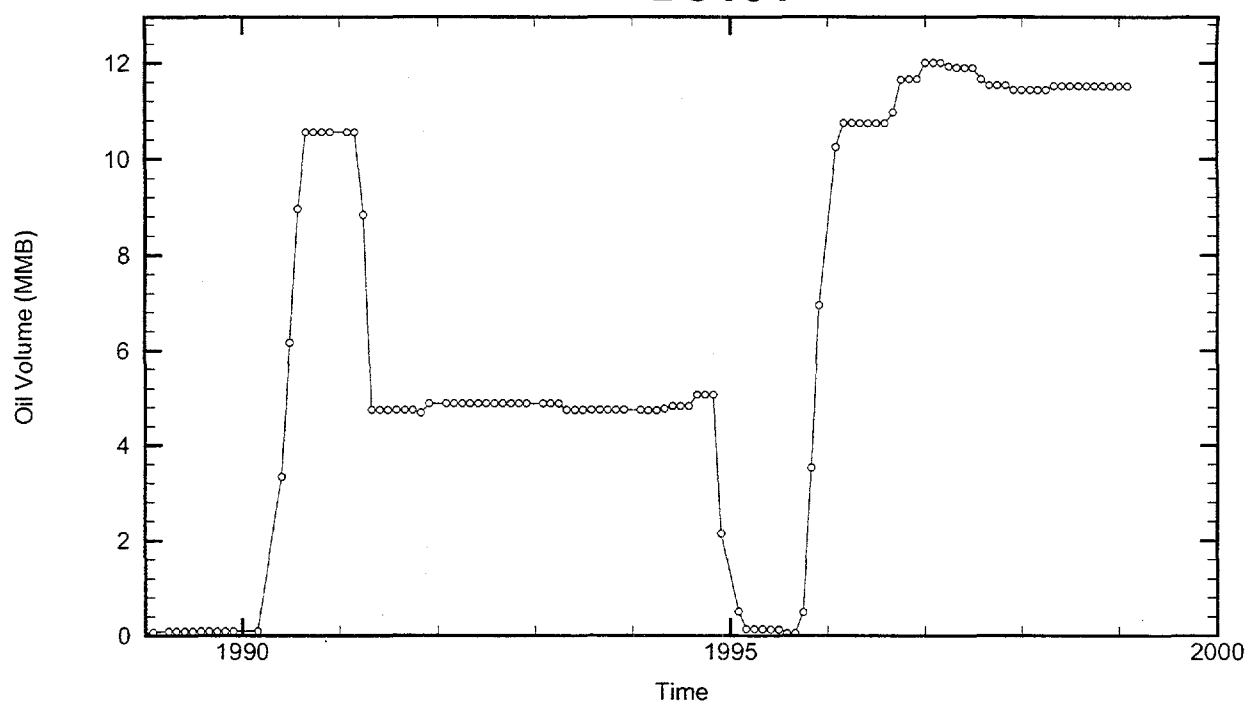
Brine Injection Temperature: 59.61 °F

Number of iterations: 231

BC20



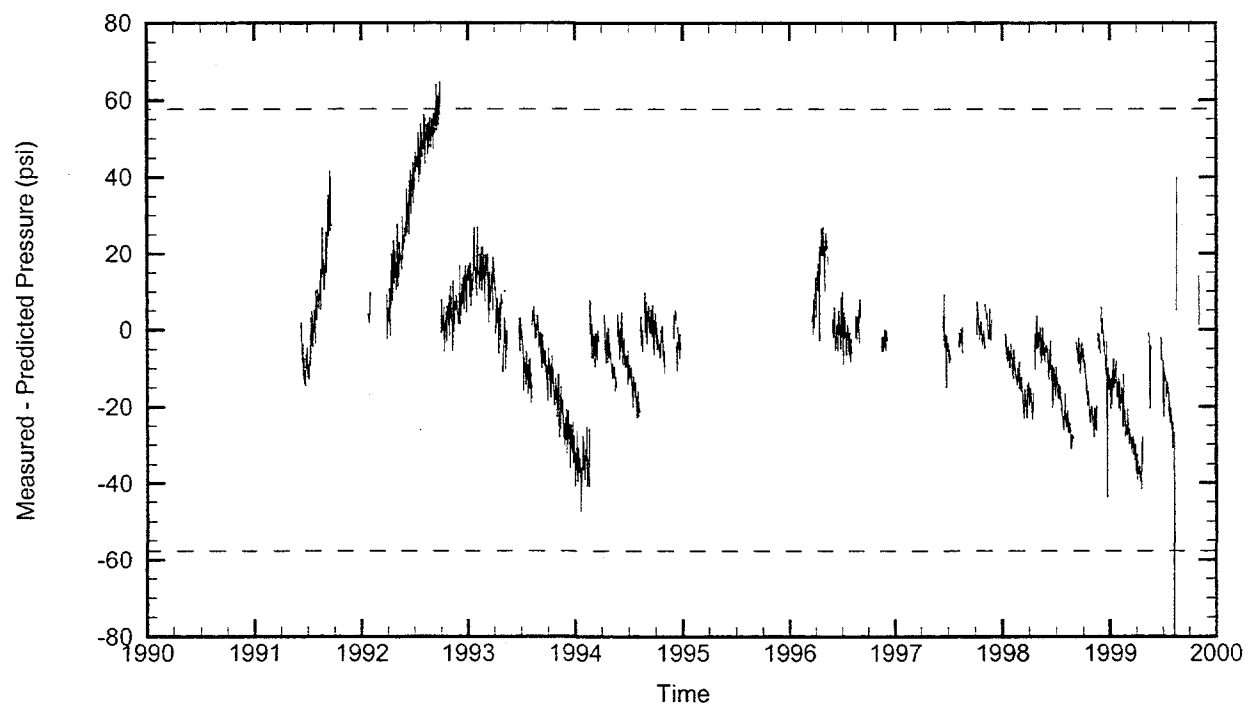
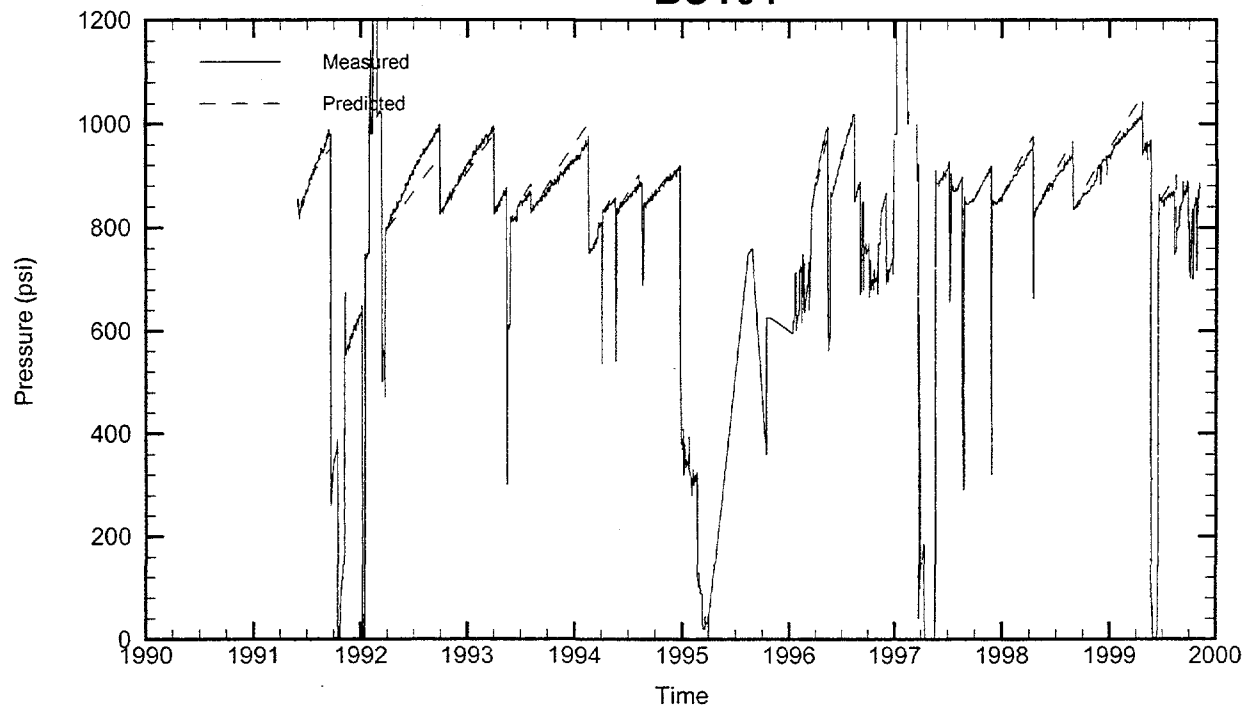
BC101



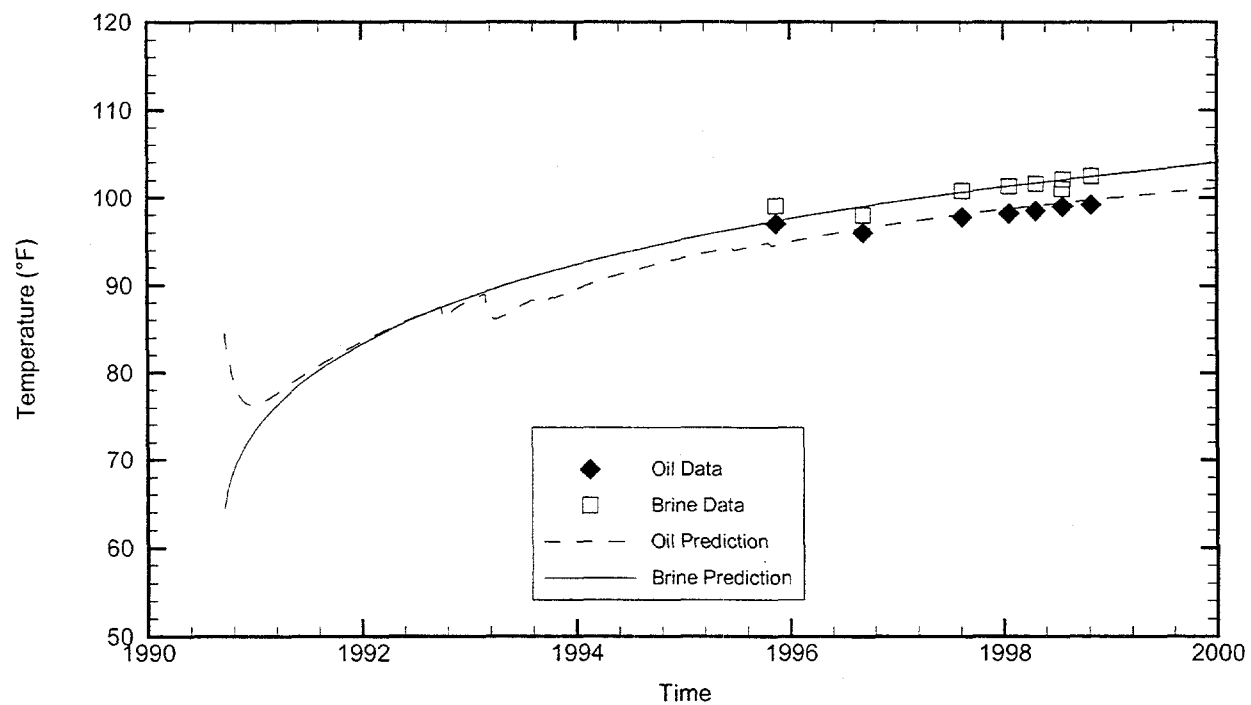
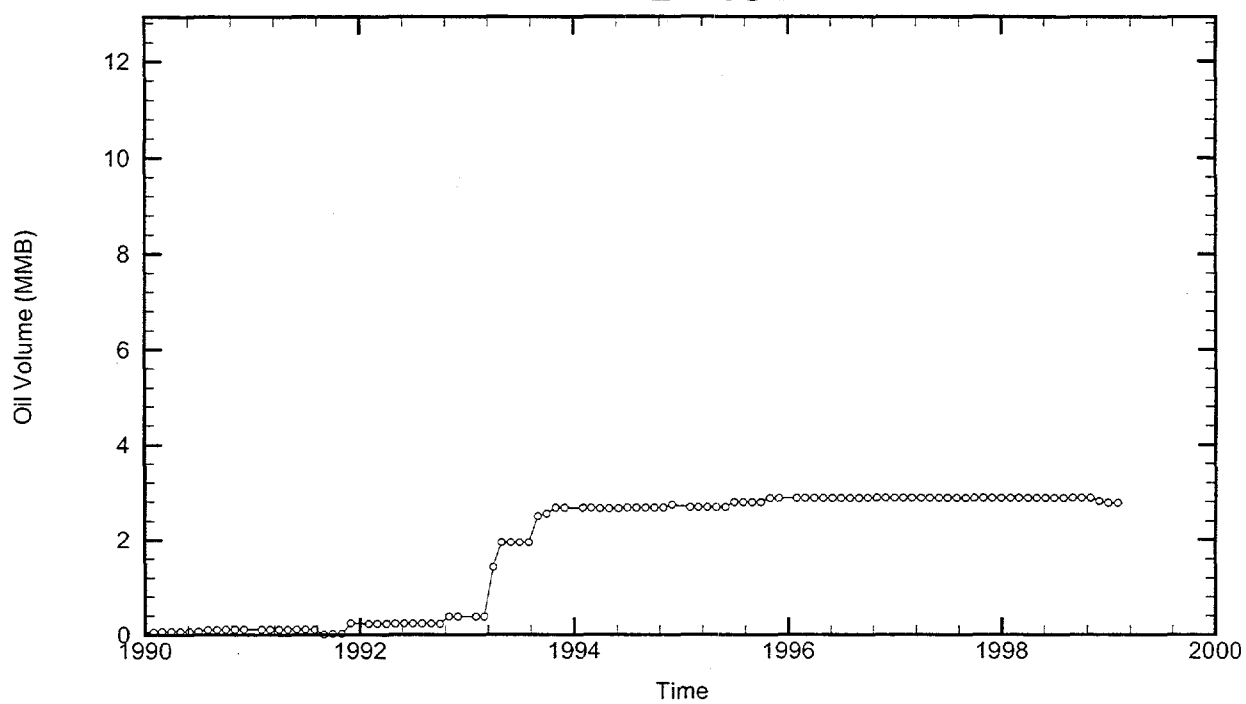
Cavern: BC101
End of Leaching: 03/30/1989
Duration of Leaching: 6.0835 years
Leaching Temperature: 70.00 °F

Degas: 09/17/1995, 80.00 °F, 11.75 MMB
Oil Injection Temperature: 124.41 °F
Brine Injection Temperature: 67.81 °F
Number of iterations: 486

BC101



BH101



Cavern: BH101

End of Leaching: 09/18/1990

Duration of Leaching: 2.0000 days

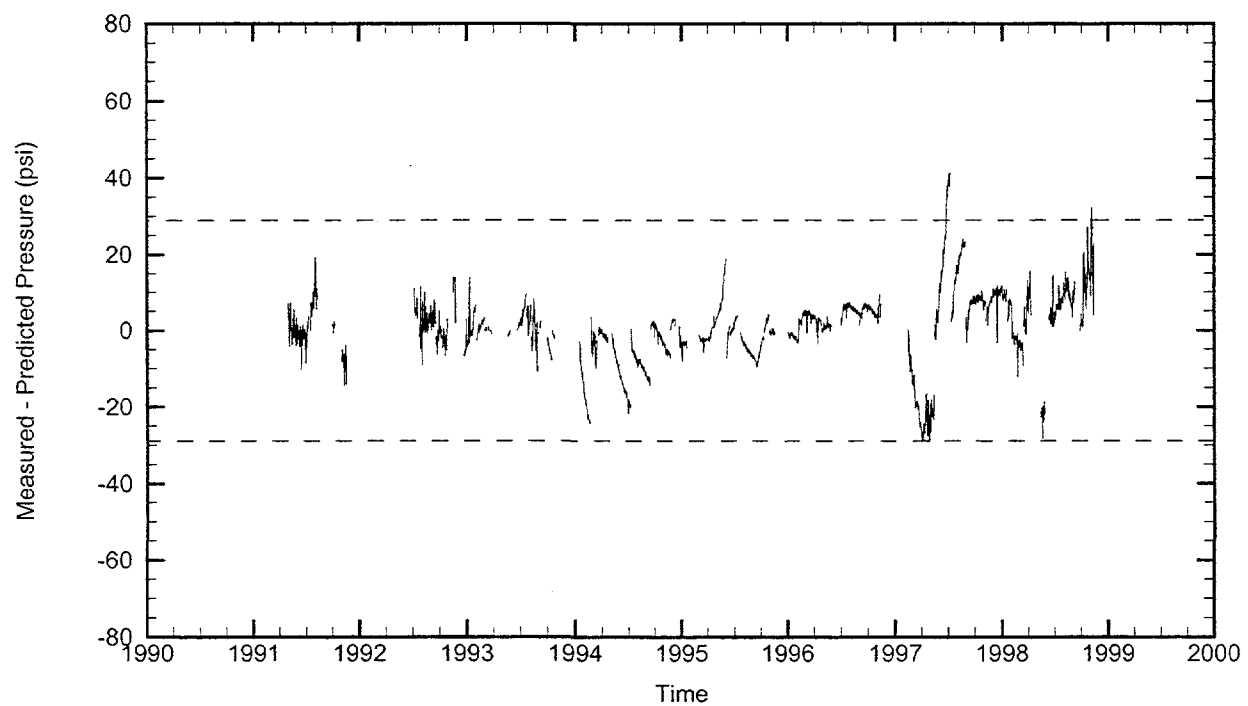
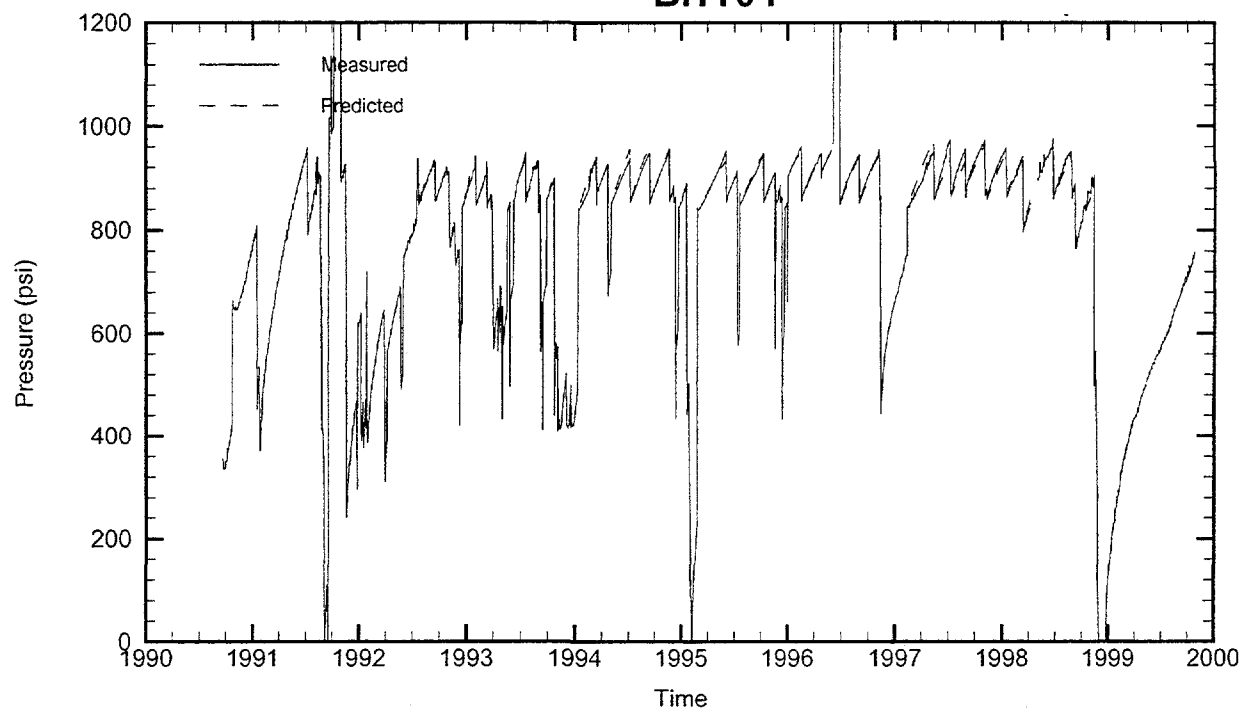
Leaching Temperature: 64.47 °F

Oil Injection Temperature: 84.48 °F

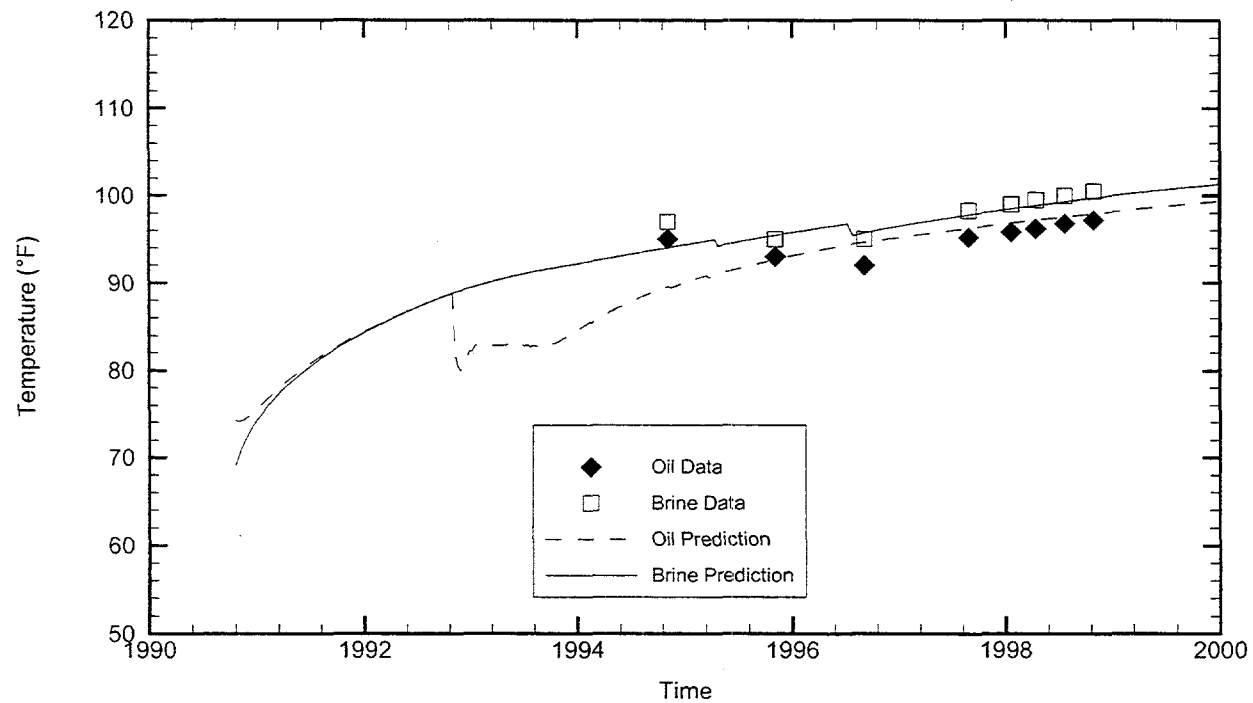
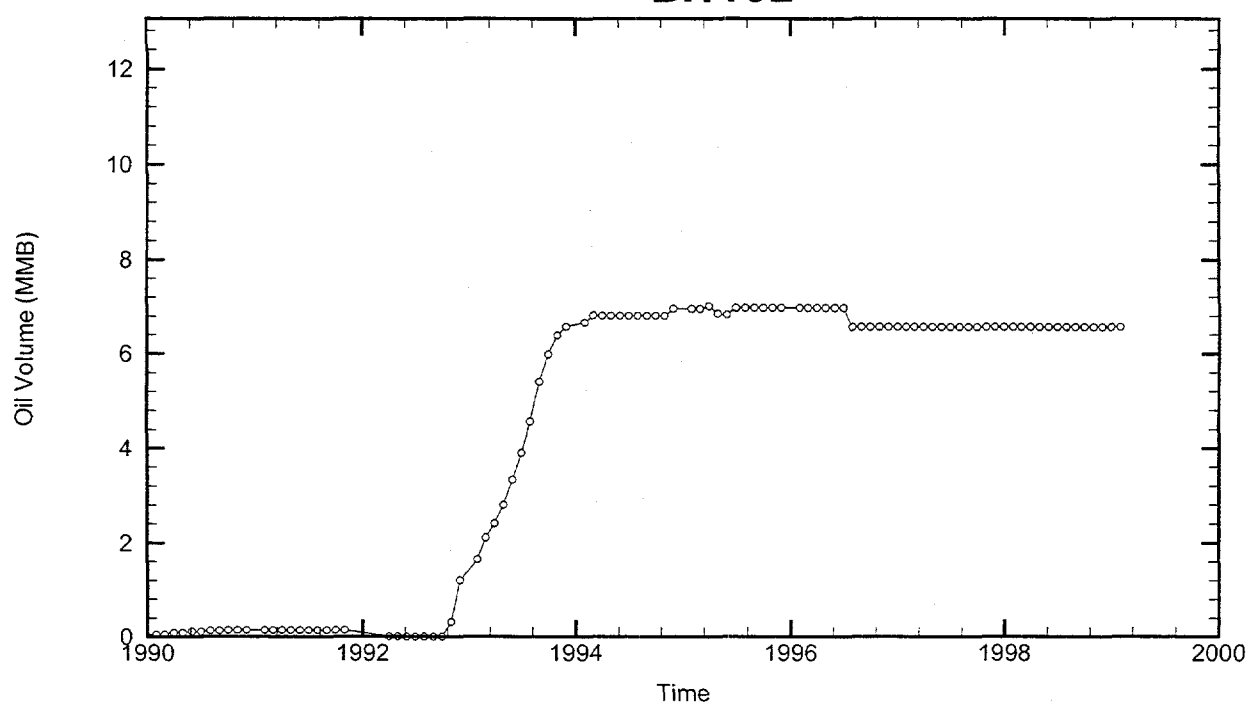
Brine Injection Temperature: 64.47 °F

Number of iterations: 355

BH101



BH102



Cavern: BH102

End of Leaching: 10/20/1990

Duration of Leaching: 1.2500 years

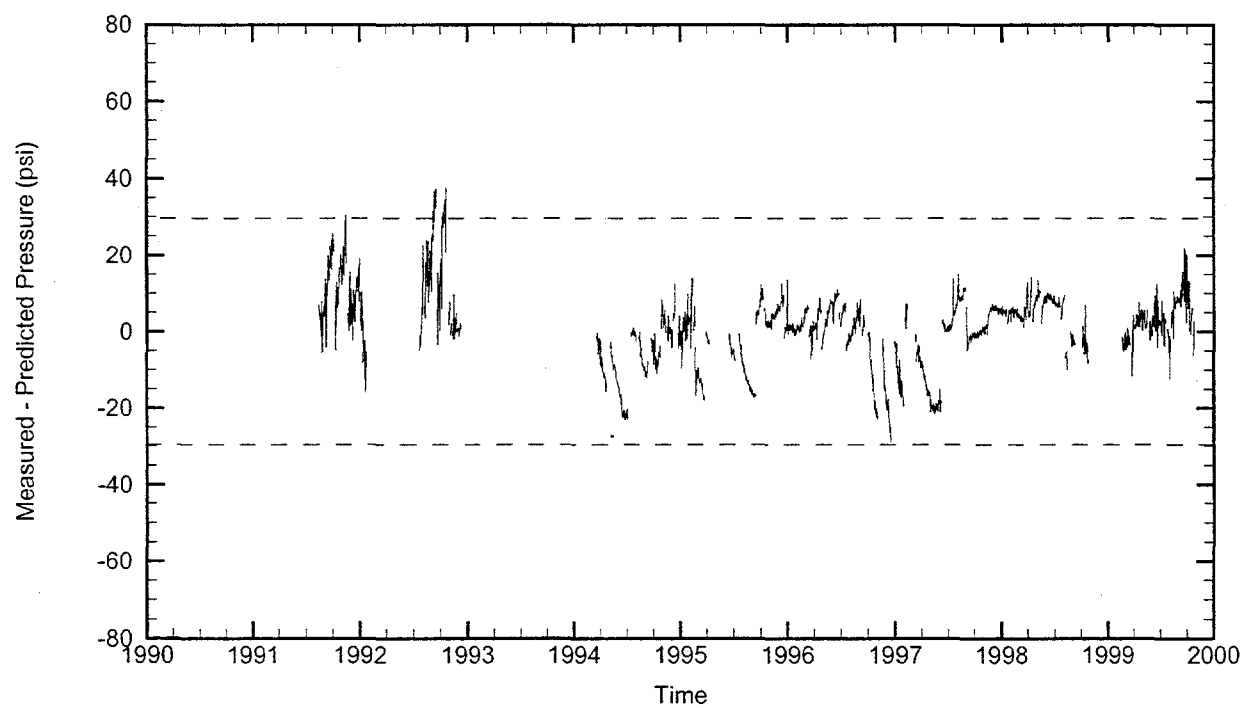
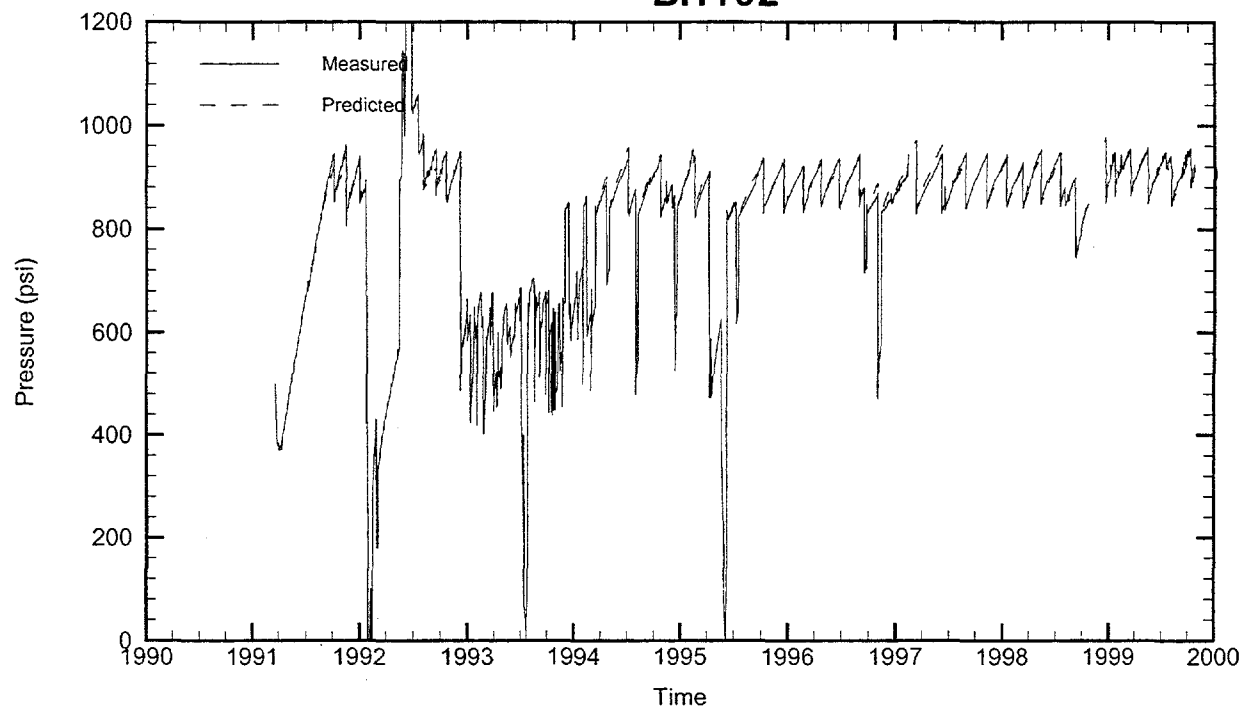
Leaching Temperature: 69.07 °F

Oil Injection Temperature: 74.21 °F

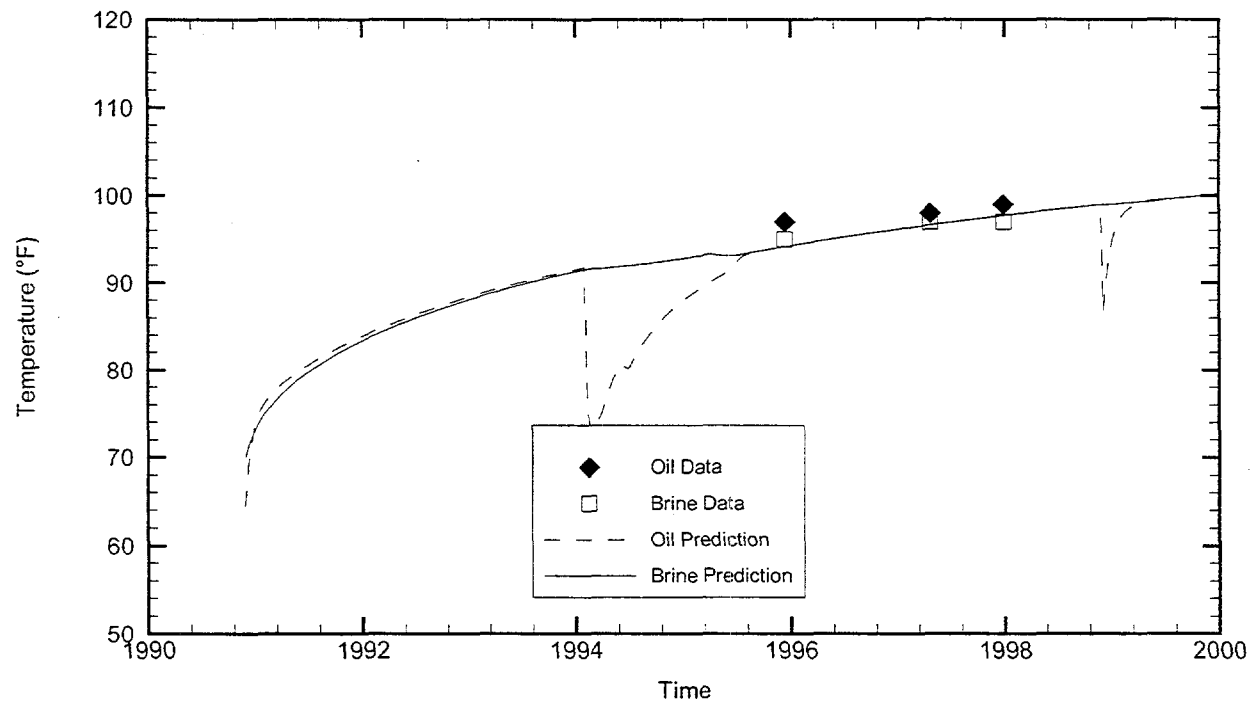
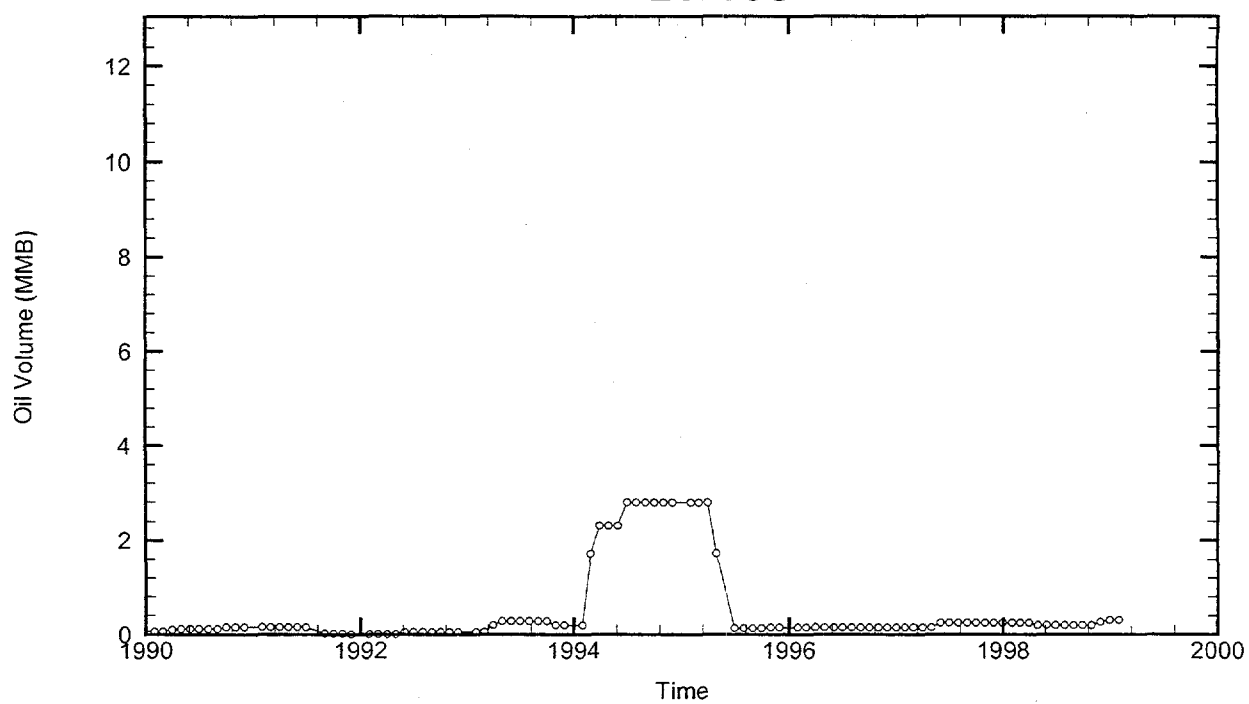
Brine Injection Temperature: 58.75 °F

Number of iterations: 177

BH102



BH103



Cavern: BH103

End of Leaching: 11/28/1990

Duration of Leaching: 5.0000 days

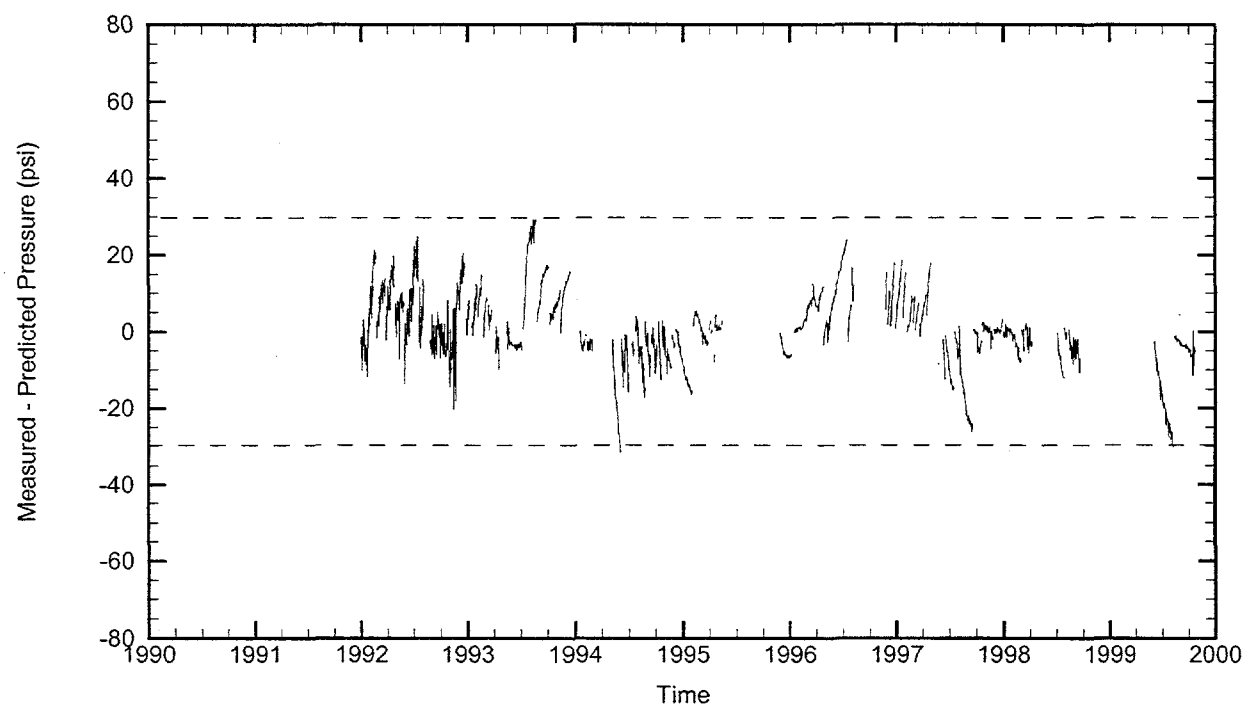
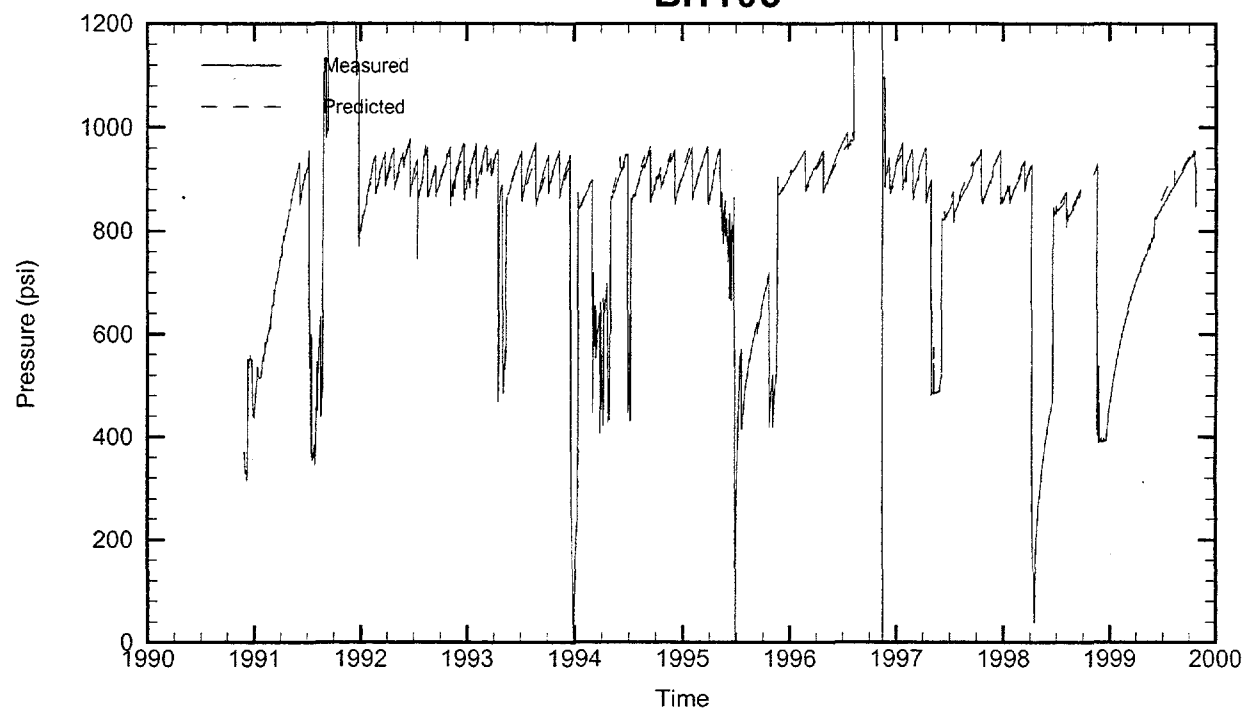
Leaching Temperature: 70.00 °F

Oil Injection Temperature: 64.51 °F

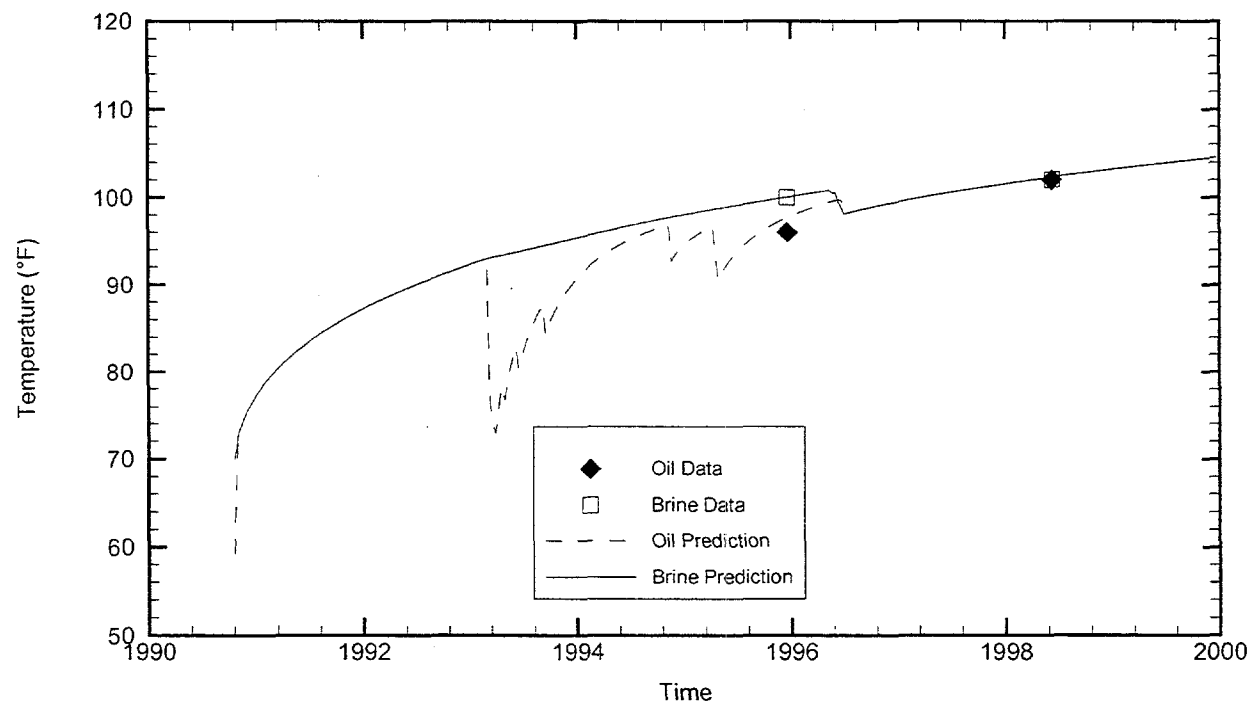
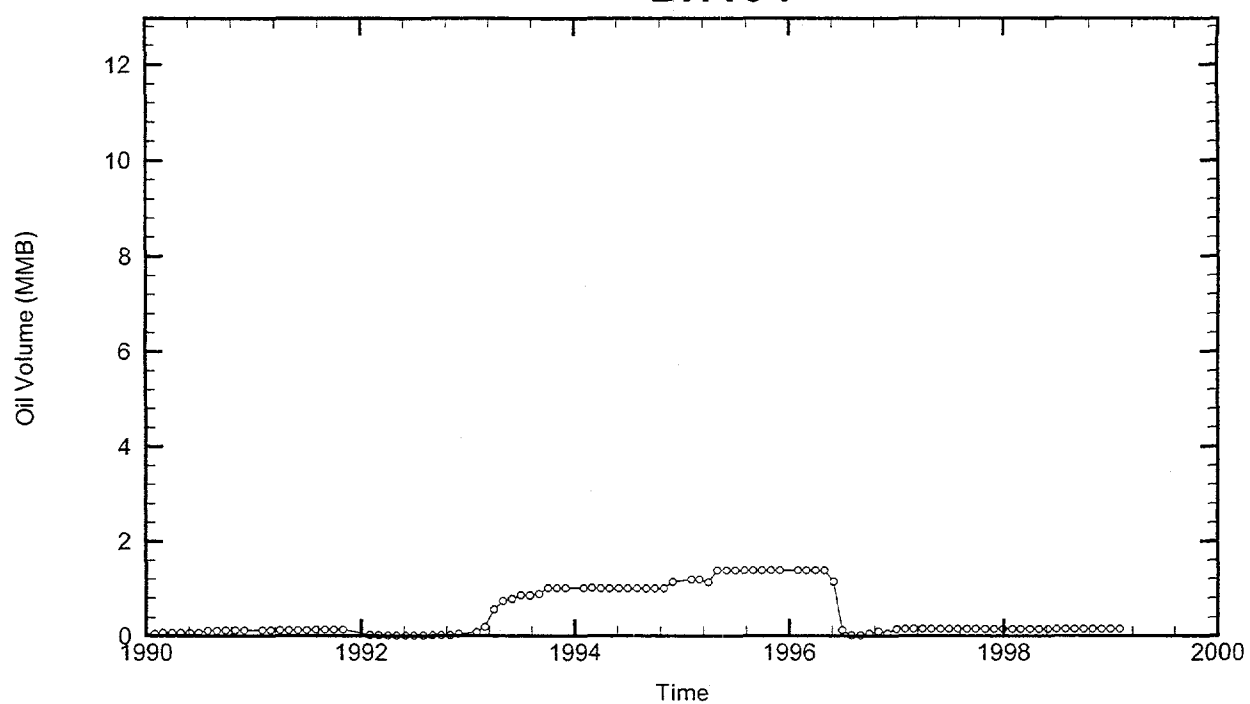
Brine Injection Temperature: 90.00 °F

Number of iterations: 303

BH103



BH104



Cavern: BH104

End of Leaching: 10/21/1990

Duration of Leaching: 0.0000 days

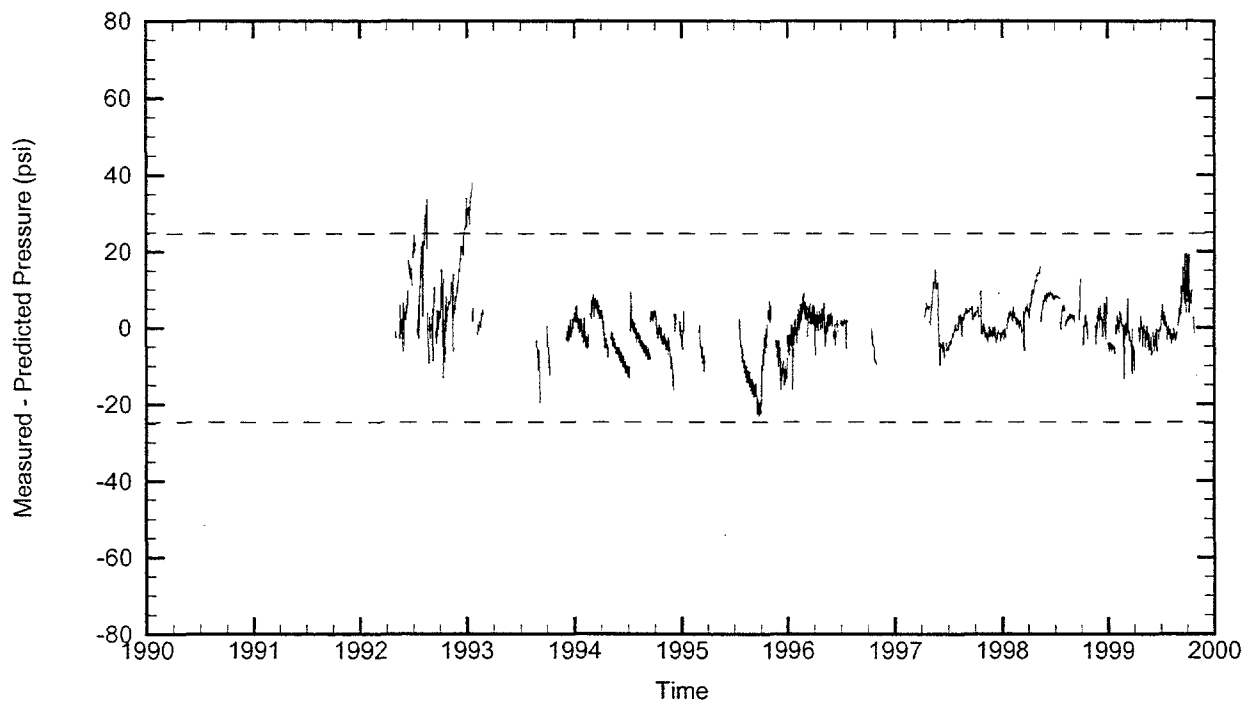
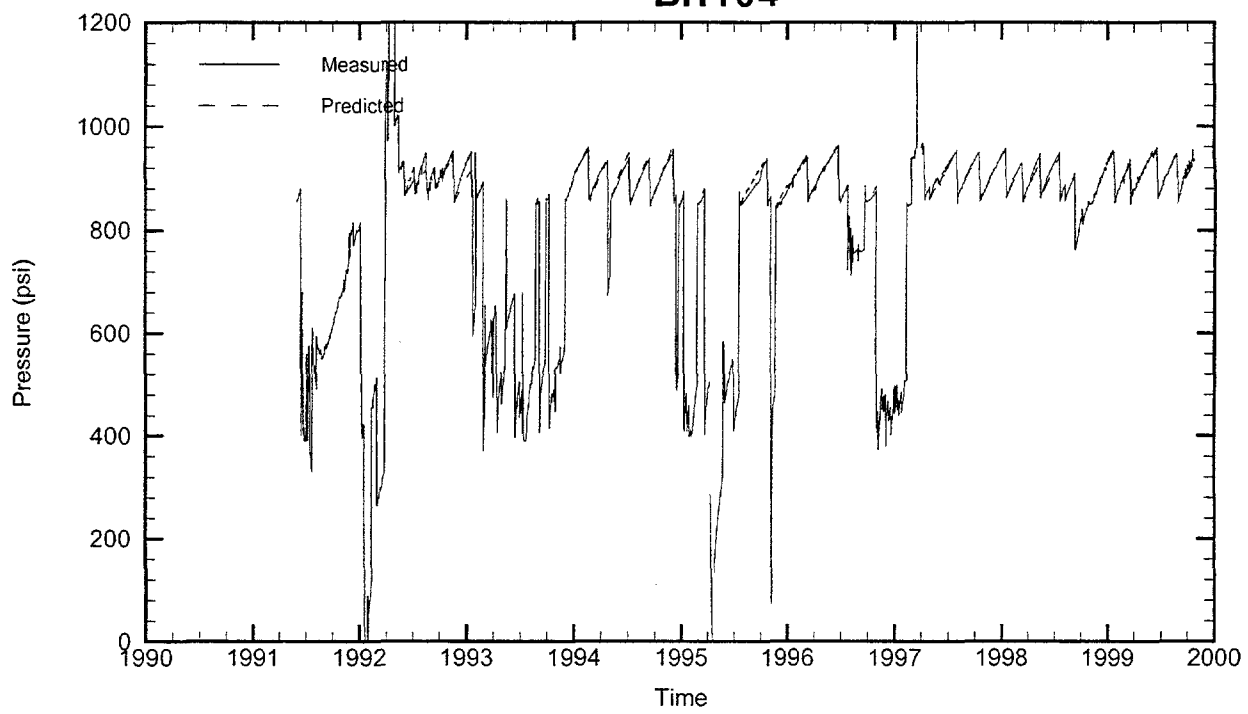
Leaching Temperature: 70.00 °F

Oil Injection Temperature: 59.20 °F

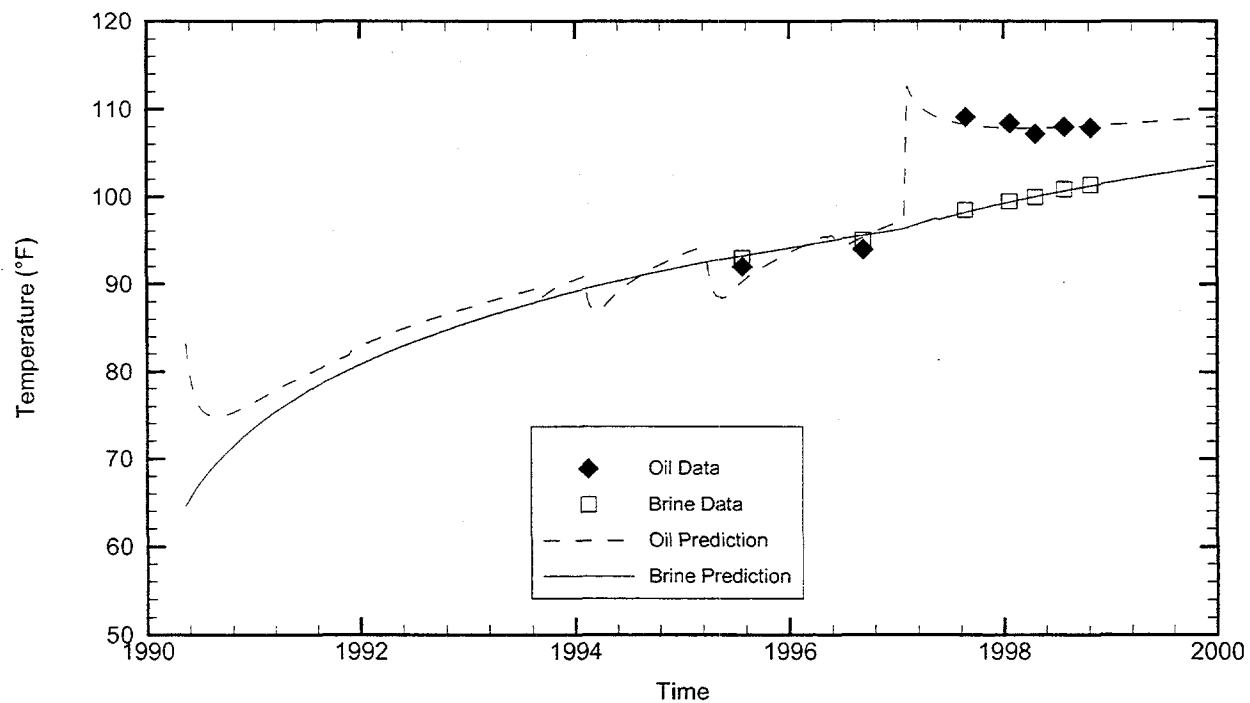
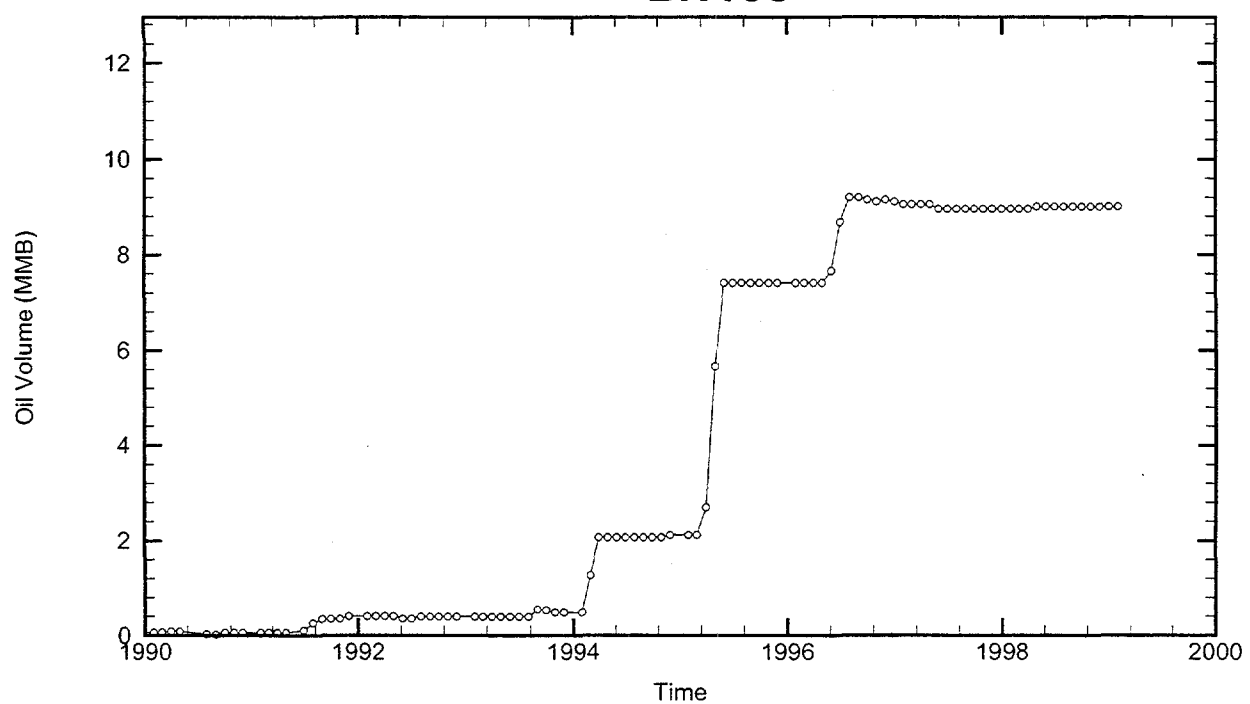
Brine Injection Temperature: 68.00 °F

Number of iterations: 245

BH104



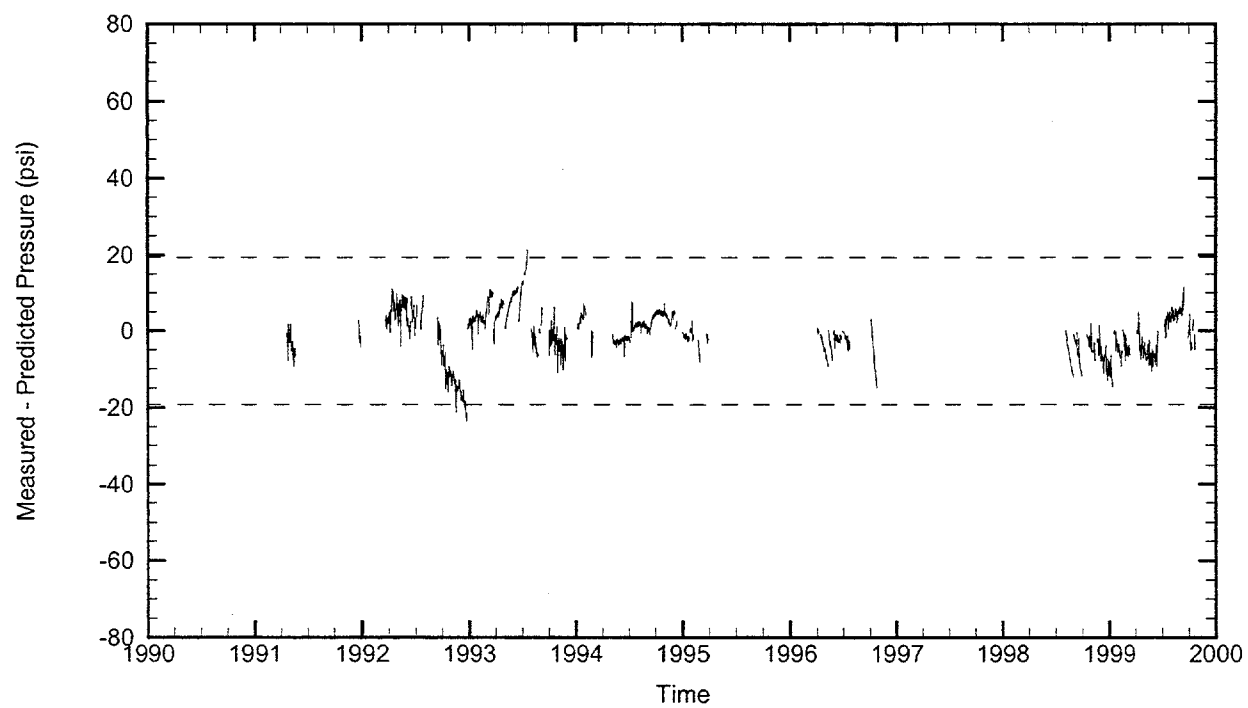
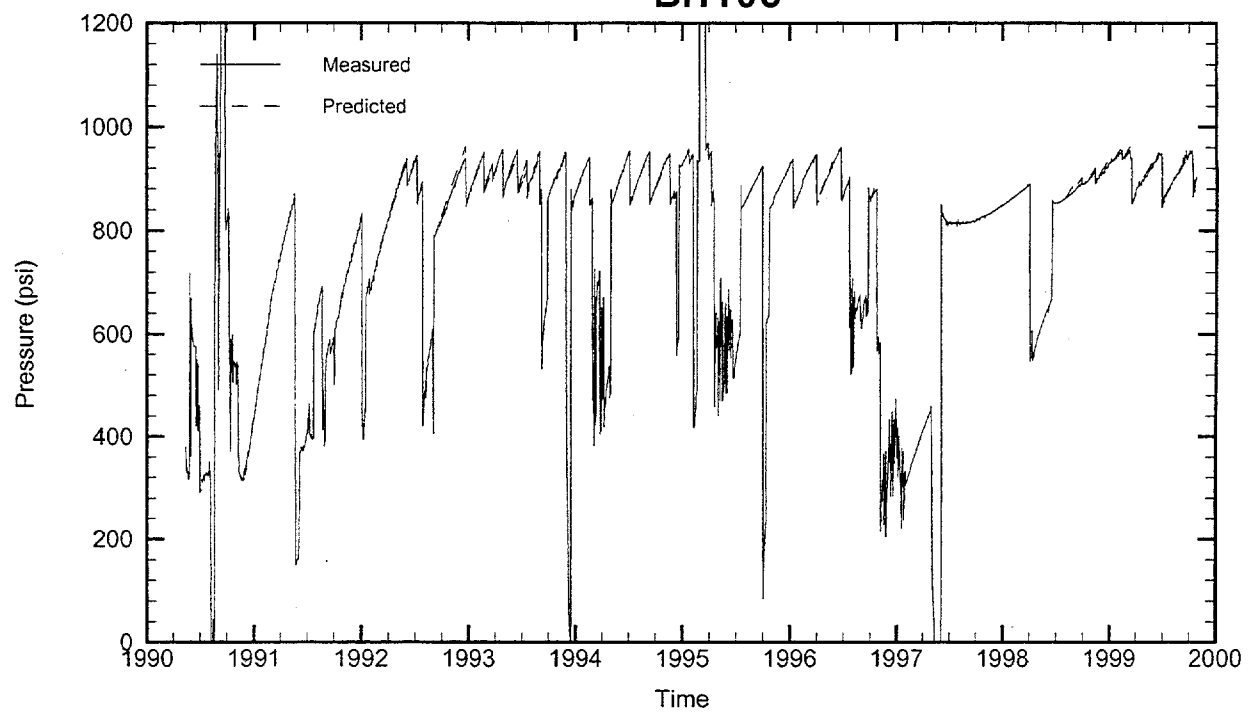
BH105

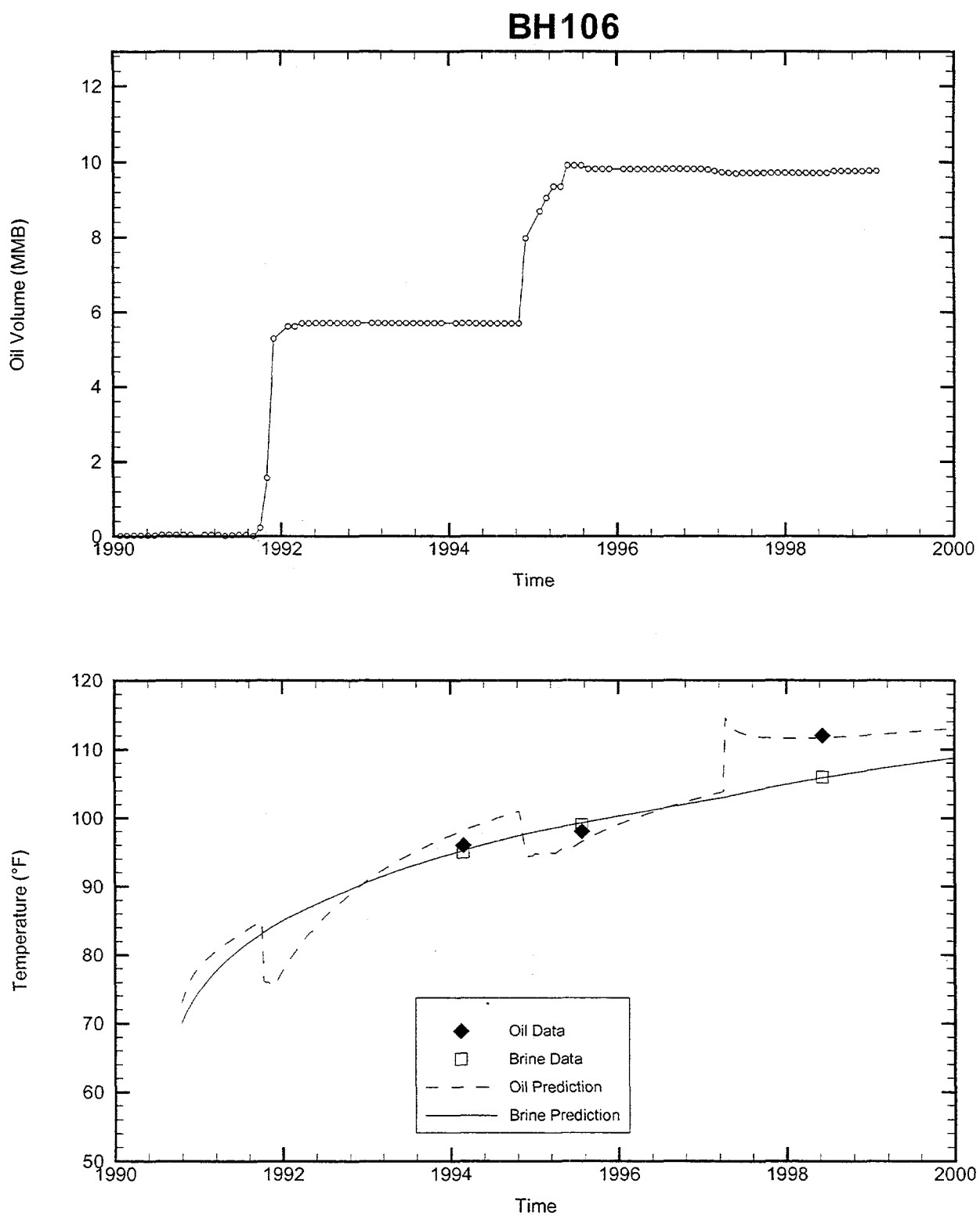


Cavern: BH105
End of Leaching: 05/14/1990
Duration of Leaching: 2.6283 months
Leaching Temperature: 64.59 °F

Degas: 01/31/1997, 114.11 °F, 8.98 MMB
Oil Injection Temperature: 83.21 °F
Brine Injection Temperature: 90.00 °F
Number of iterations: 763

BH105

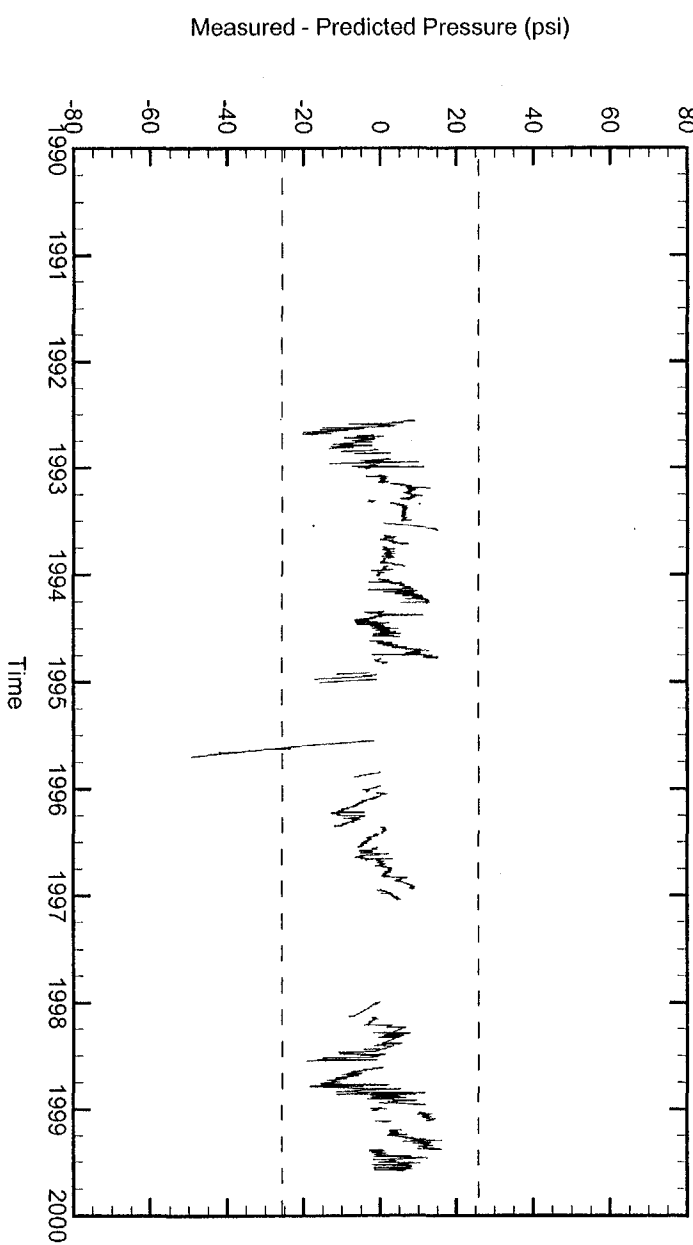
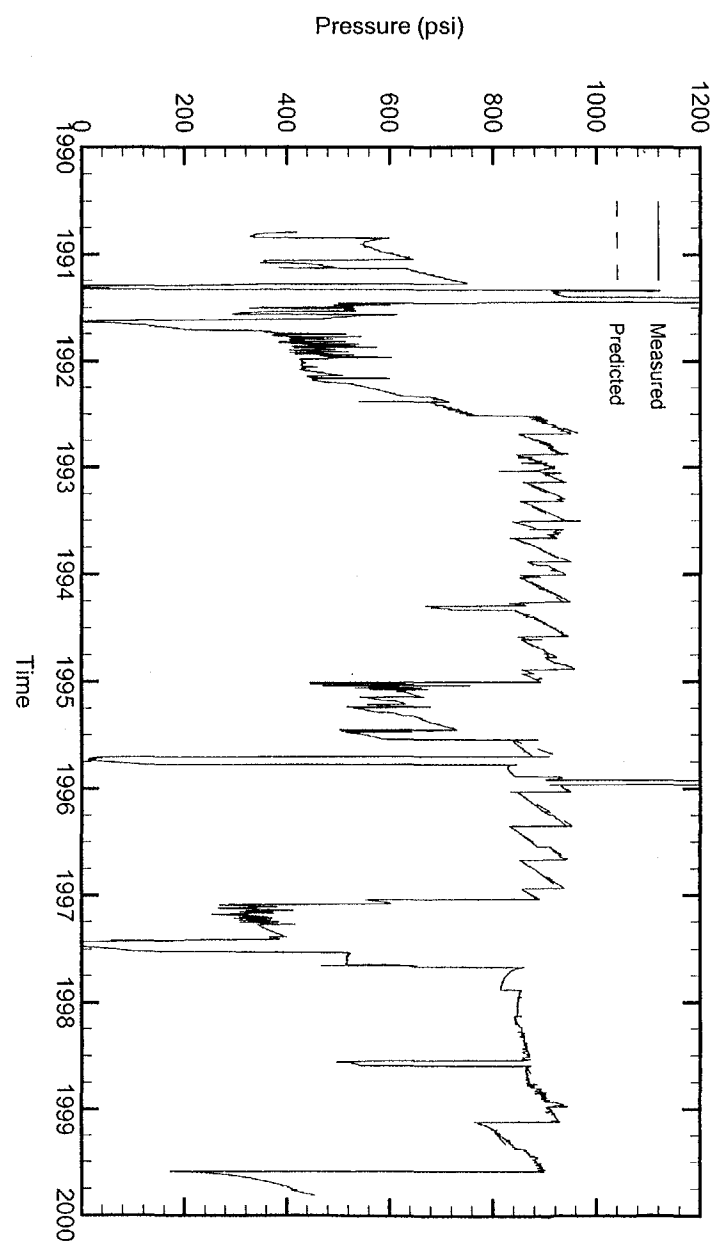




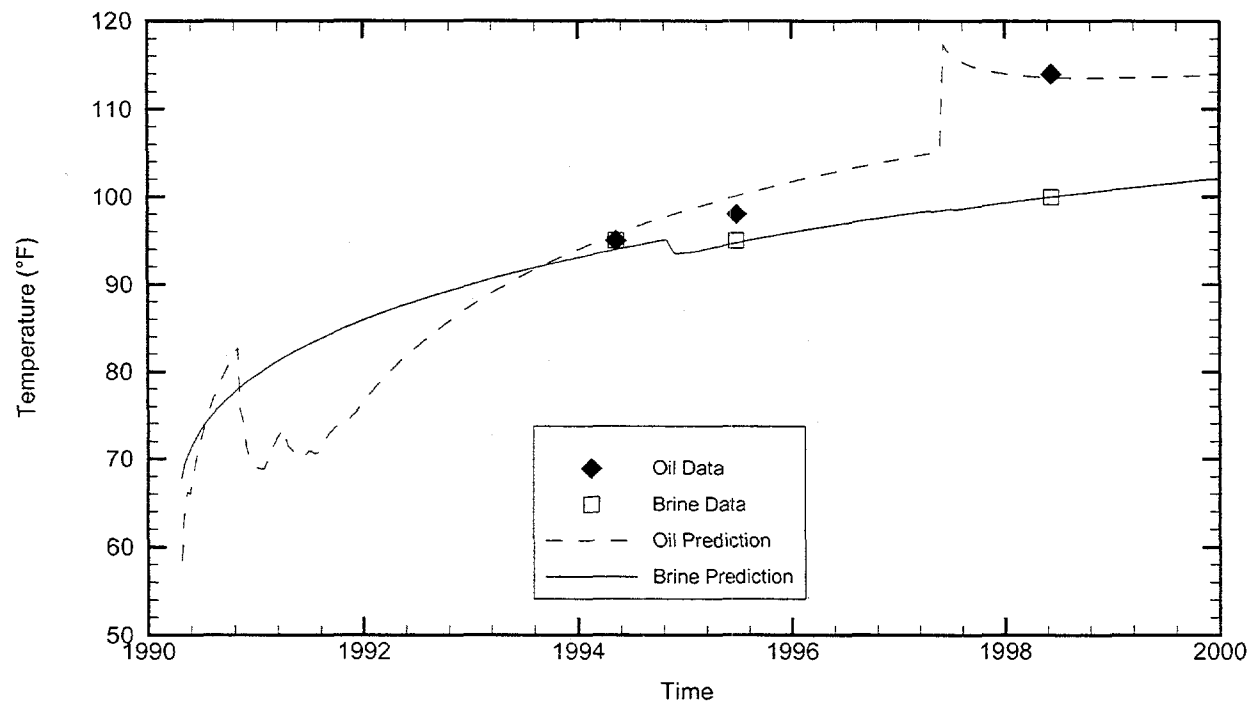
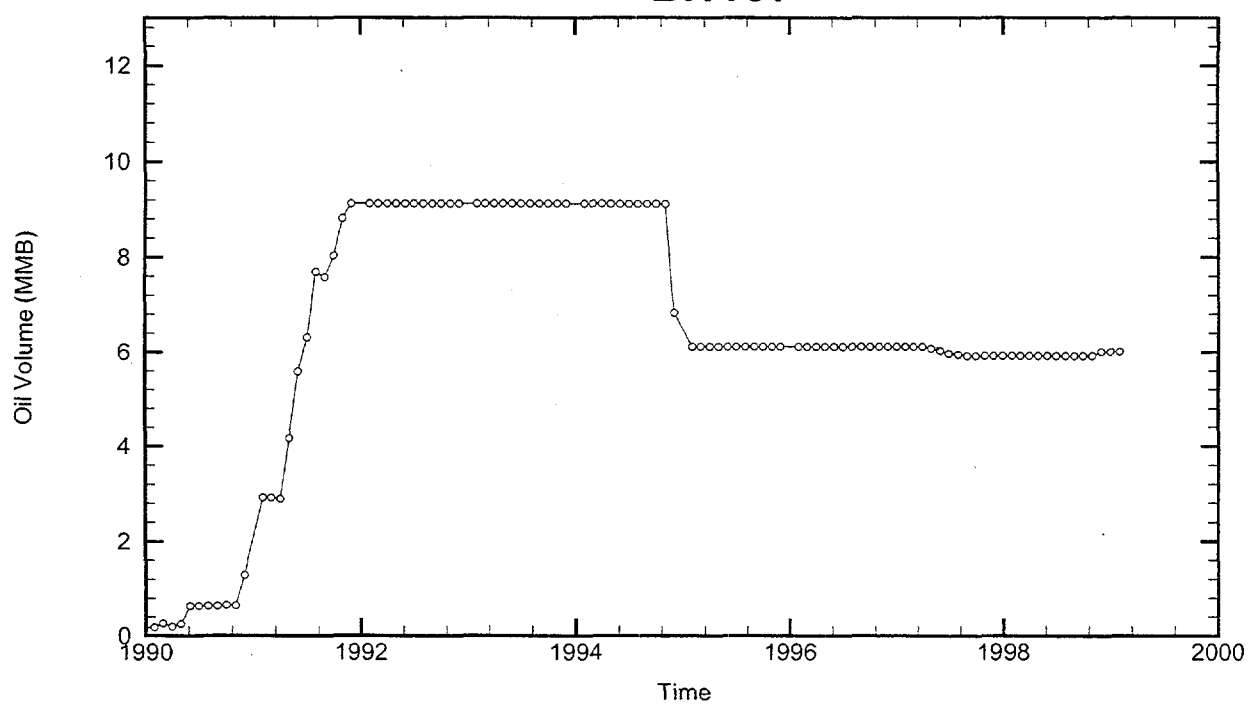
Cavern: BH106
 End of Leaching: 10/16/1990
 Duration of Leaching: 1.3142 months
 Leaching Temperature: 69.97 °F

Degas: 04/11/1997, 115.00 °F, 9.61 MMB
 Oil Injection Temperature: 72.90 °F
 Brine Injection Temperature: 69.97 °F
 Number of iterations: 727

BH106



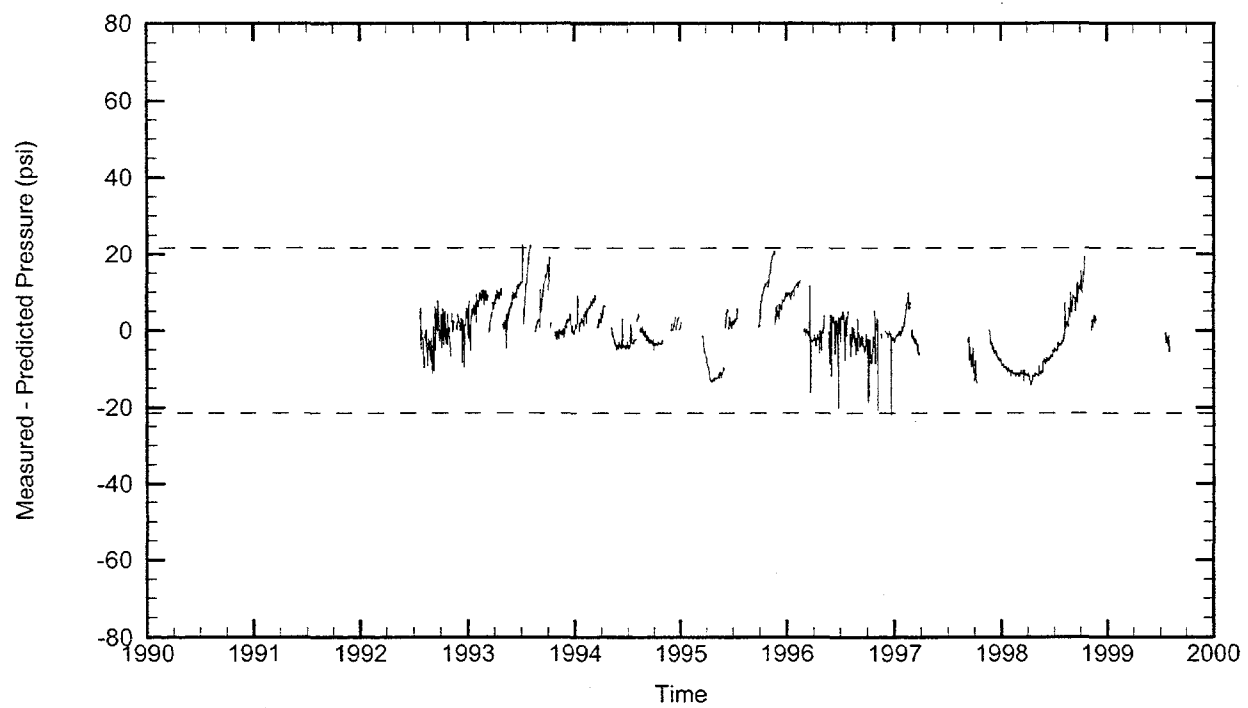
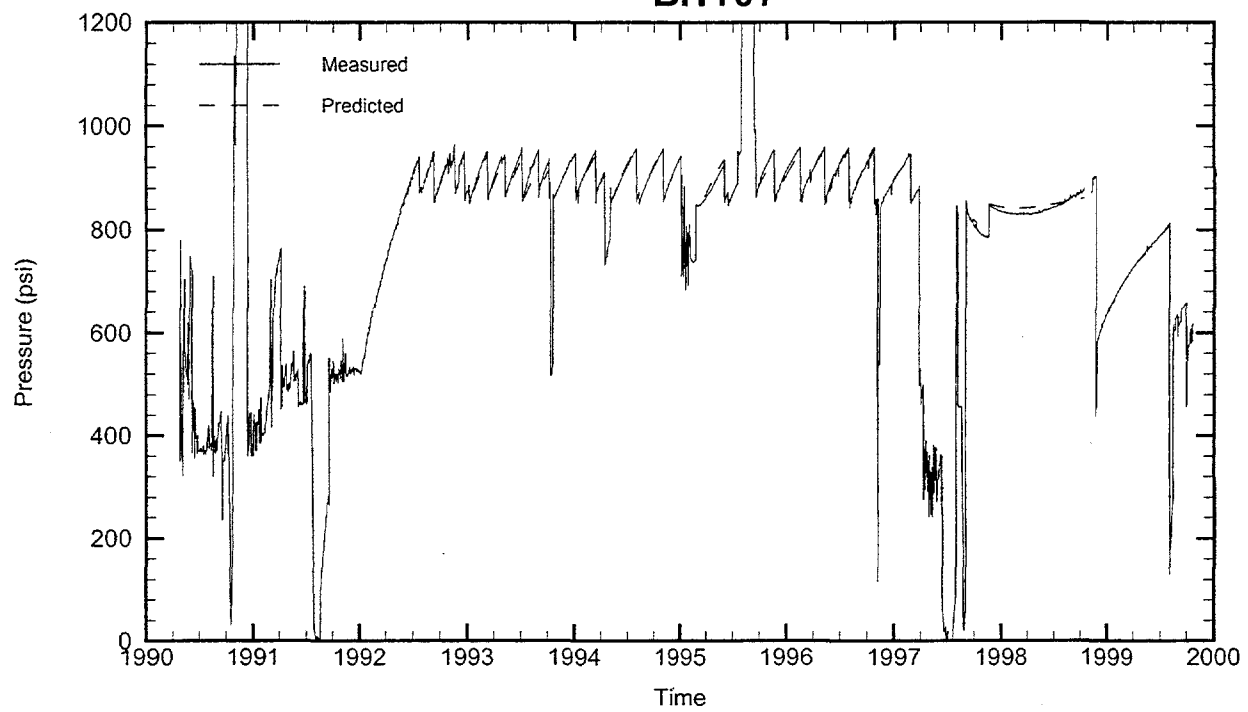
BH107



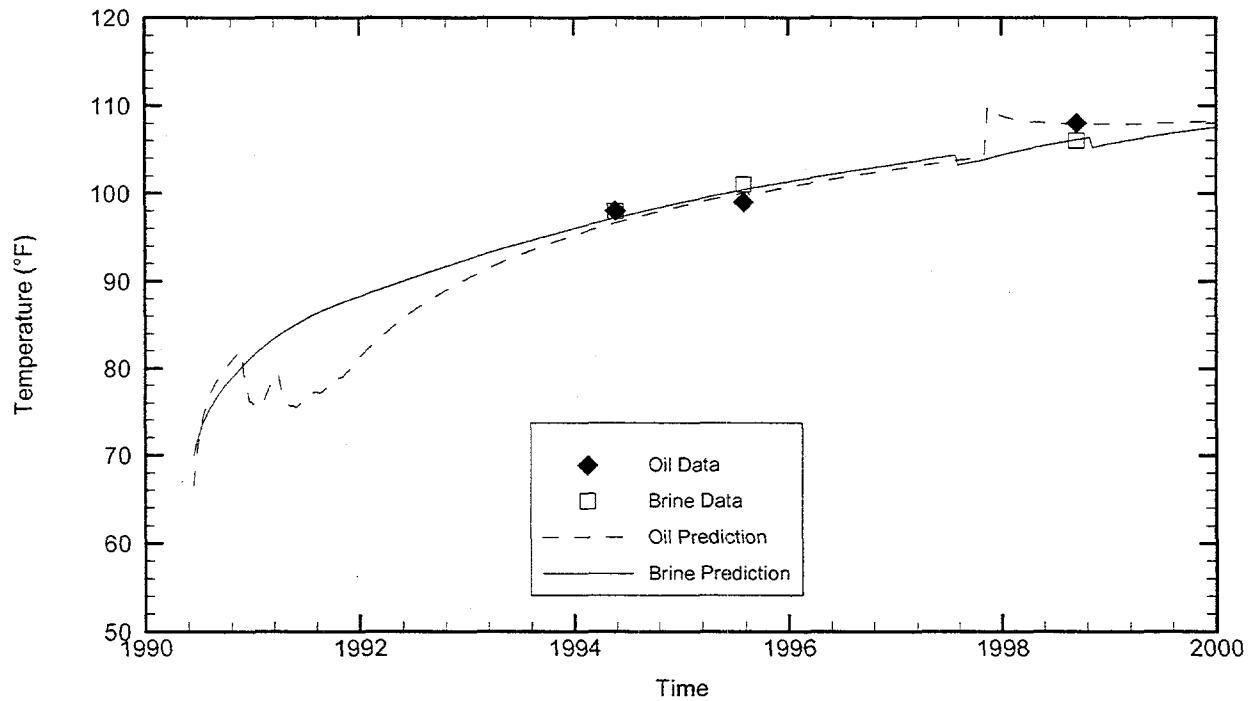
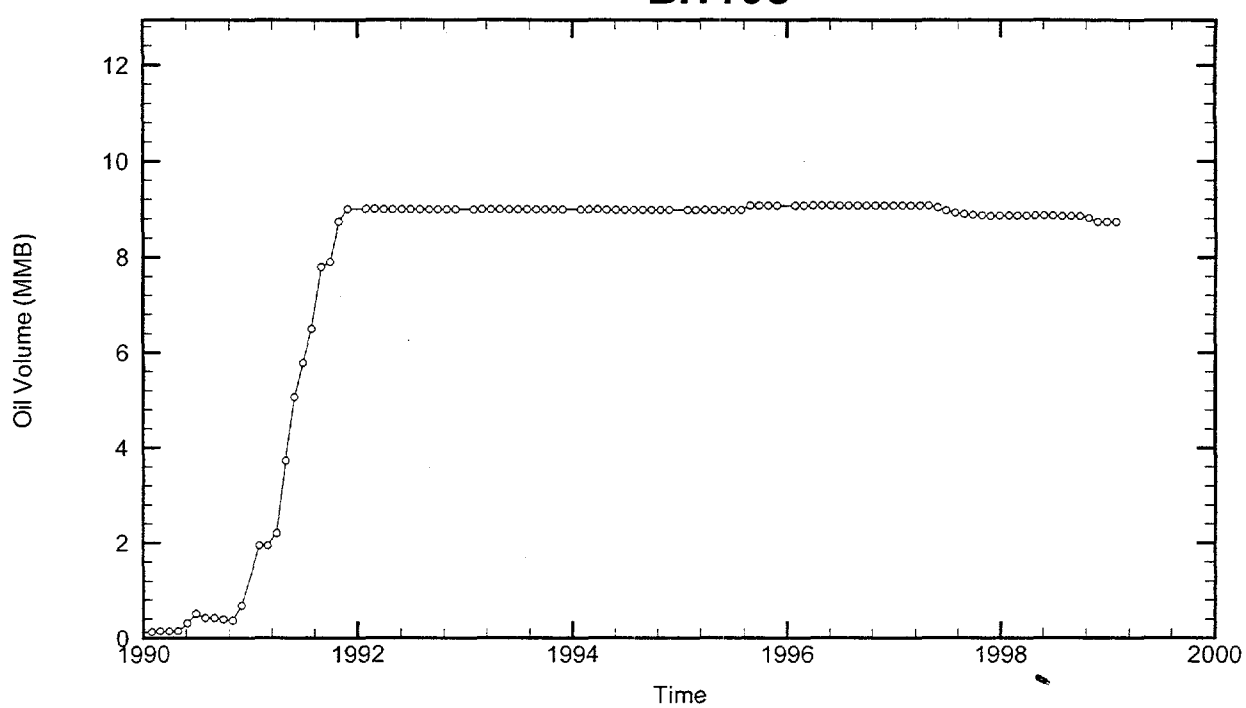
Cavern: BH107
End of Leaching: 04/24/1990
Duration of Leaching: 5.0000 days
Leaching Temperature: 67.75 °F

Degas: 05/28/1997, 118.76 °F, 5.97 MMB
Oil Injection Temperature: 58.47 °F
Brine Injection Temperature: 90.00 °F
Number of iterations: 522

BH107



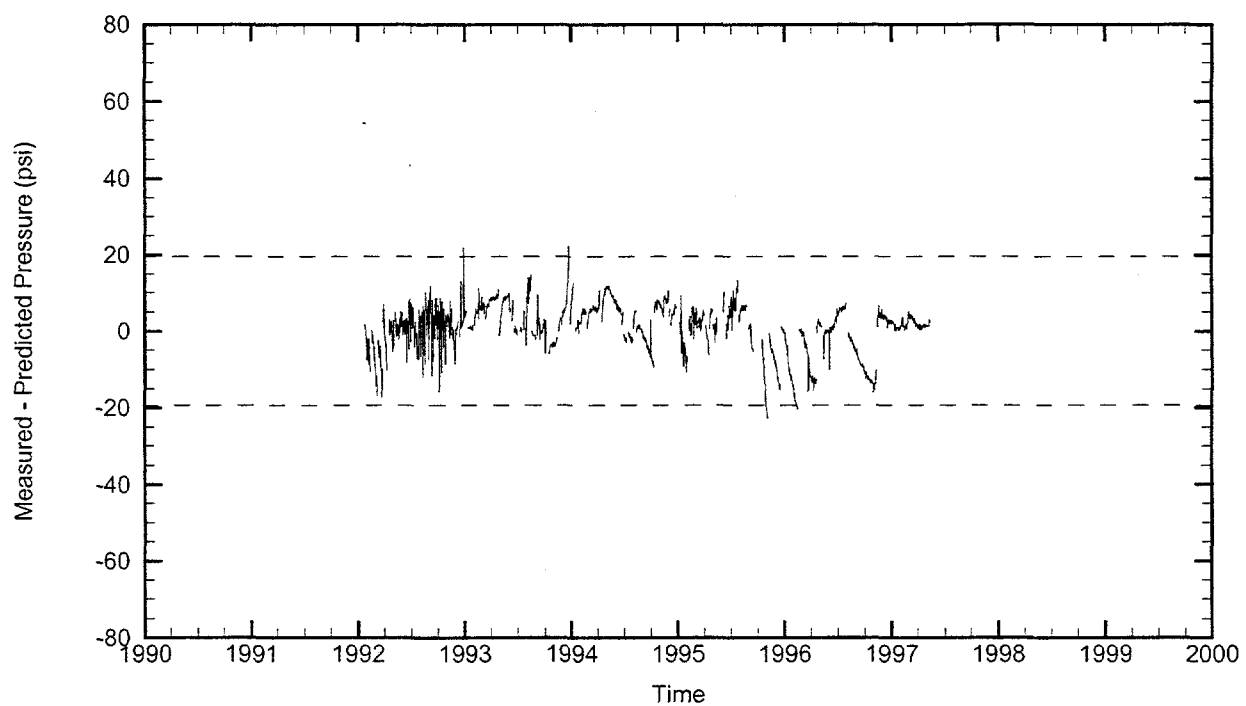
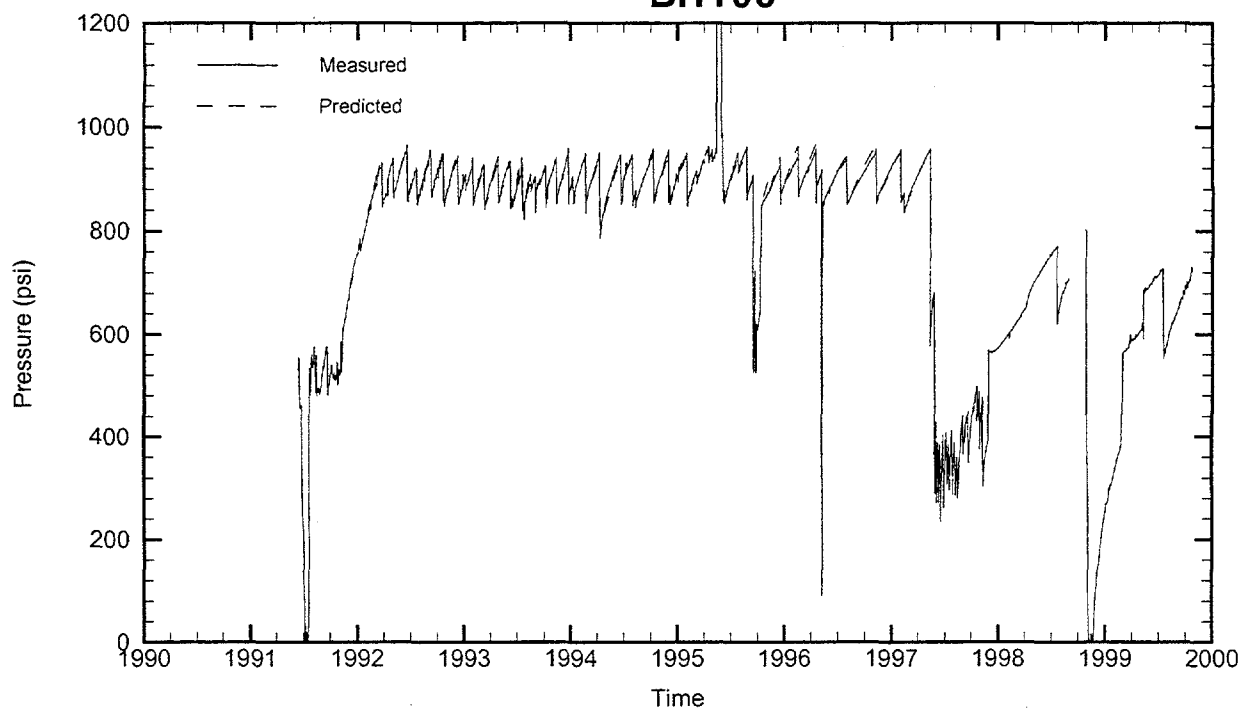
BH108



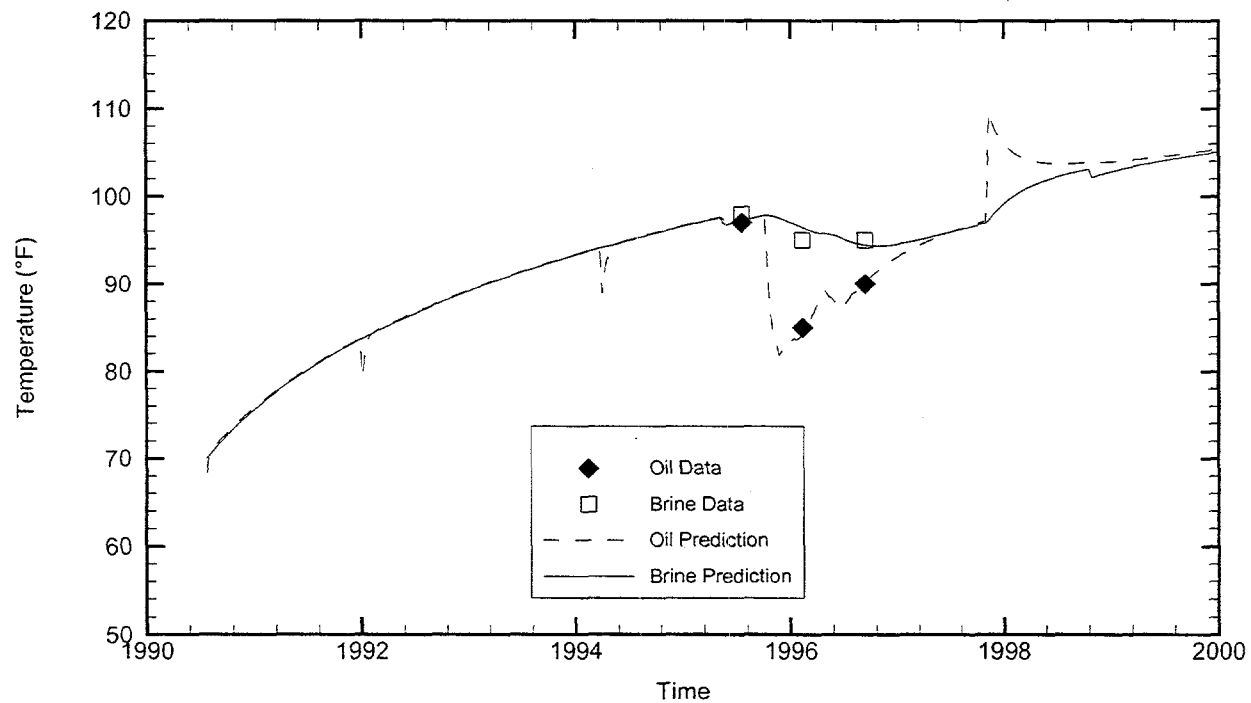
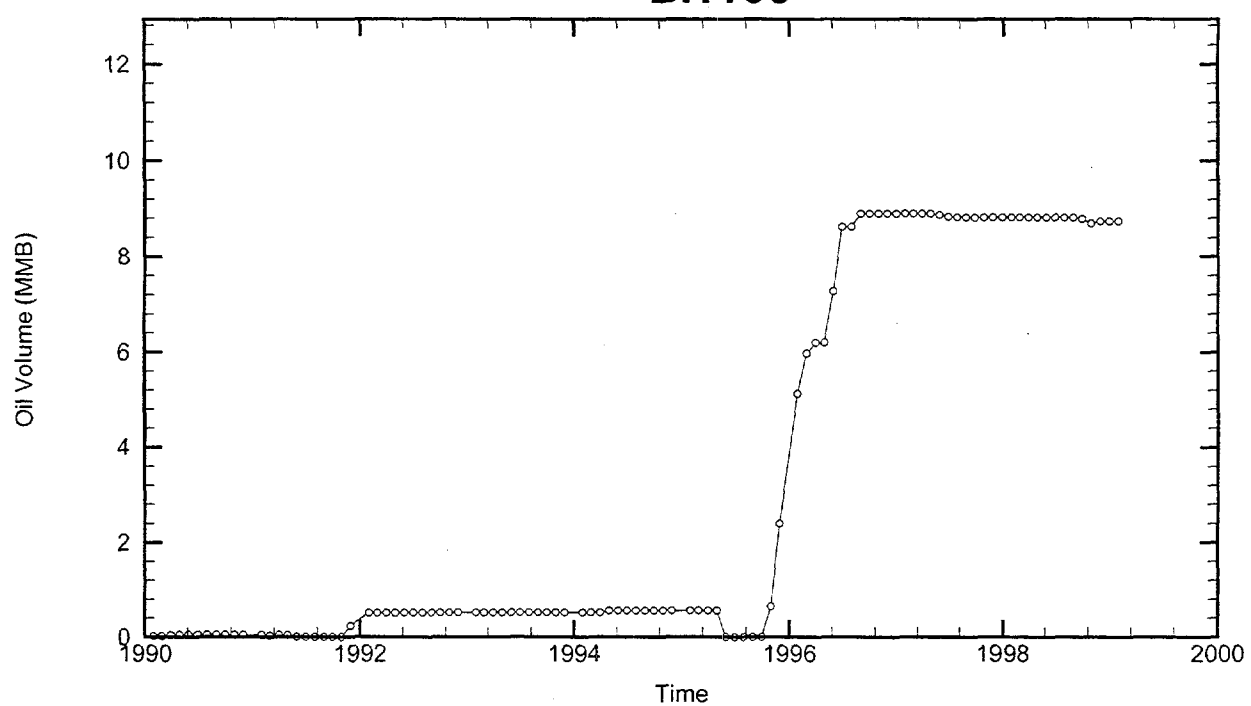
Cavern: BH108
End of Leaching: 06/14/1990
Duration of Leaching: 7.0000 days
Leaching Temperature: 69.90 °F

Degas: 11/11/1997, 110.18 °F, 9.01 MMB
Oil Injection Temperature: 66.48 °F
Brine Injection Temperature: 67.78 °F
Number of iterations: 214

BH108



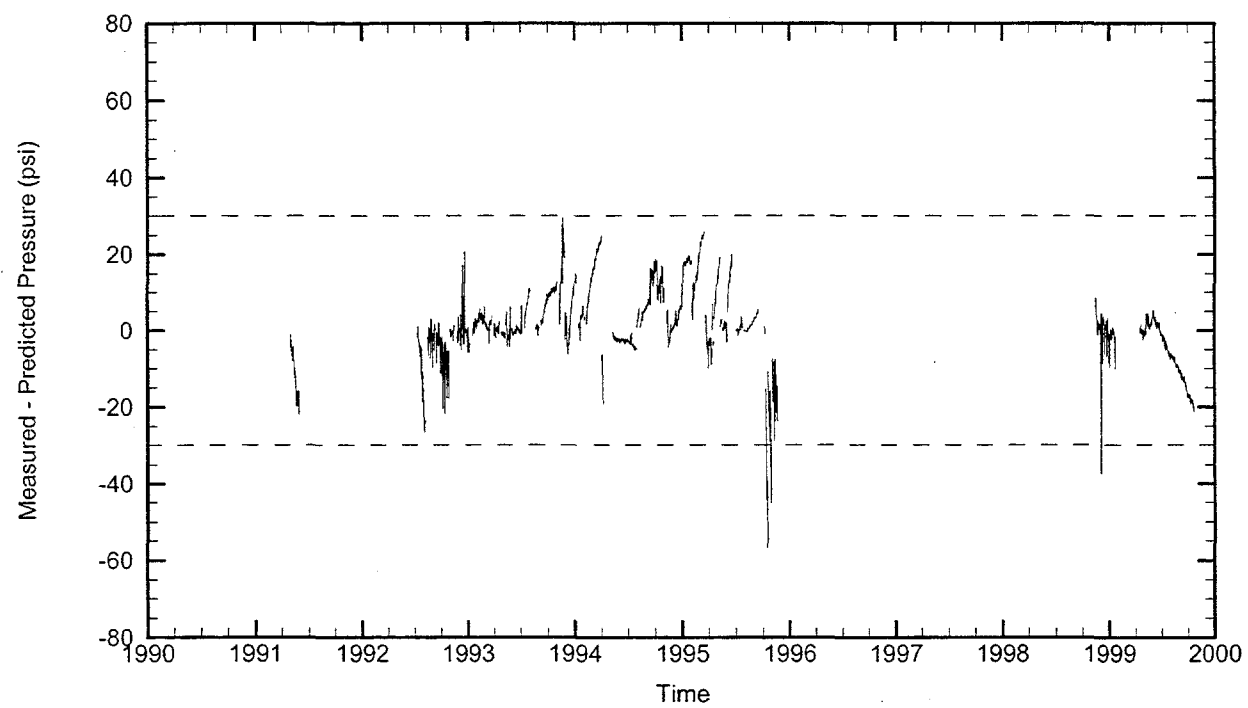
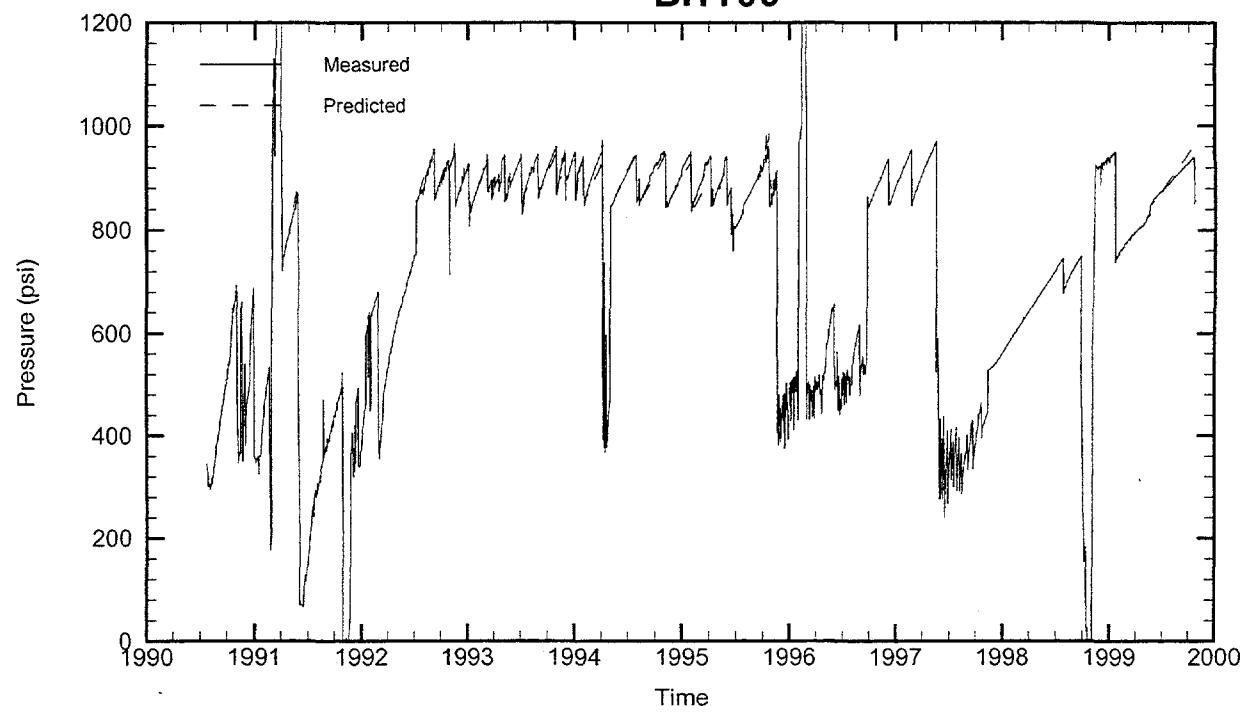
BH109

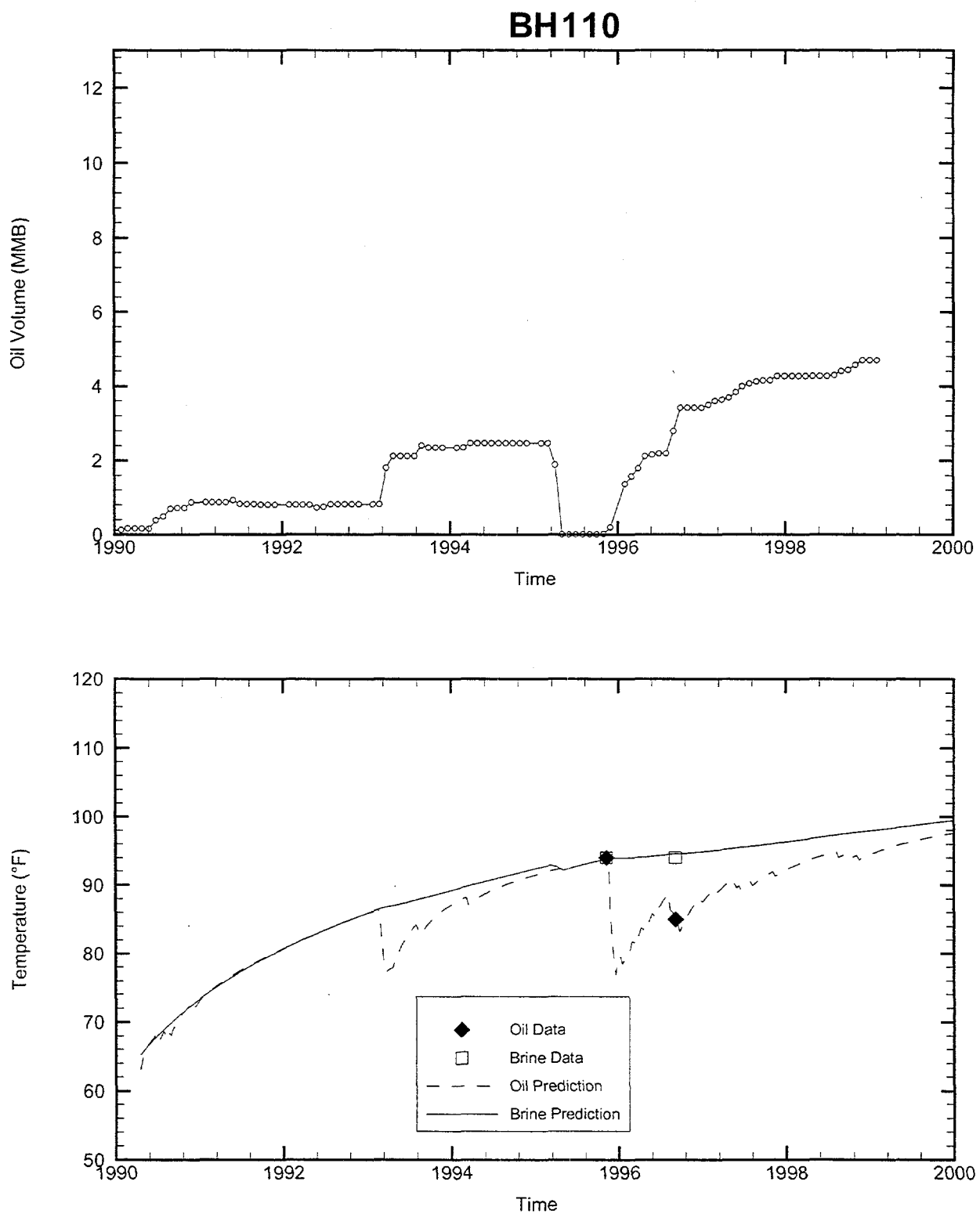


Cavern: BH109
End of Leaching: 07/24/1990
Duration of Leaching: 7.1294 months
Leaching Temperature: 70.00 °F

Degas: 11/11/1997, 110.18 °F, 9.01 MMB
Oil Injection Temperature: 68.32 °F
Brine Injection Temperature: 66.69 °F
Number of iterations: 231

BH109

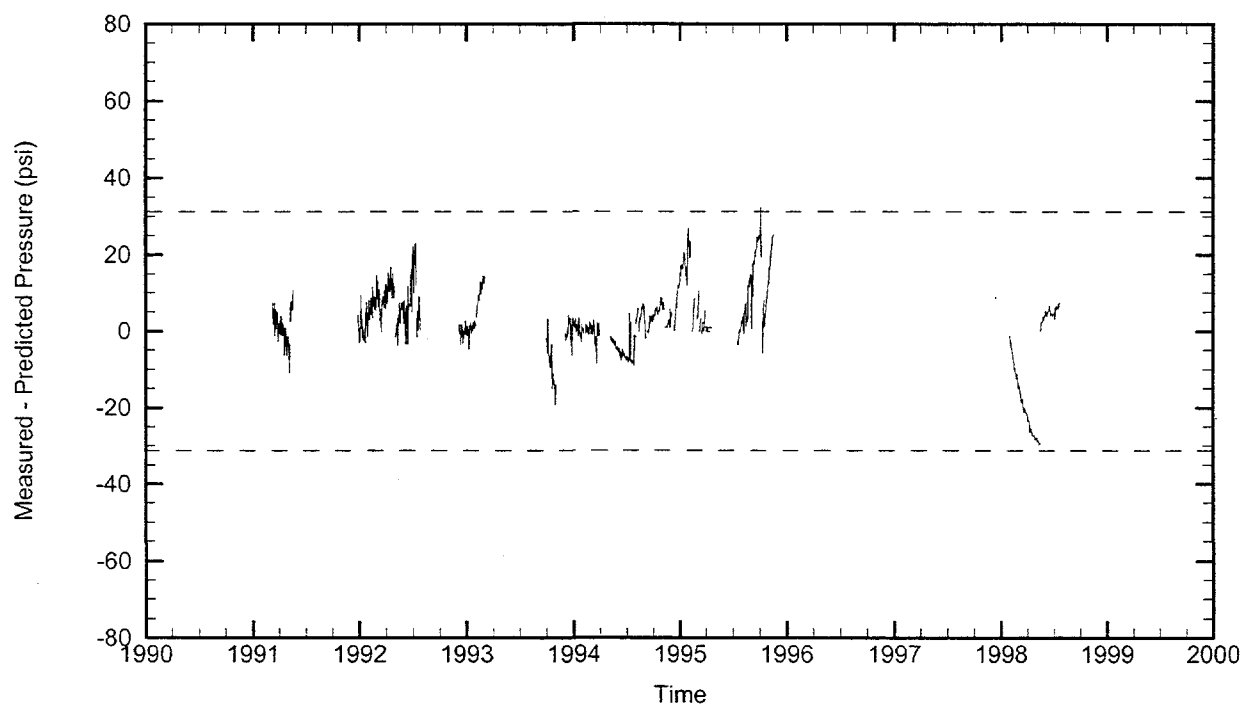
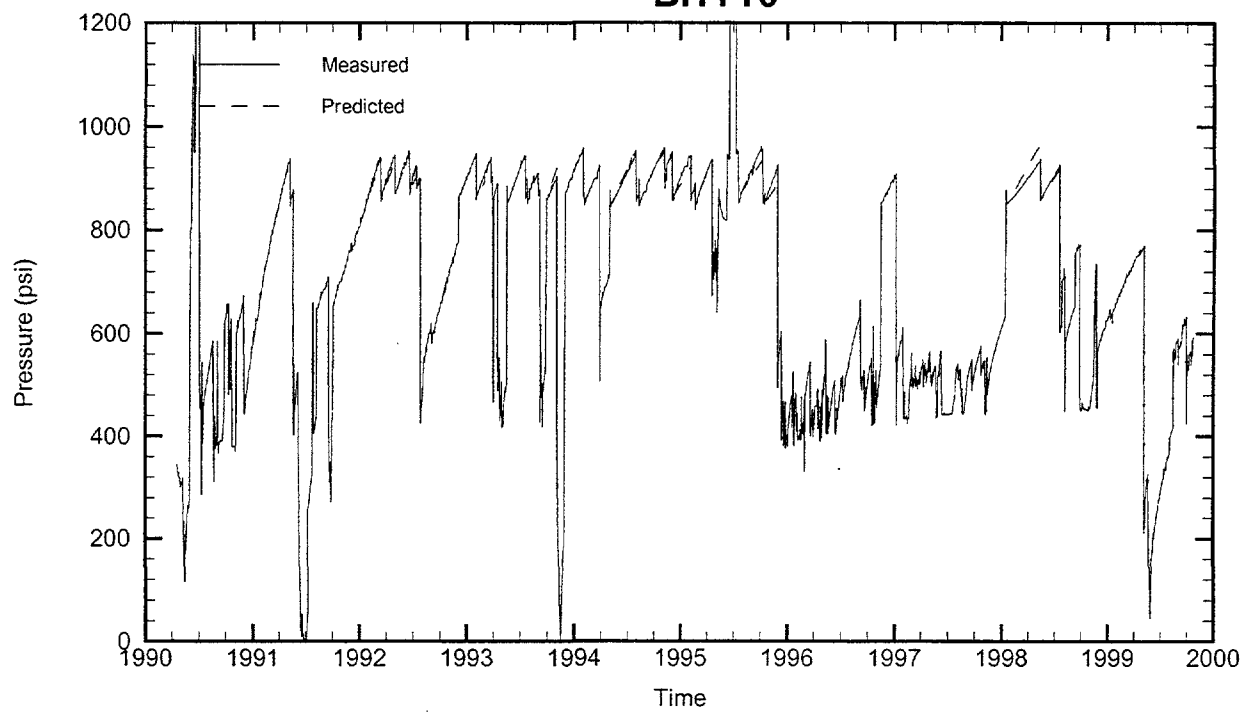


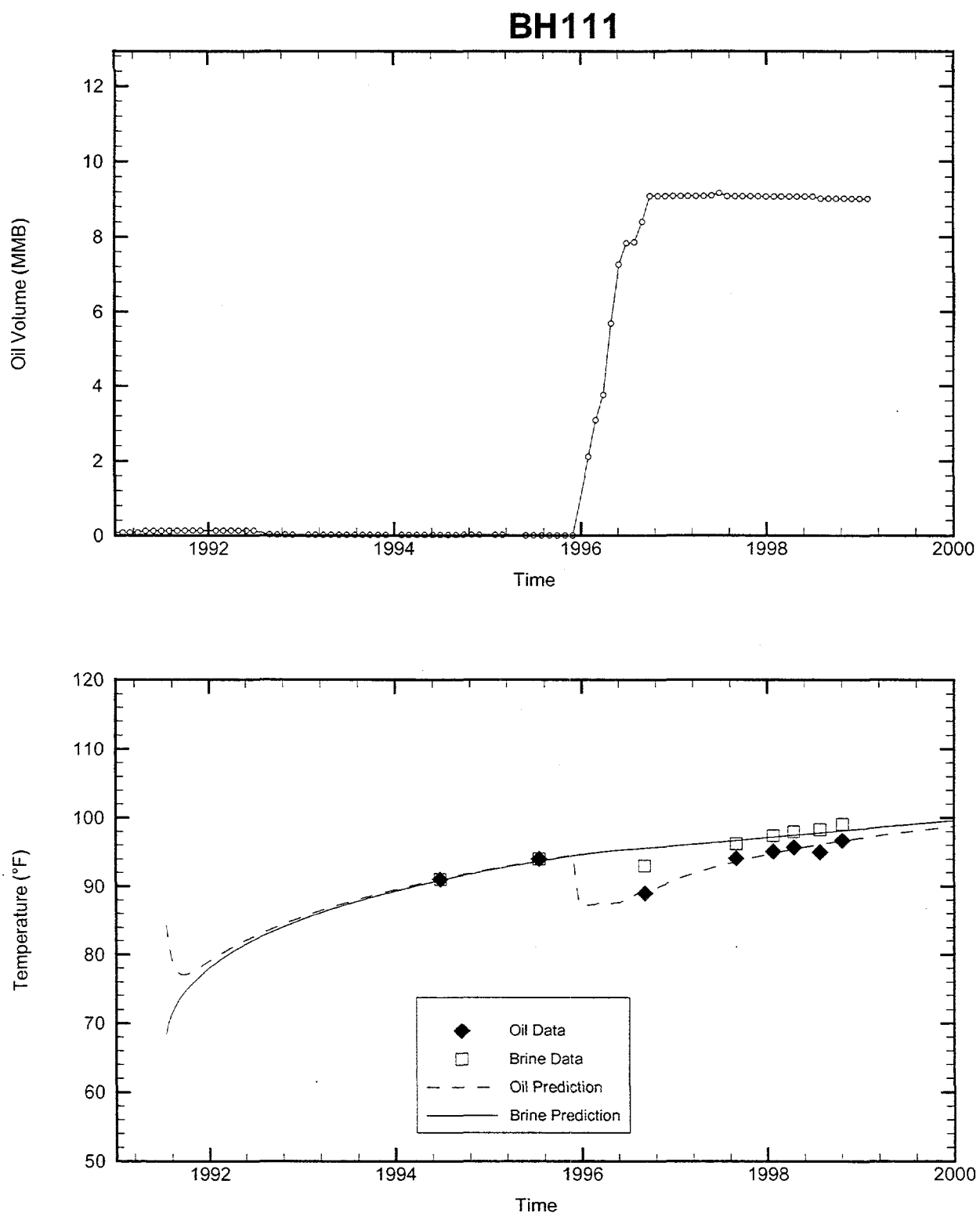


Cavern: BH110
 End of Leaching: 04/19/1990
 Duration of Leaching: 8.2464 months
 Leaching Temperature: 65.26 °F

Oil Injection Temperature: 63.12 °F
 Brine Injection Temperature: 86.40 °F
 Number of iterations: 482

BH110





Cavern: BH111

End of Leaching: 07/15/1991

Duration of Leaching: 2.0000 days

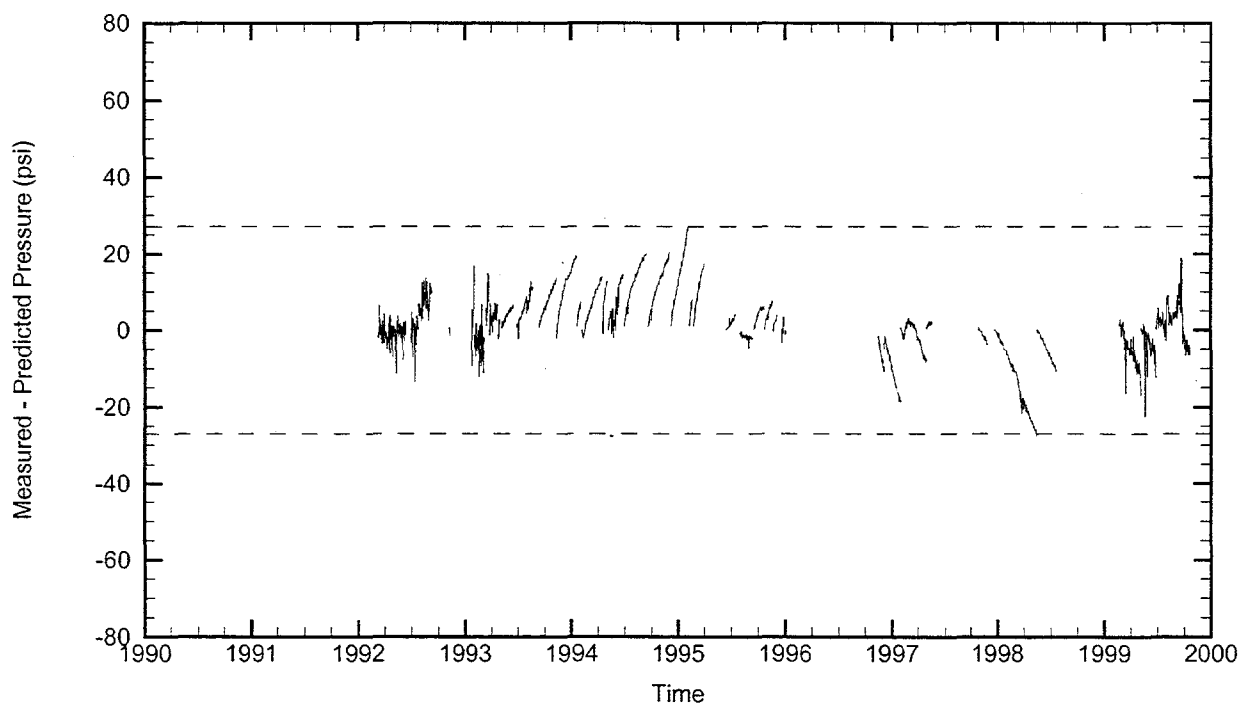
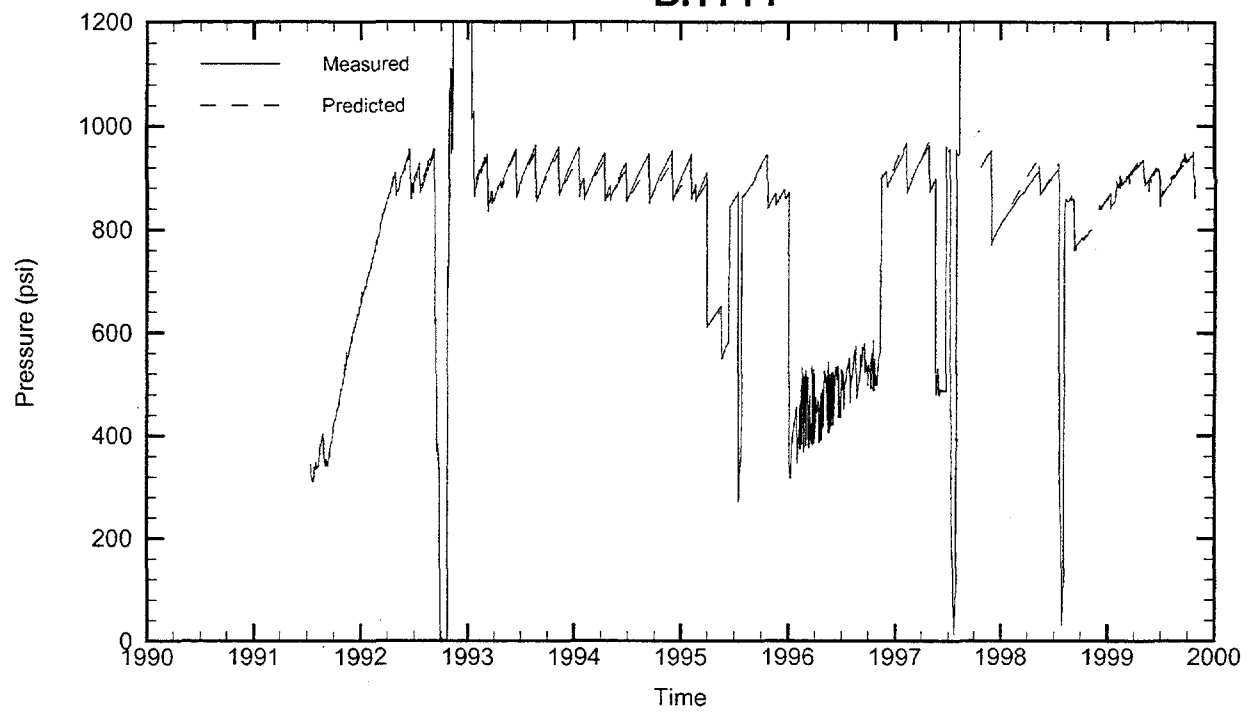
Leaching Temperature: 68.36 °F

Oil Injection Temperature: 84.30 °F

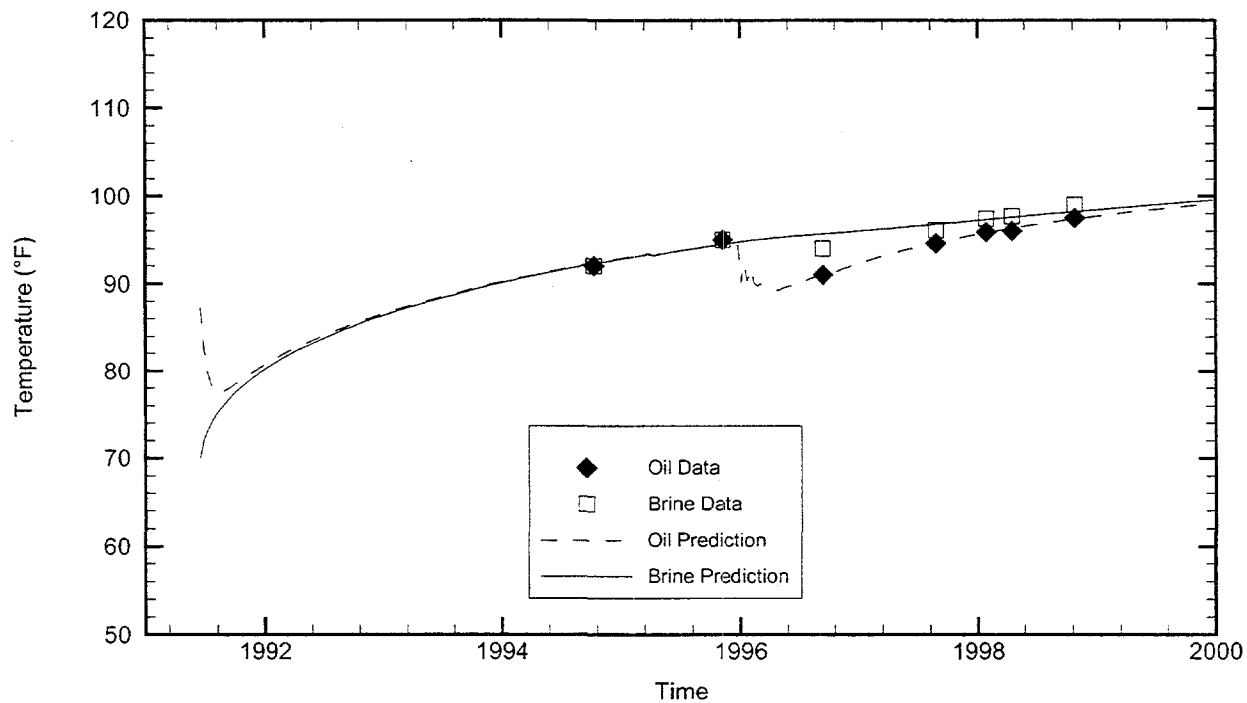
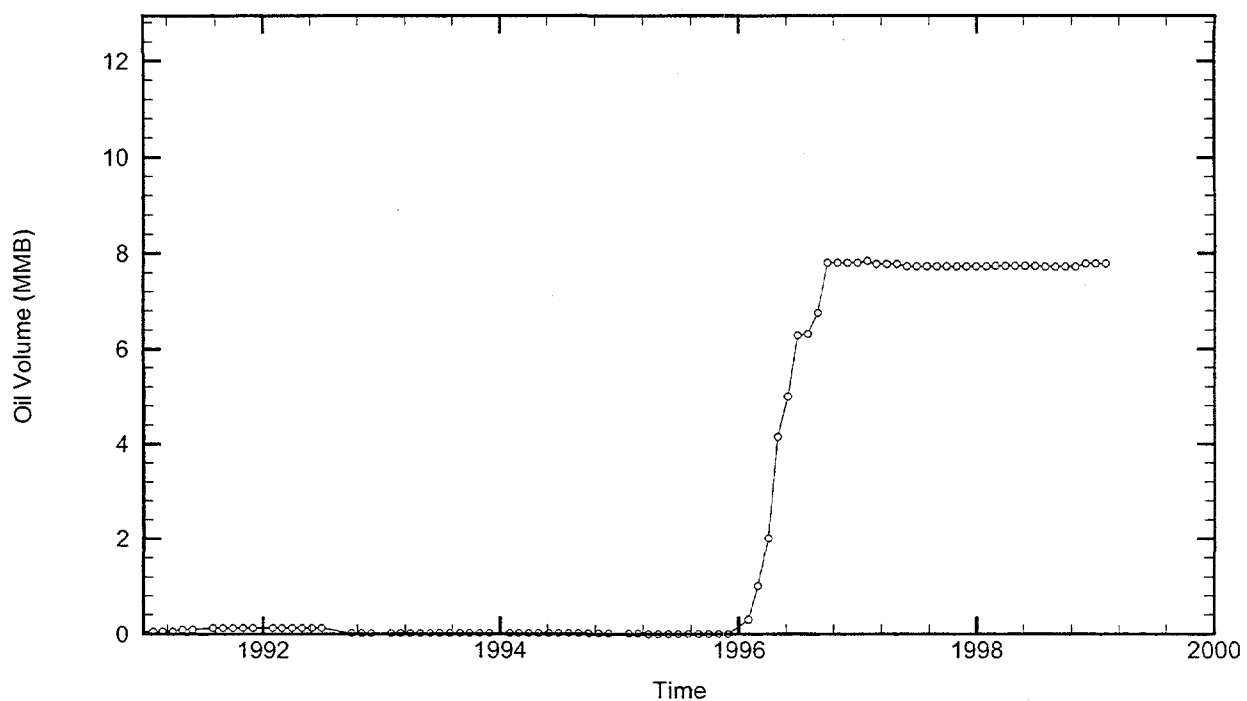
Brine Injection Temperature: 68.36 °F

Number of iterations: 260

BH111



BH112



Cavern: BH112

End of Leaching: 06/18/1991

Duration of Leaching: 0.0000 days

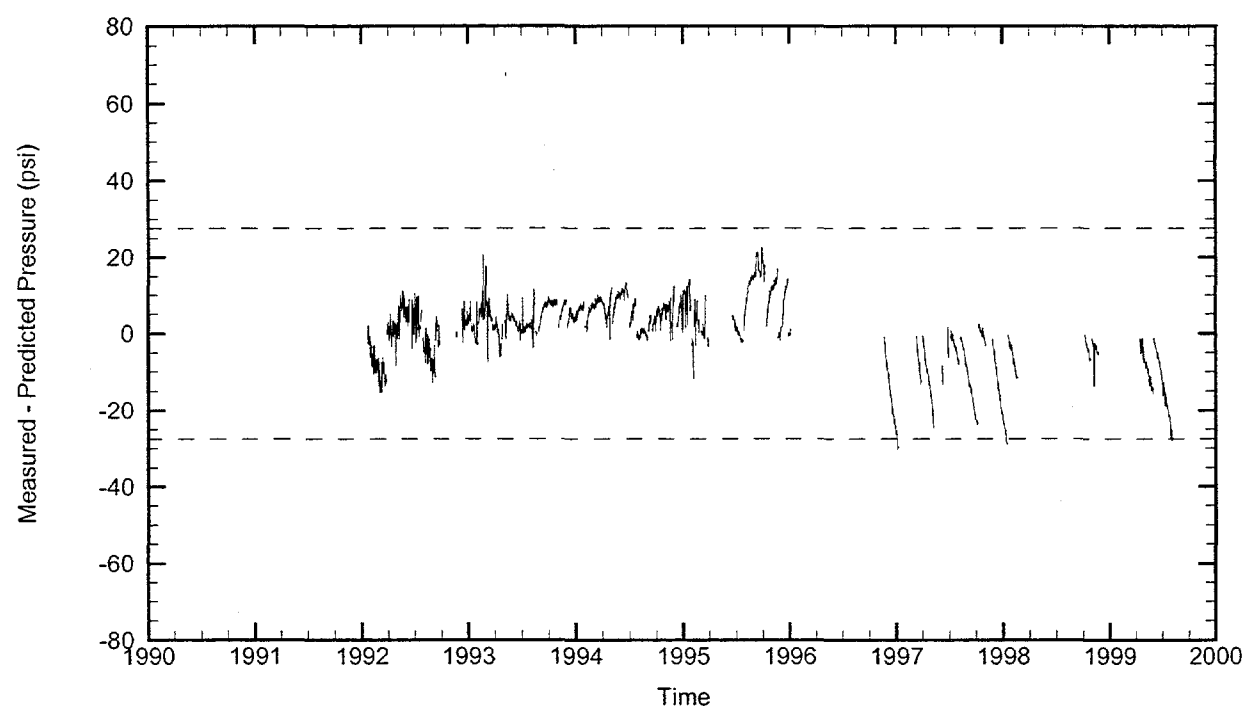
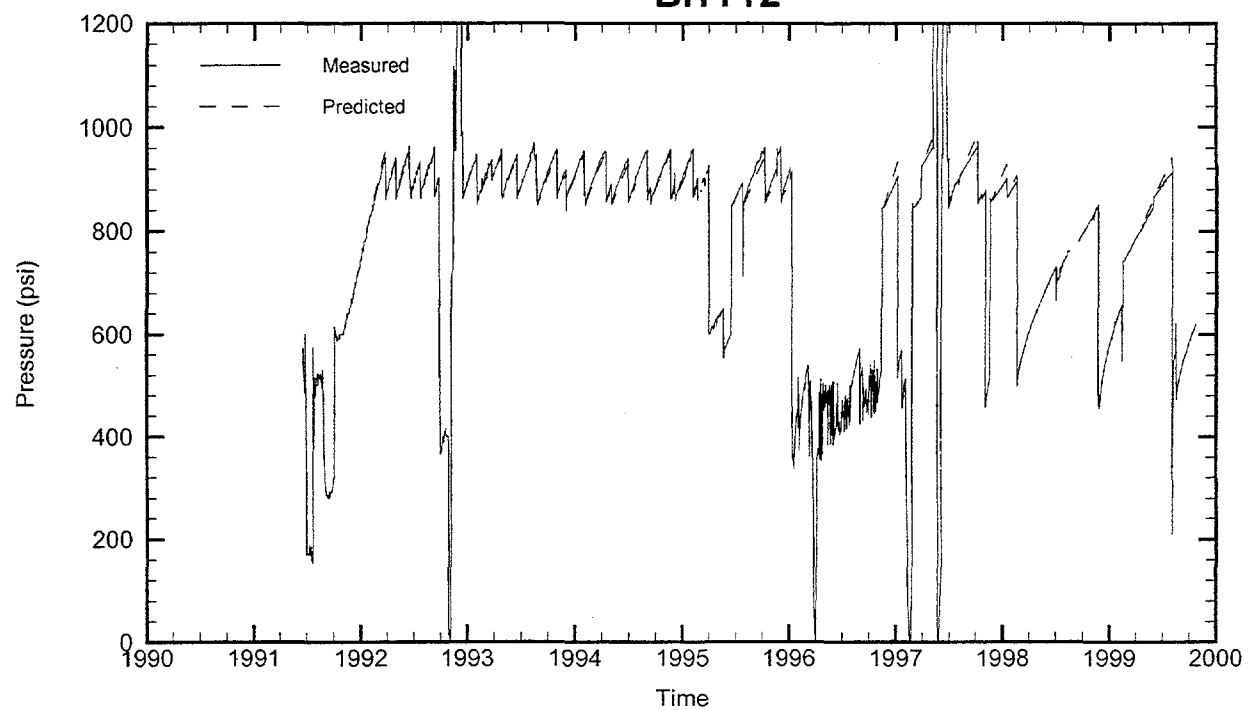
Leaching Temperature: 70.00 °F

Oil Injection Temperature: 87.18 °F

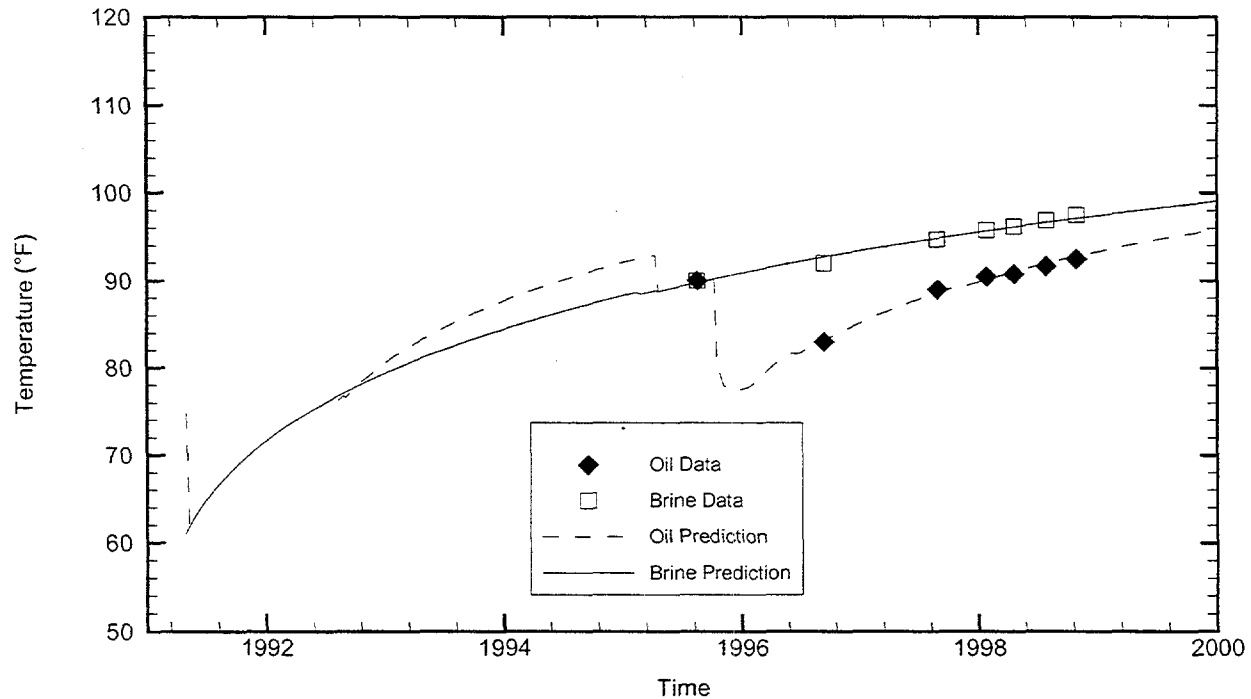
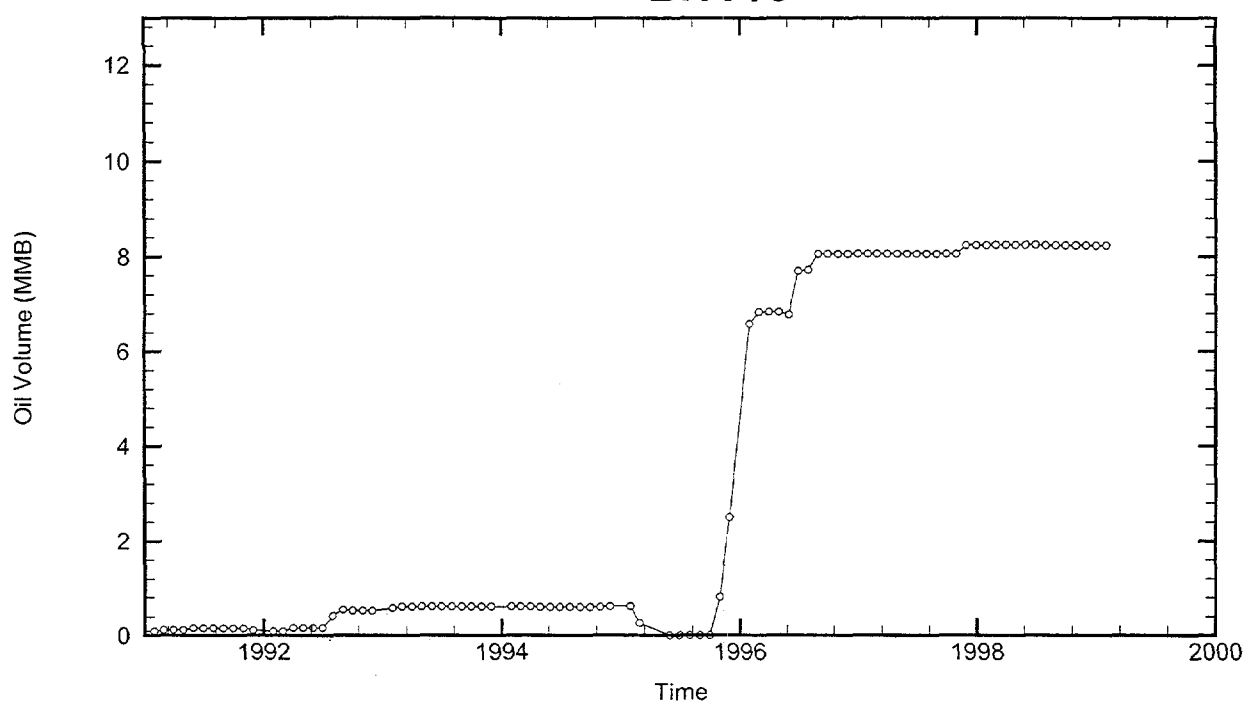
Brine Injection Temperature: 73.73 °F

Number of iterations: 282

BH112



BH113



Cavern: BH113

End of Leaching: 05/01/1991

Duration of Leaching: 1.7741 months

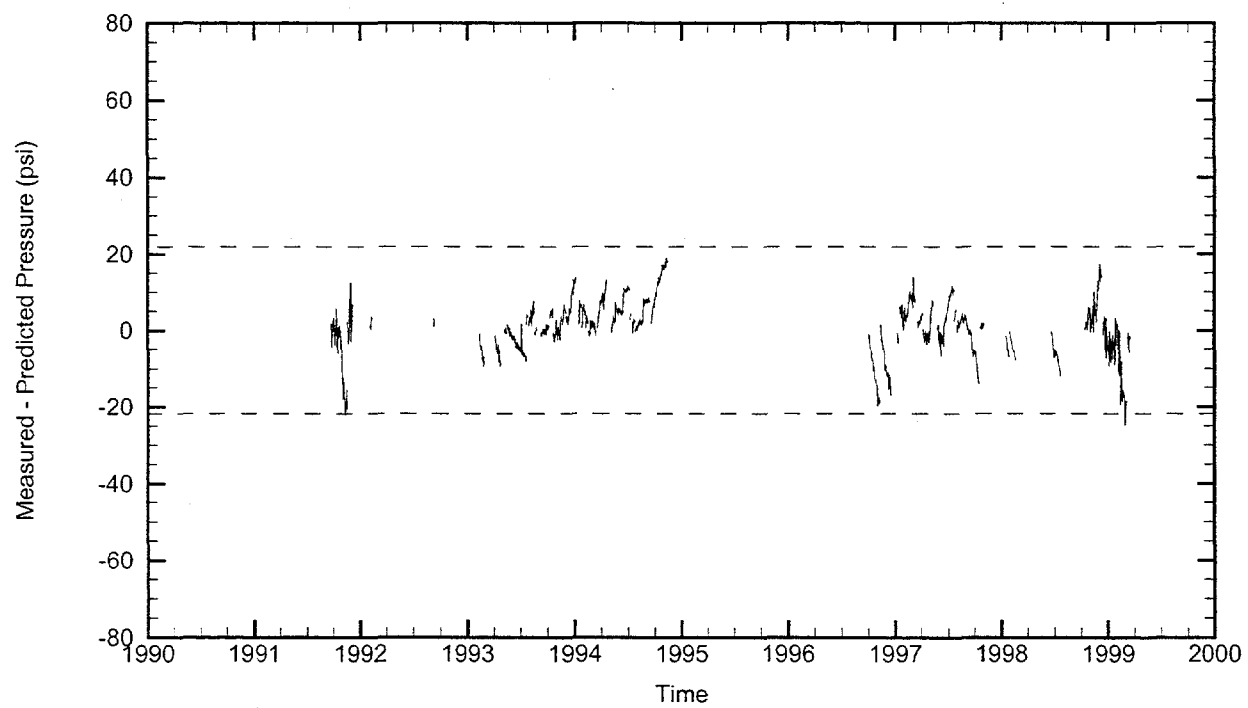
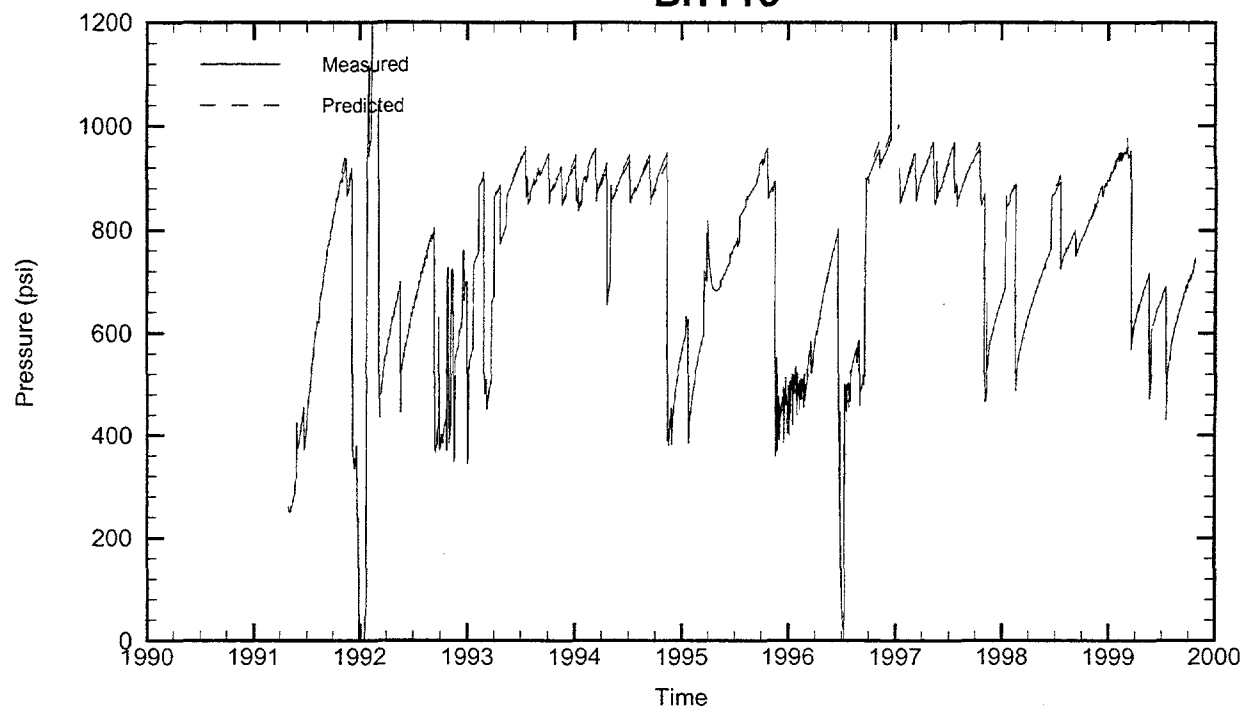
Leaching Temperature: 61.04 °F

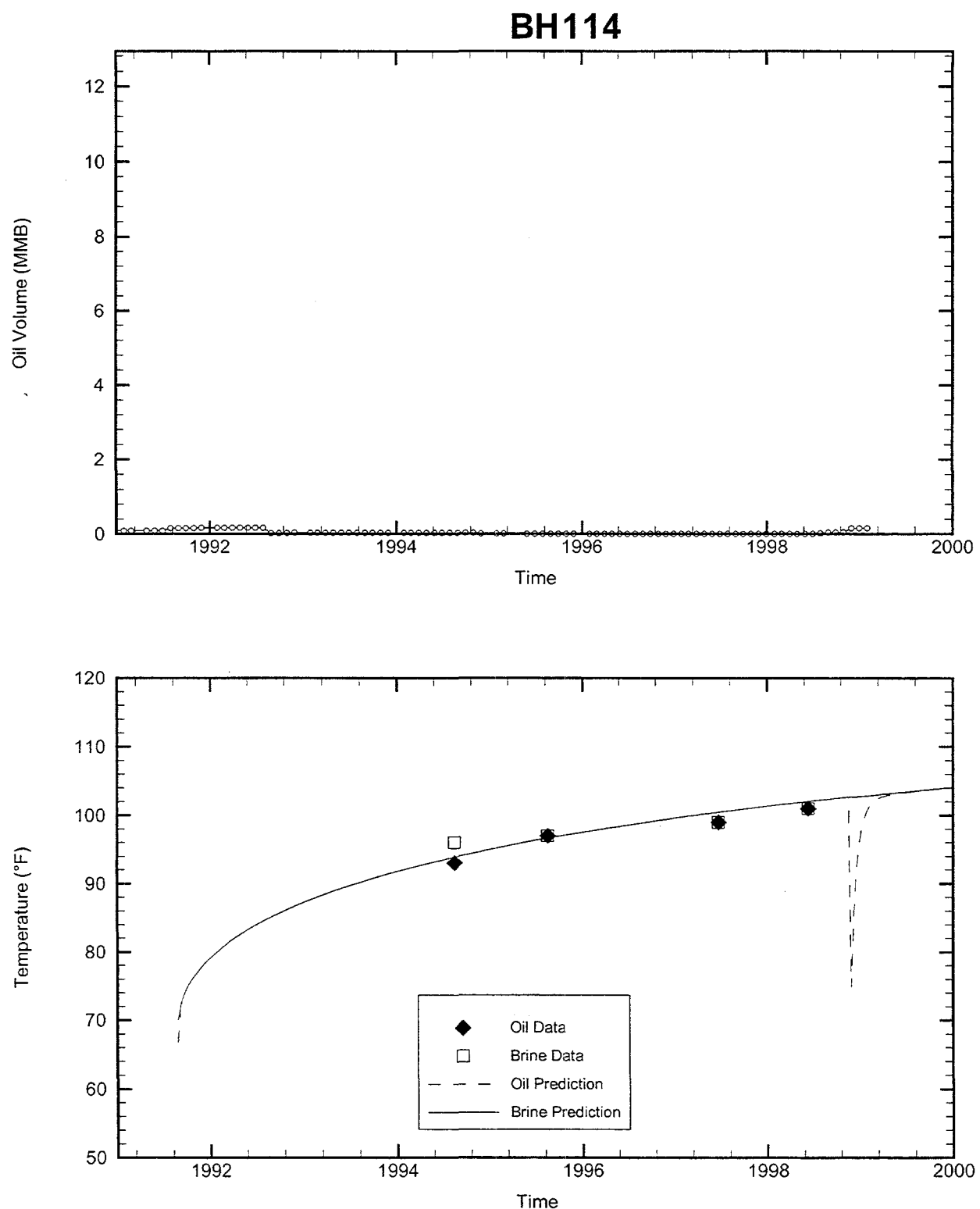
Oil Injection Temperature: 74.78 °F

Brine Injection Temperature: 72.61 °F

Number of iterations: 188

BH113

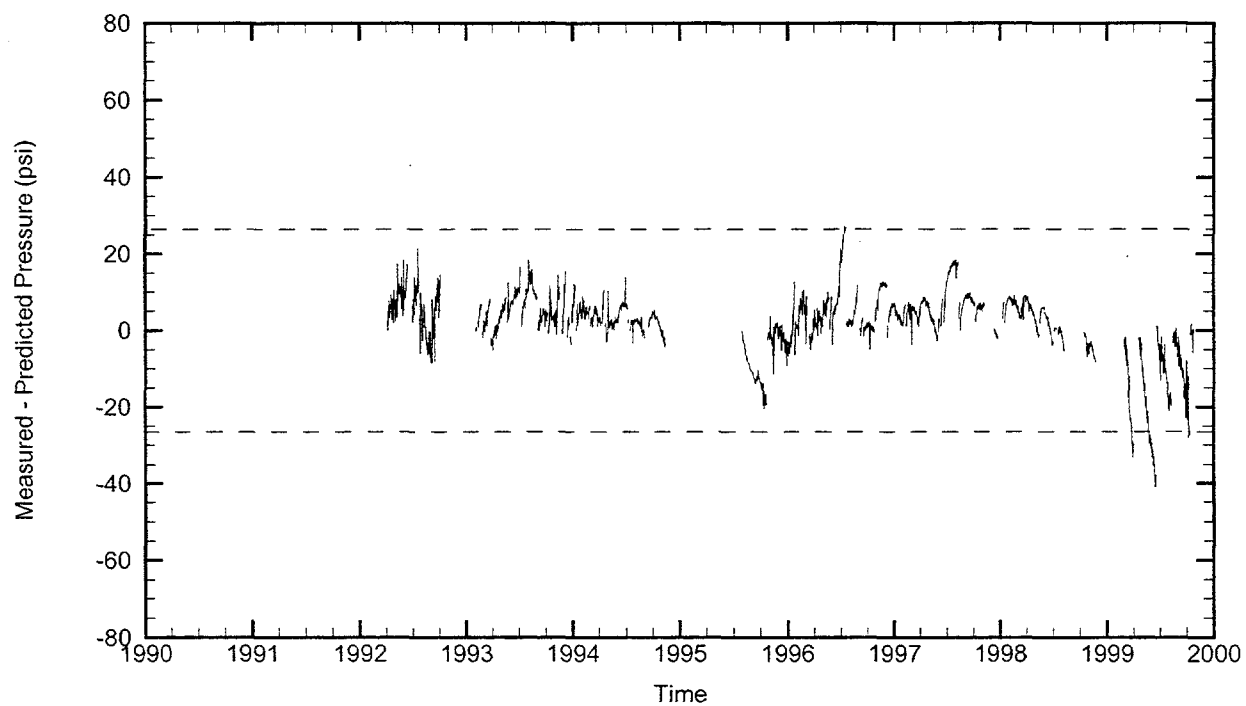
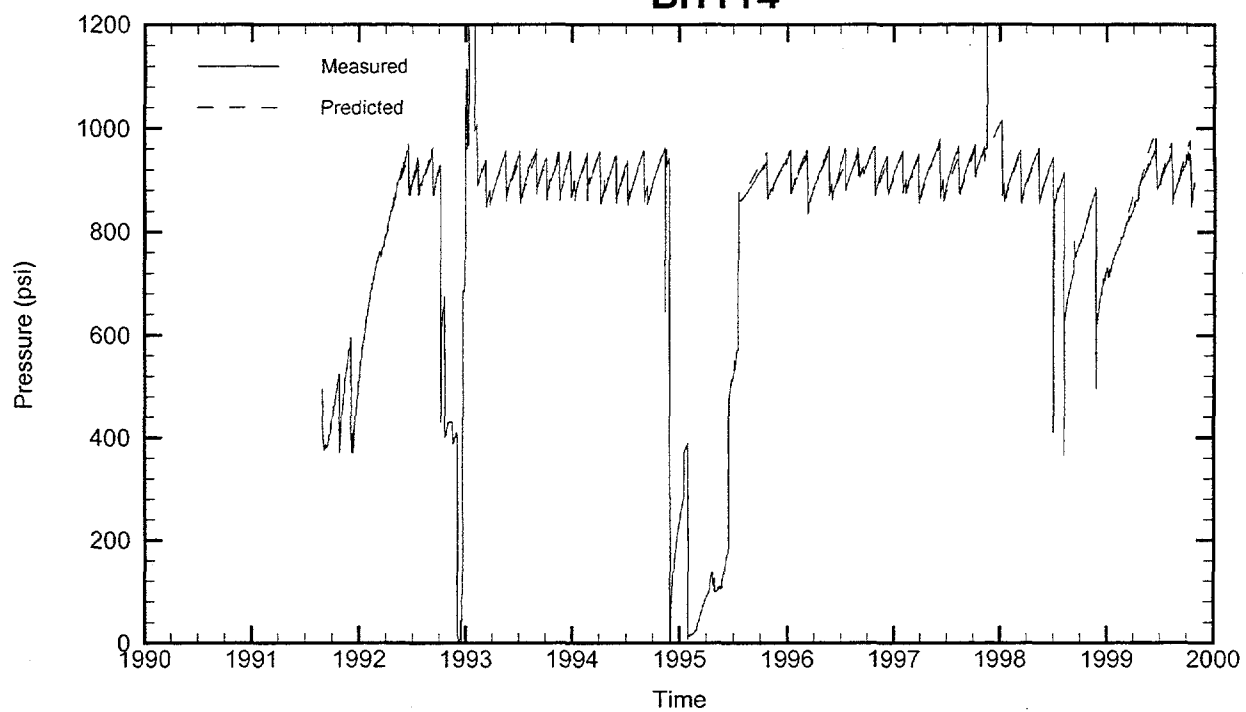




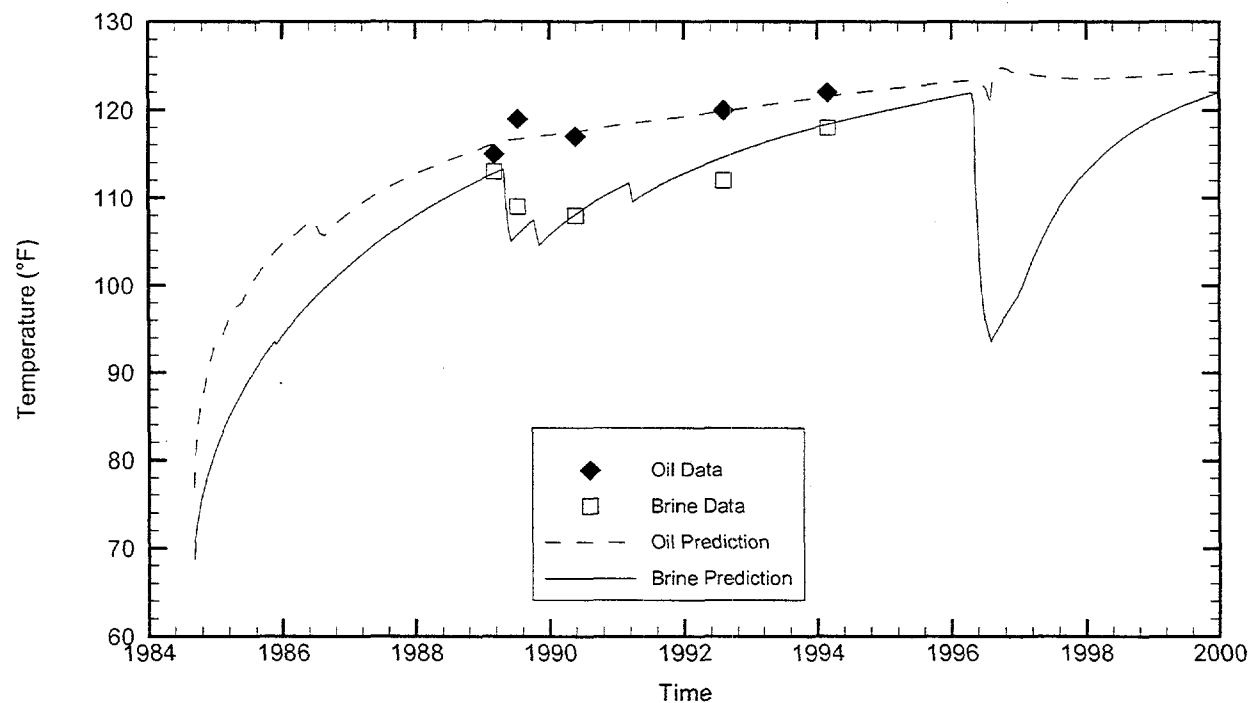
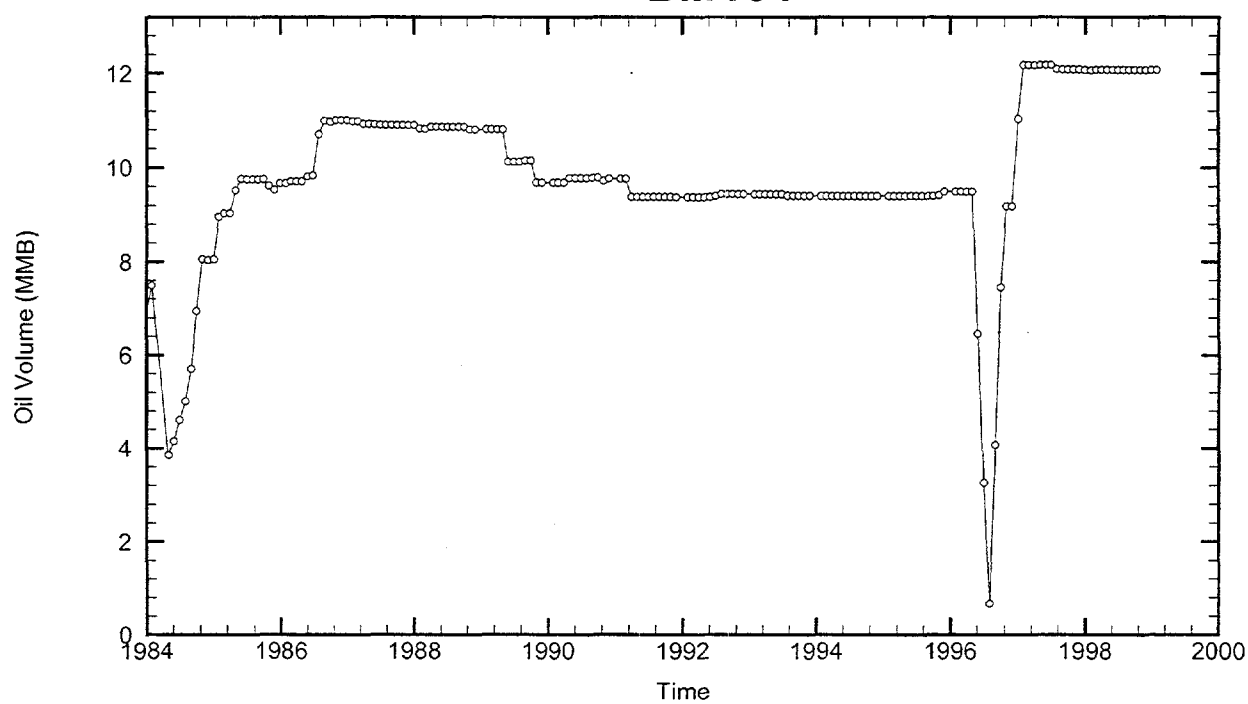
Cavern: BH114
 End of Leaching: 08/27/1991
 Duration of Leaching: 0.0000 days
 Leaching Temperature: 70.00 °F

Oil Injection Temperature: 66.77 °F
 Brine Injection Temperature: 70.00 °F
 Number of iterations: 199

BH114



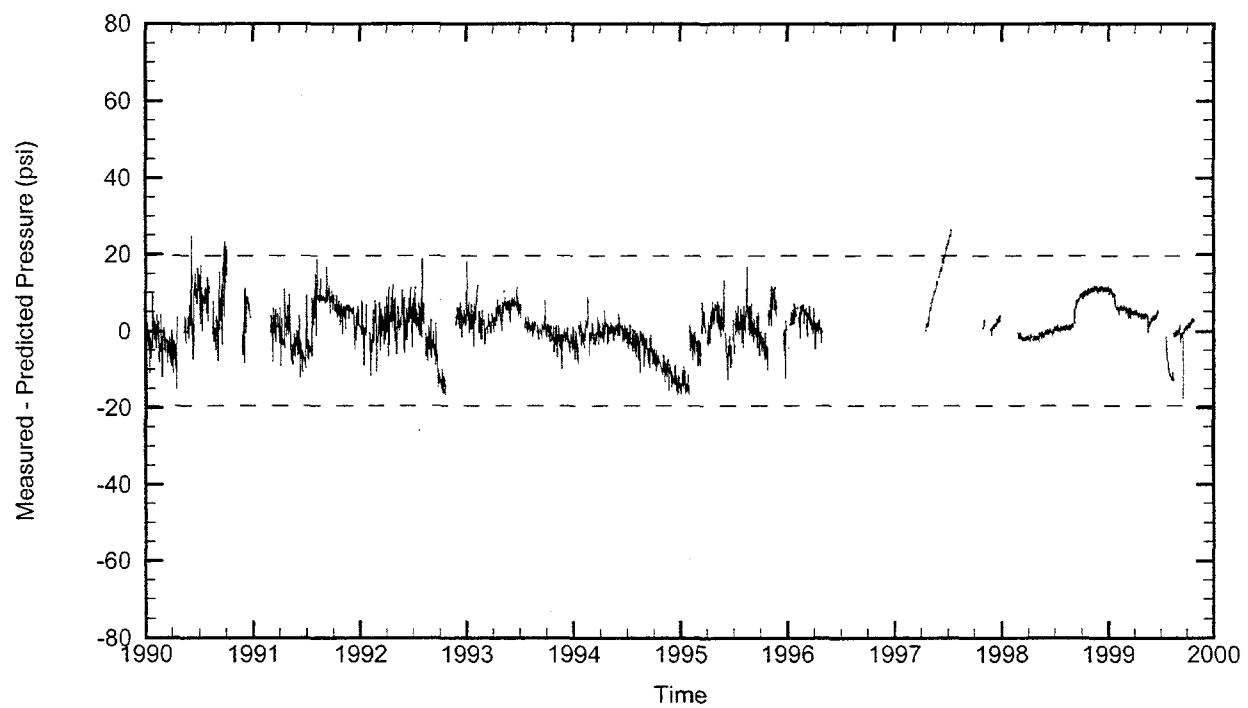
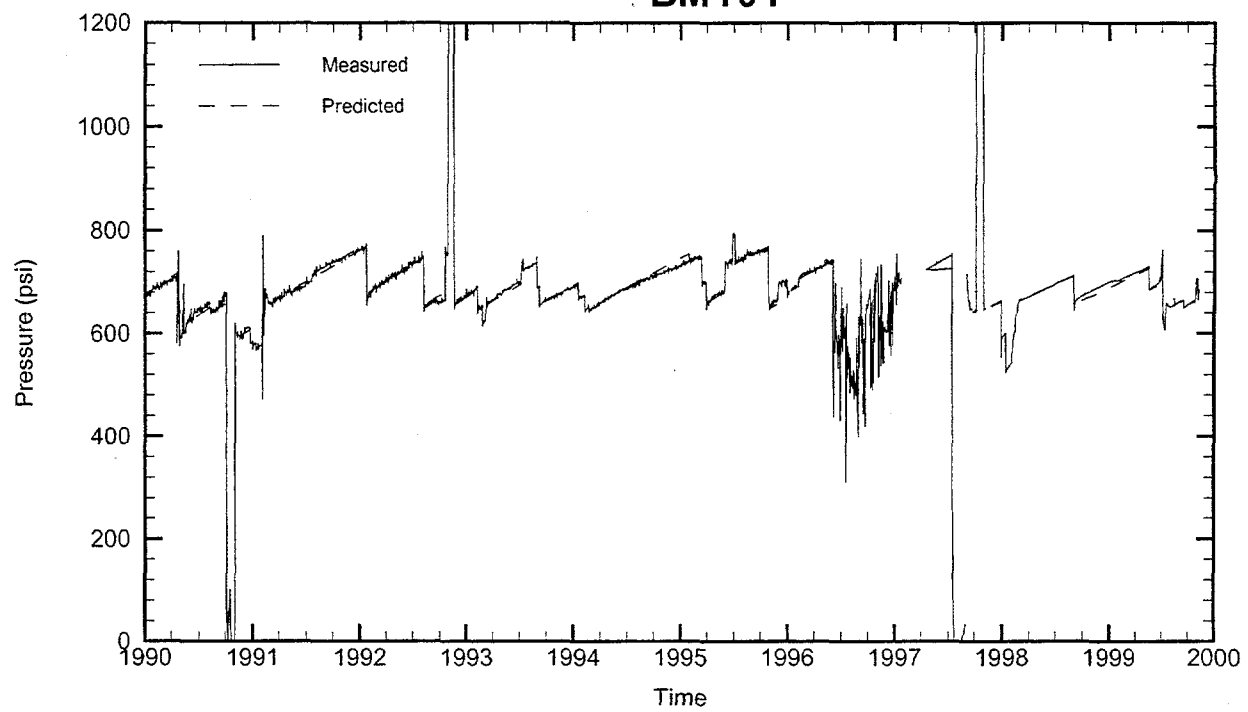
BM101



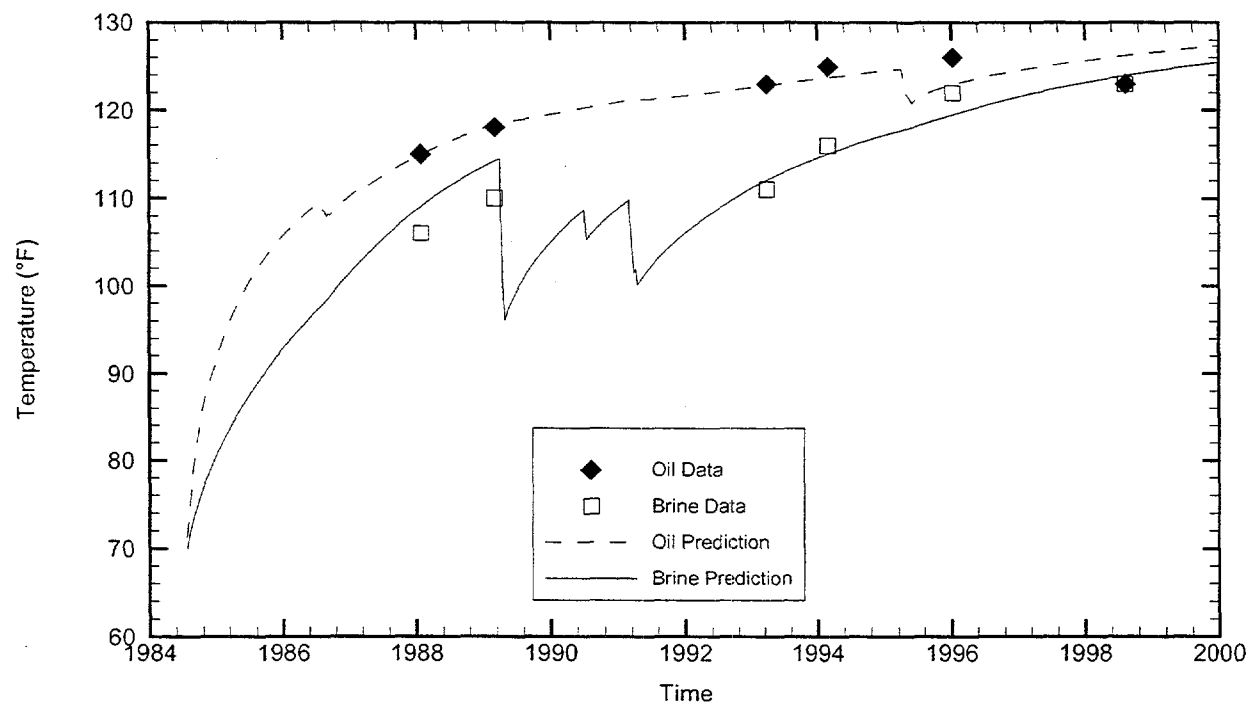
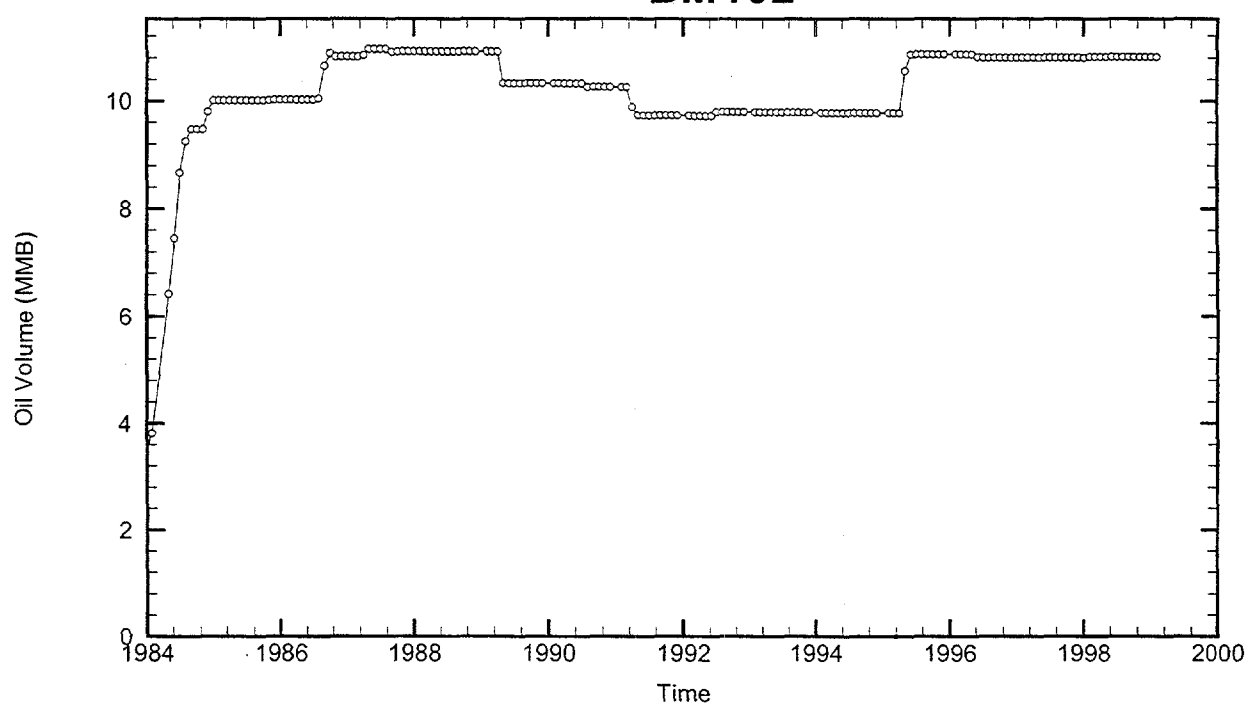
Cavern: BM101
 End of Leaching: 09/03/1984
 Duration of Leaching: 2.0000 days
 Leaching Temperature: 68.66 °F

Degas: 08/02/1996, 126.87 °F, 11.46 MMB
 Oil Injection Temperature: 76.89 °F
 Brine Injection Temperature: 77.16 °F
 Number of iterations: 336

BM101



BM102



Cavern: BM102

End of Leaching: 07/26/1984

Duration of Leaching: 1.6667 years

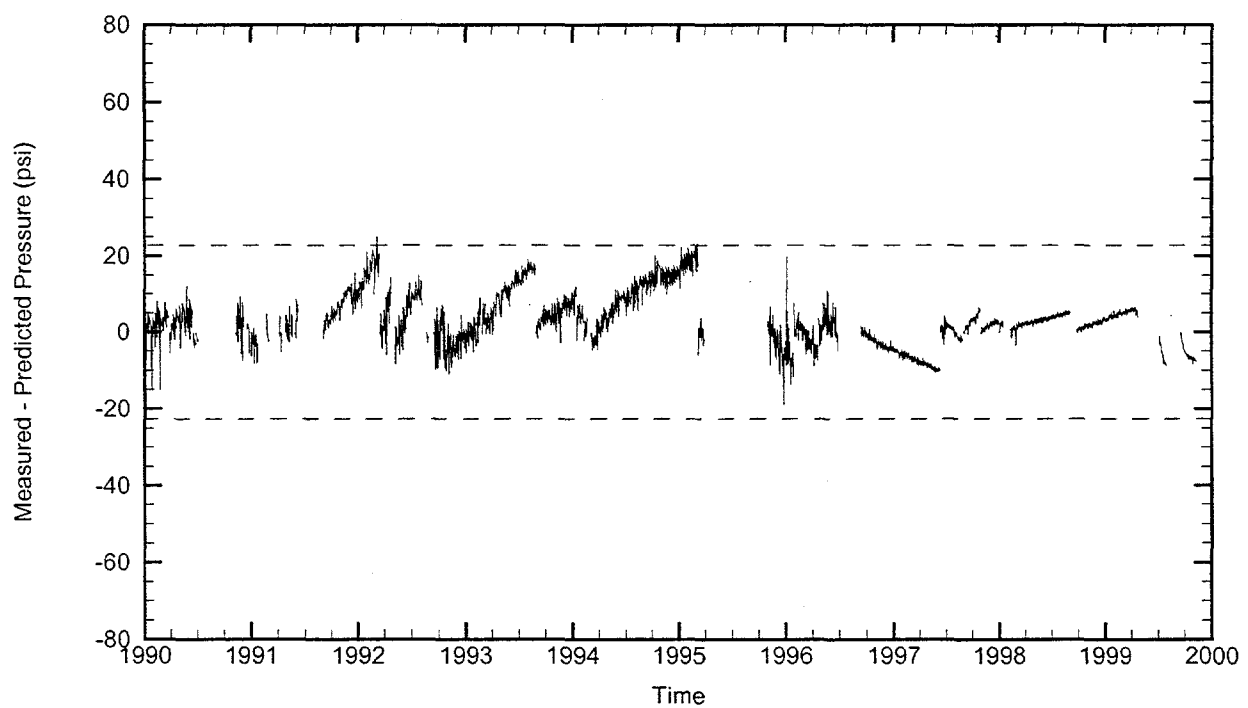
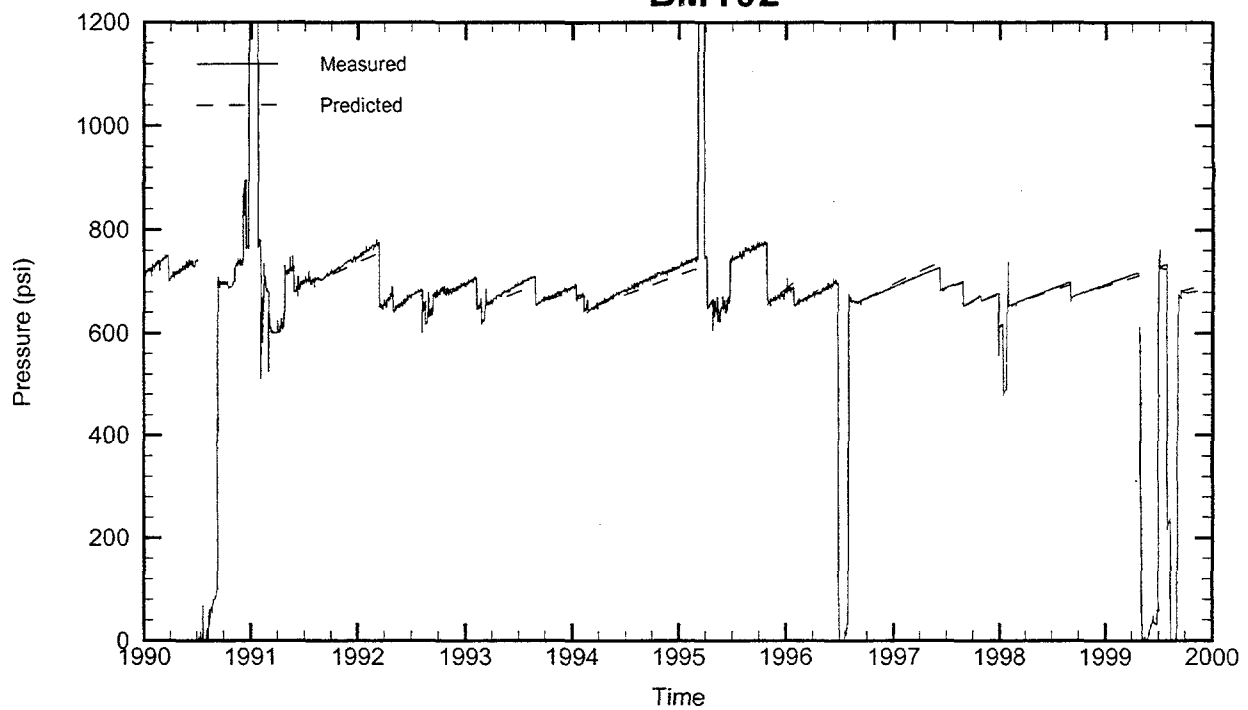
Leaching Temperature: 70.00 °F

Oil Injection Temperature: 71.25 °F

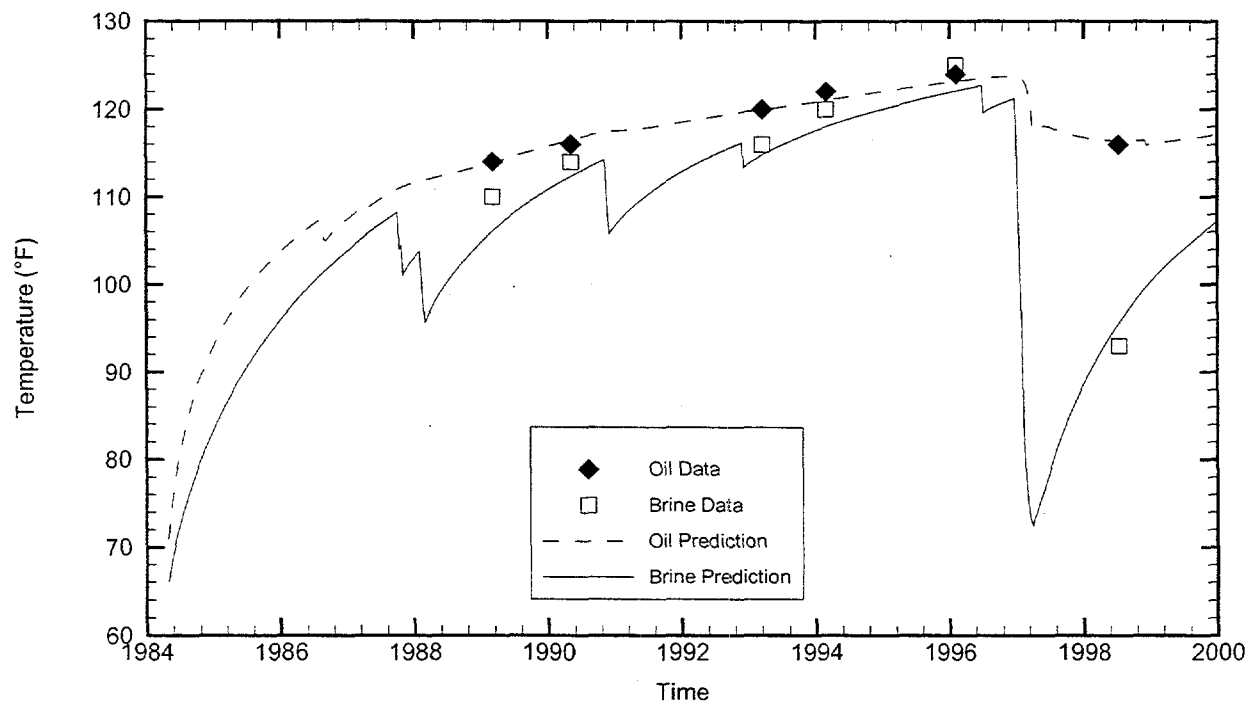
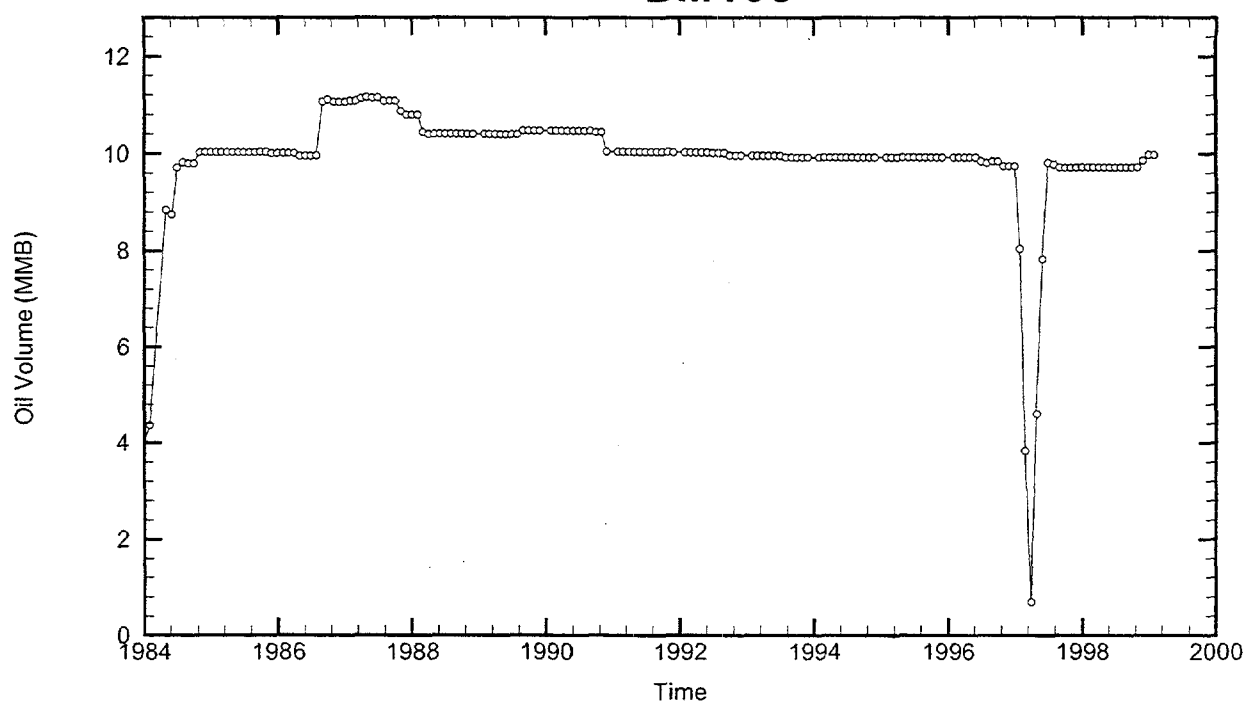
Brine Injection Temperature: 69.56 °F

Number of iterations: 370

BM102



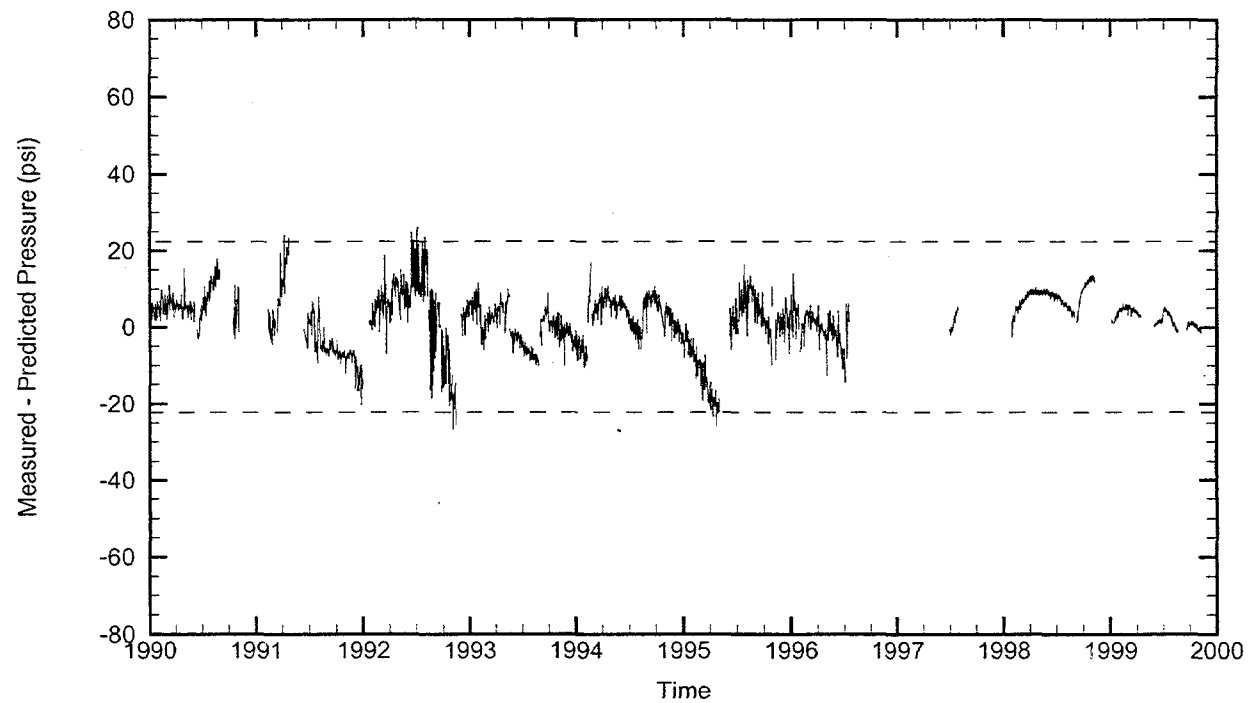
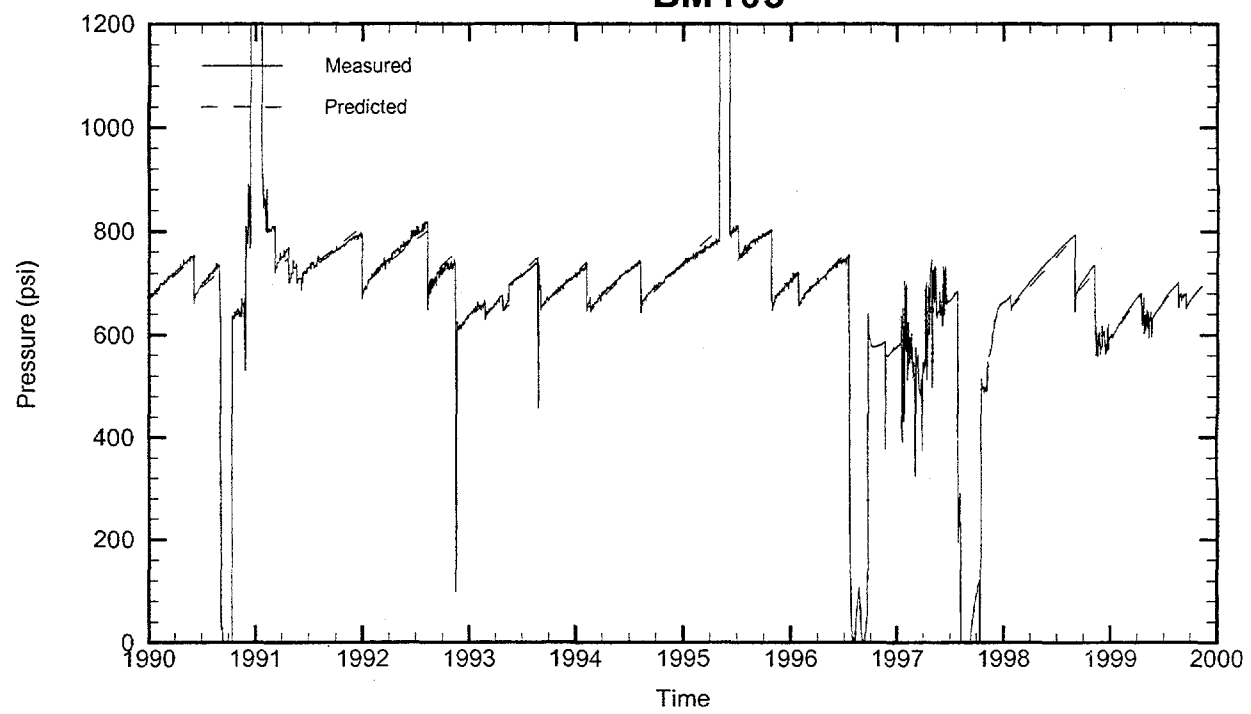
BM103



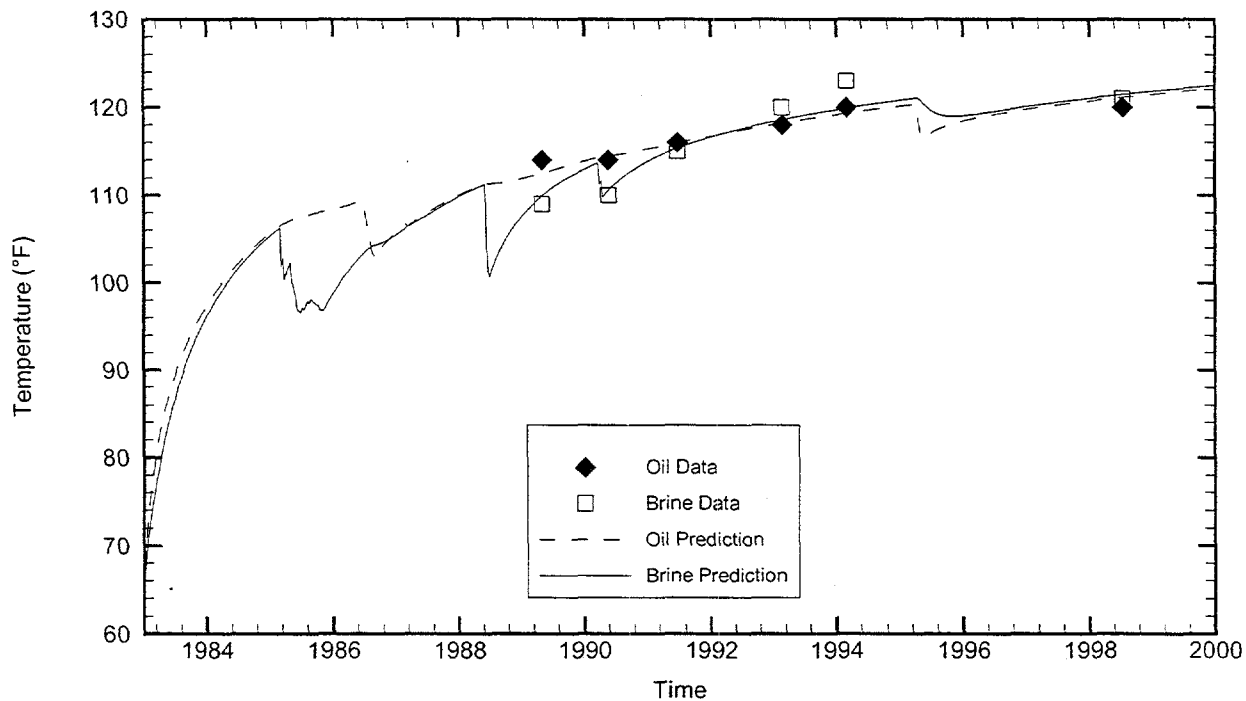
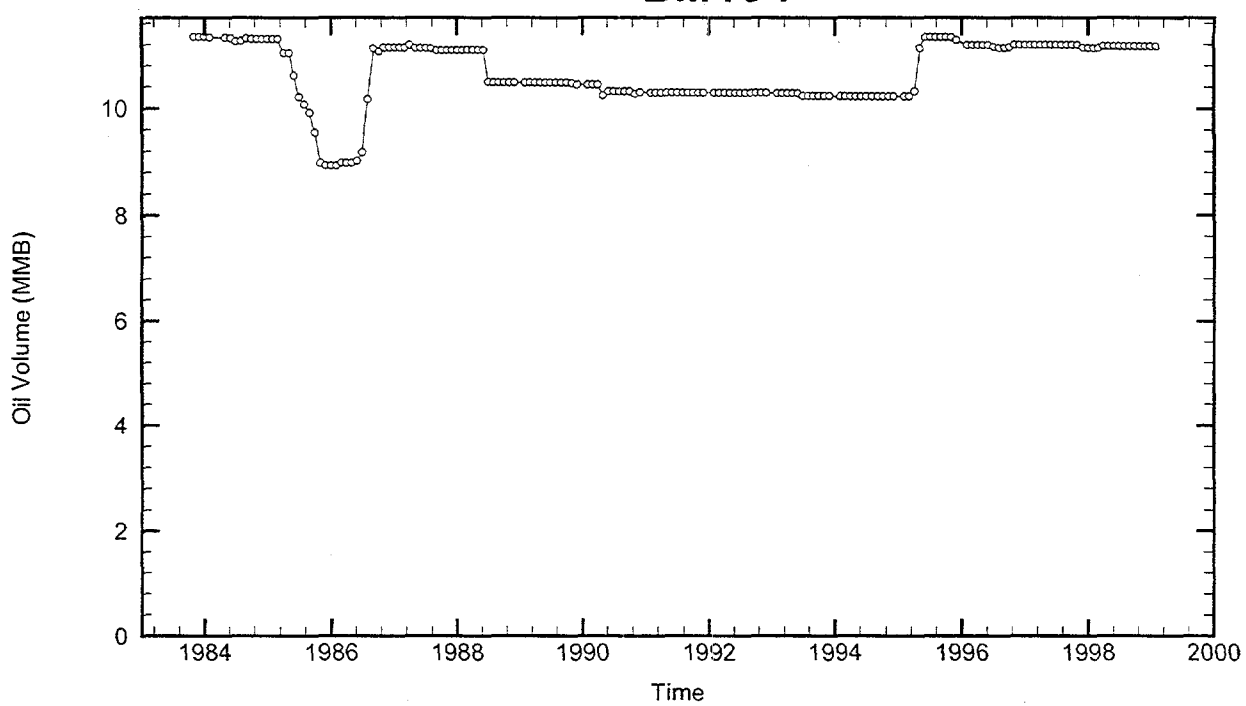
Cavern: BM103
End of Leaching: 04/30/1984
Duration of Leaching: 2.3333 years
Leaching Temperature: 66.03 °F

Degas: 04/02/1997, 120.00 °F, 8.96 MMB
Oil Injection Temperature: 70.90 °F
Brine Injection Temperature: 50.00 °F
Number of iterations: 251

BM103



BM104



Cavern: BM104

End of Leaching: 01/01/1983

Duration of Leaching: 0.0000 days

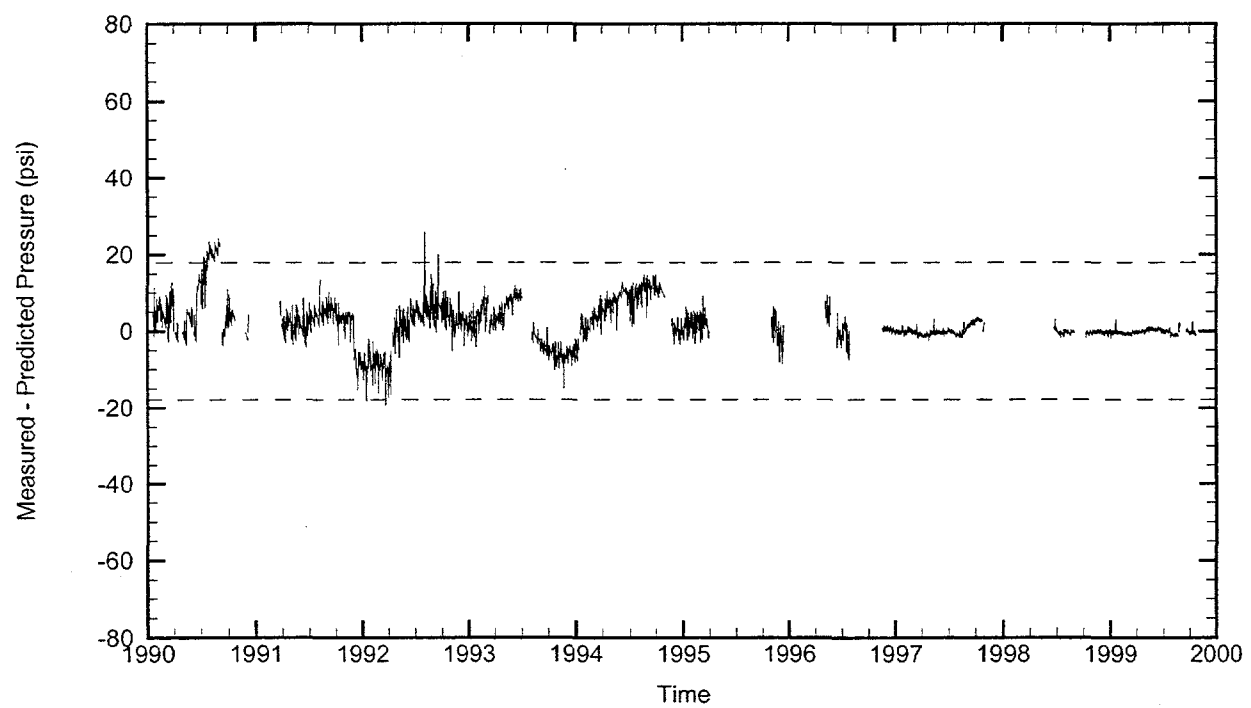
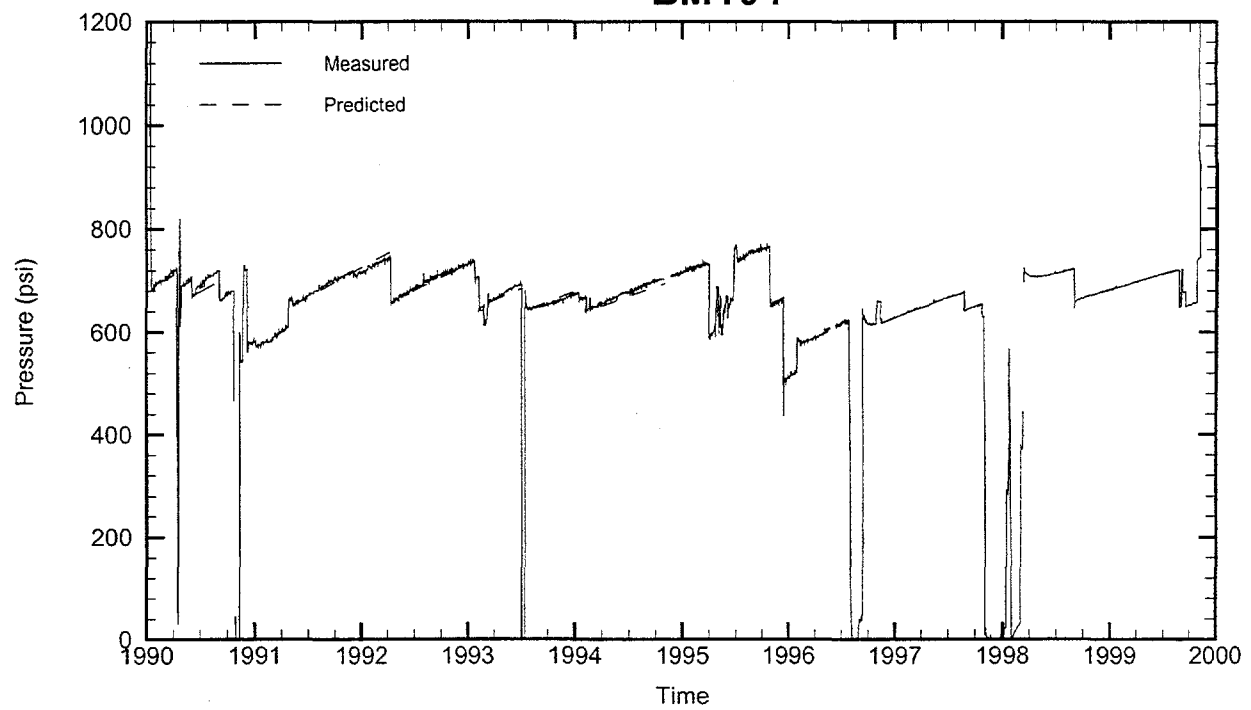
Leaching Temperature: 64.00 °F

Oil Injection Temperature: 59.90 °F

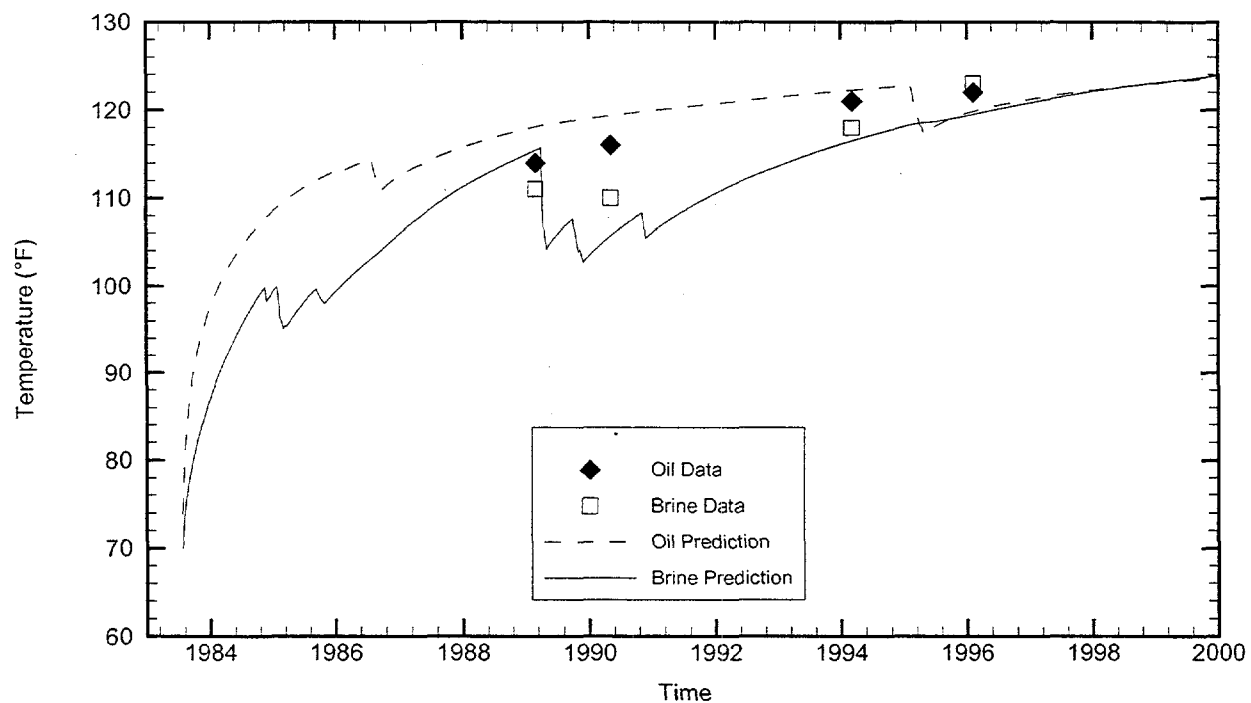
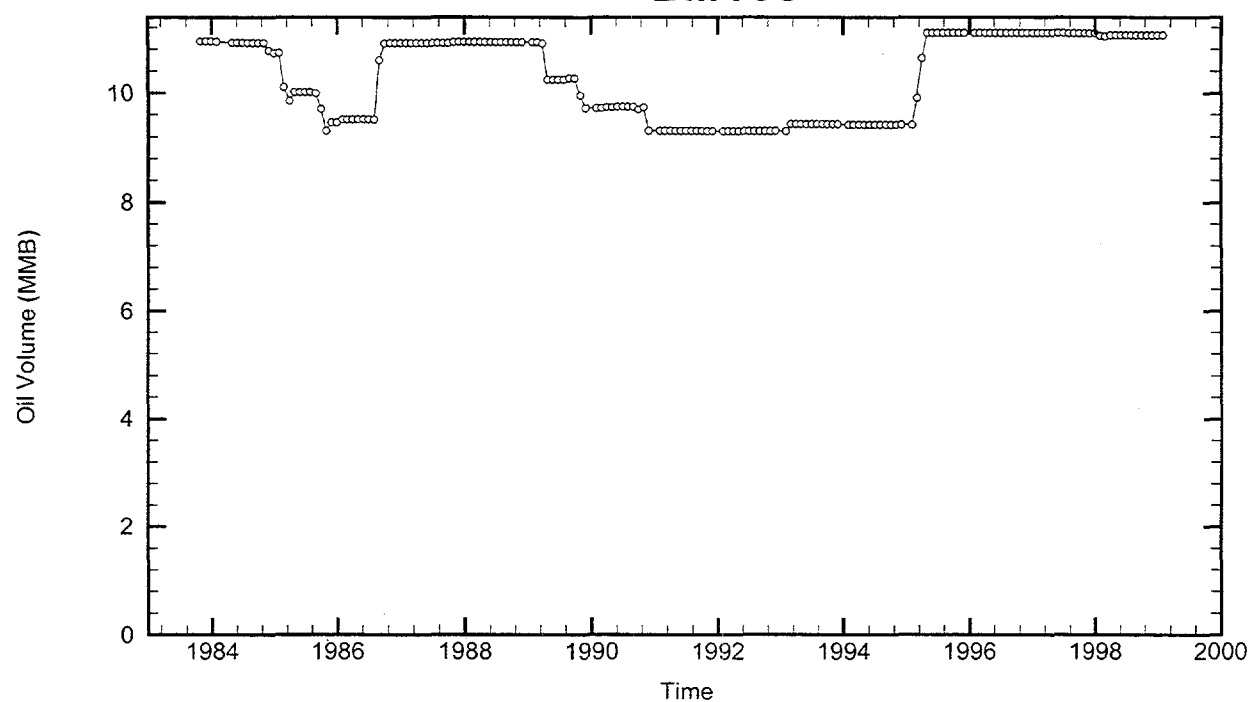
Brine Injection Temperature: 88.15 °F

Number of iterations: 410

BM104



BM105



Cavern: BM105

End of Leaching: 07/25/1983

Duration of Leaching: 0.0000 days

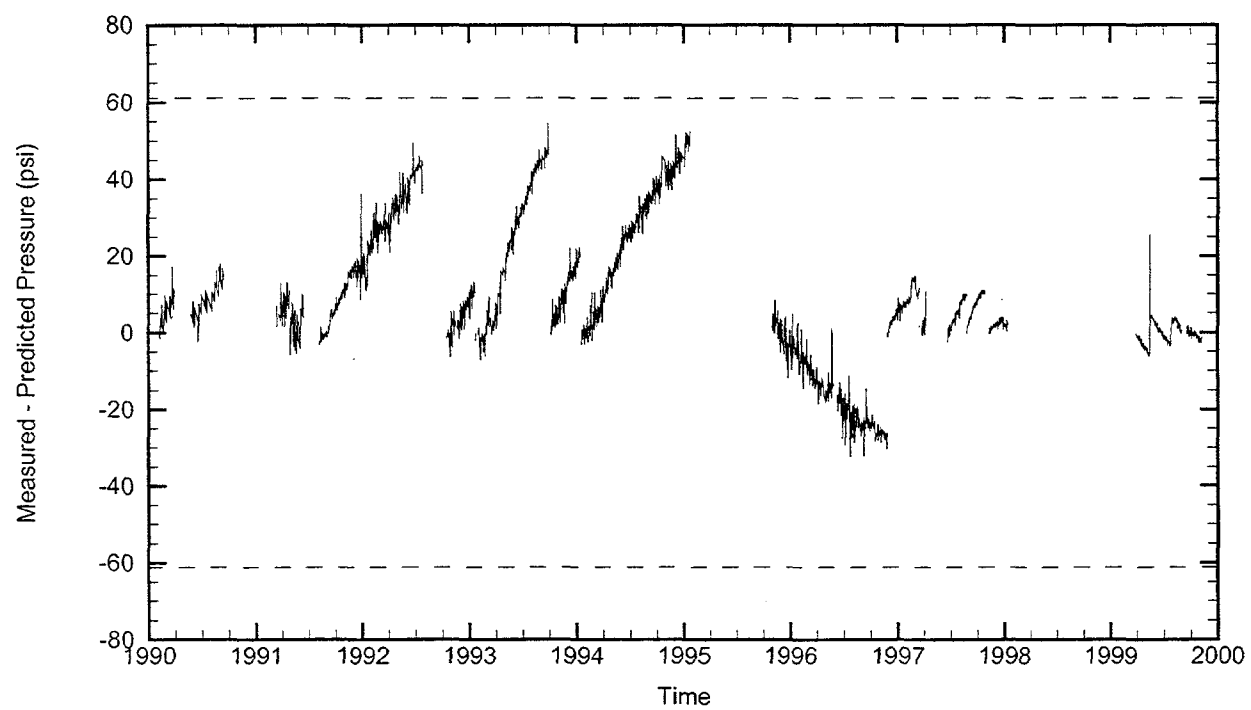
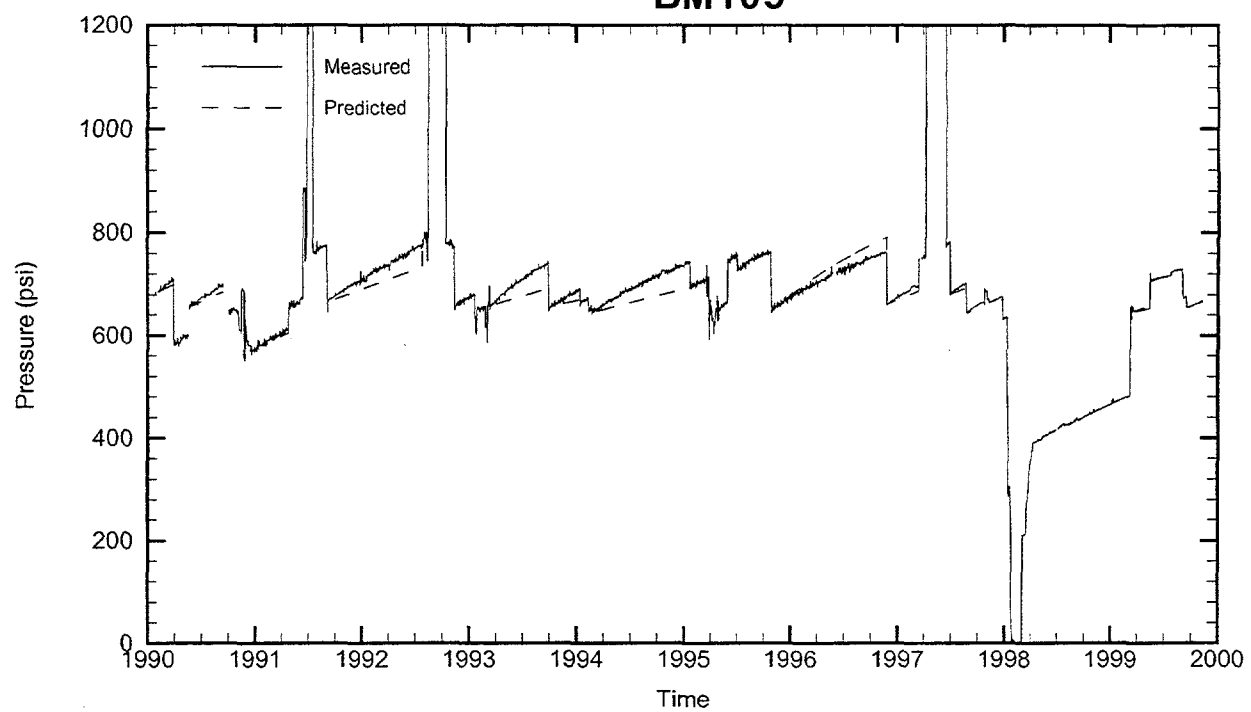
Leaching Temperature: 69.97 °F

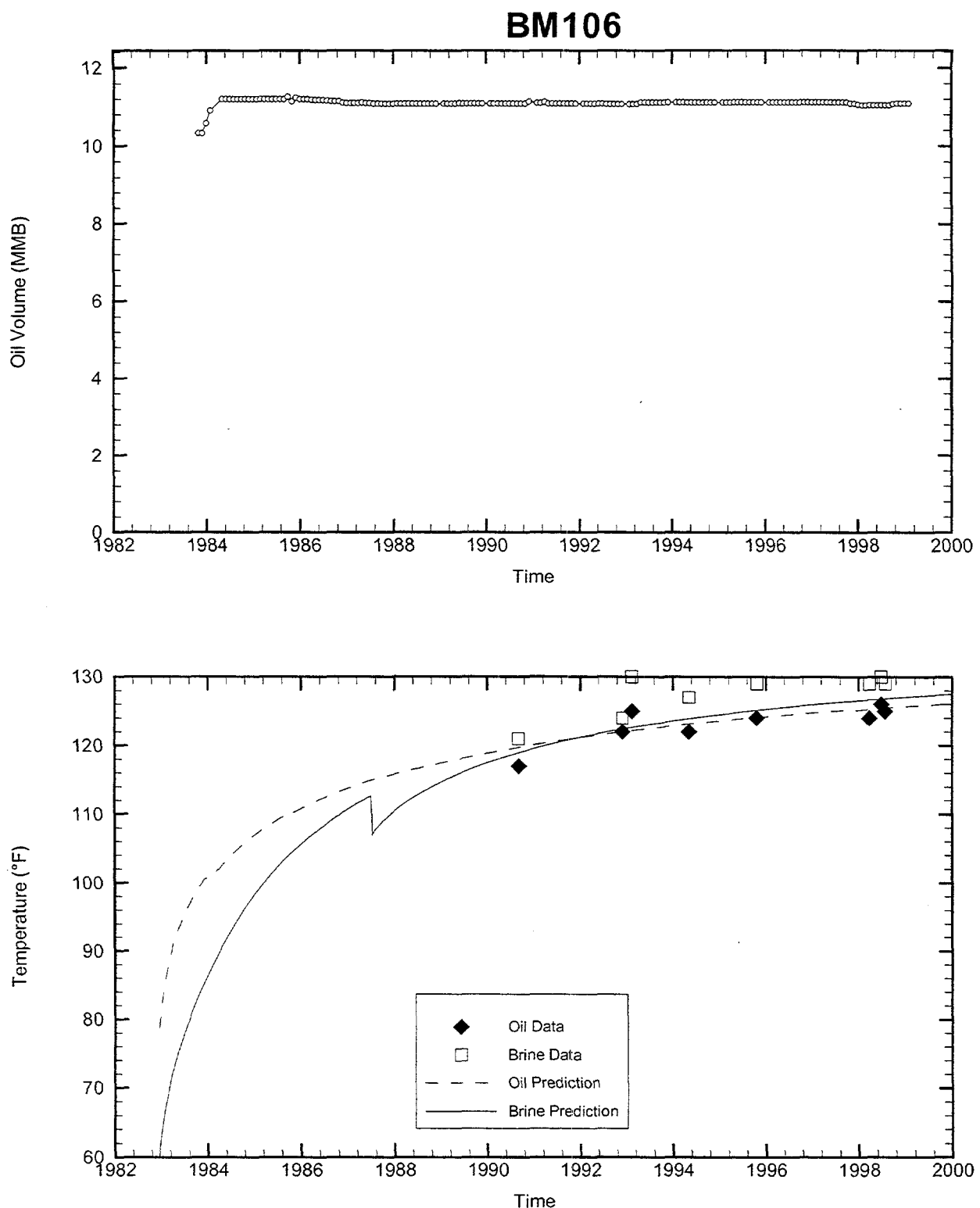
Oil Injection Temperature: 73.90 °F

Brine Injection Temperature: 89.85 °F

Number of iterations: 262

BM105

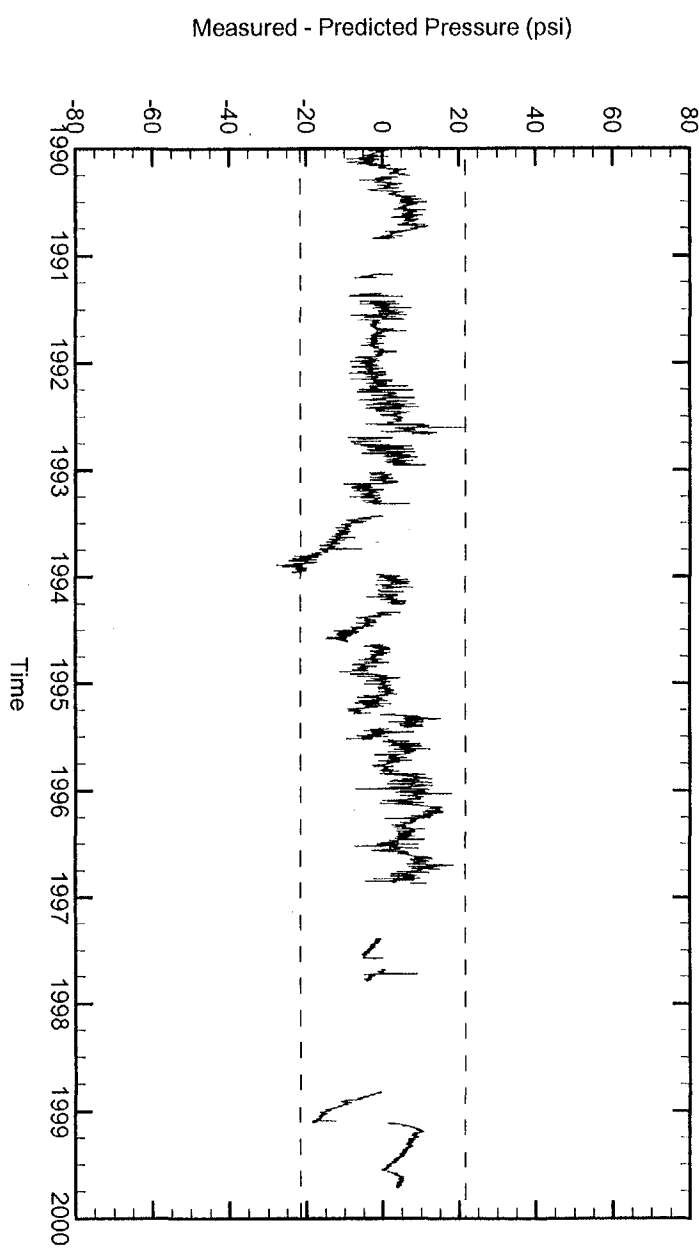
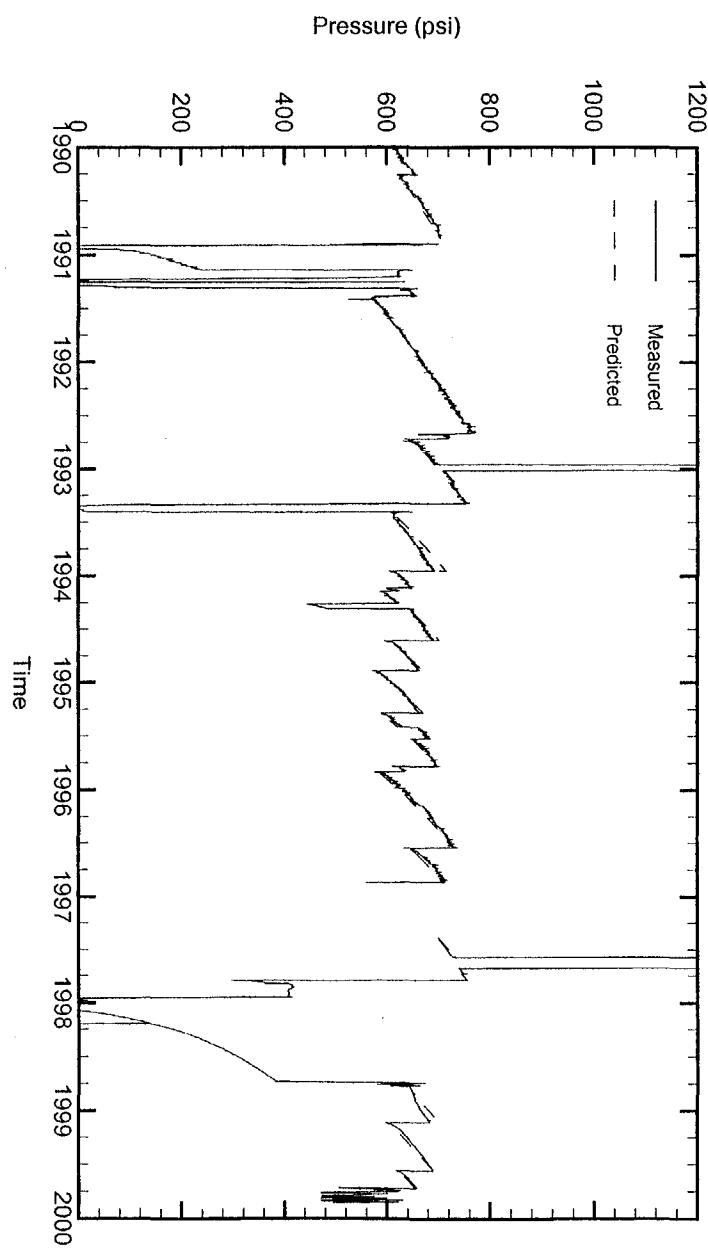




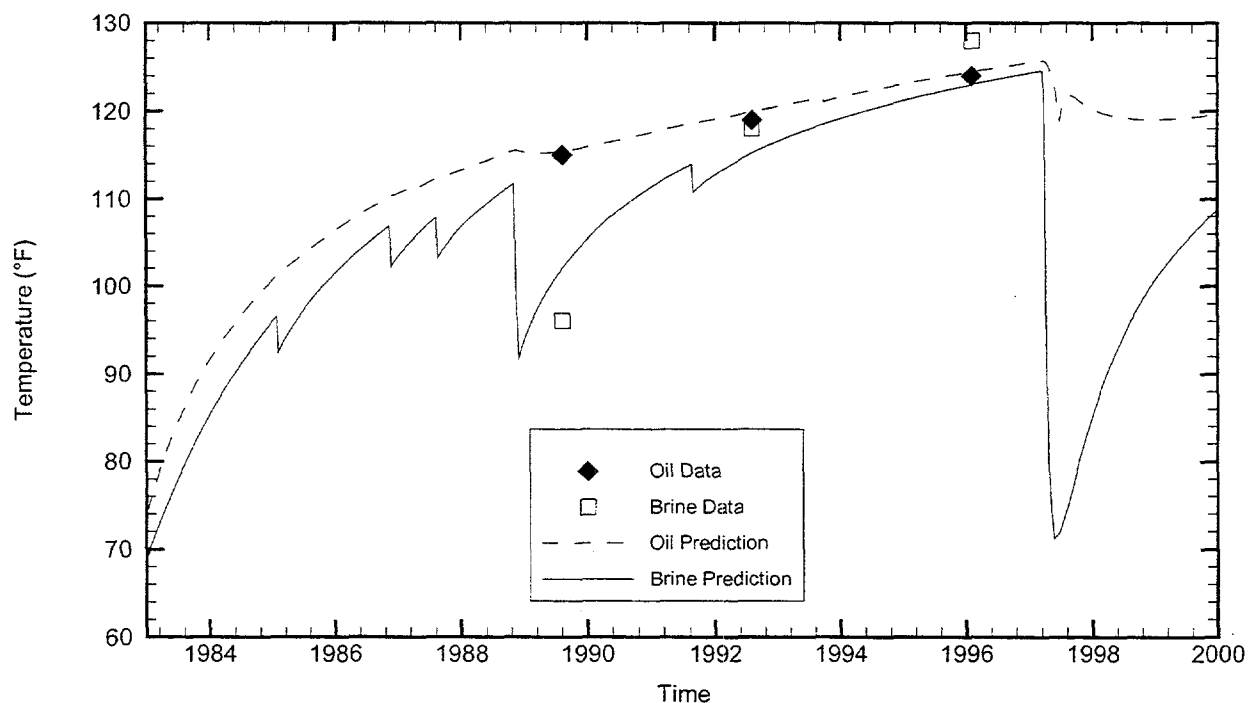
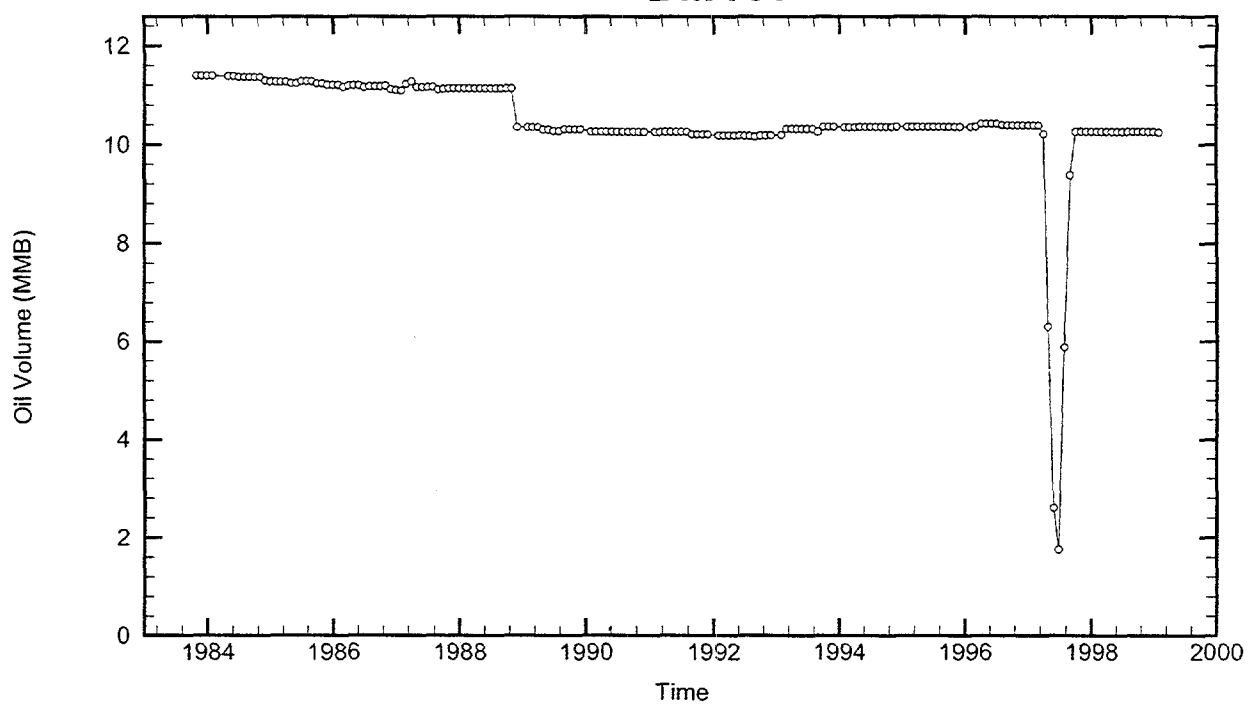
Cavern: BM106
 End of Leaching: 12/16/1982
 Duration of Leaching: 1.2500 years
 Leaching Temperature: 60.14 °F

Degas: 12/13/1997, 125.00 °F, 6.70 MMB
 Oil Injection Temperature: 78.70 °F
 Brine Injection Temperature: 50.30 °F
 Number of iterations: 275

BM106



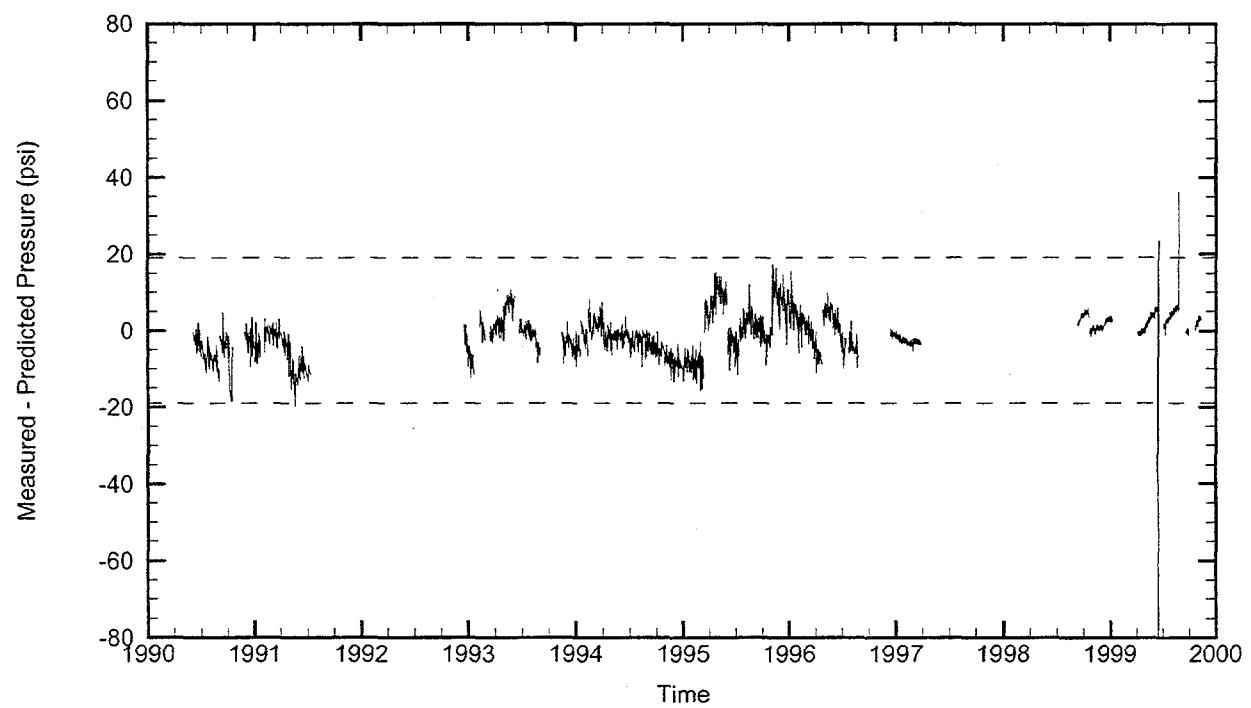
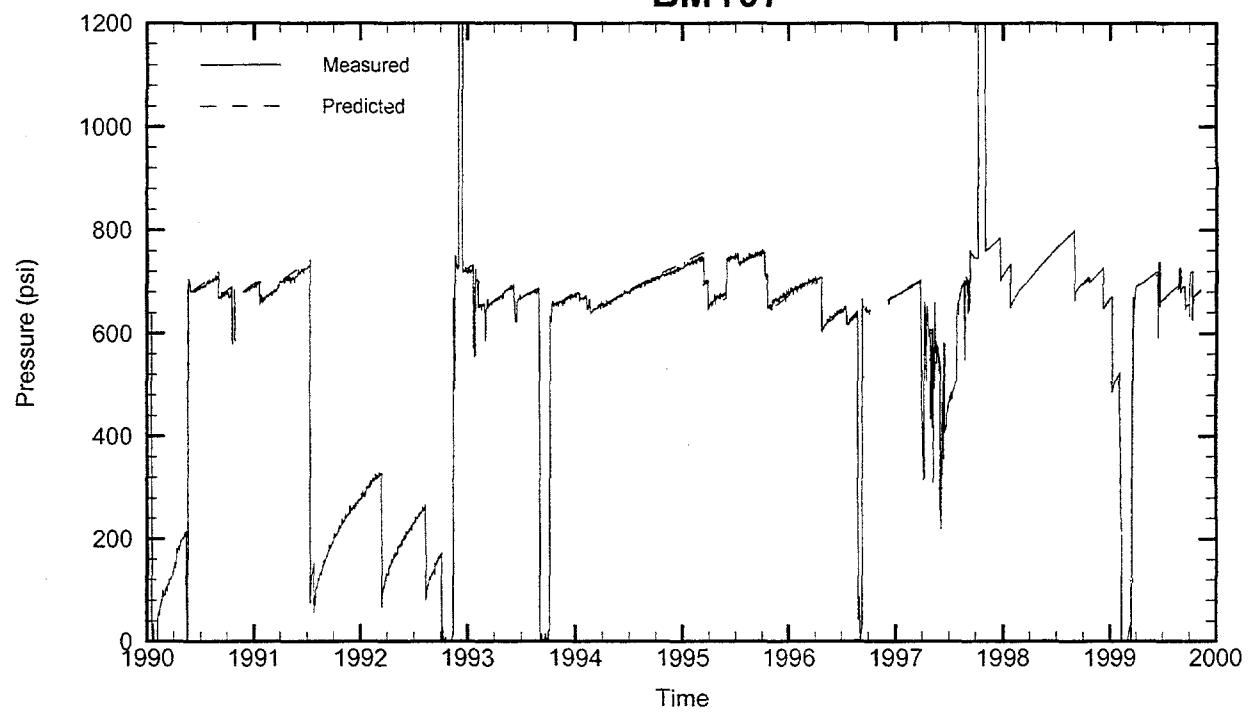
BM107



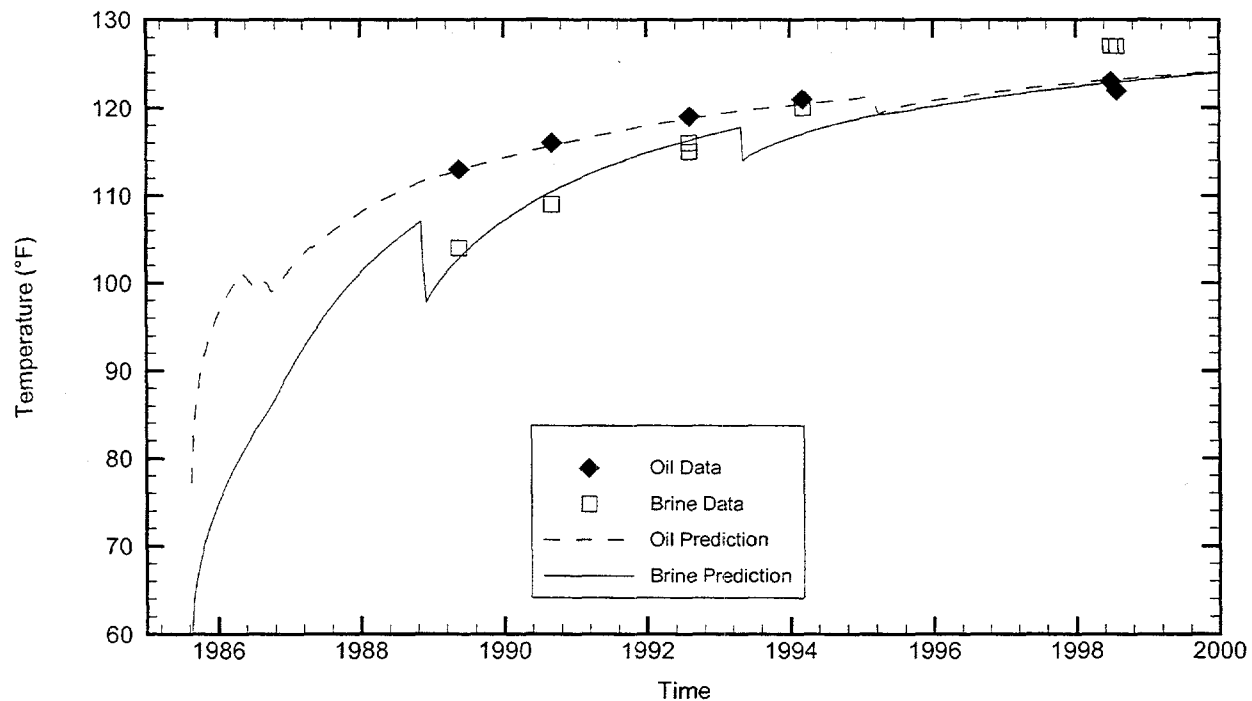
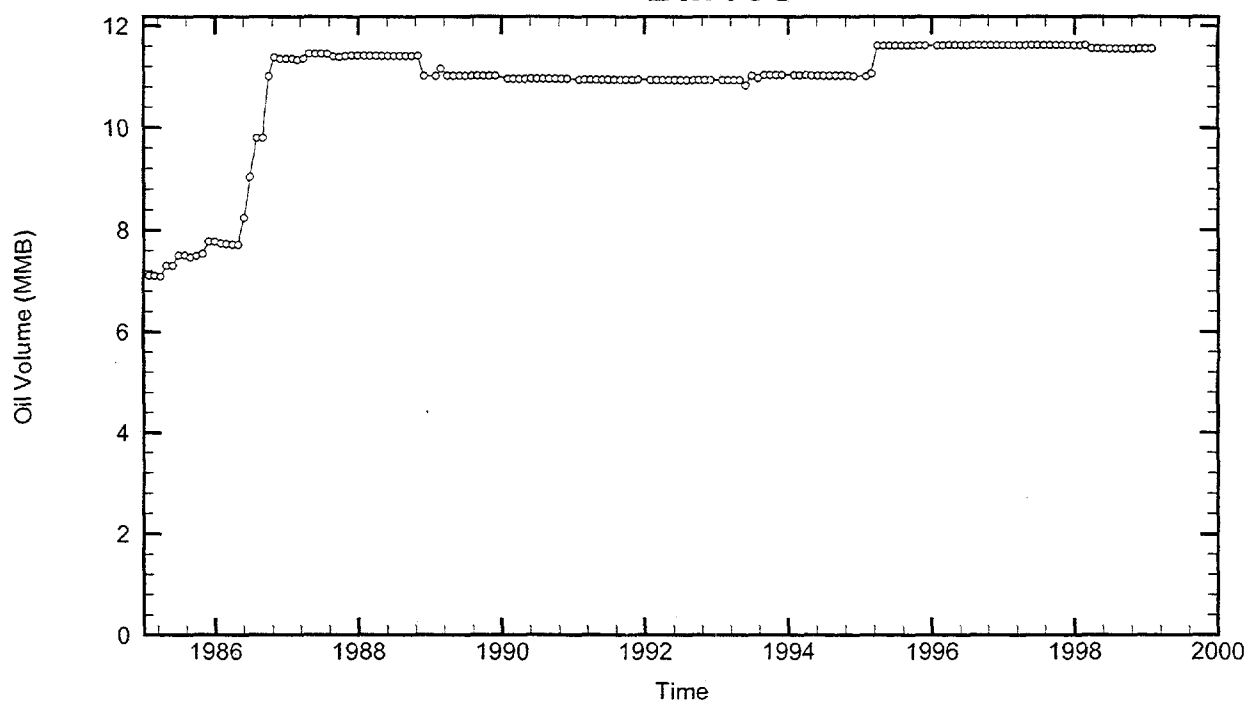
Cavern: BM107
 End of Leaching: 01/04/1983
 Duration of Leaching: 10.1520 months
 Leaching Temperature: 68.89 °F

Degas: 07/02/1997, 125.00 °F, 8.27 MMB
 Oil Injection Temperature: 74.19 °F
 Brine Injection Temperature: 50.03 °F
 Number of iterations: 135

BM107



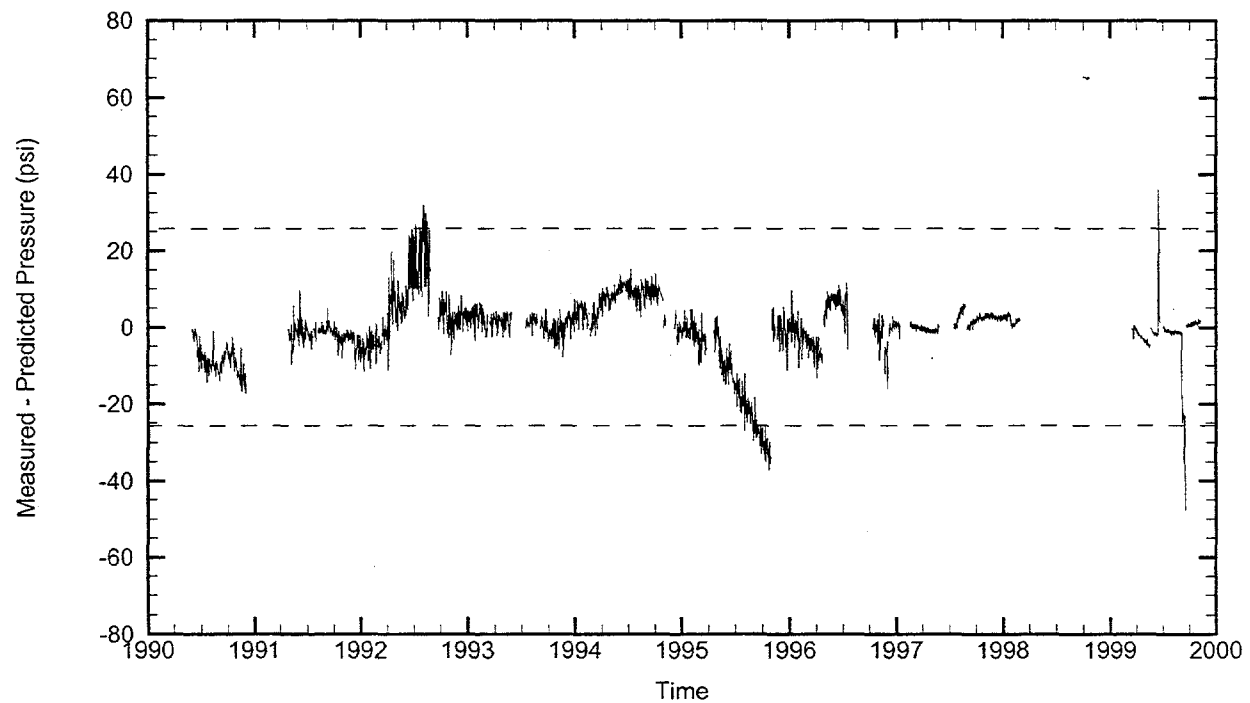
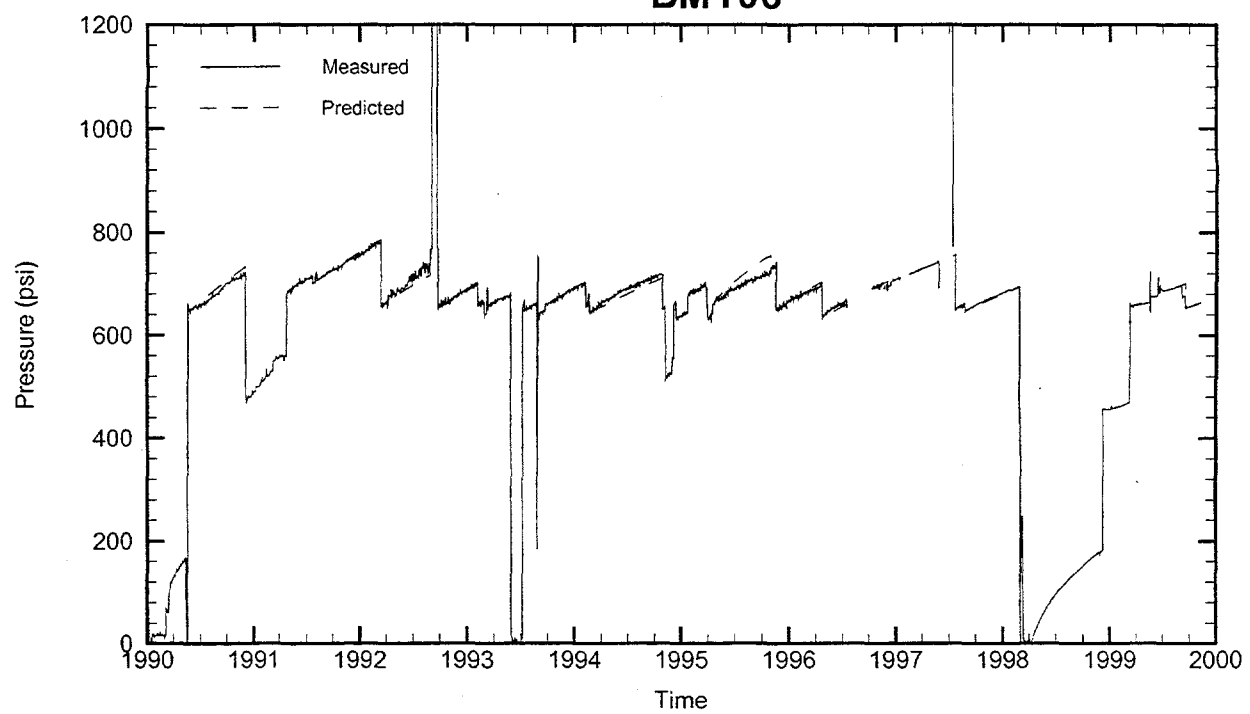
BM108



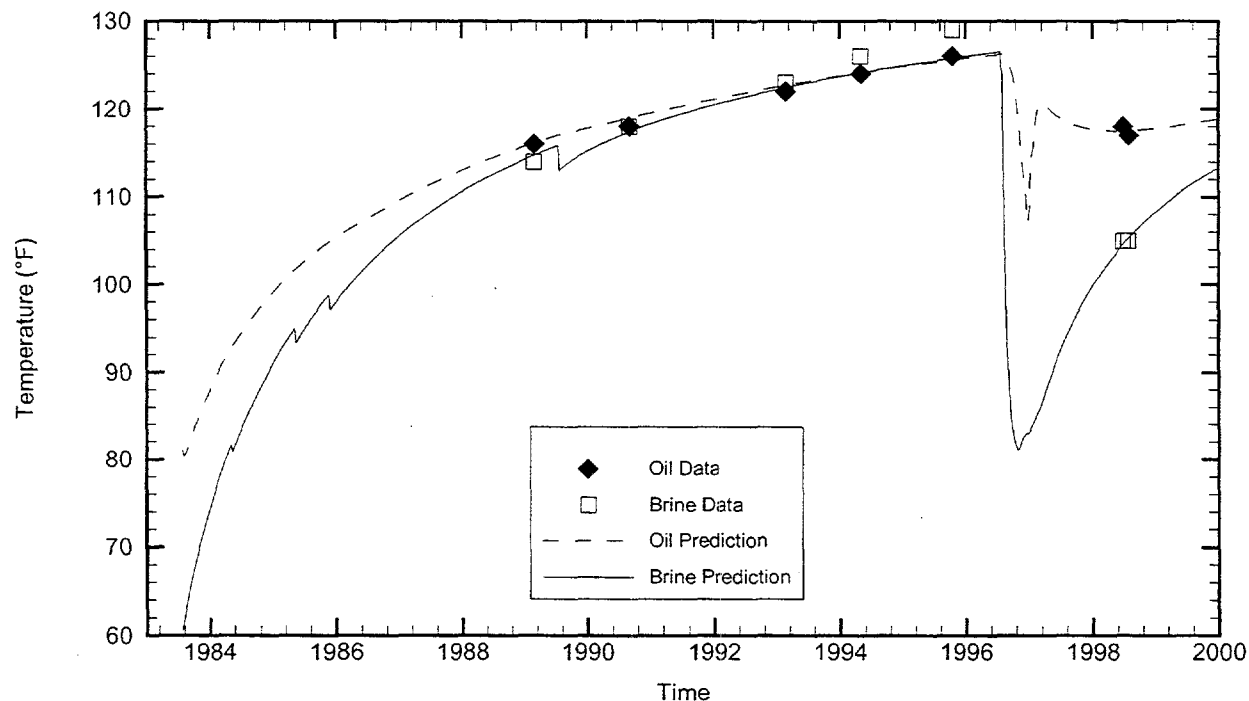
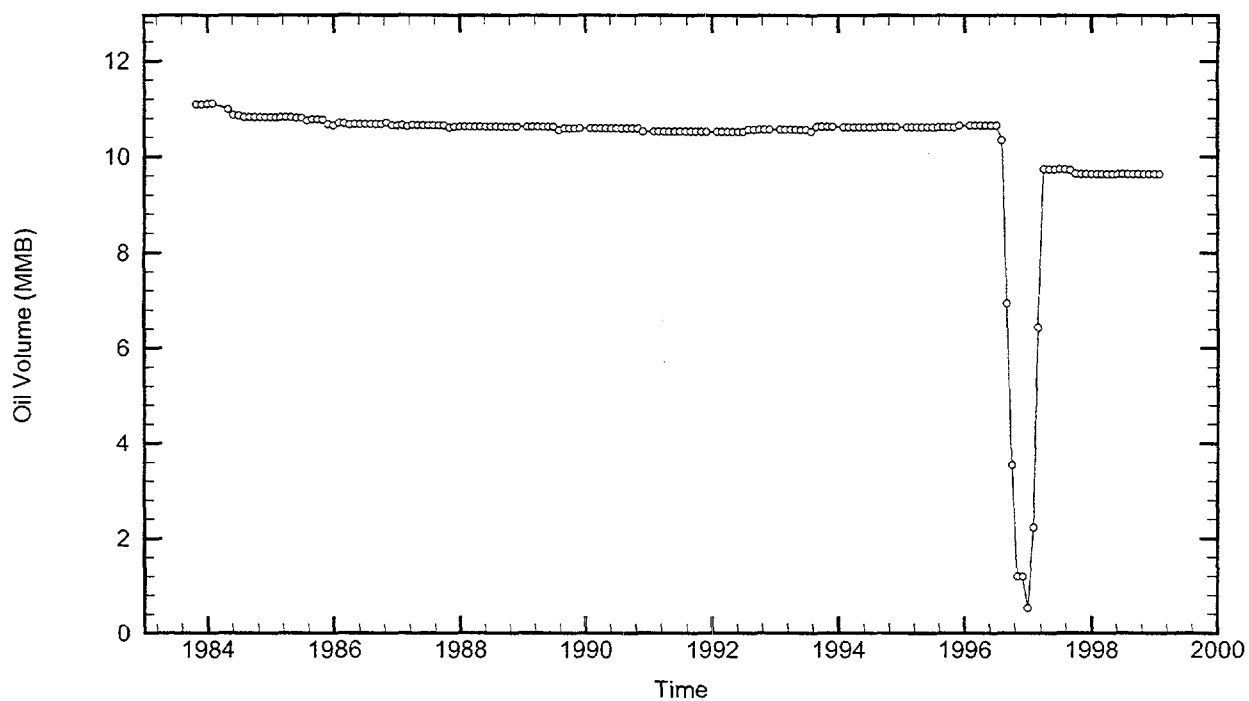
Cavern: BM108
End of Leaching: 08/20/1985
Duration of Leaching: 0.0000 days
Leaching Temperature: 60.00 °F

Oil Injection Temperature: 77.18 °F
Brine Injection Temperature: 77.12 °F
Number of iterations: 452

BM108



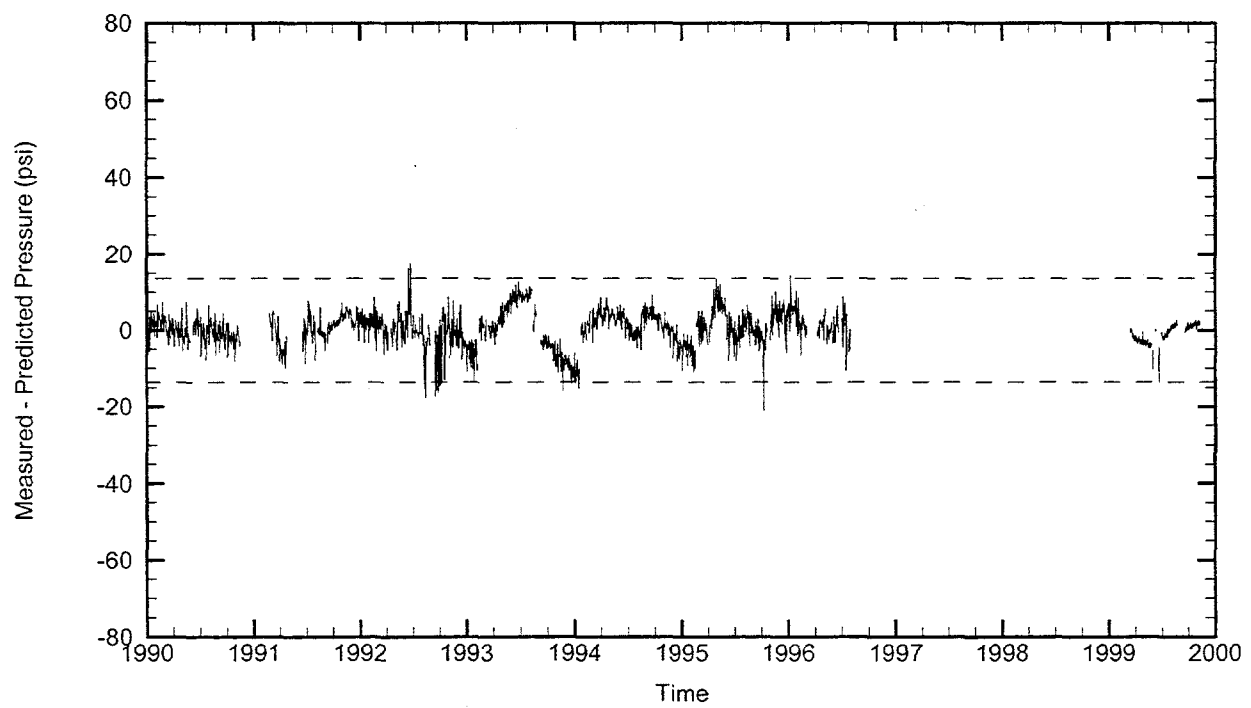
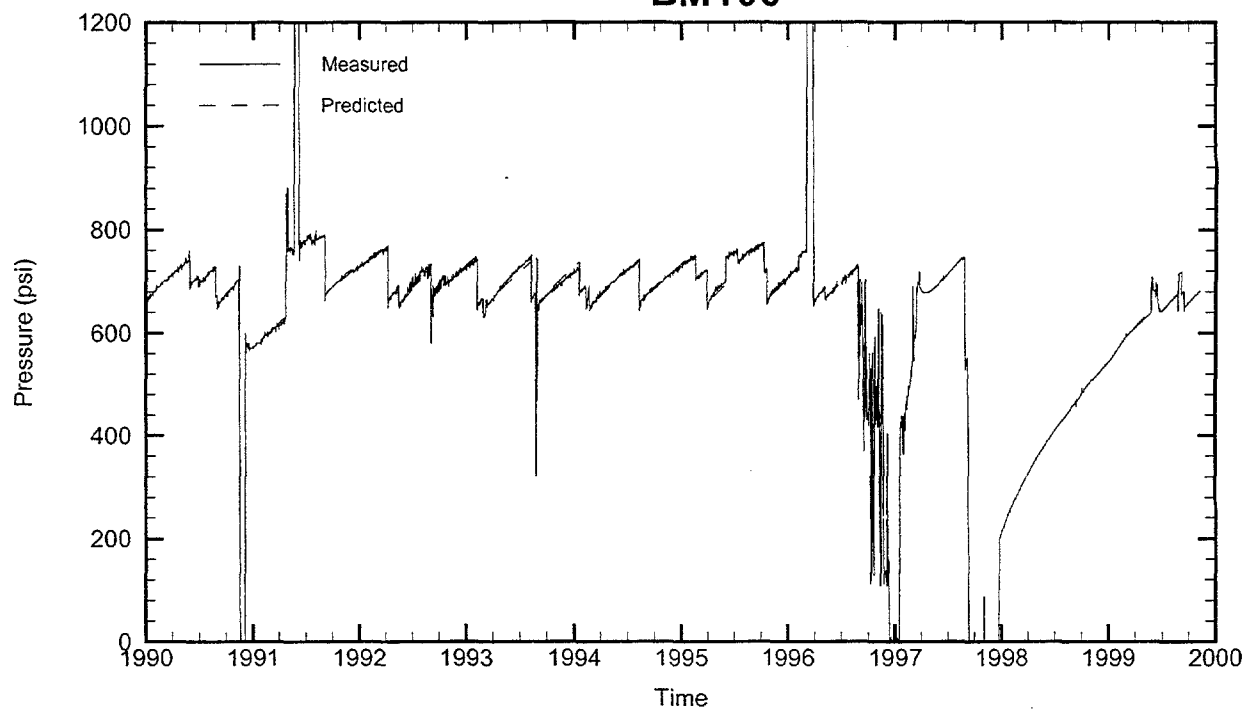
BM109

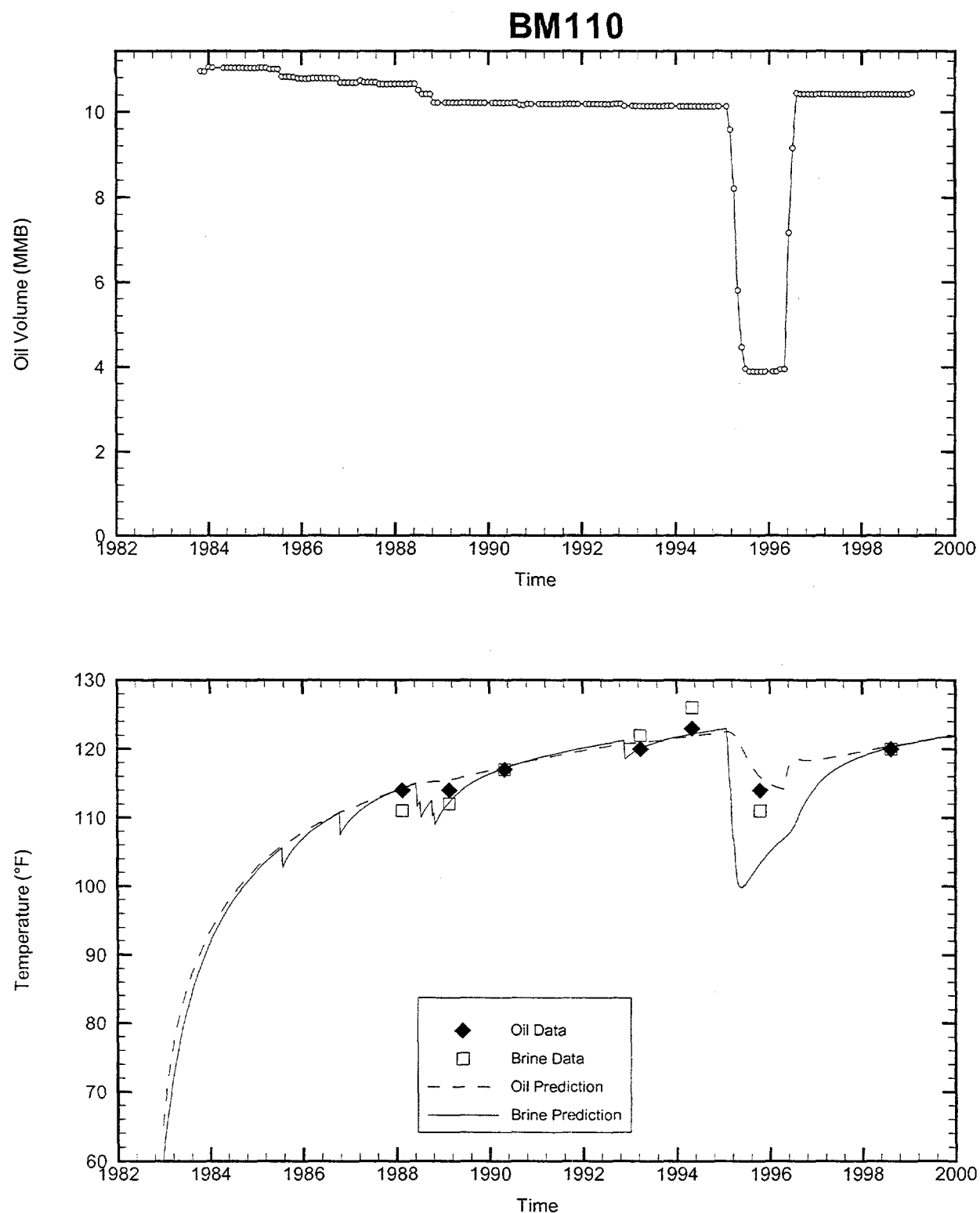


Cavern: BM109
 End of Leaching: 07/28/1983
 Duration of Leaching: 4.0739 months
 Leaching Temperature: 60.51 °F

Degas: 01/03/1997, 125.00 °F, 9.10 MMB
 Oil Injection Temperature: 81.00 °F
 Brine Injection Temperature: 62.56 °F
 Number of iterations: 216

BM109

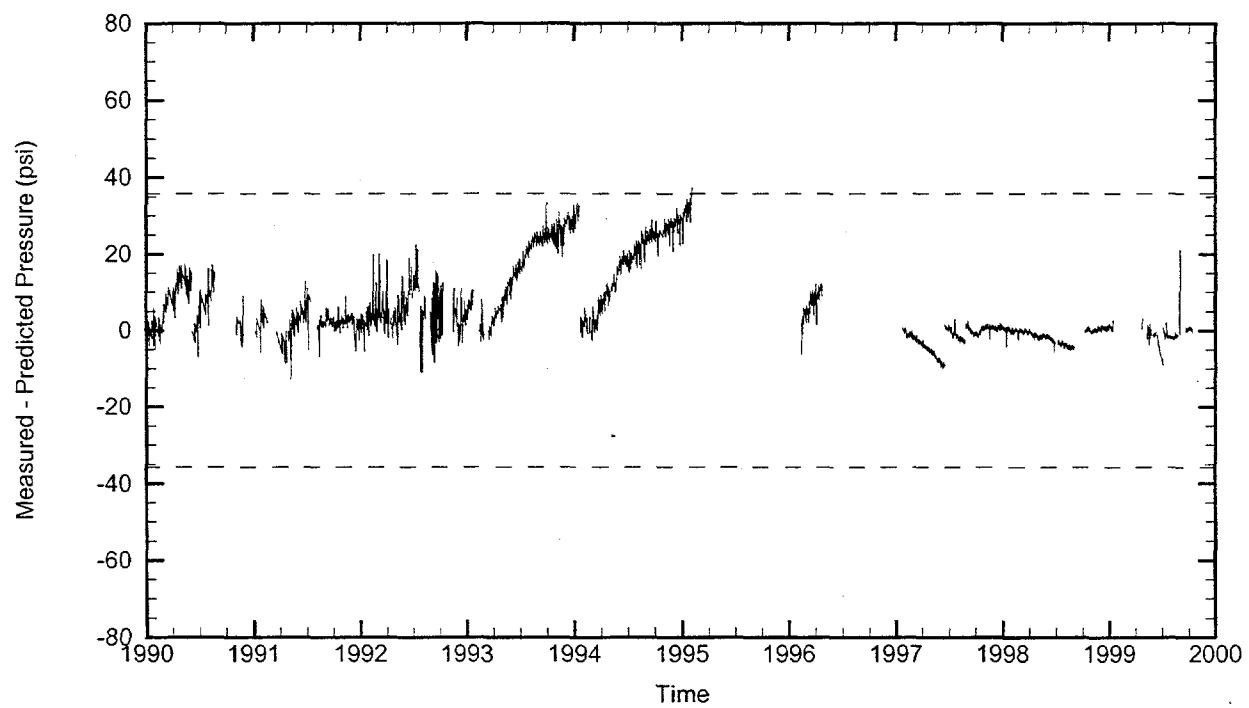
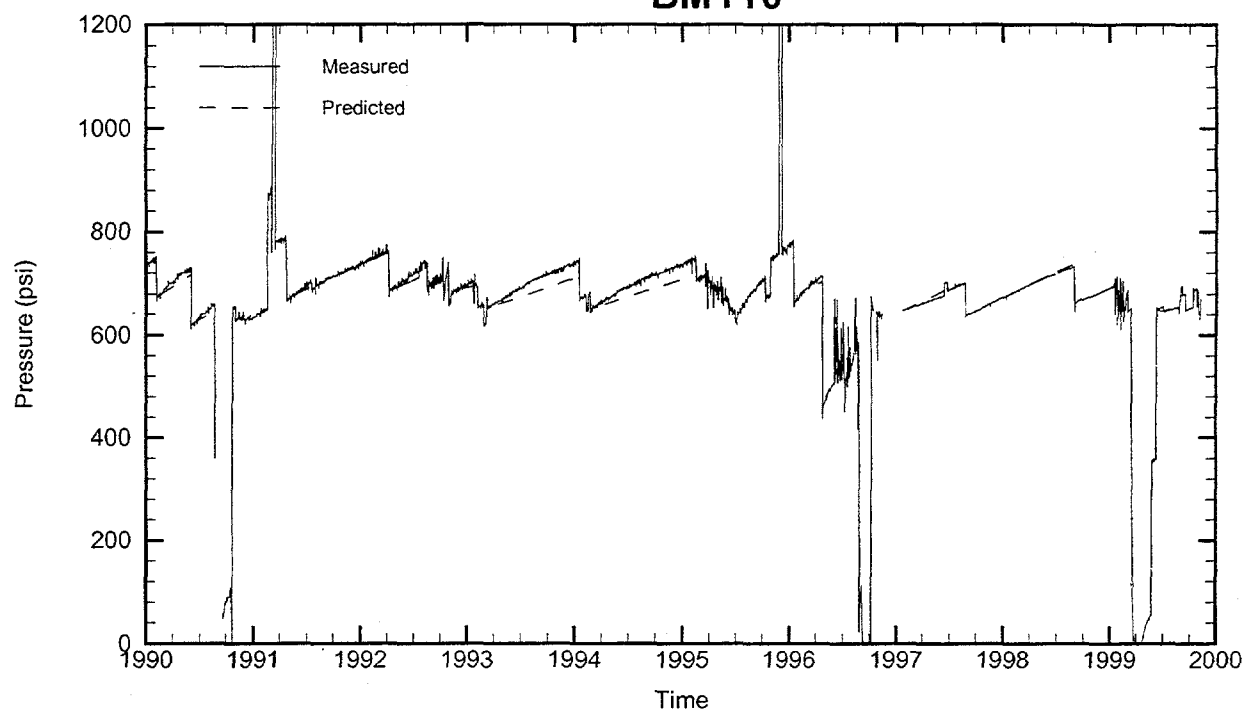




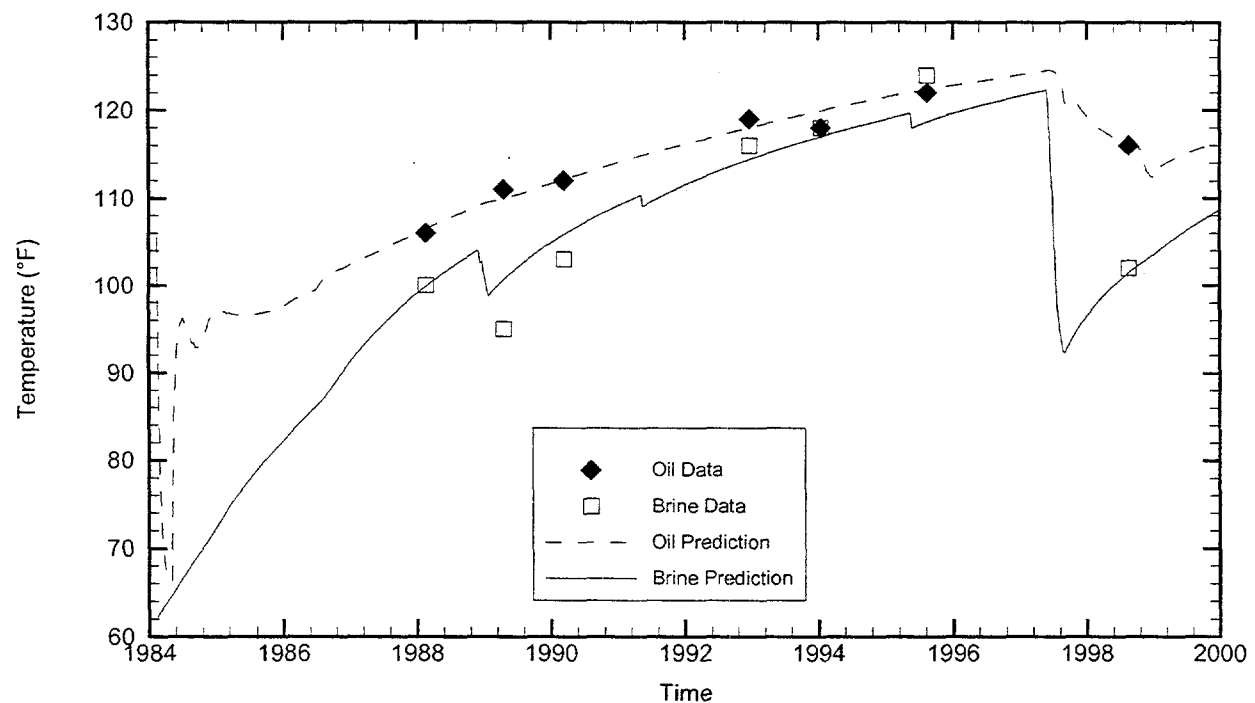
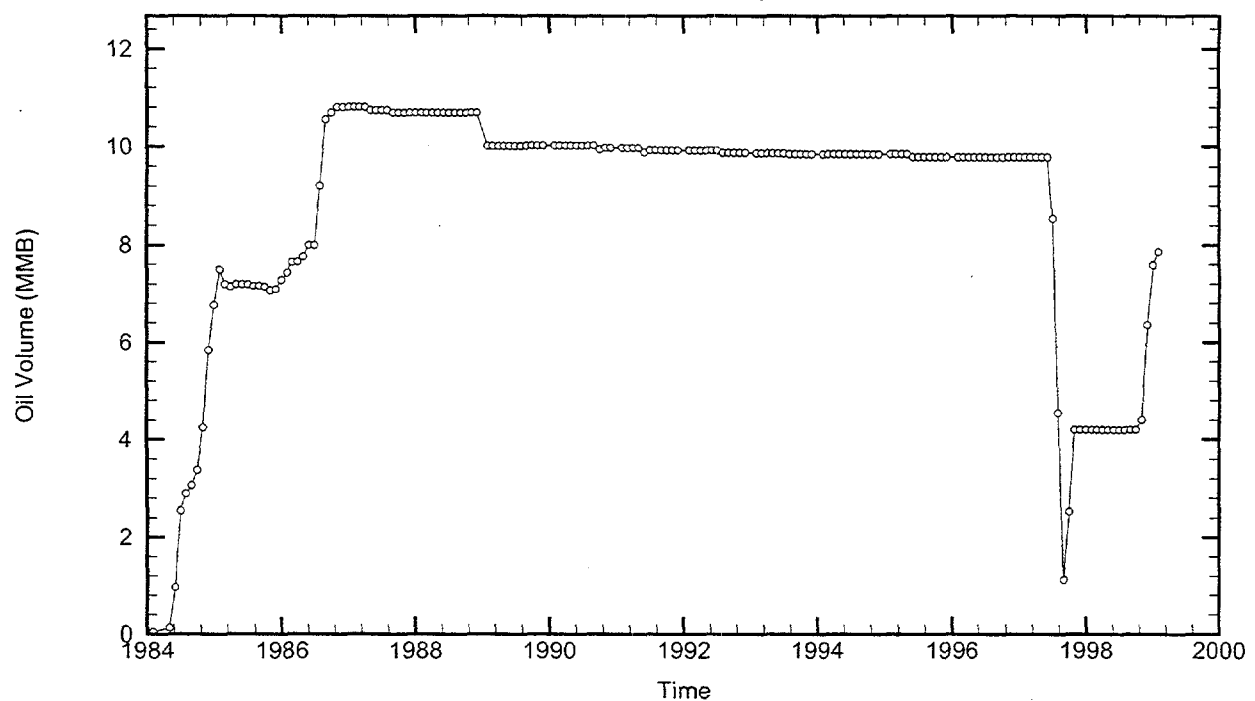
Cavern: BM110
 End of Leaching: 12/23/1982
 Duration of Leaching: 1.3142 months
 Leaching Temperature: 60.22 °F

Degas: 05/01/1996, 123.00 °F, 6.50 MMB
 Oil Injection Temperature: 65.07 °F
 Brine Injection Temperature: 89.98 °F
 Number of iterations: 281

BM110



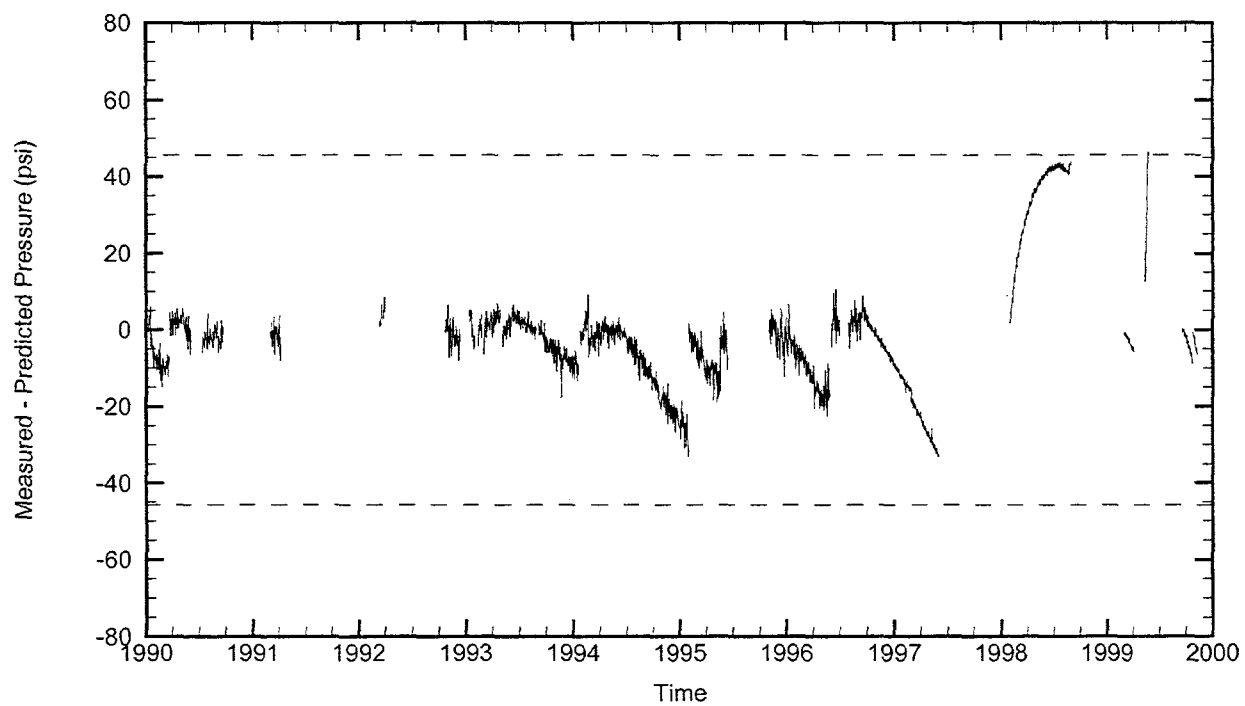
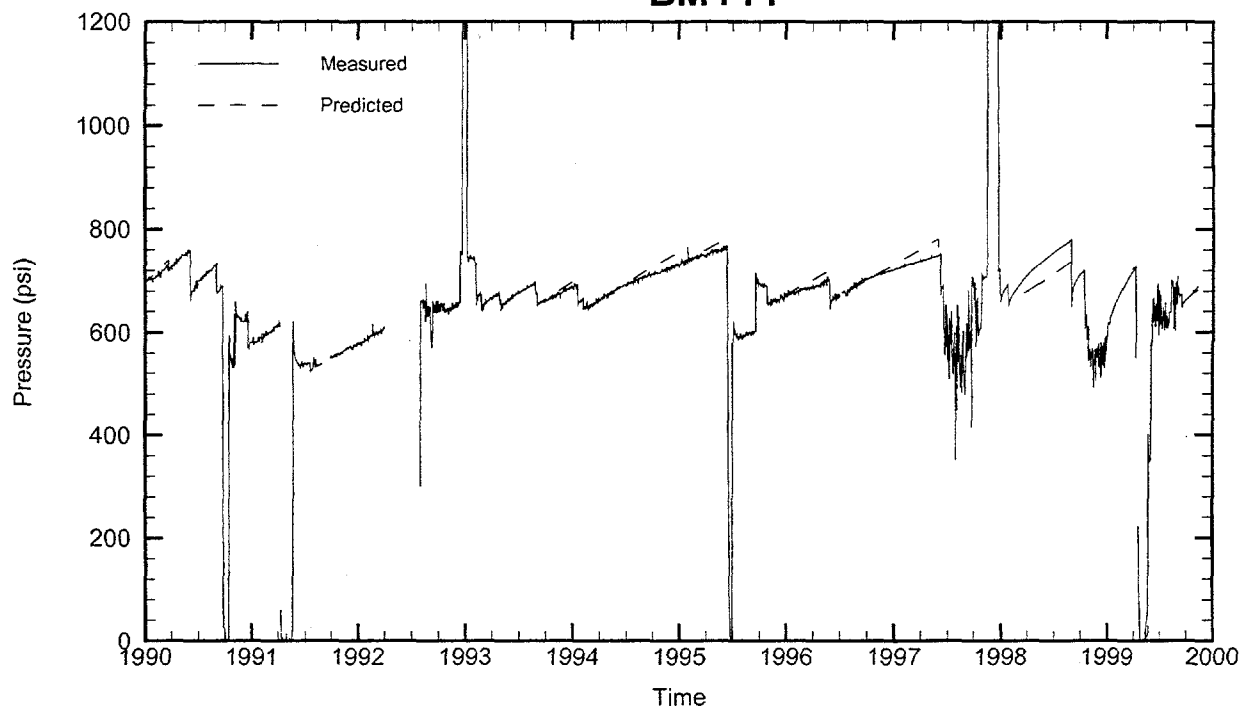
BM111



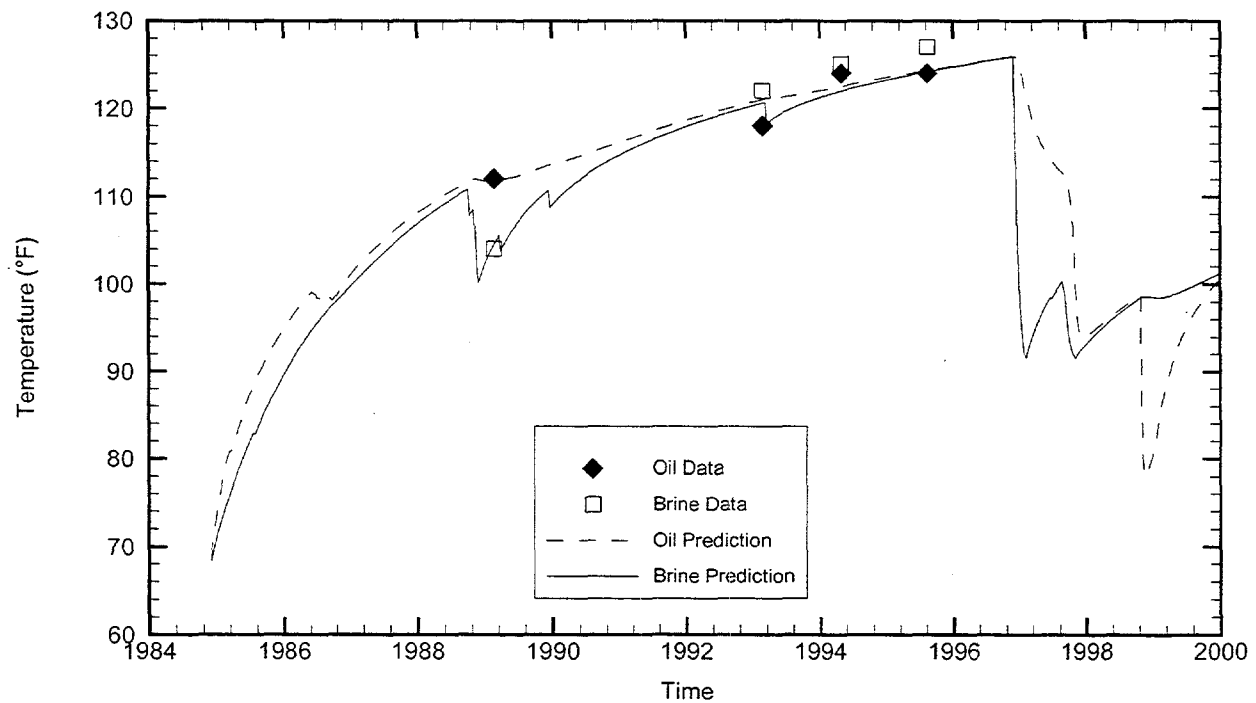
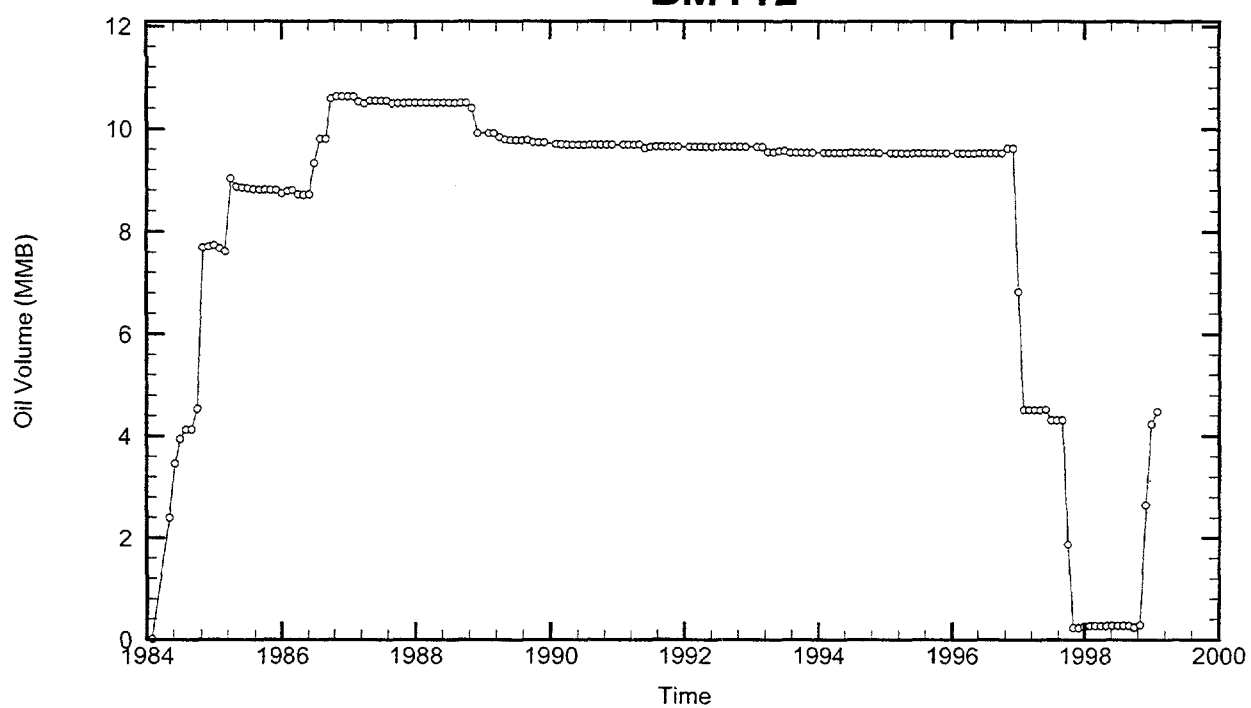
Cavern: BM111
 End of Leaching: 02/14/1984
 Duration of Leaching: 3.3374 years
 Leaching Temperature: 62.16 °F

Degas: 09/06/1997, 125.00 °F, 3.55 MMB
 Oil Injection Temperature: 105.52 °F
 Brine Injection Temperature: 78.18 °F
 Number of iterations: 444

BM111



BM112



Cavern: BM112

End of Leaching: 11/30/1984

Duration of Leaching: 2.6612 months

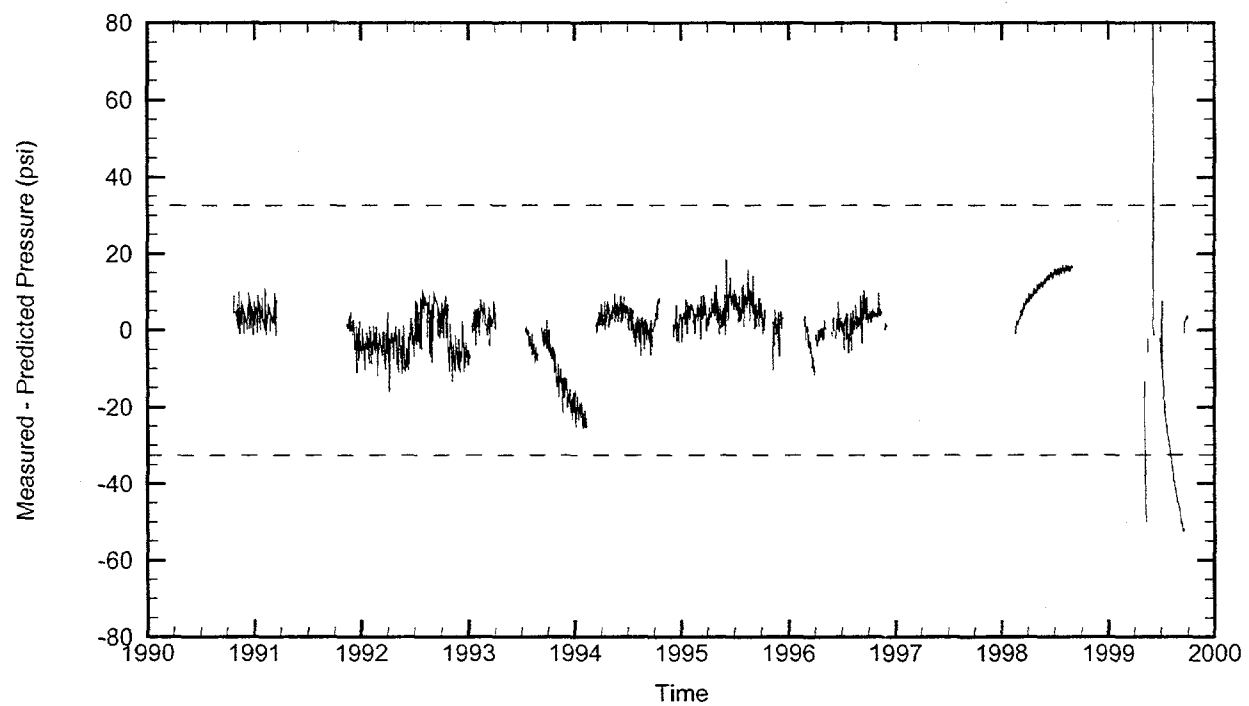
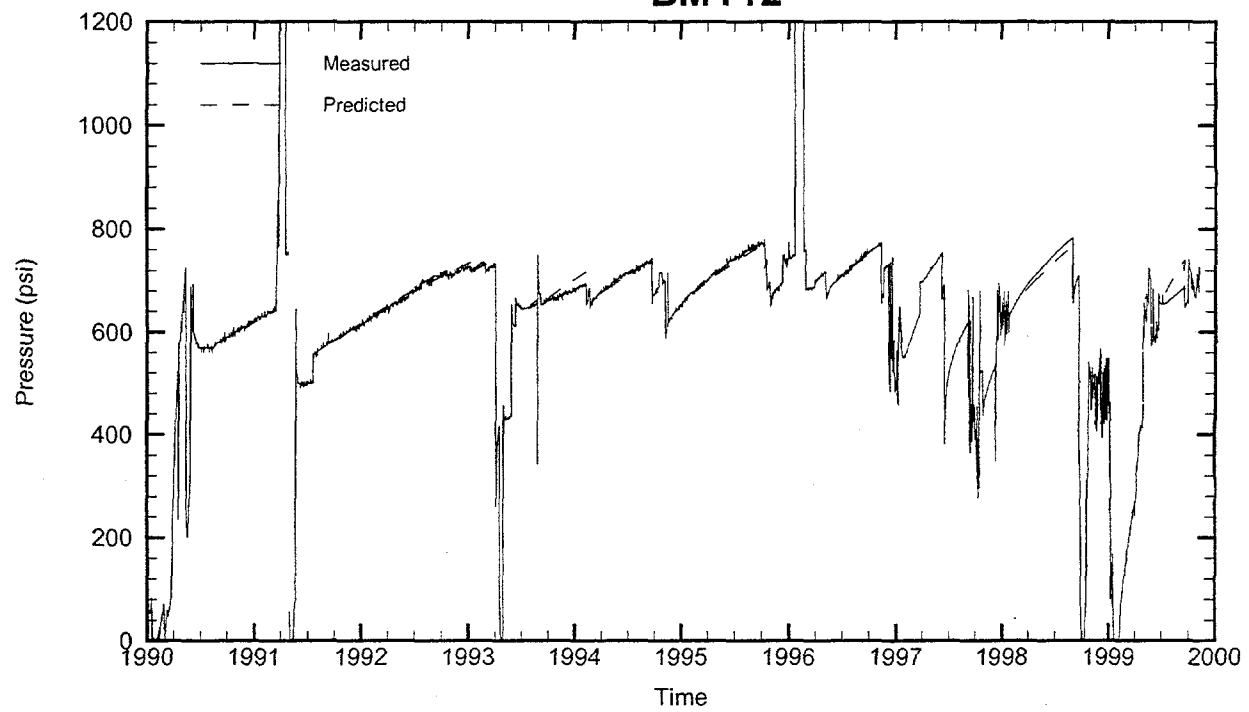
Leaching Temperature: 68.38 °F

Oil Injection Temperature: 68.68 °F

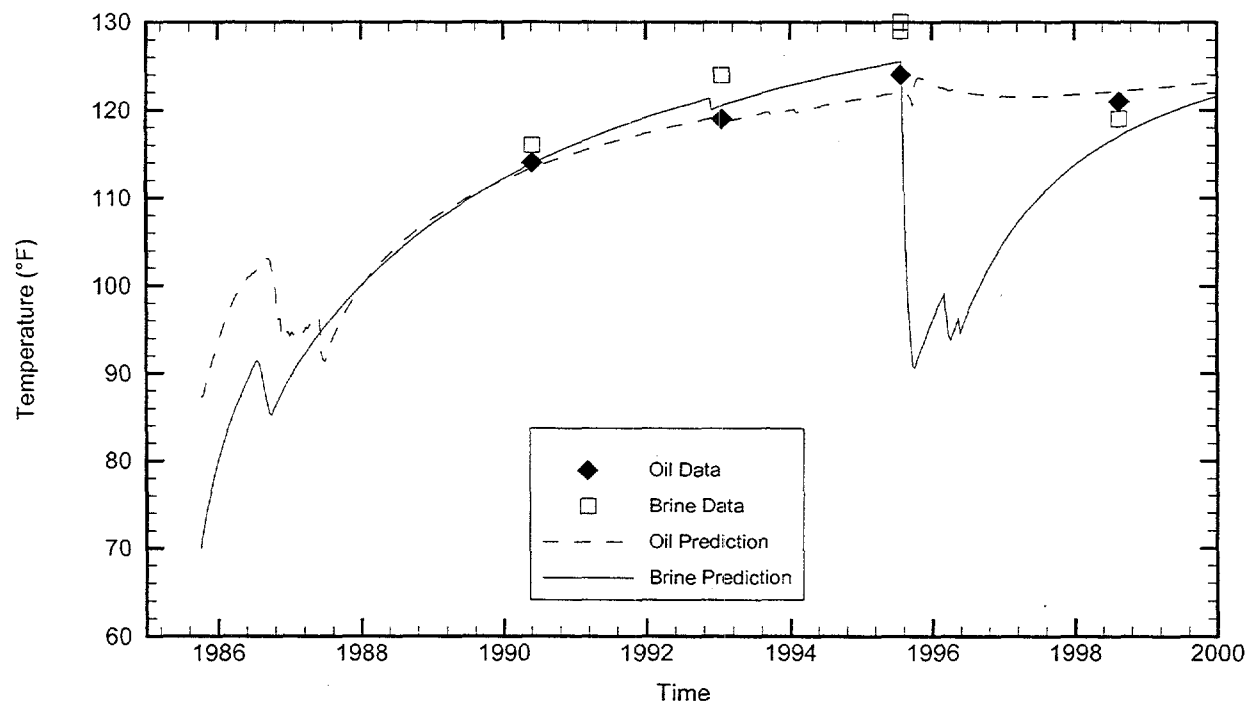
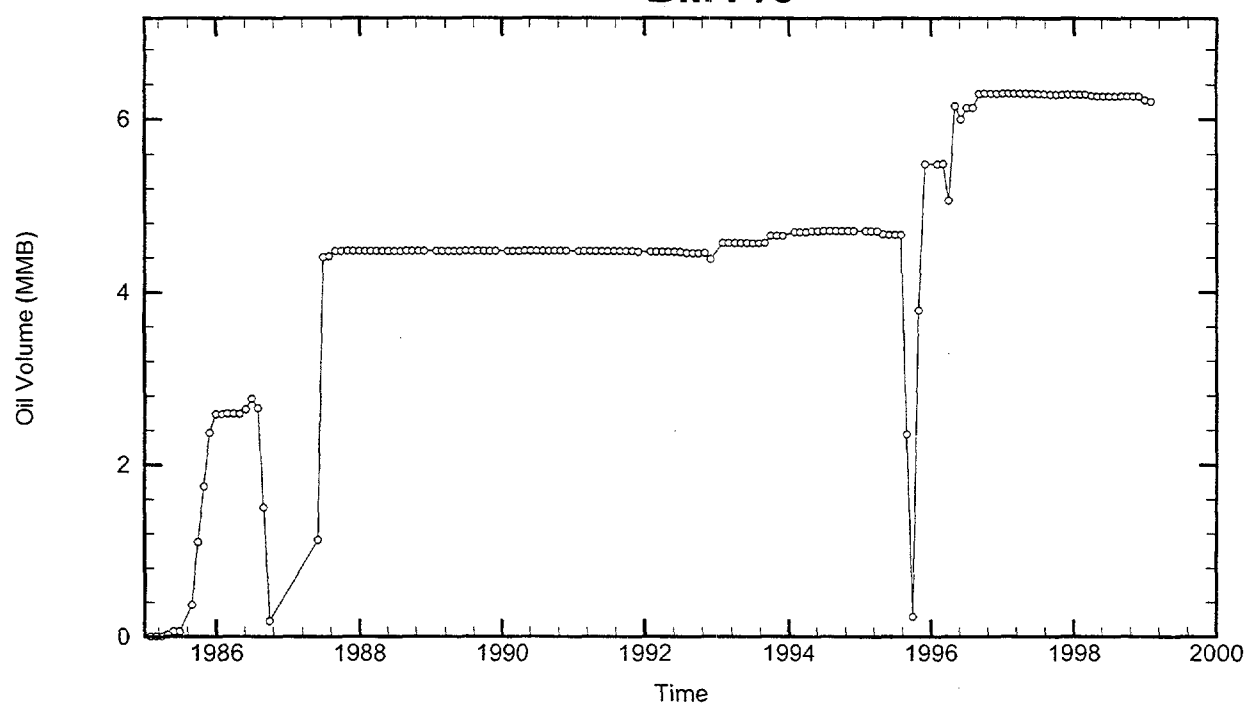
Brine Injection Temperature: 67.87 °F

Number of iterations: 705

BM112



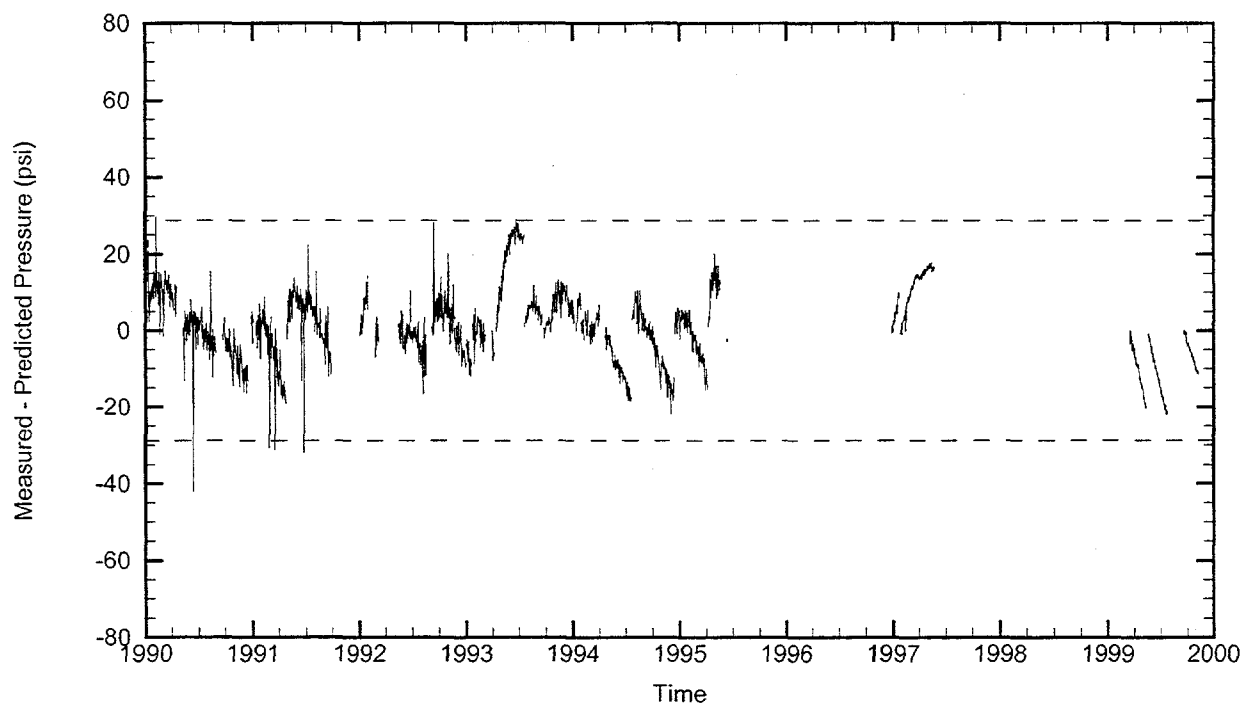
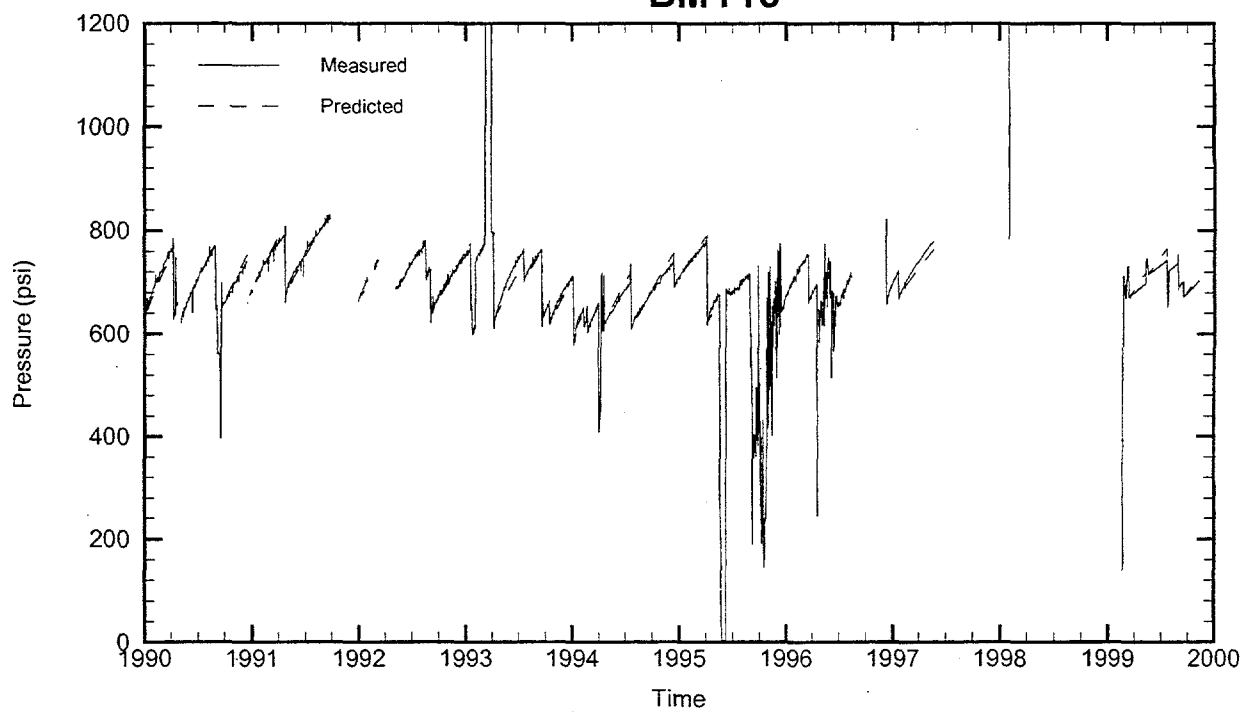
BM113



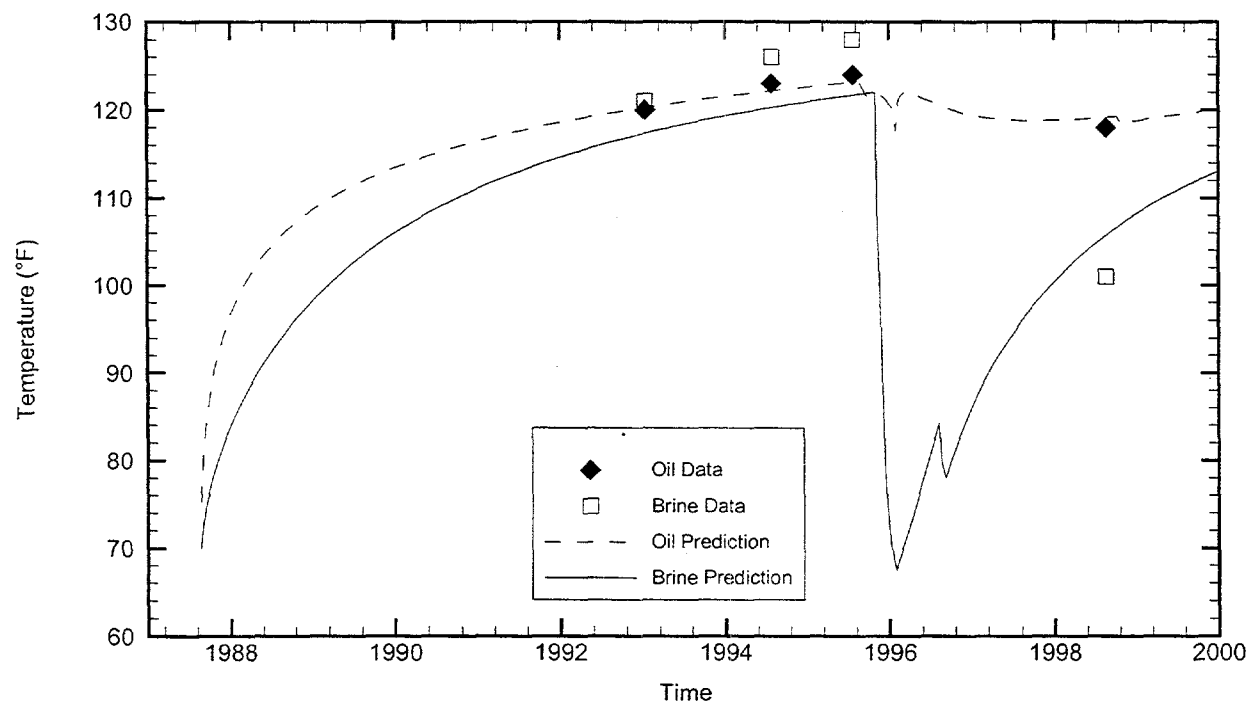
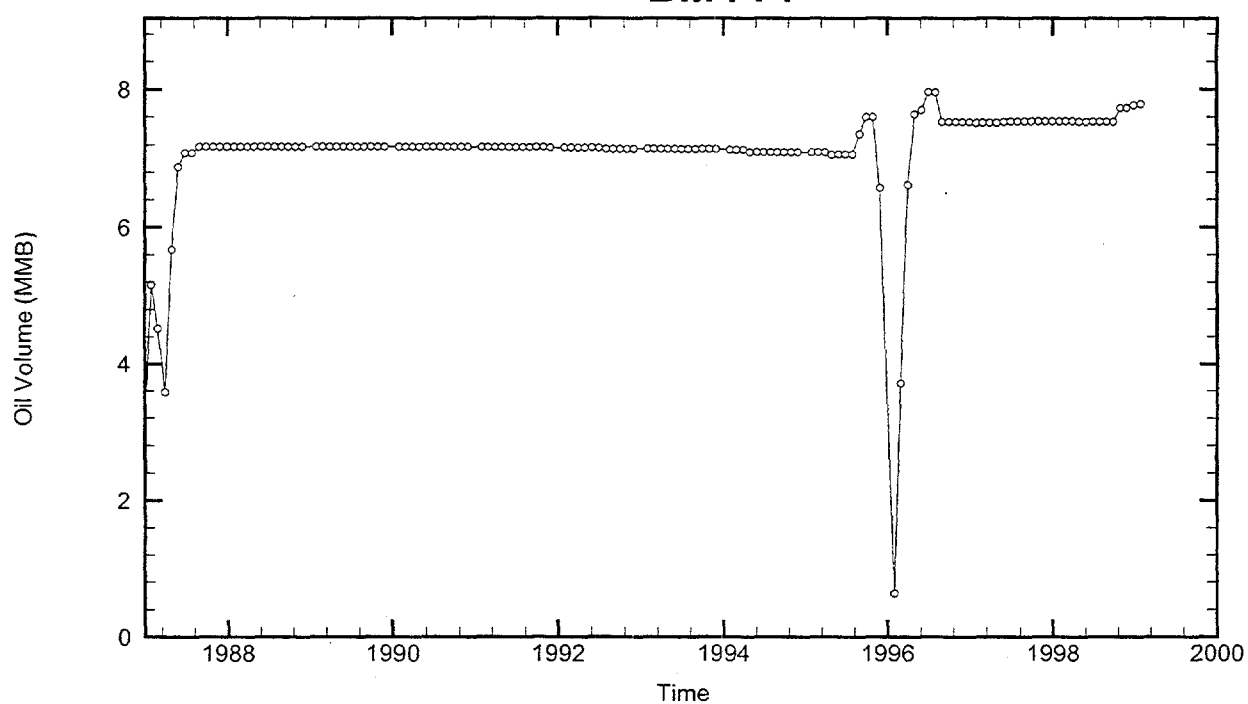
Cavern: BM113
End of Leaching: 10/08/1985
Duration of Leaching: 1.1828 months
Leaching Temperature: 70.00 °F

Degas: 10/01/1995, 125.00 °F, 6.51 MMB
Oil Injection Temperature: 87.20 °F
Brine Injection Temperature: 64.69 °F
Number of iterations: 242

BM113



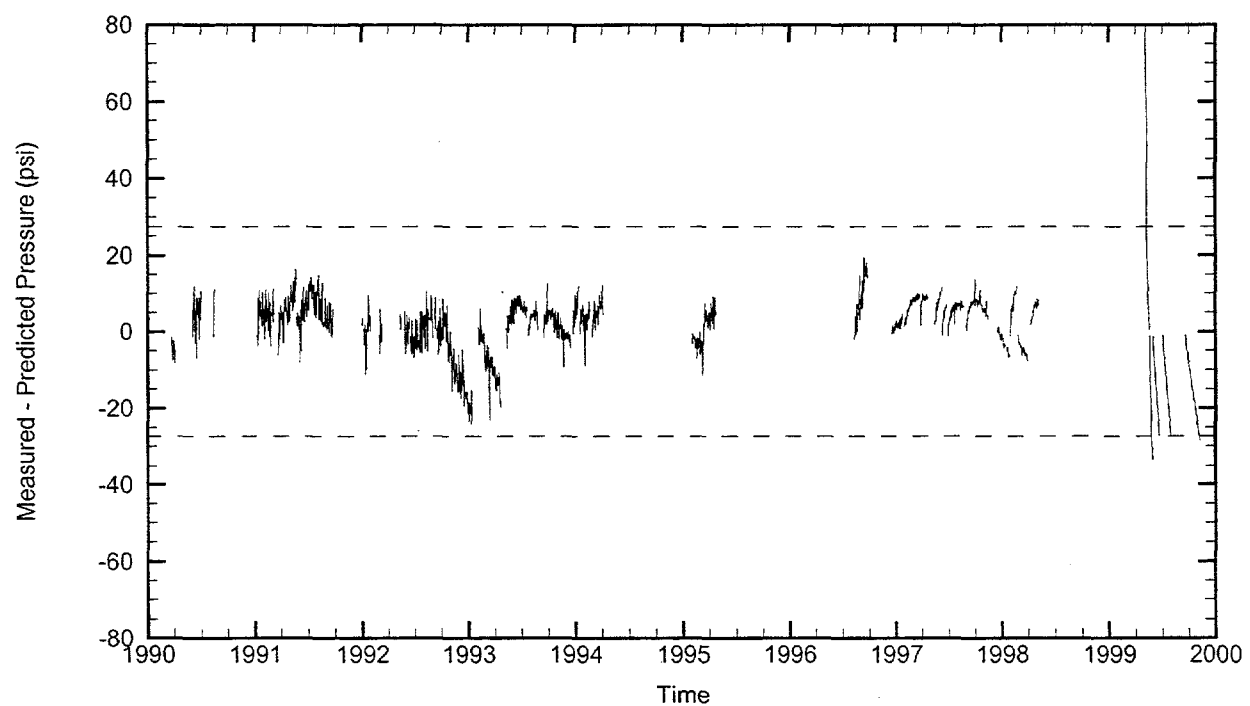
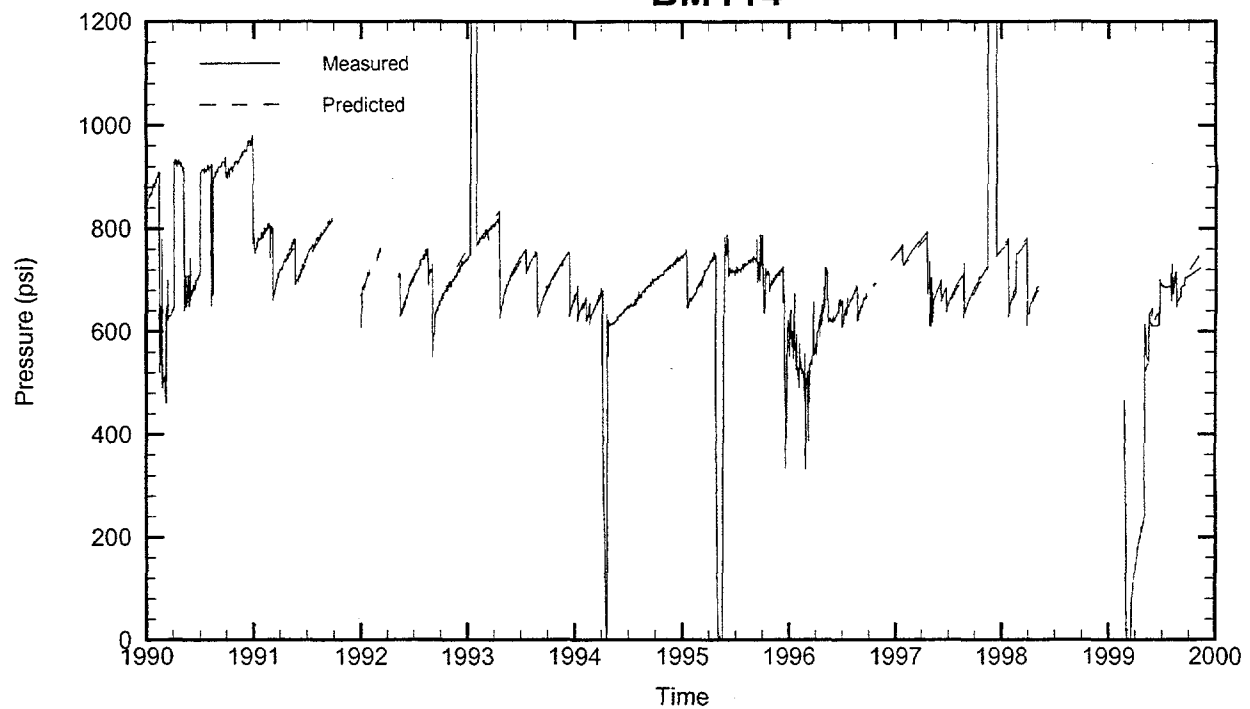
BM114



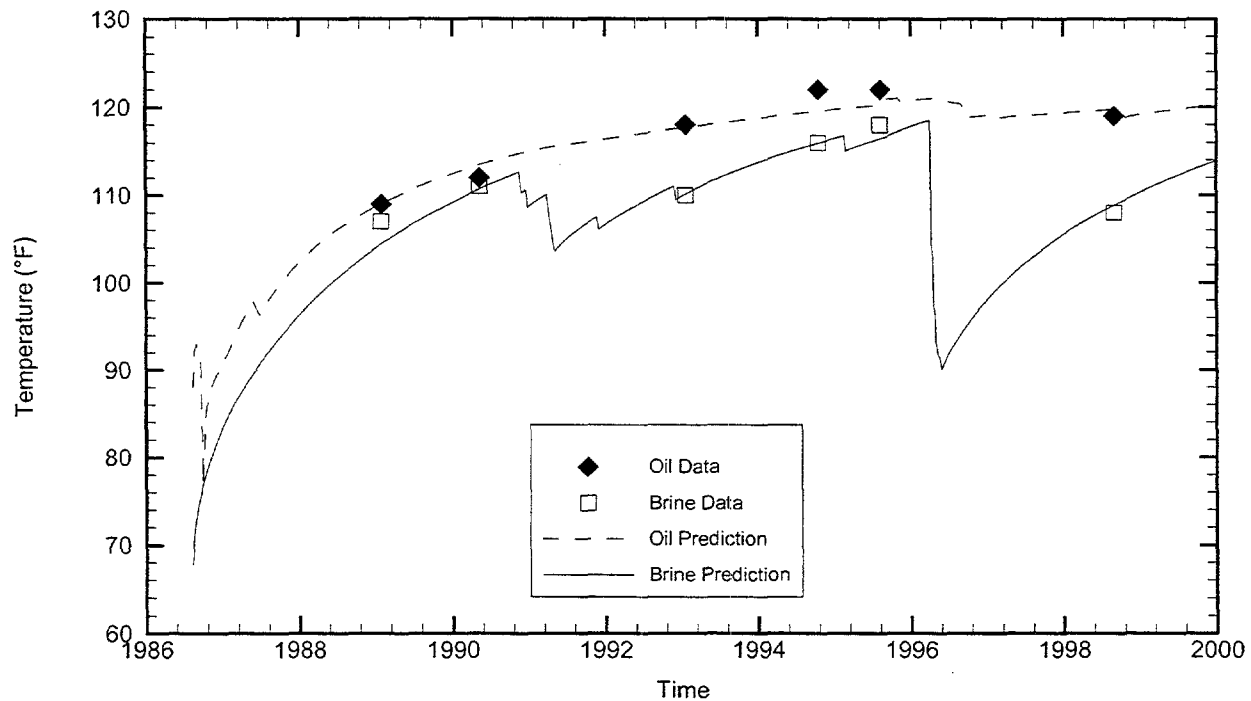
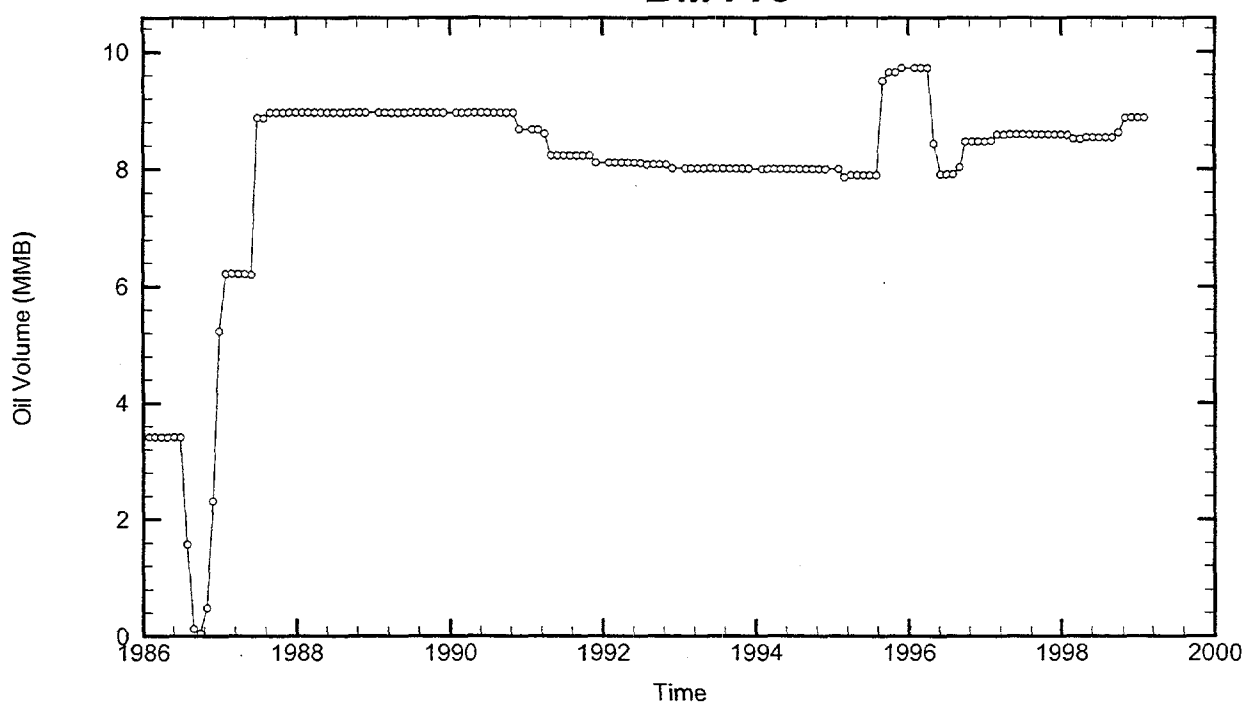
Cavern: BM114
End of Leaching: 08/26/1987
Duration of Leaching: 2.0000 days
Leaching Temperature: 70.00 °F

Degas: 02/01/1996, 125.00 °F, 7.28 MMB
Oil Injection Temperature: 75.25 °F
Brine Injection Temperature: 50.00 °F
Number of iterations: 154

BM114



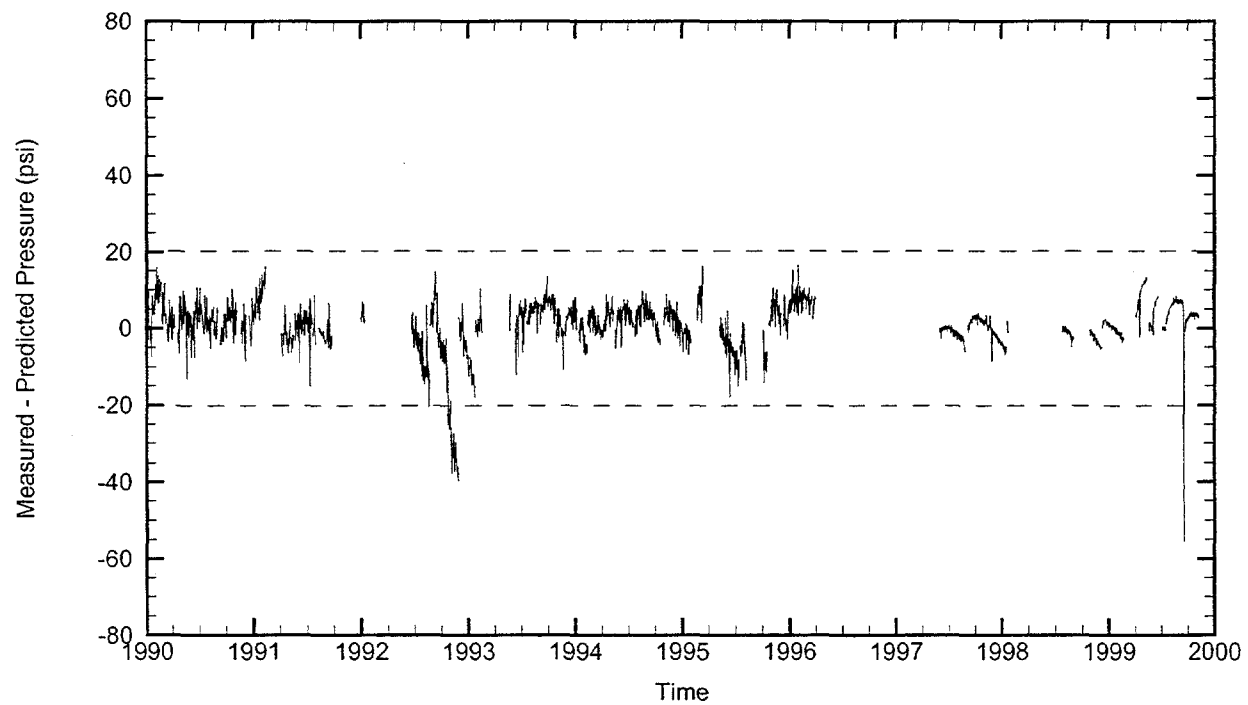
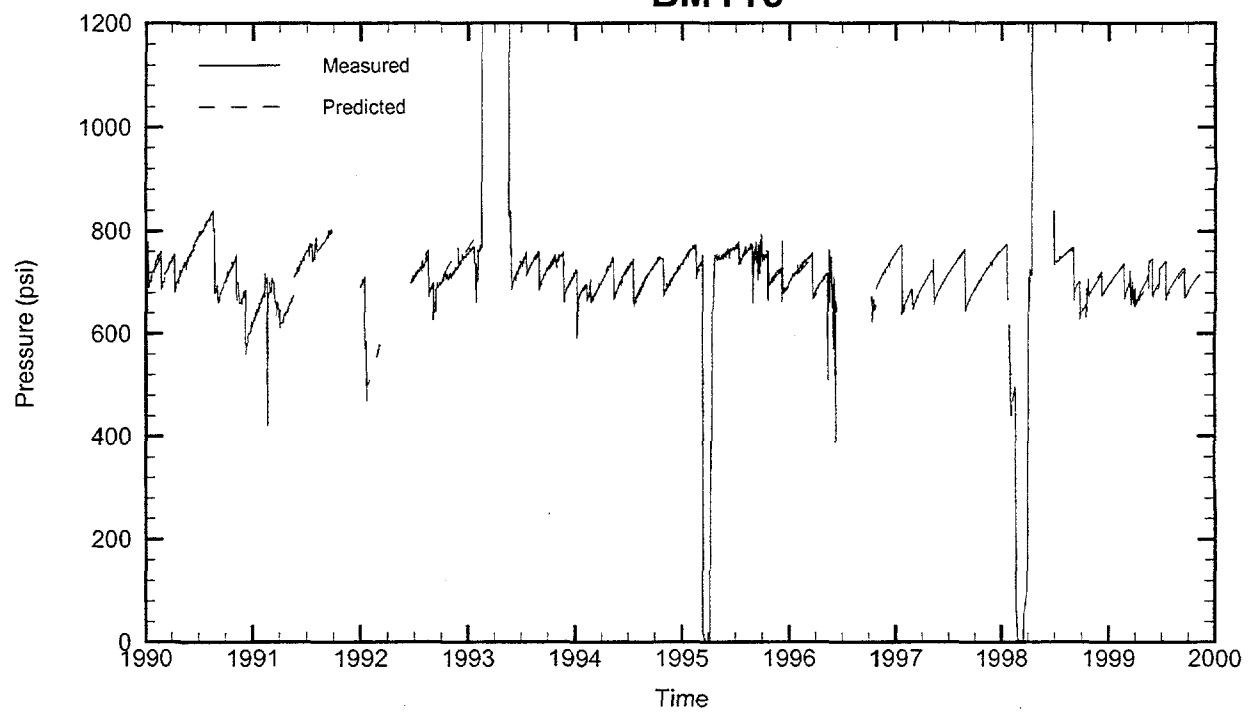
BM115



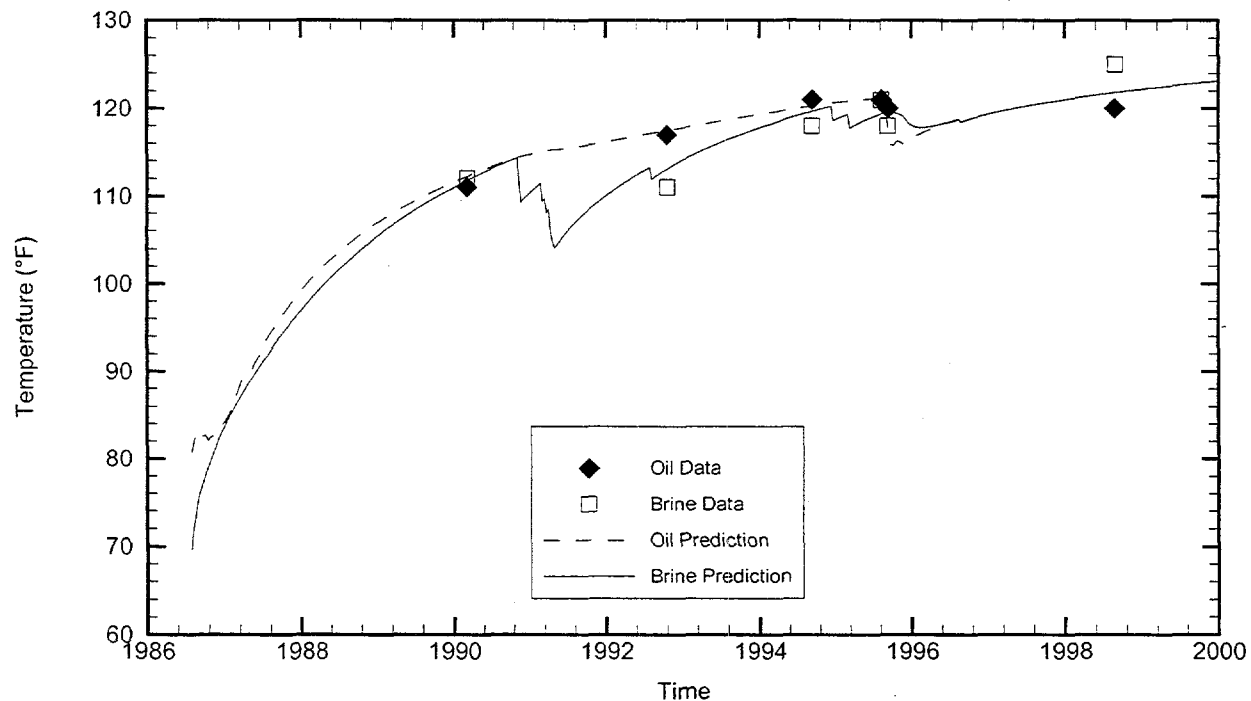
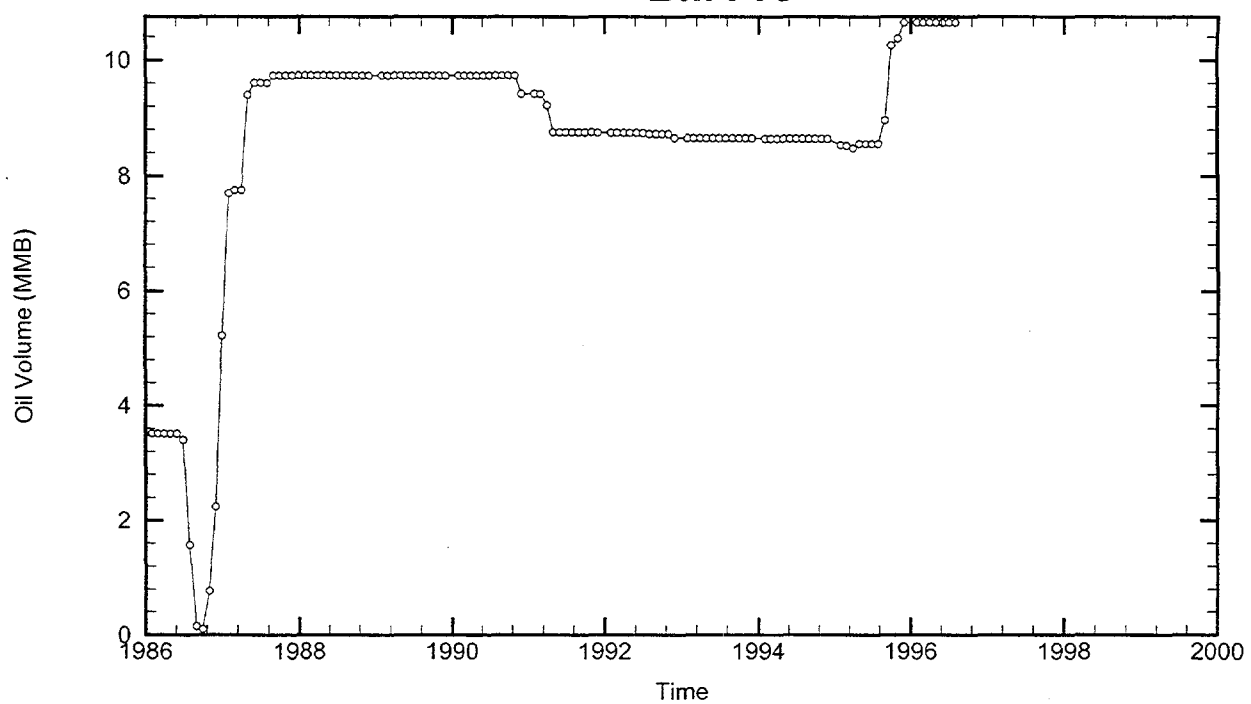
Cavern: BM115
End of Leaching: 08/11/1986
Duration of Leaching: 0.0000 days
Leaching Temperature: 67.80 °F

Degas: 08/03/1995, 125.00 °F, 1.66 MMB
Oil Injection Temperature: 88.01 °F
Brine Injection Temperature: 70.52 °F
Number of iterations: 610

BM115



BM116



Cavern: BM116

End of Leaching: 07/28/1986

Duration of Leaching: 1.2156 months

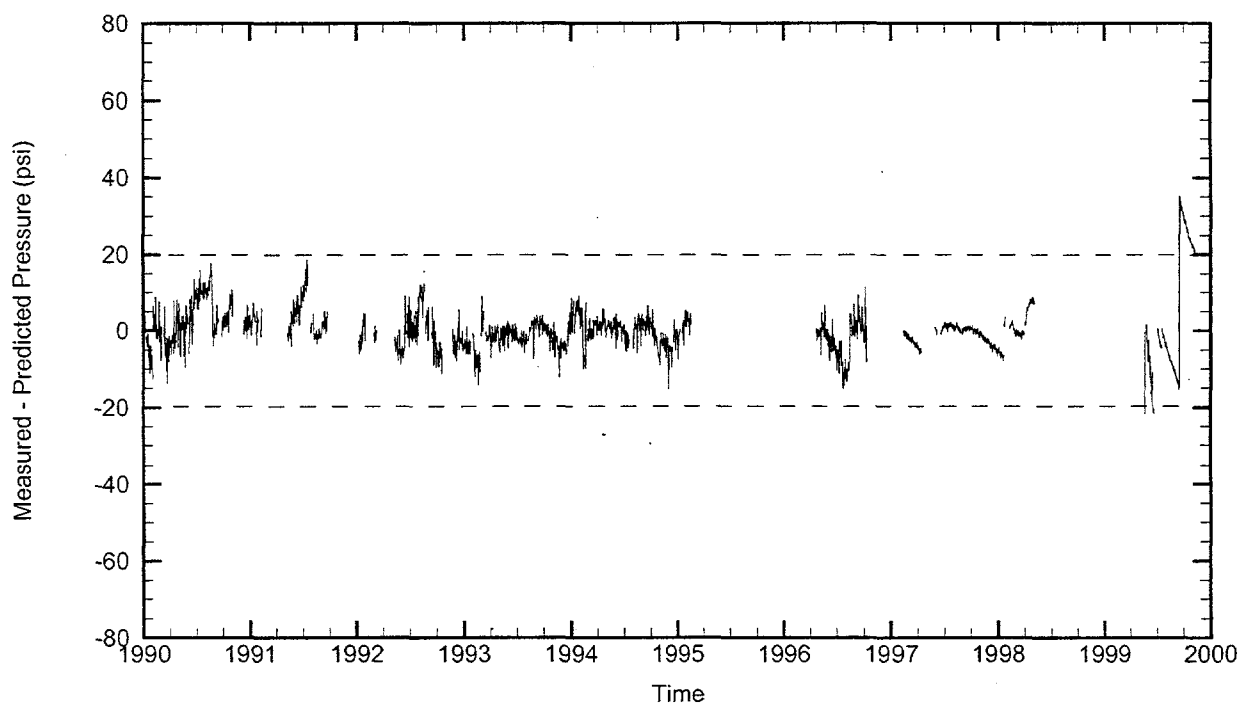
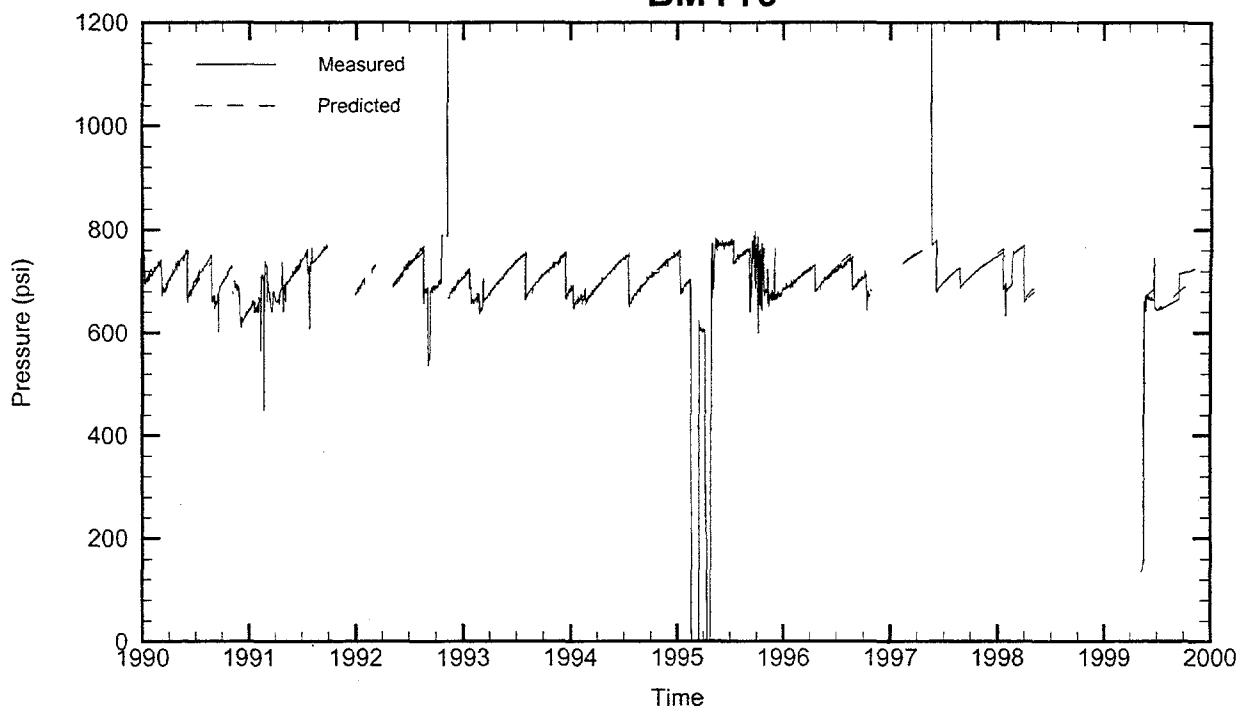
Leaching Temperature: 69.62 °F

Oil Injection Temperature: 80.71 °F

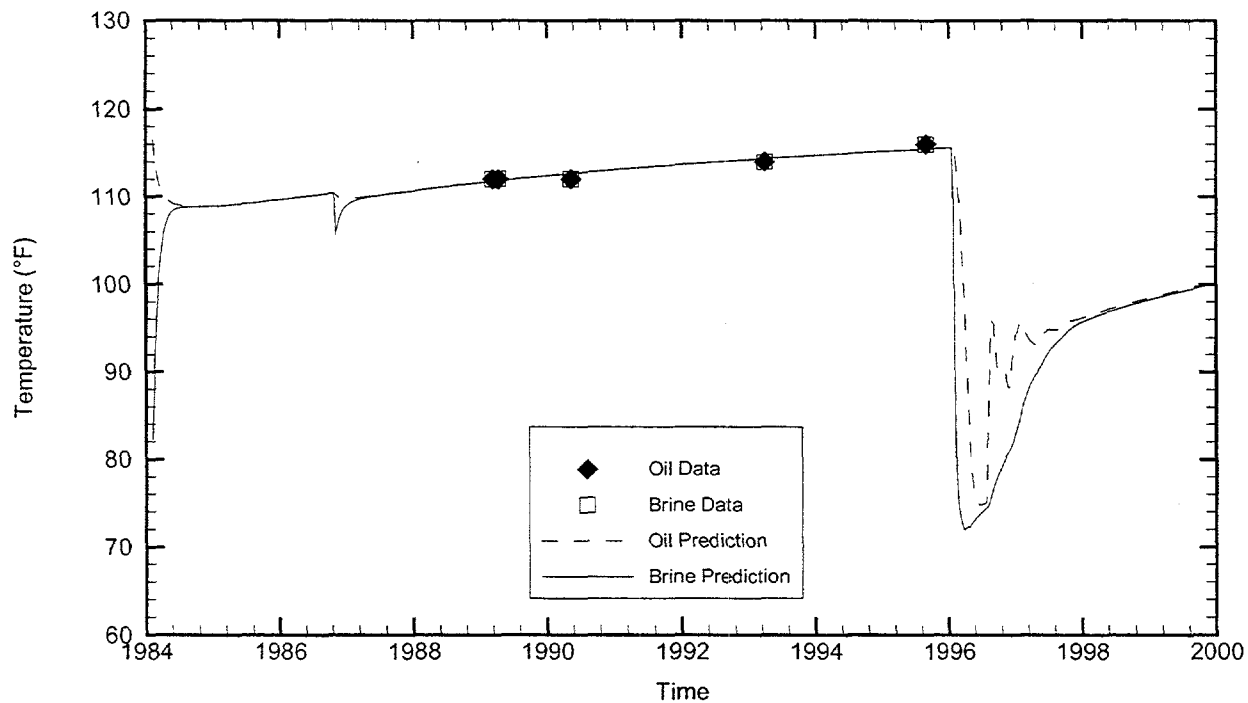
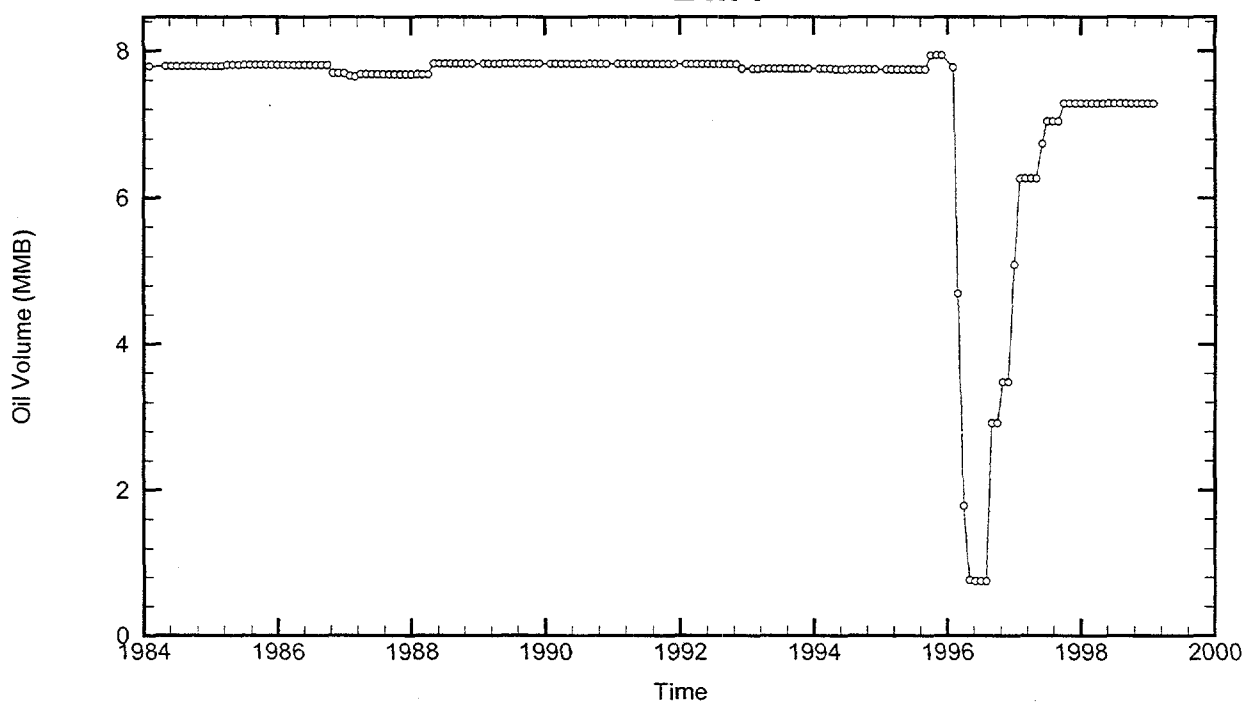
Brine Injection Temperature: 84.86 °F

Number of iterations: 227

BM116



BM1



Cavern: BM1

End of Leaching: 02/10/1984

Duration of Leaching: 1.9959 years

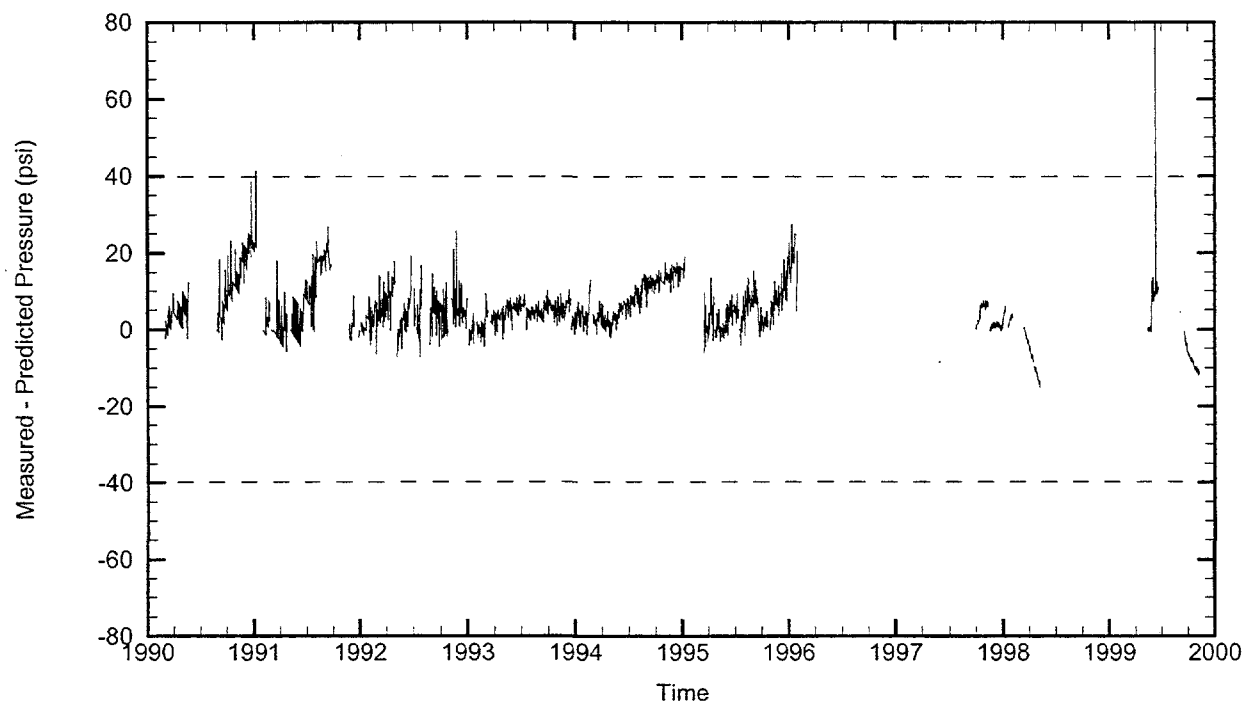
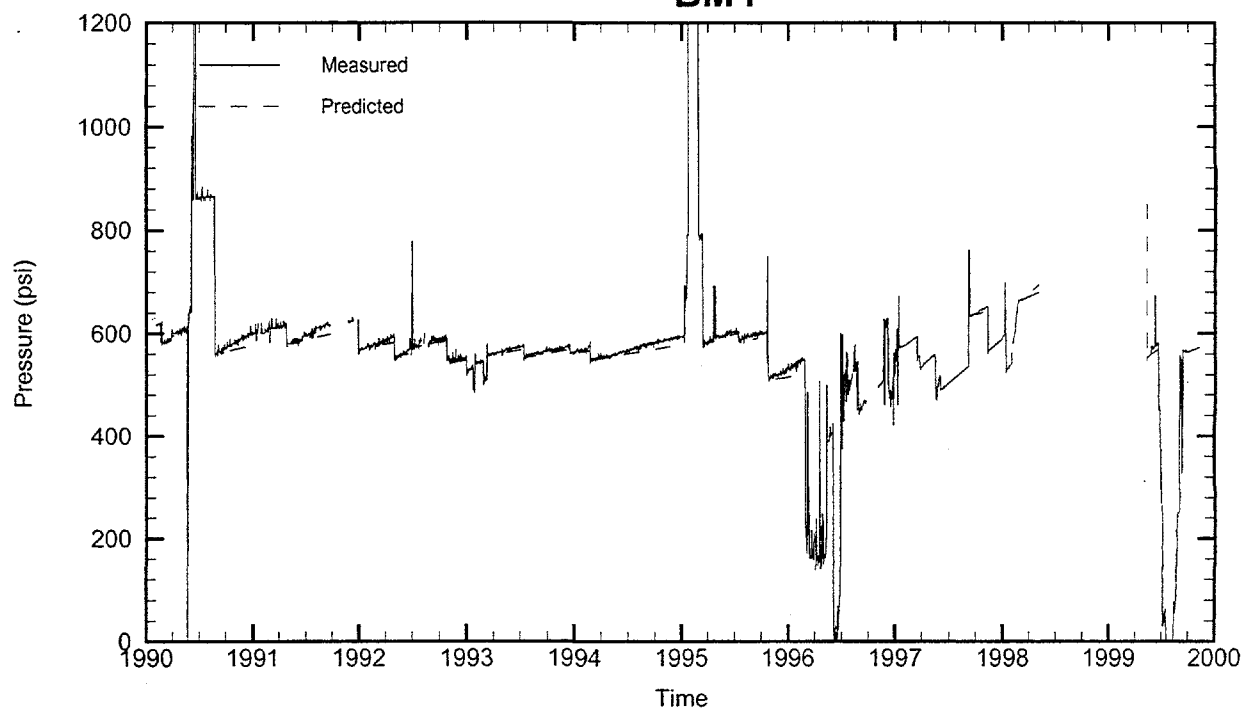
Leaching Temperature: 82.26 °F

Oil Injection Temperature: 116.50 °F

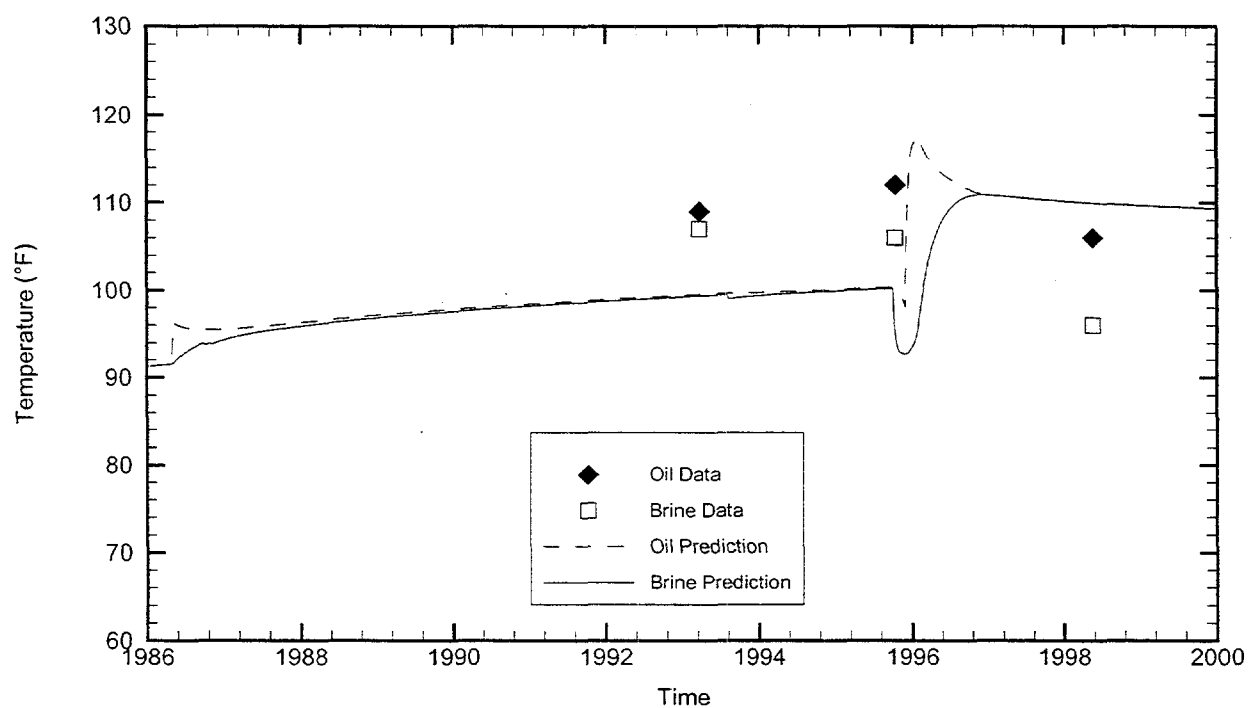
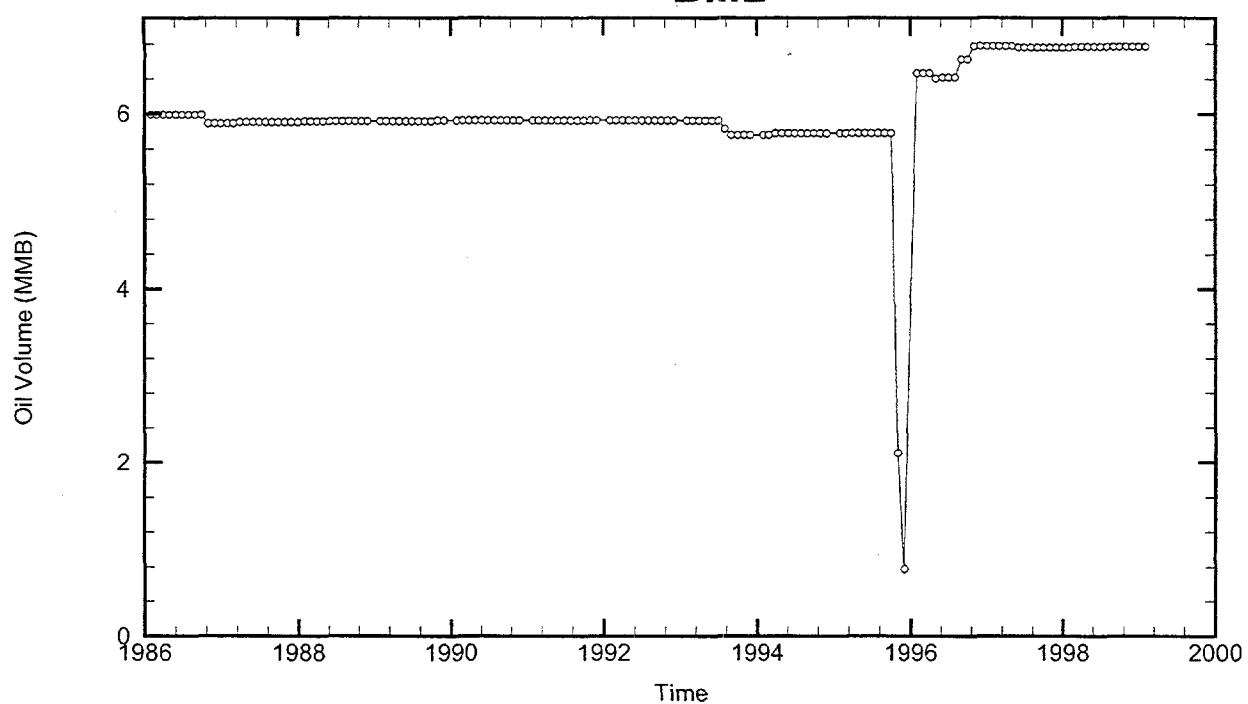
Brine Injection Temperature: 60.30 °F

Number of iterations: 329

BM1



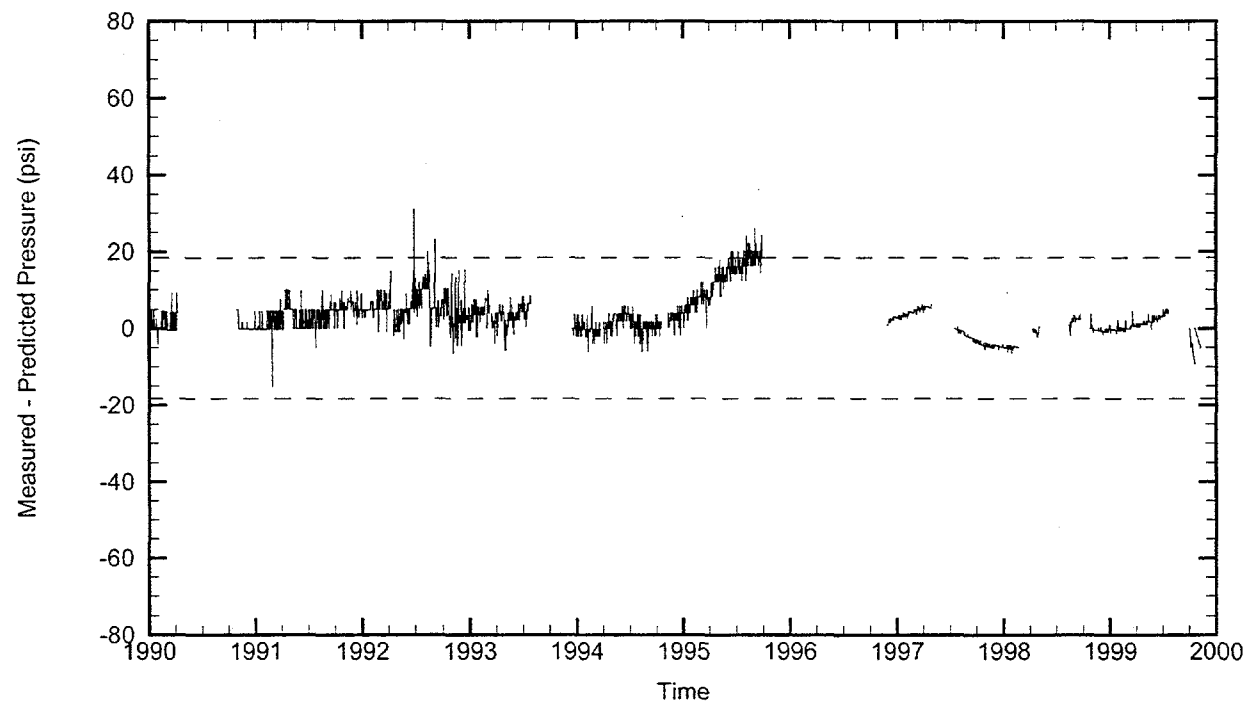
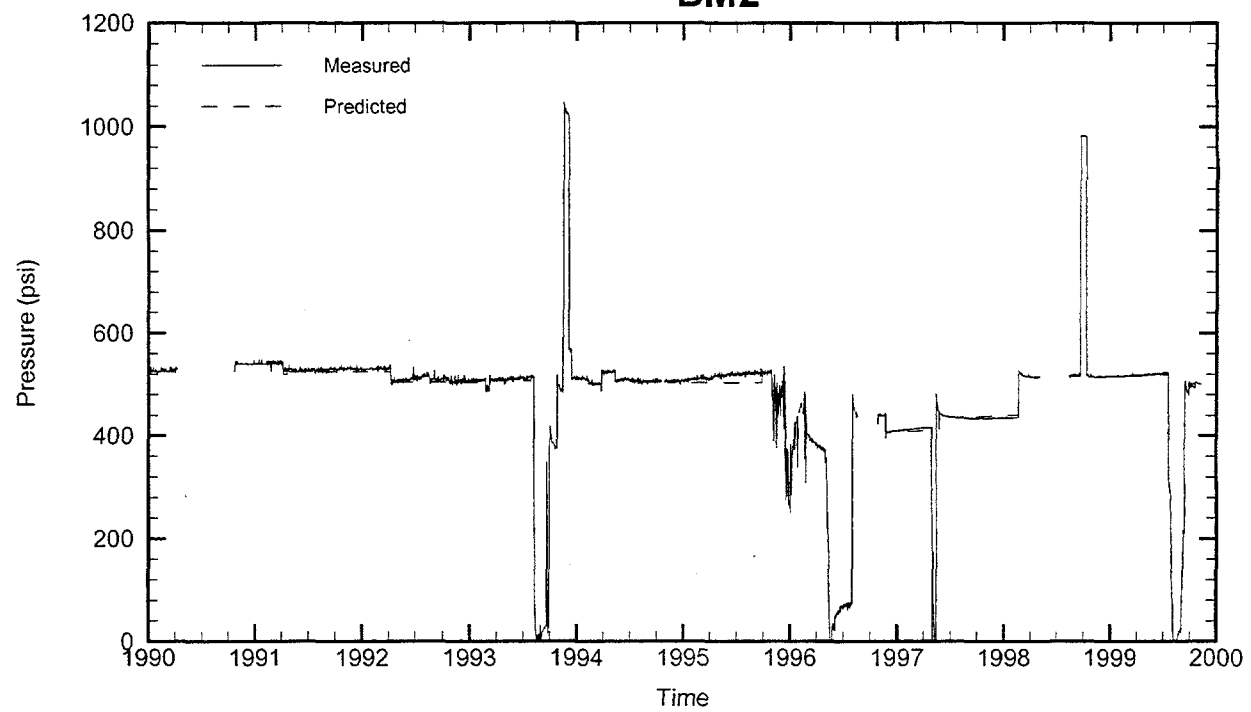
BM2



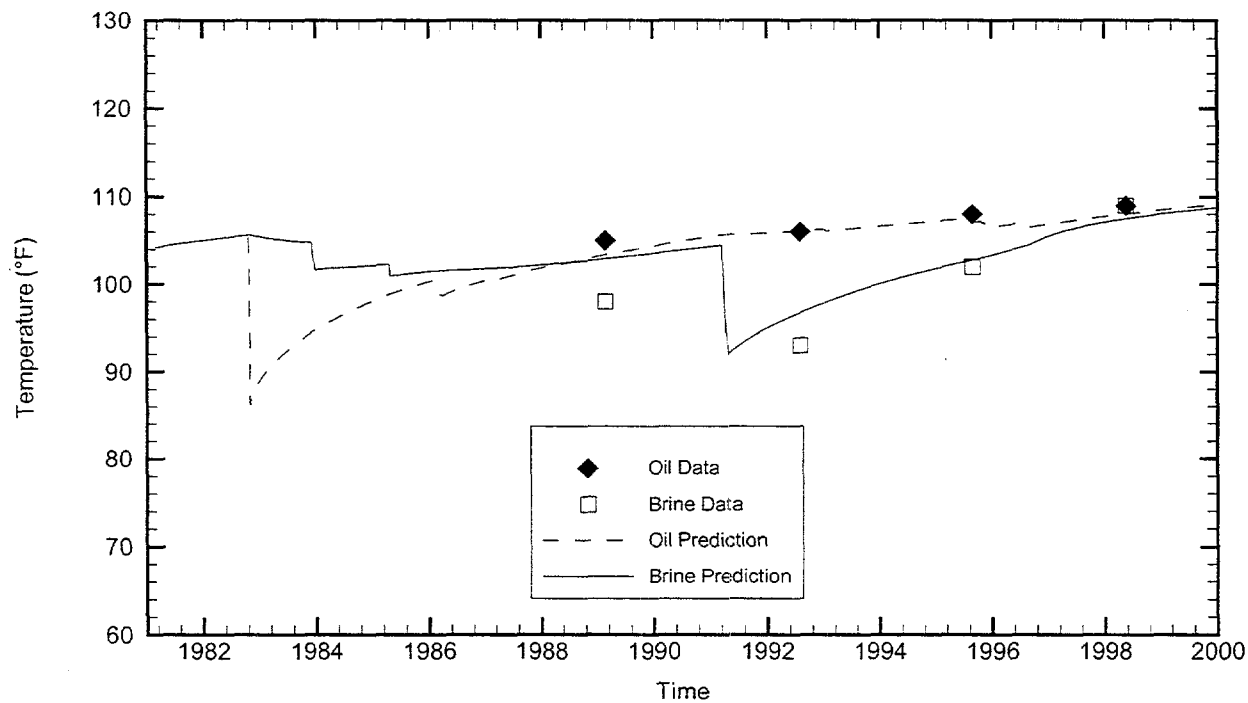
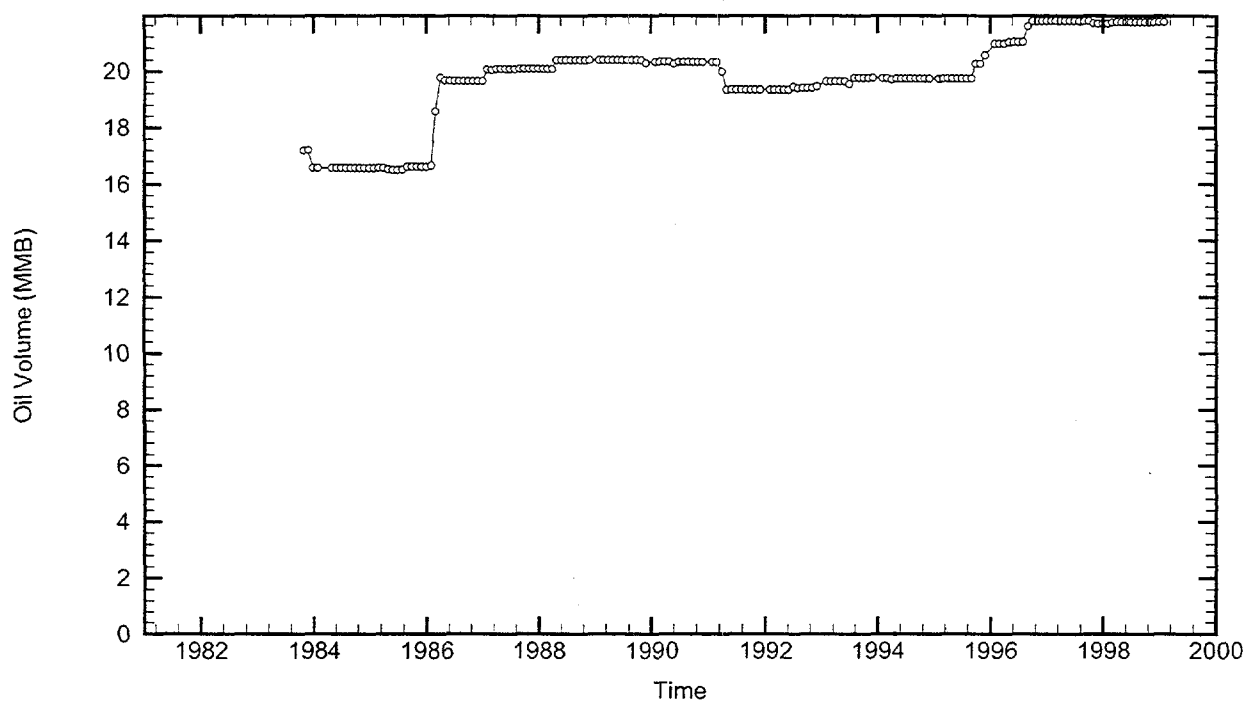
Cavern: BM2
End of Leaching: 01/19/1986
Duration of Leaching: 1.9959 years
Leaching Temperature: 91.24 °F

Degas: 12/01/1995, 125.00 °F, 5.69 MMB
Oil Injection Temperature: 96.38 °F
Brine Injection Temperature: 90.00 °F
Number of iterations: 308

BM2



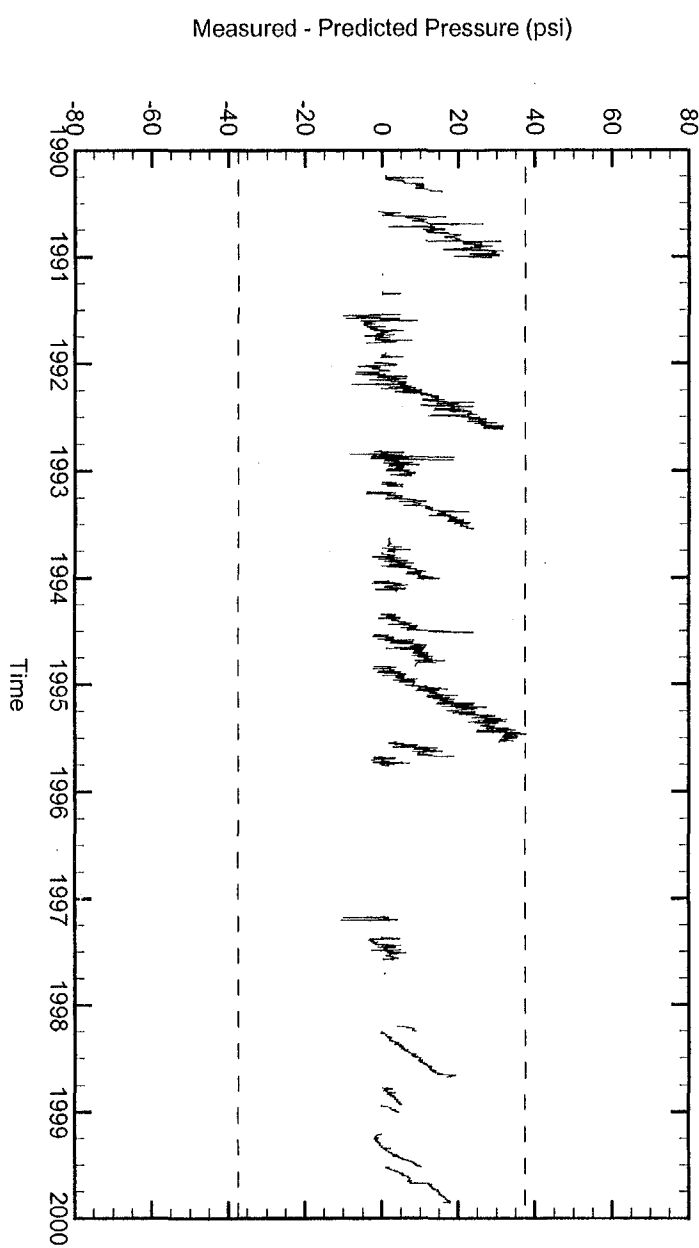
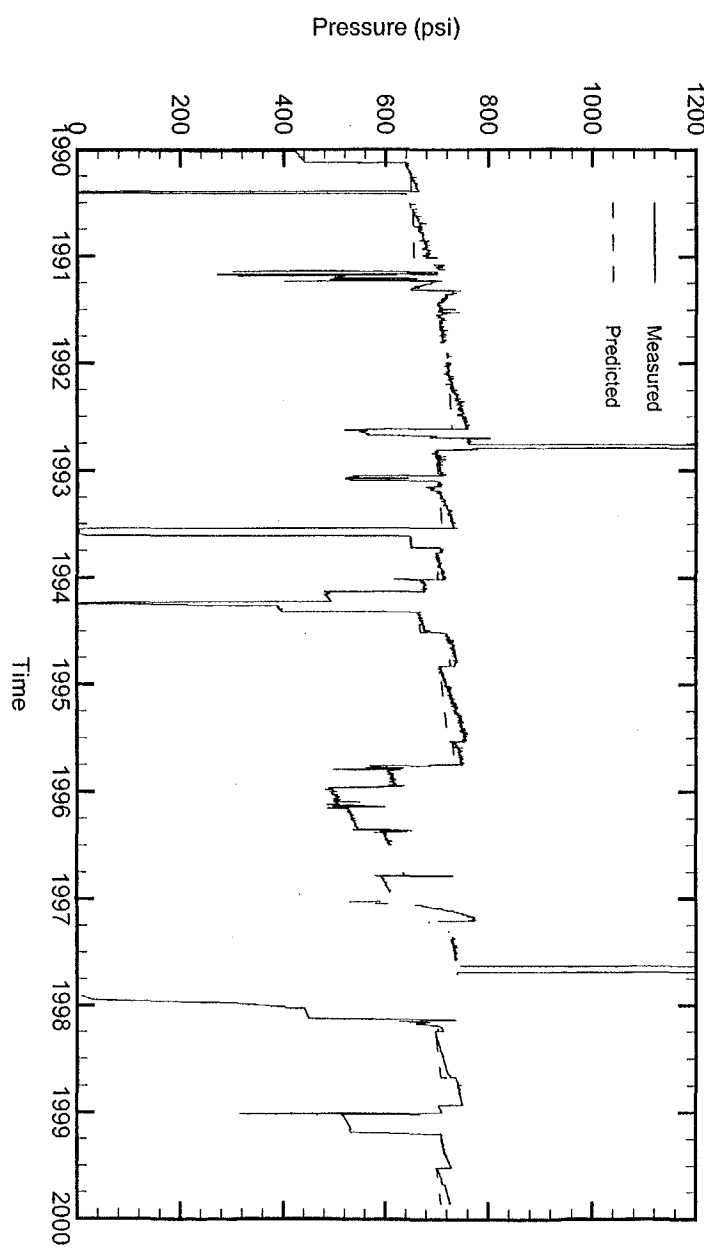
BM4



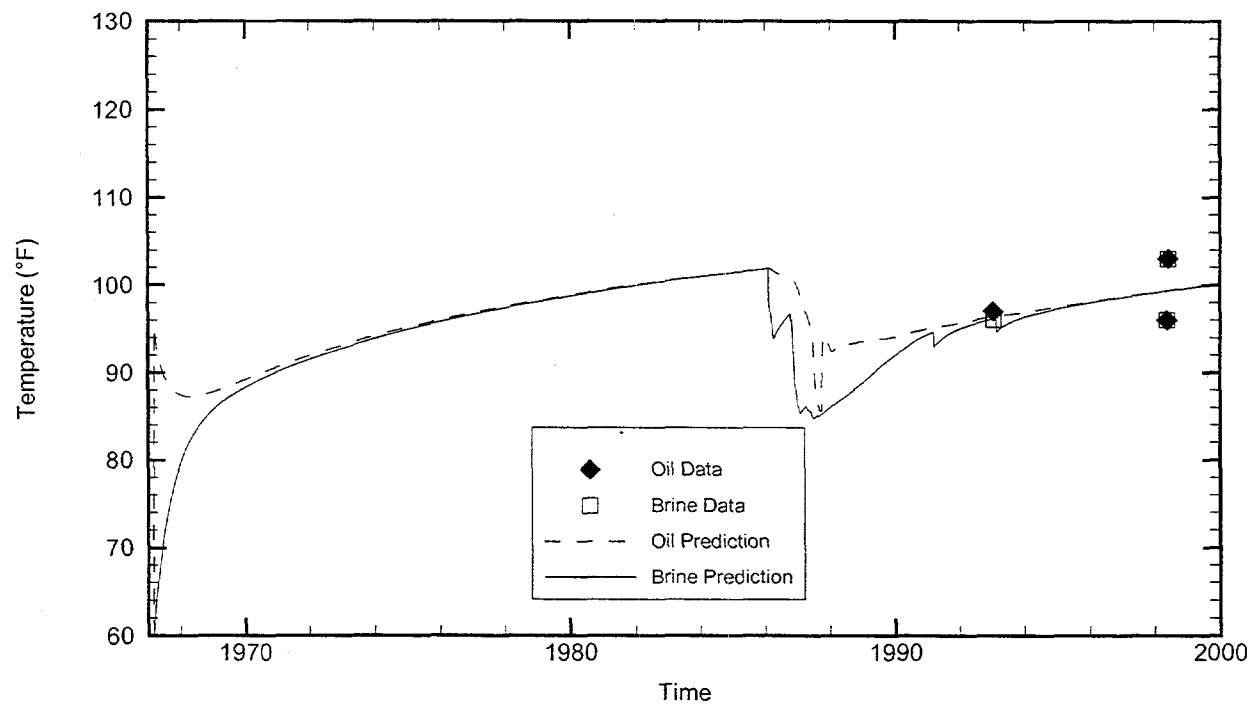
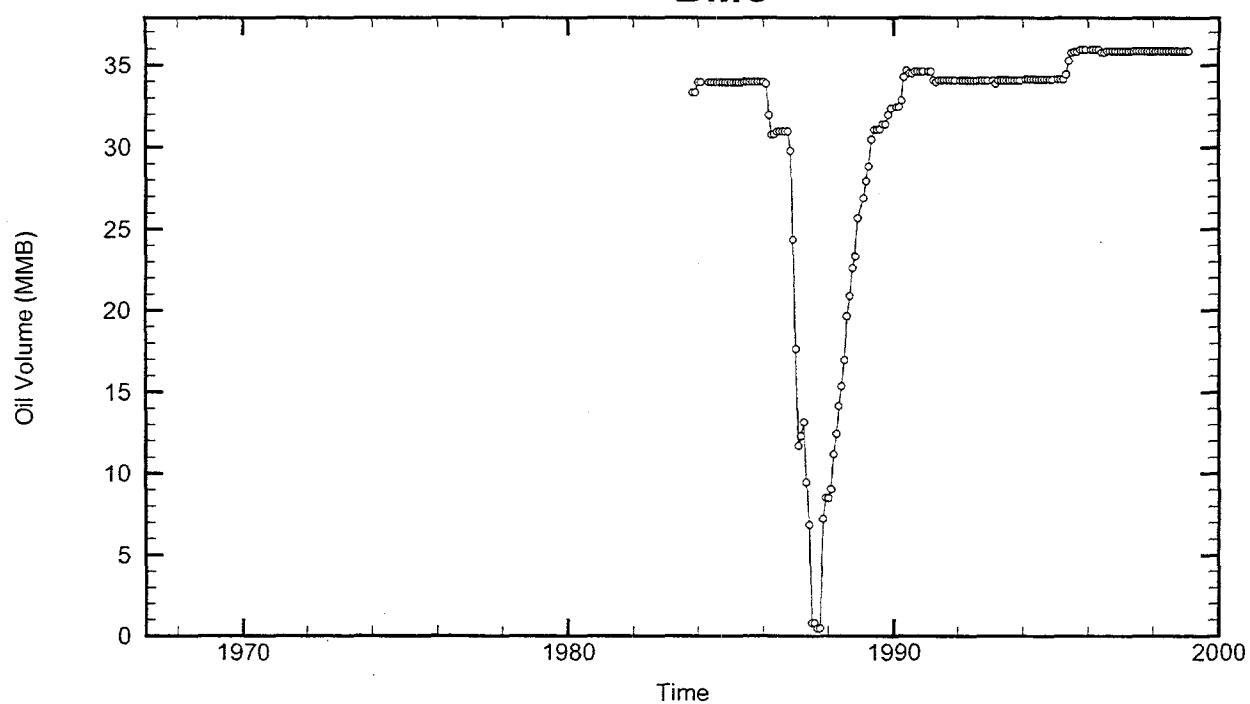
Cavern: BM4
End of Leaching: 03/02/1981
Duration of Leaching: 1.9959 years
Leaching Temperature: 104.20 °F

Oil Injection Temperature: 85.98 °F
Brine Injection Temperature: 68.25 °F
Number of iterations: 580

BM4



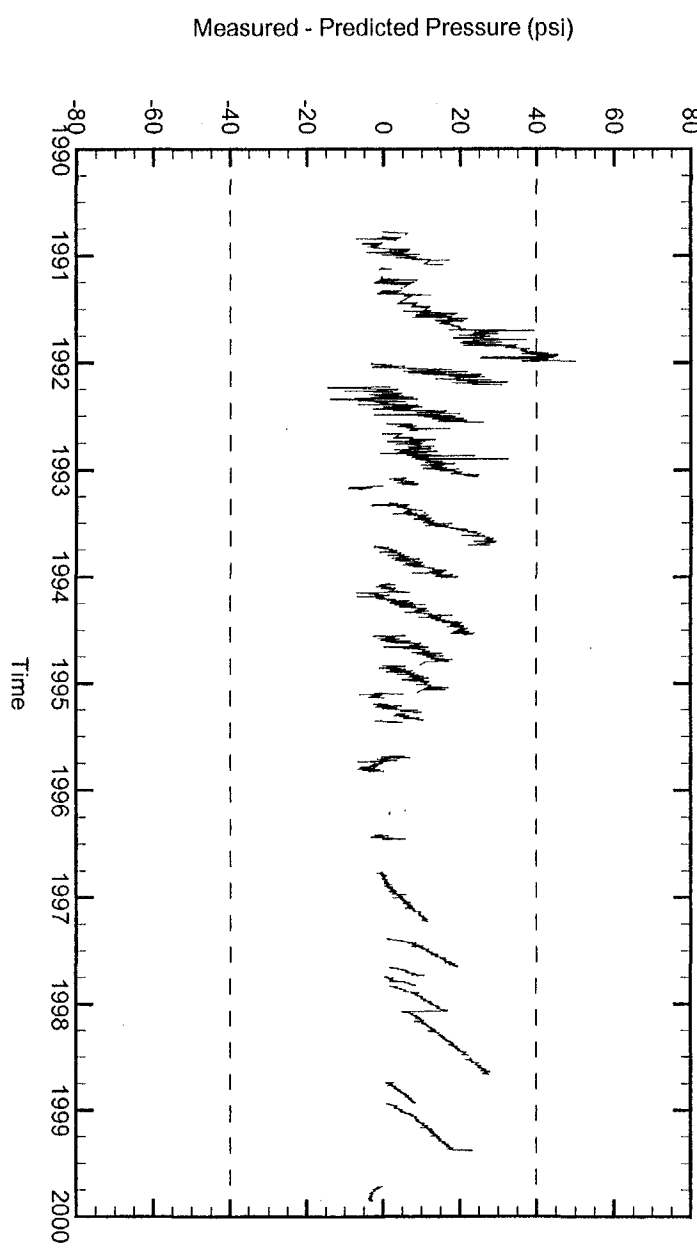
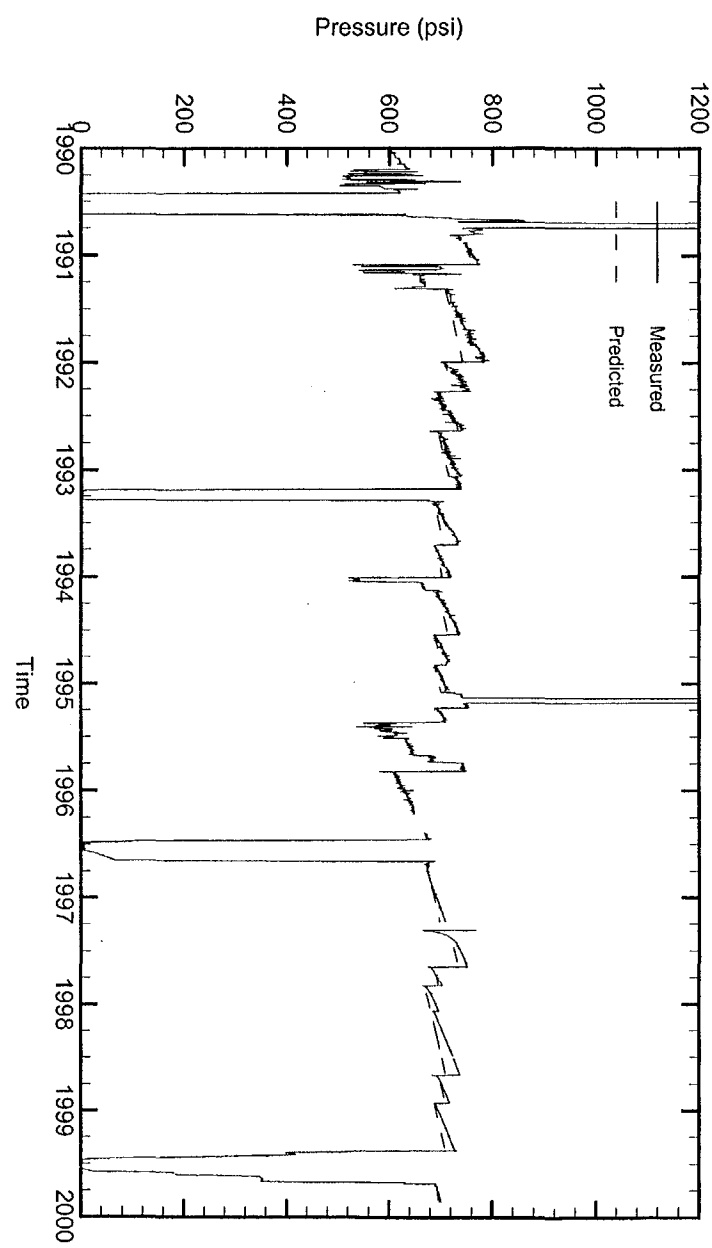
BM5



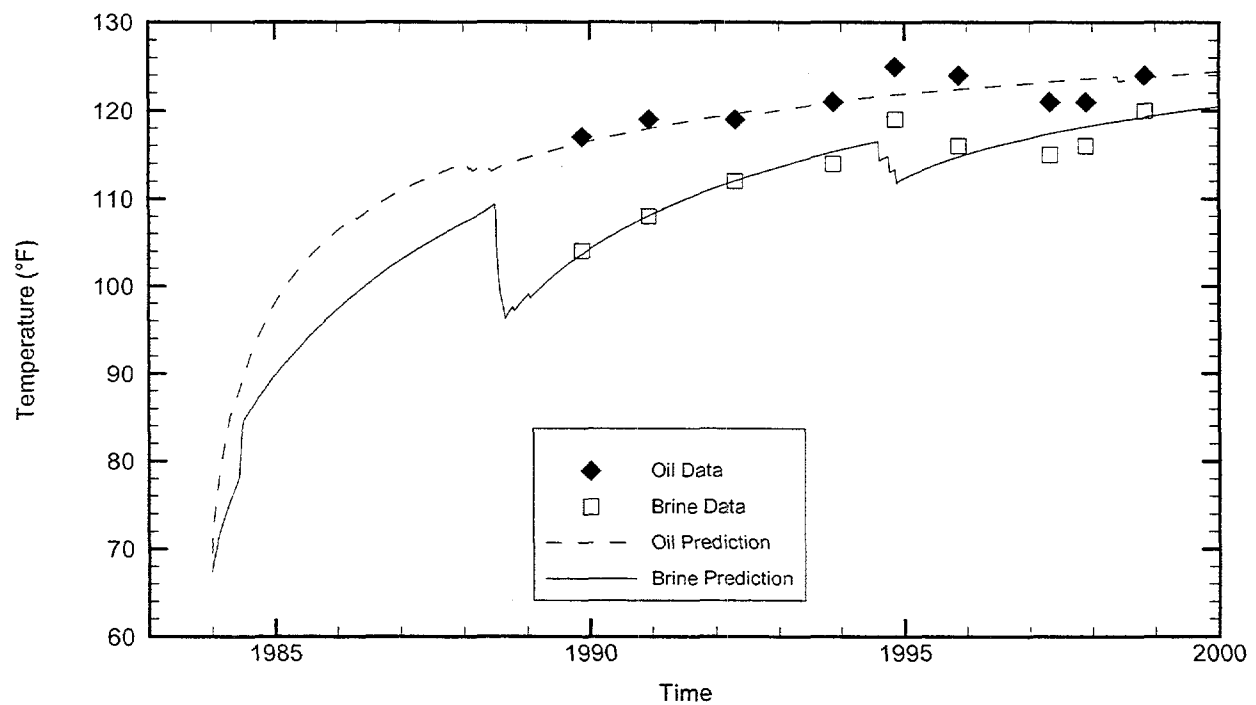
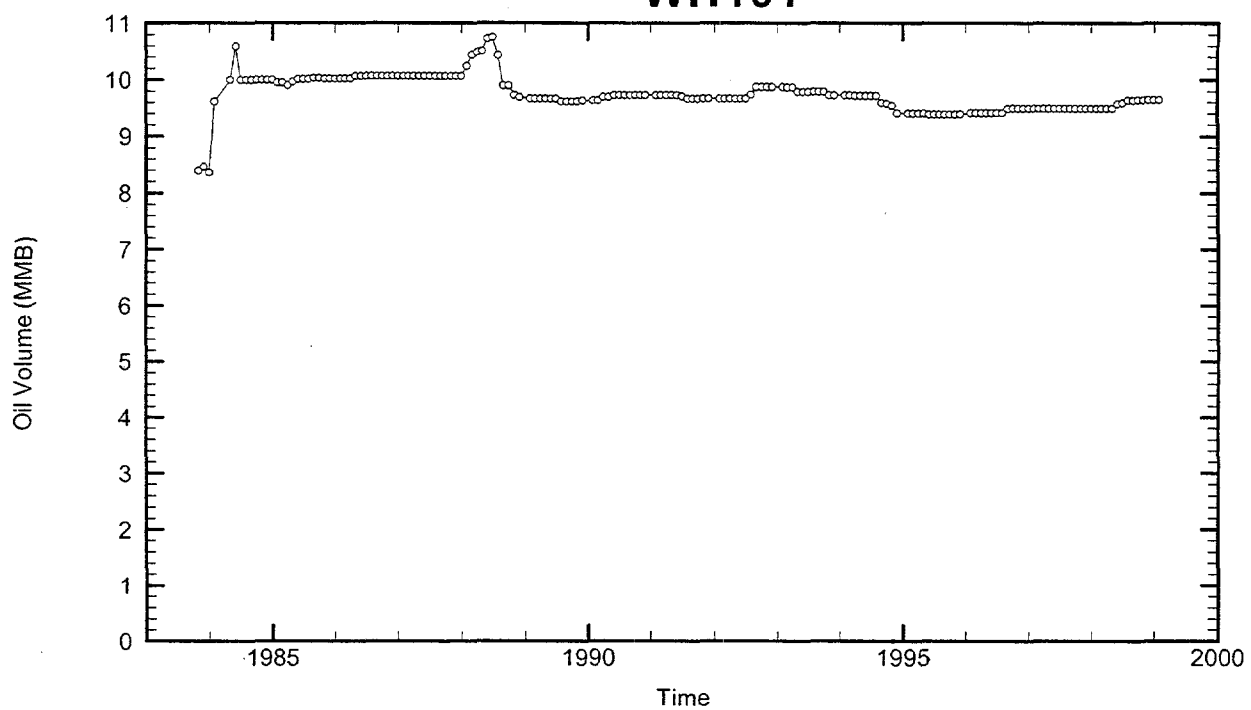
Cavern: BM5
End of Leaching: 02/14/1967
Duration of Leaching: 1.9986 years
Leaching Temperature: 60.01 °F

Oil Injection Temperature: 96.80 °F
Brine Injection Temperature: 79.37 °F
Number of iterations: 207

BM5



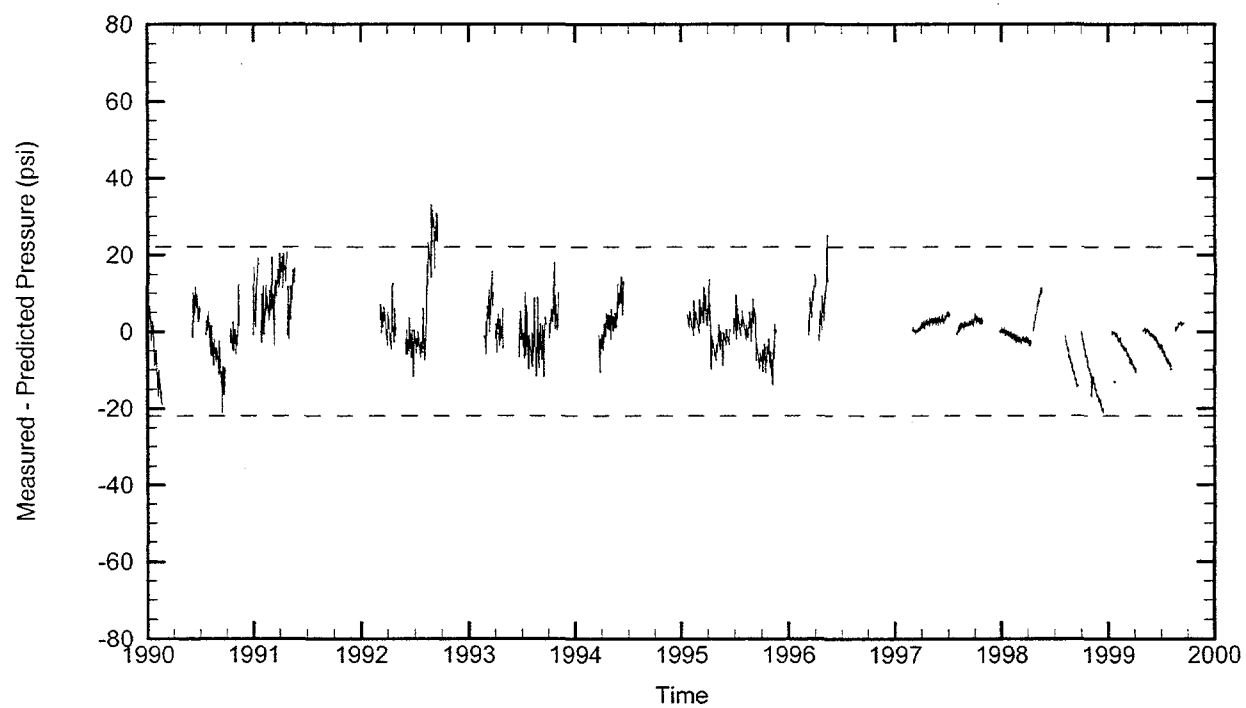
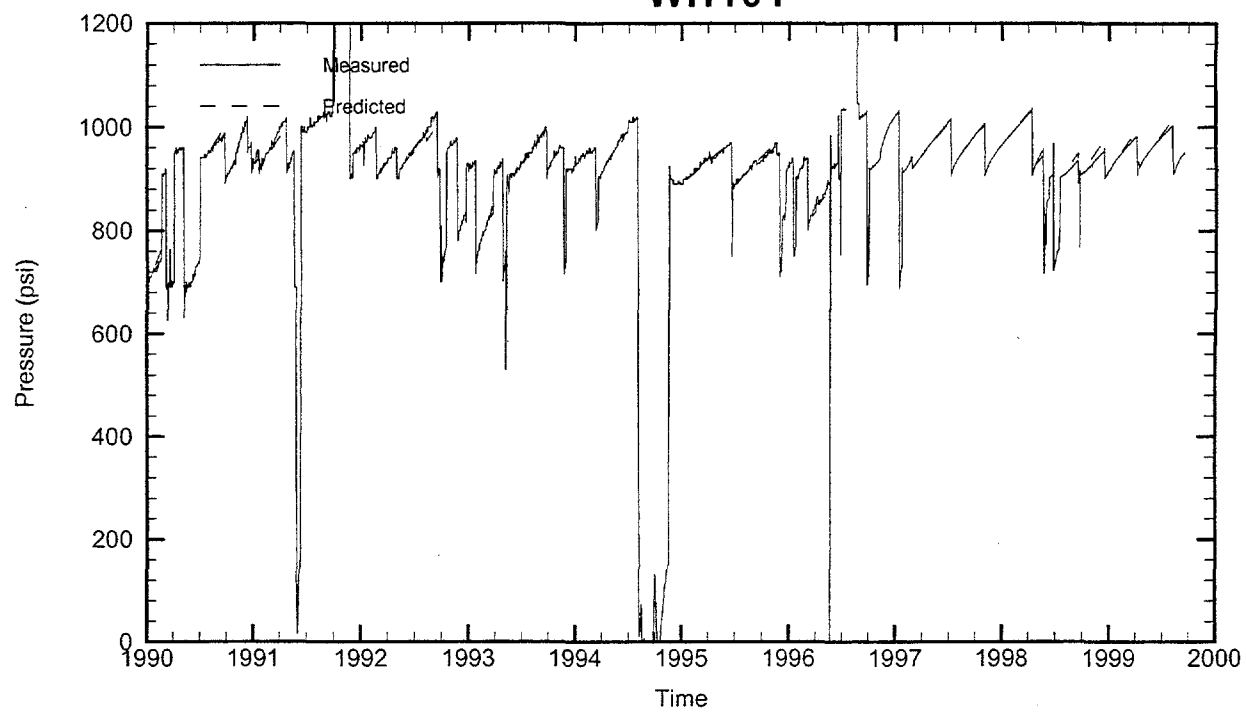
WH101



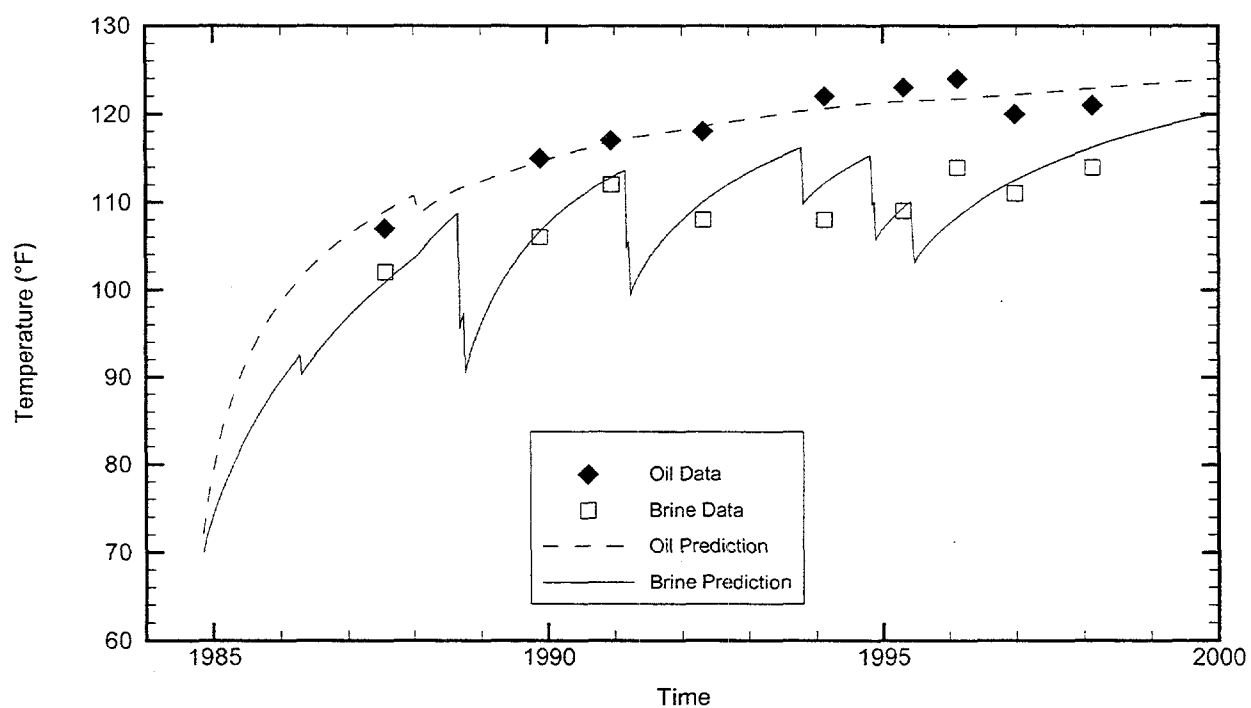
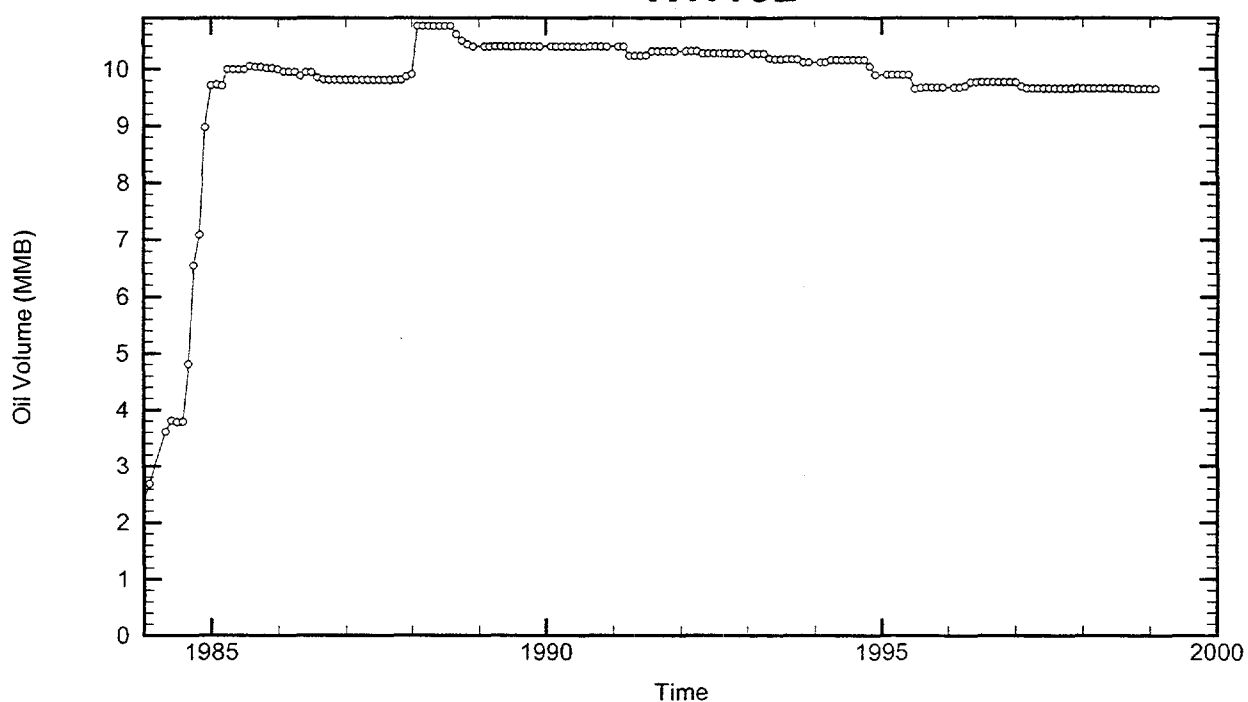
Cavern: WH101
End of Leaching: 12/28/1983
Duration of Leaching: 1.6667 years
Leaching Temperature: 67.34 °F

Oil Injection Temperature: 69.44 °F
Brine Injection Temperature: 90.00 °F
Number of iterations: 230

WH101



WH102



Cavern: WH102

End of Leaching: 11/08/1984

Duration of Leaching: 1.6756 months

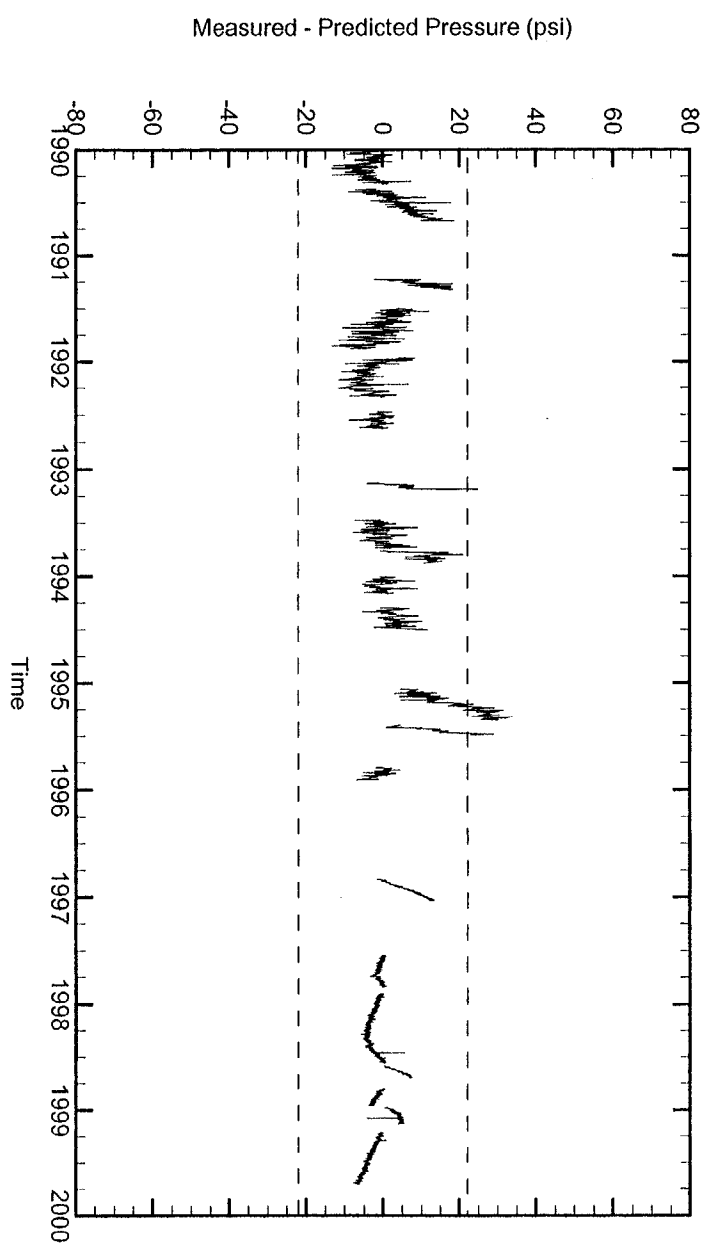
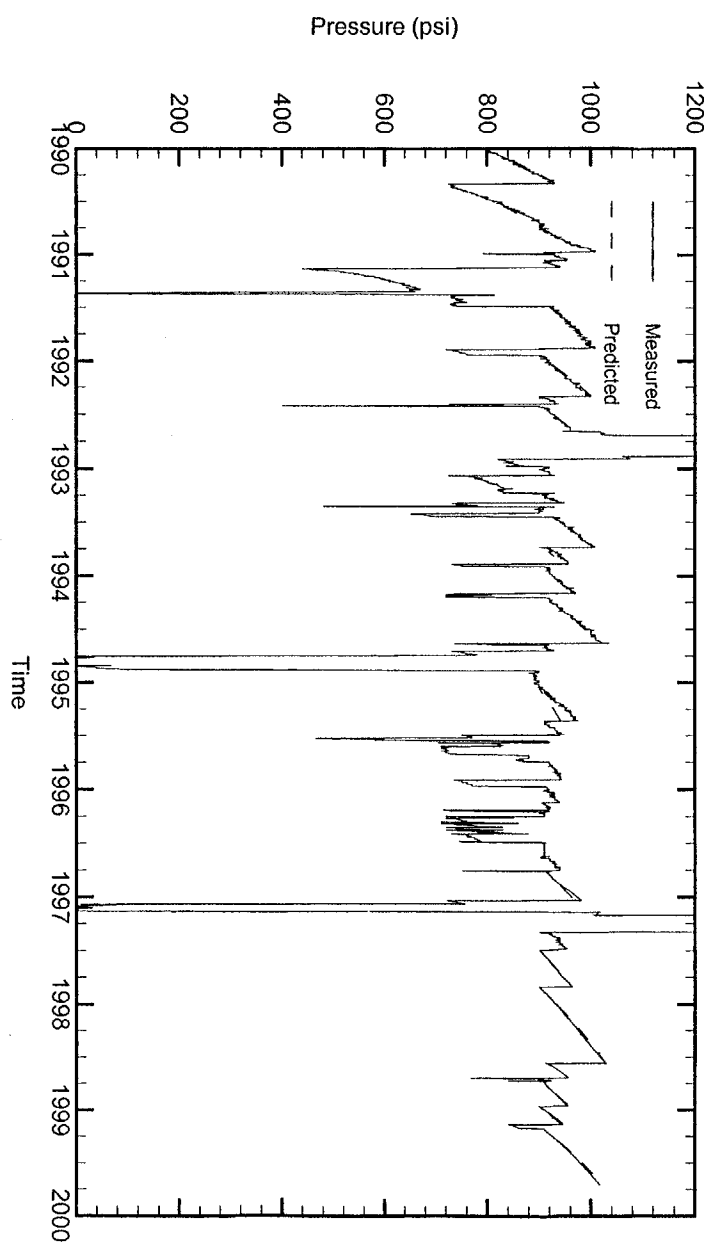
Leaching Temperature: 70.00 °F

Oil Injection Temperature: 72.13 °F

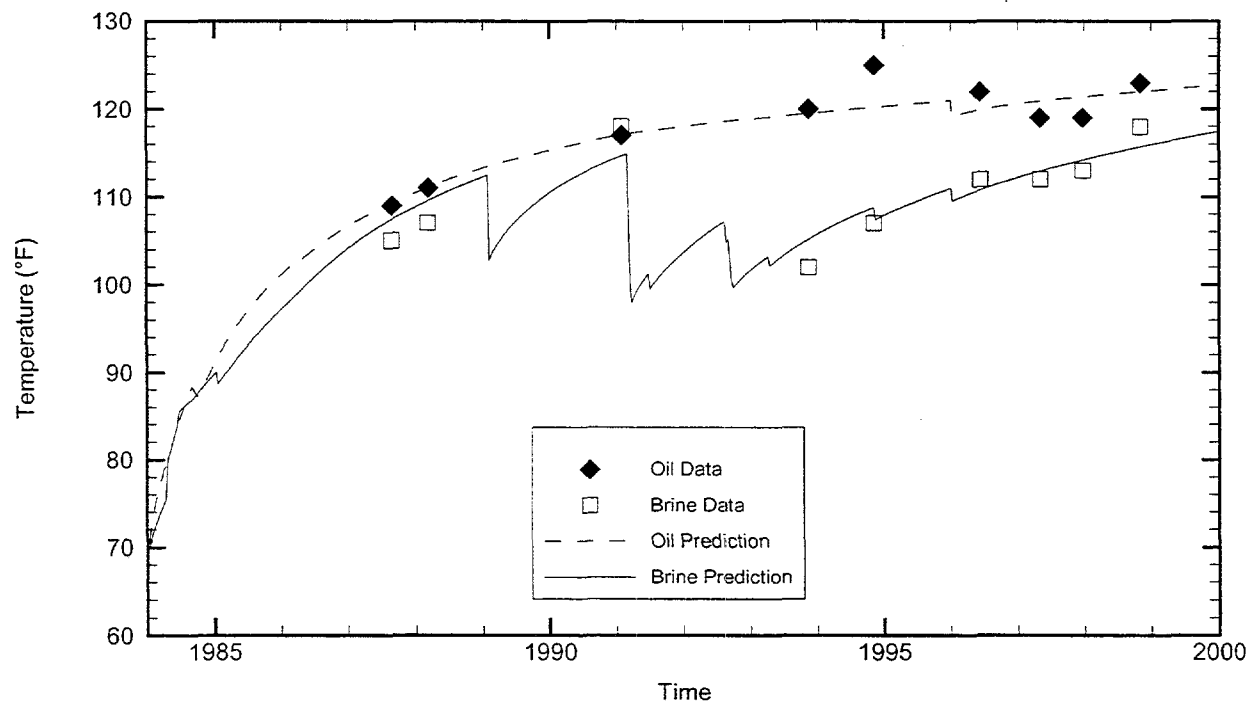
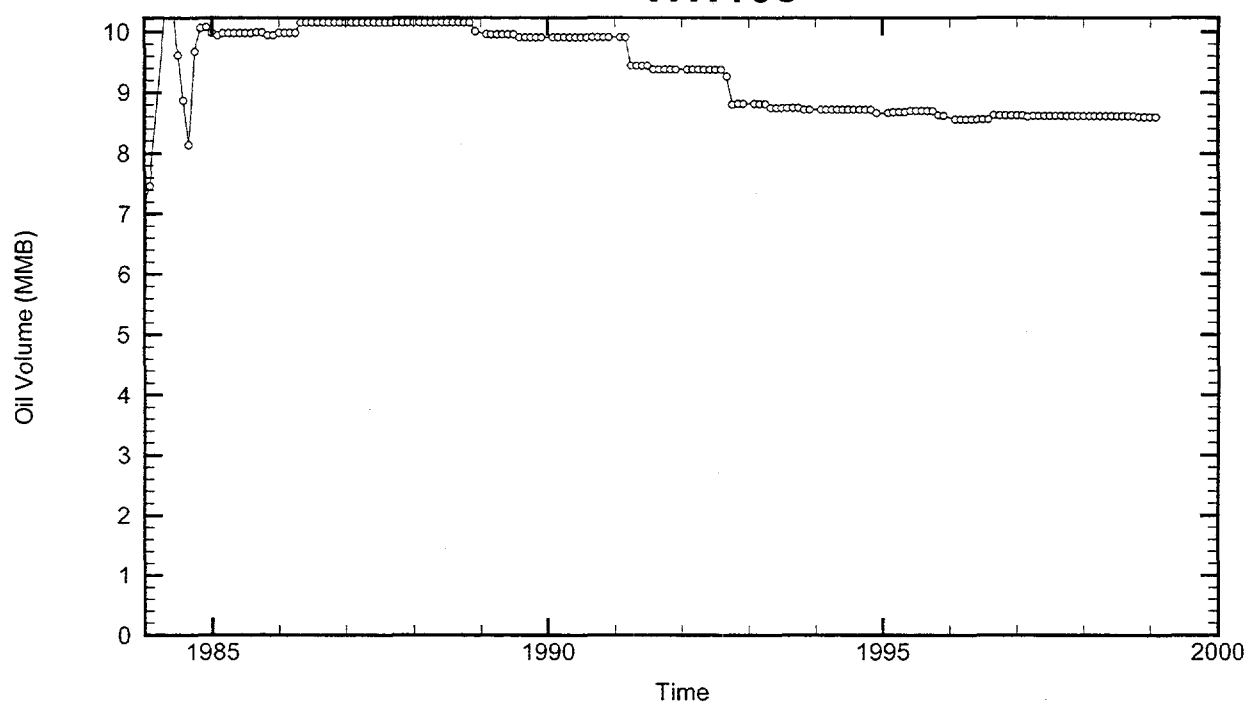
Brine Injection Temperature: 69.55 °F

Number of iterations: 349

WH102



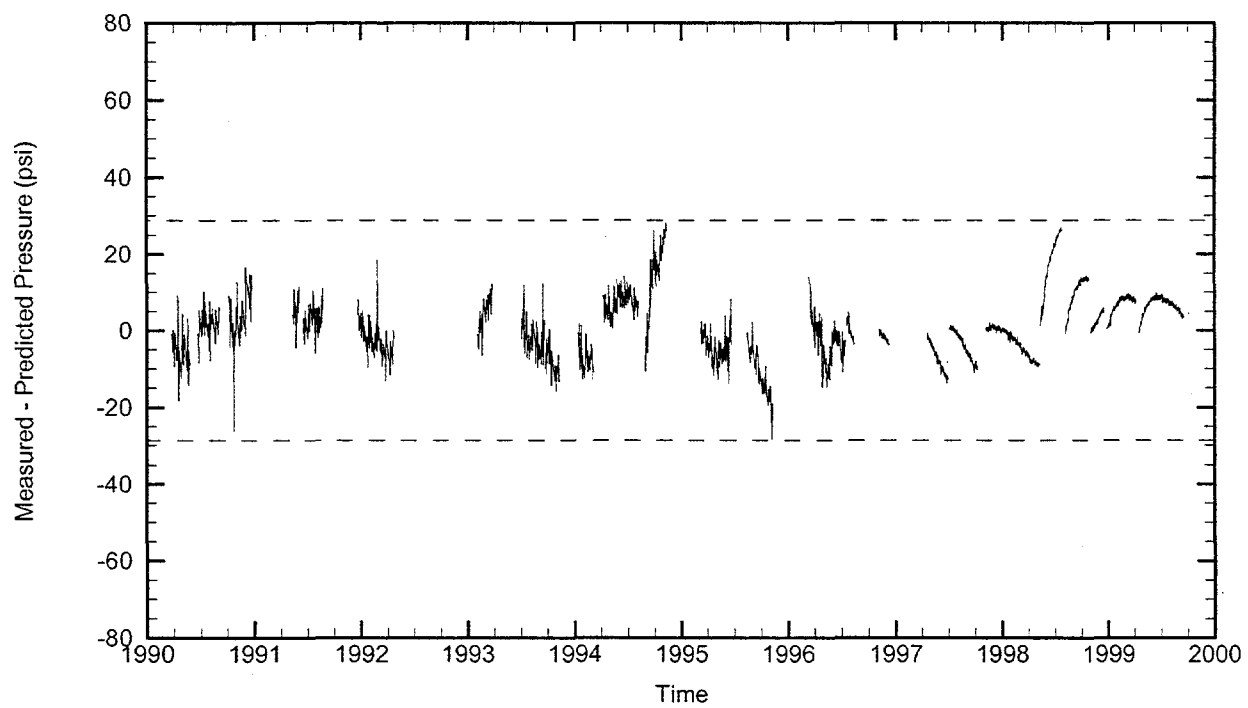
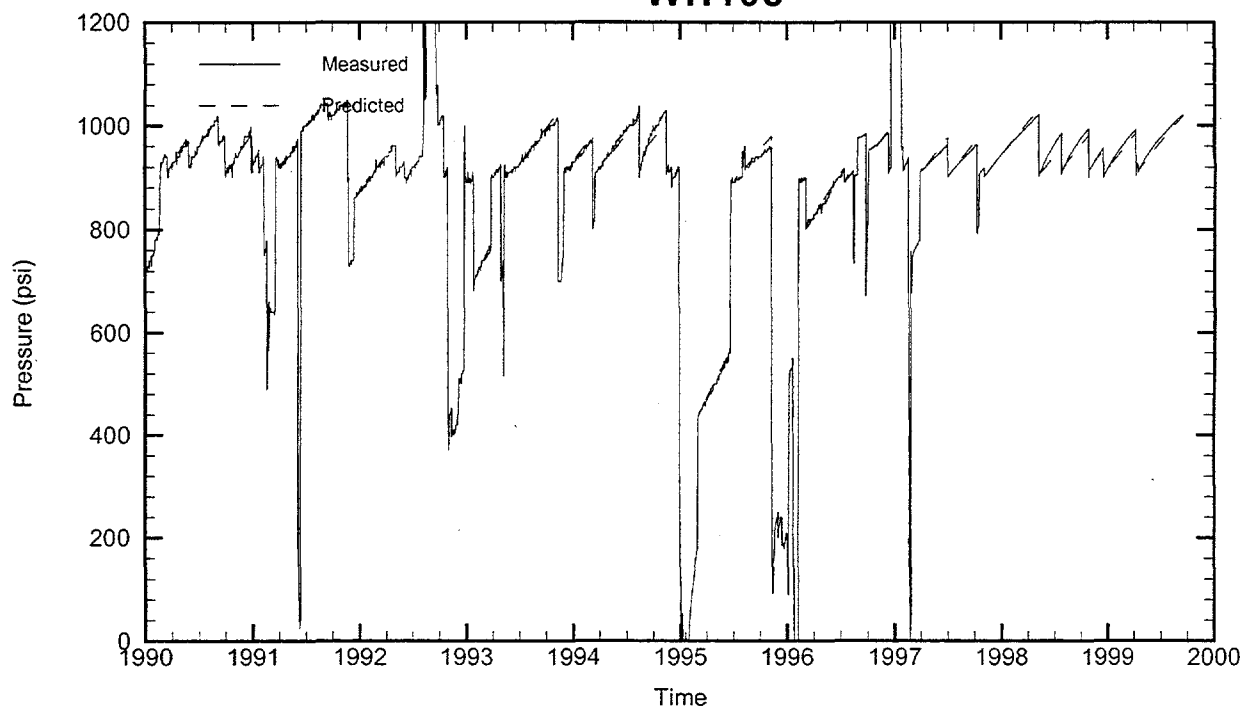
WH103



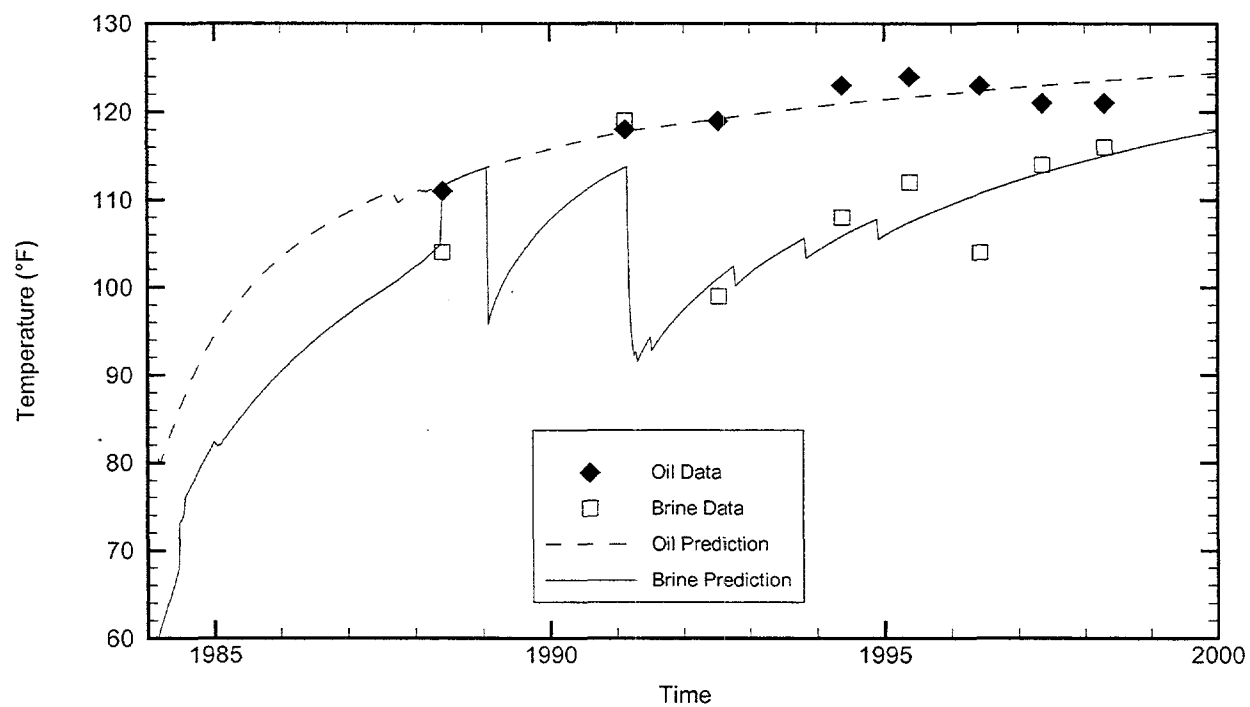
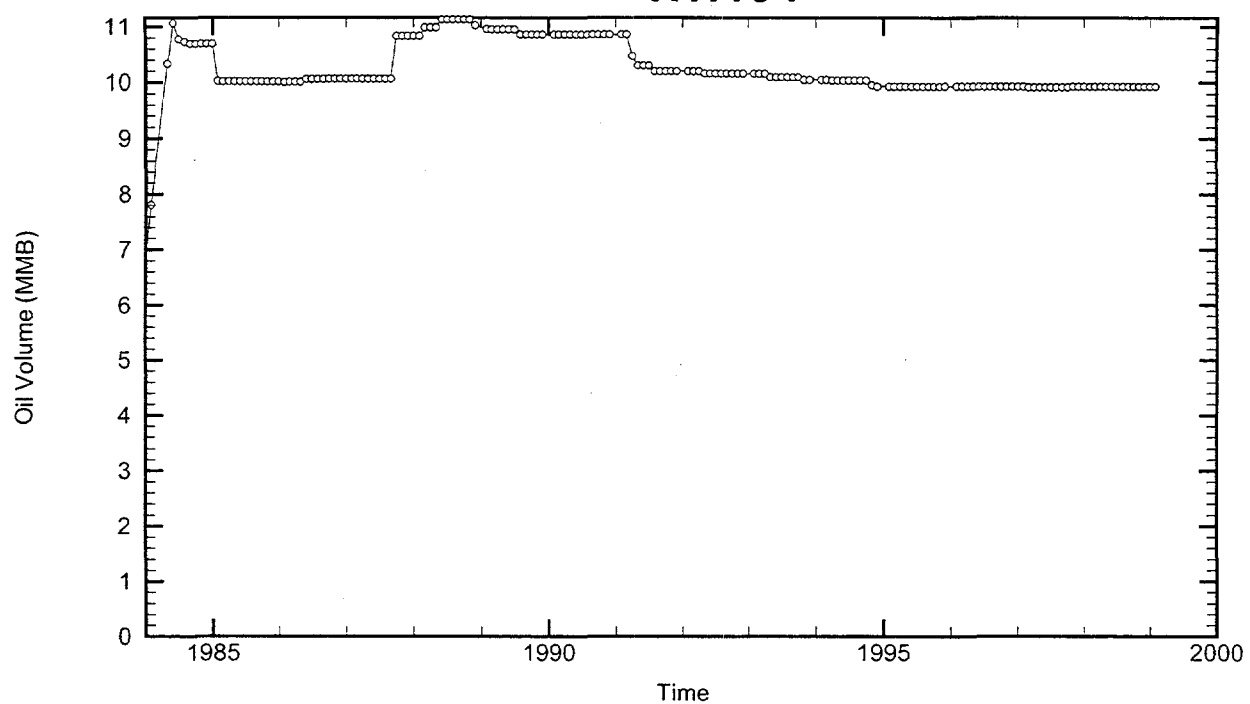
Cavern: WH103
End of Leaching: 01/14/1984
Duration of Leaching: 2.4312 months
Leaching Temperature: 70.00 °F

Degas: 01/04/1996, 118.00 °F, 6.24 MMB
Oil Injection Temperature: 70.42 °F
Brine Injection Temperature: 85.80 °F
Number of iterations: 388

WH103



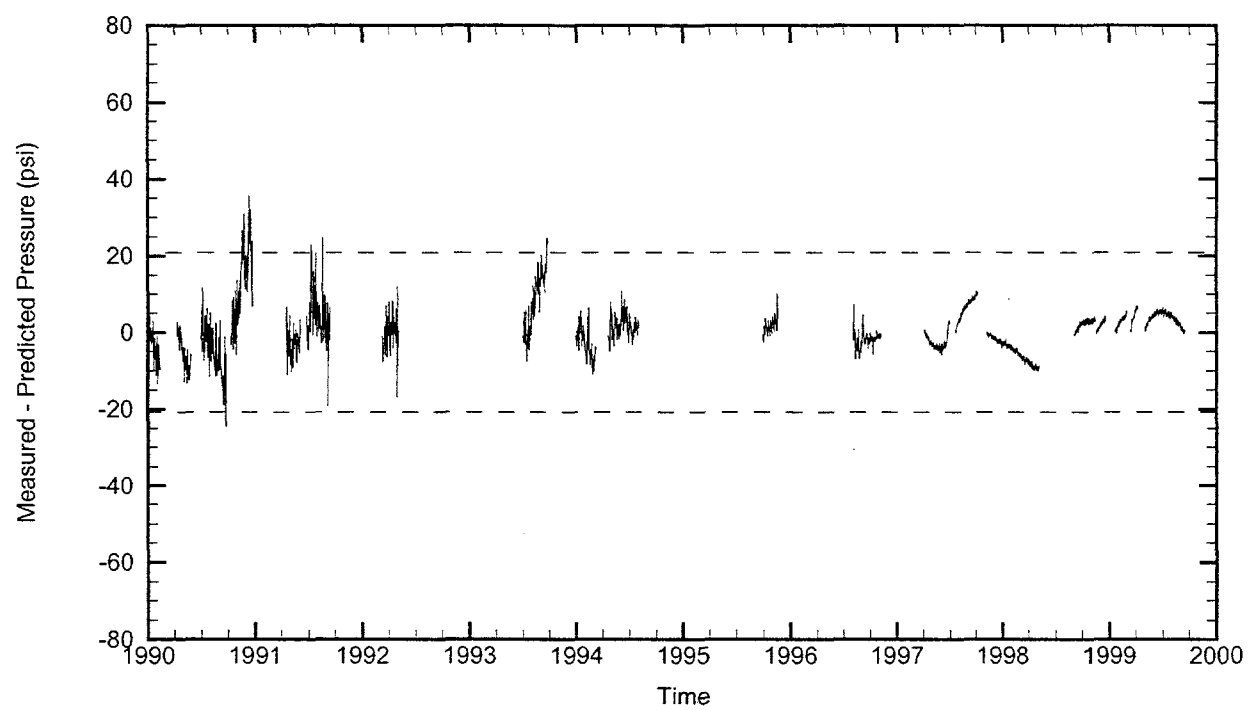
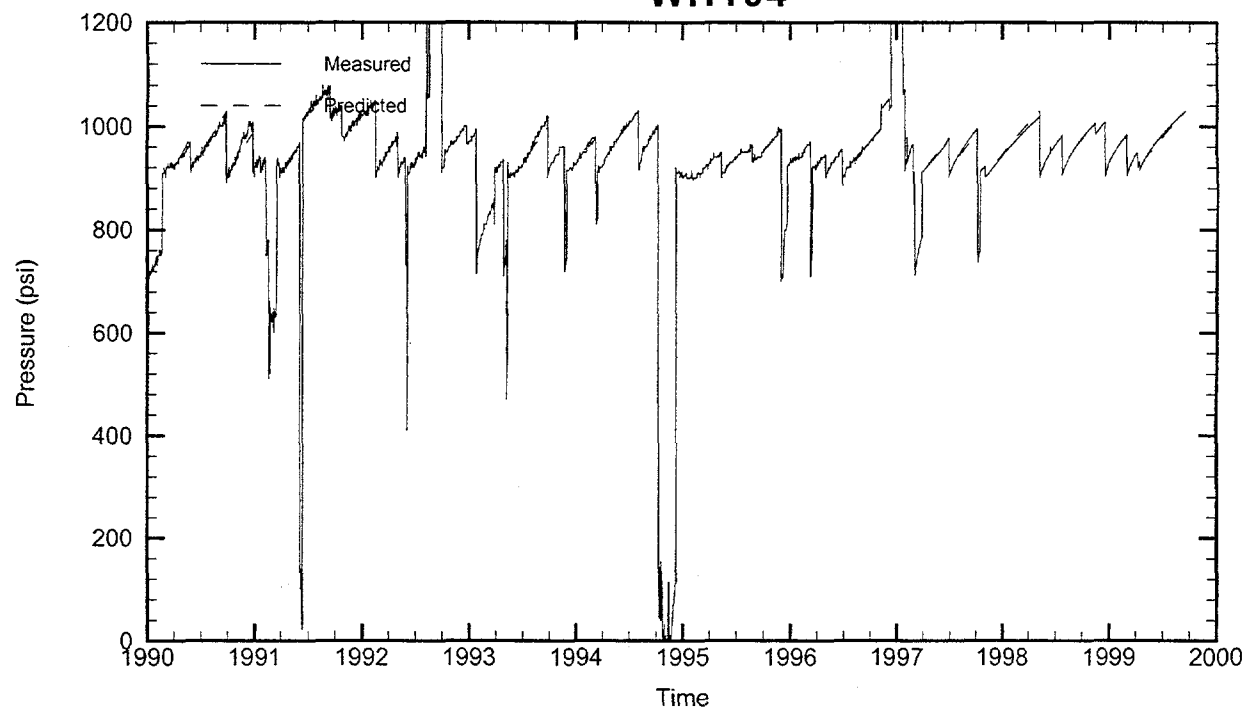
WH104



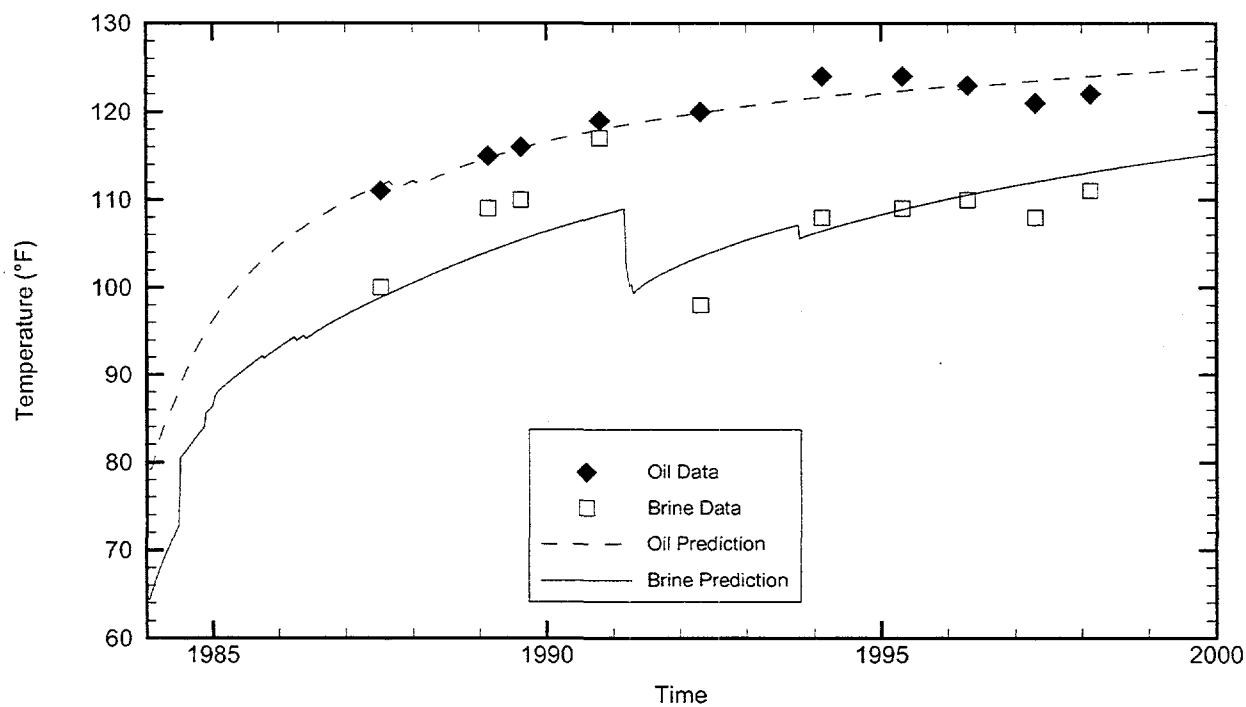
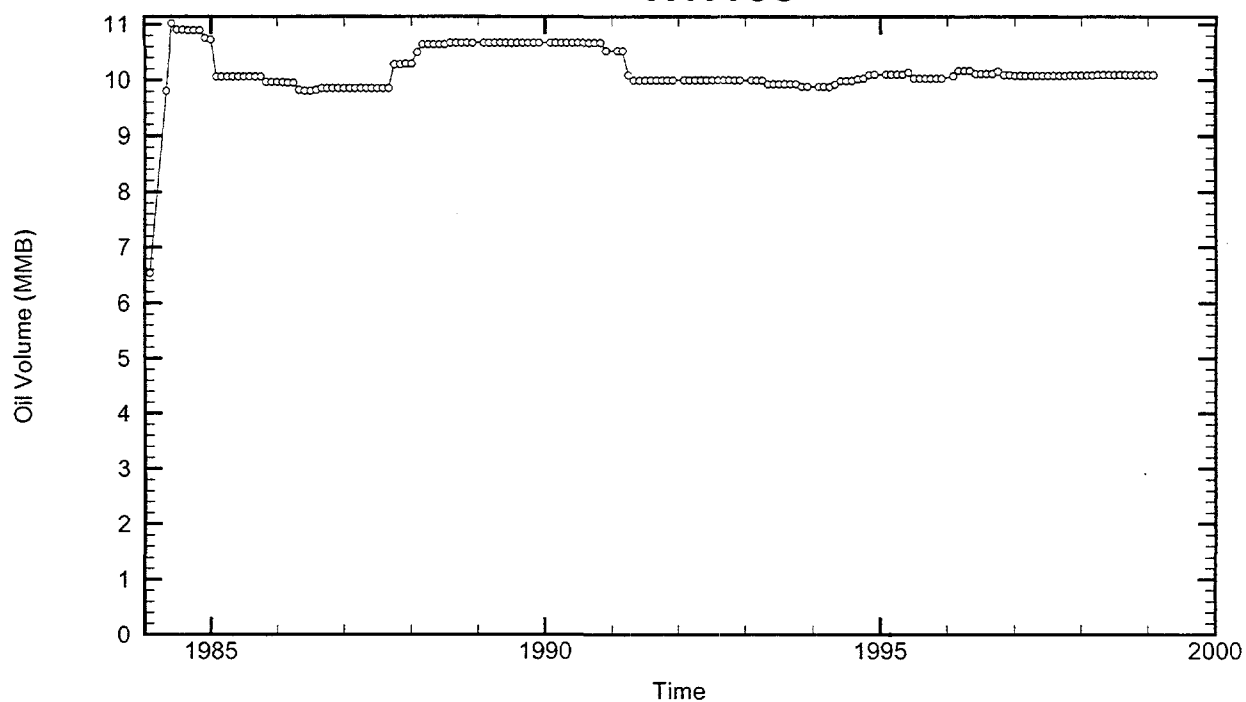
Cavern: WH104
End of Leaching: 02/27/1984
Duration of Leaching: 3.8768 months
Leaching Temperature: 60.00 °F

Oil Injection Temperature: 80.42 °F
Brine Injection Temperature: 80.63 °F
Number of iterations: 330

WH104



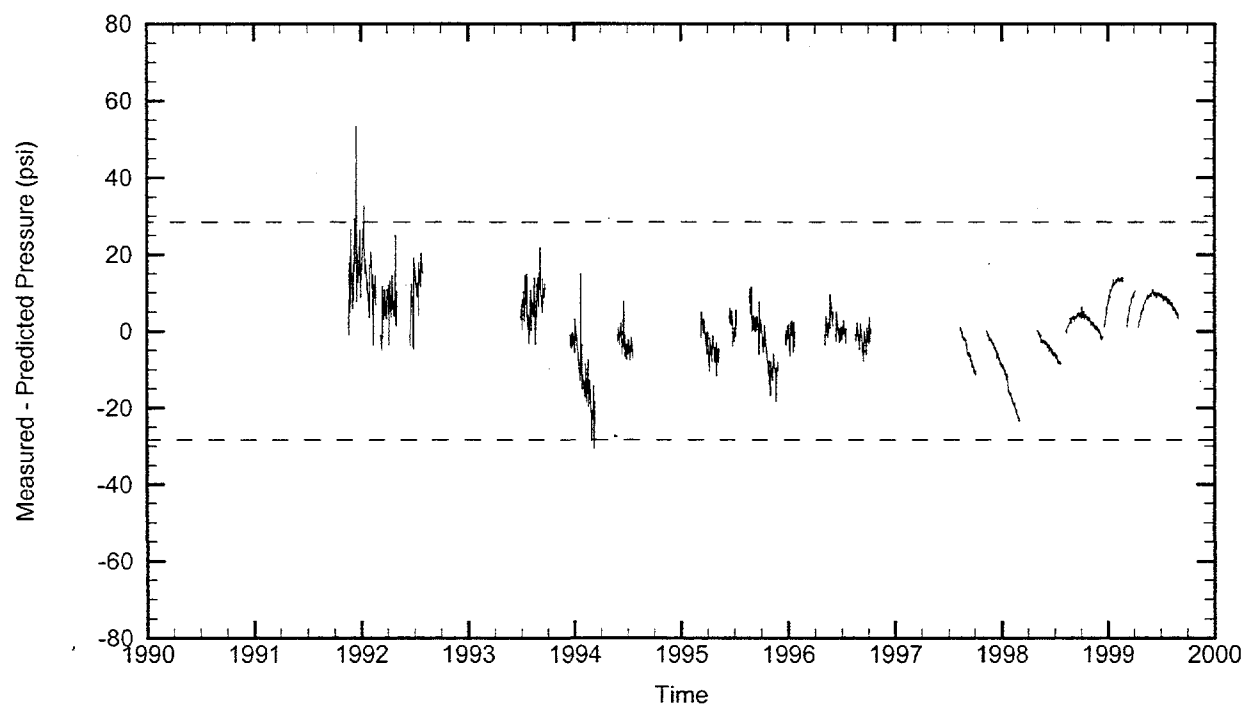
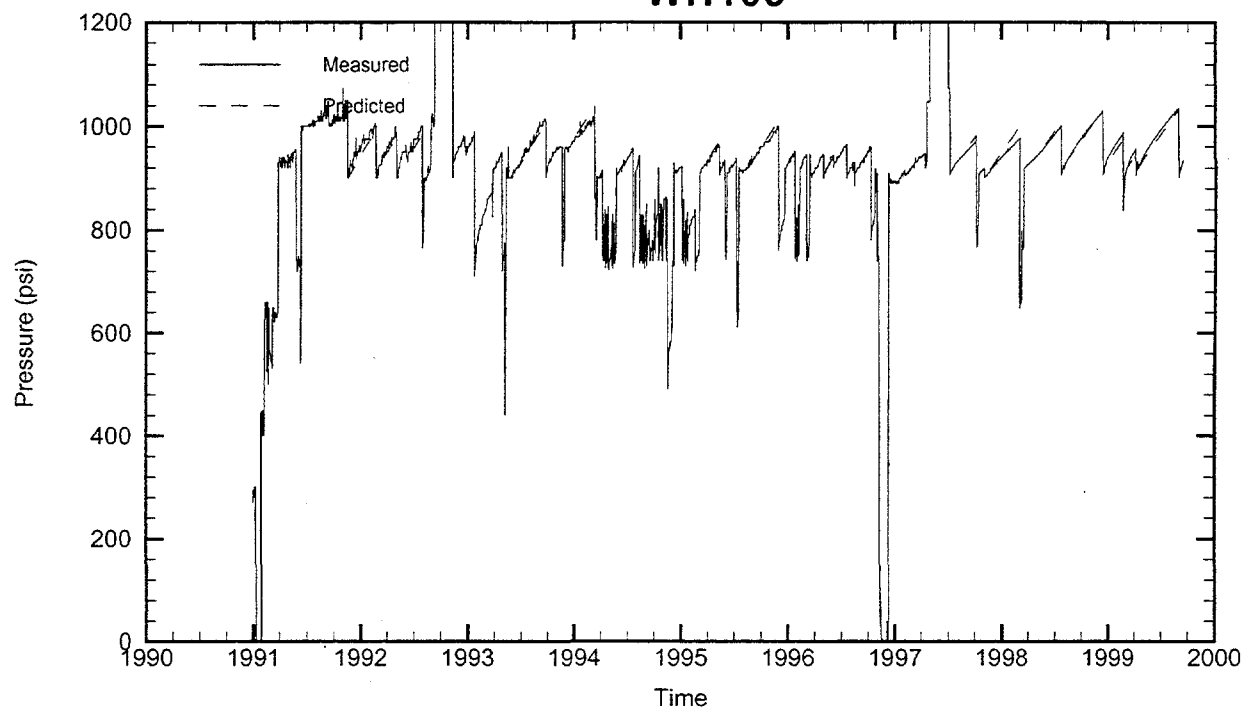
WH105



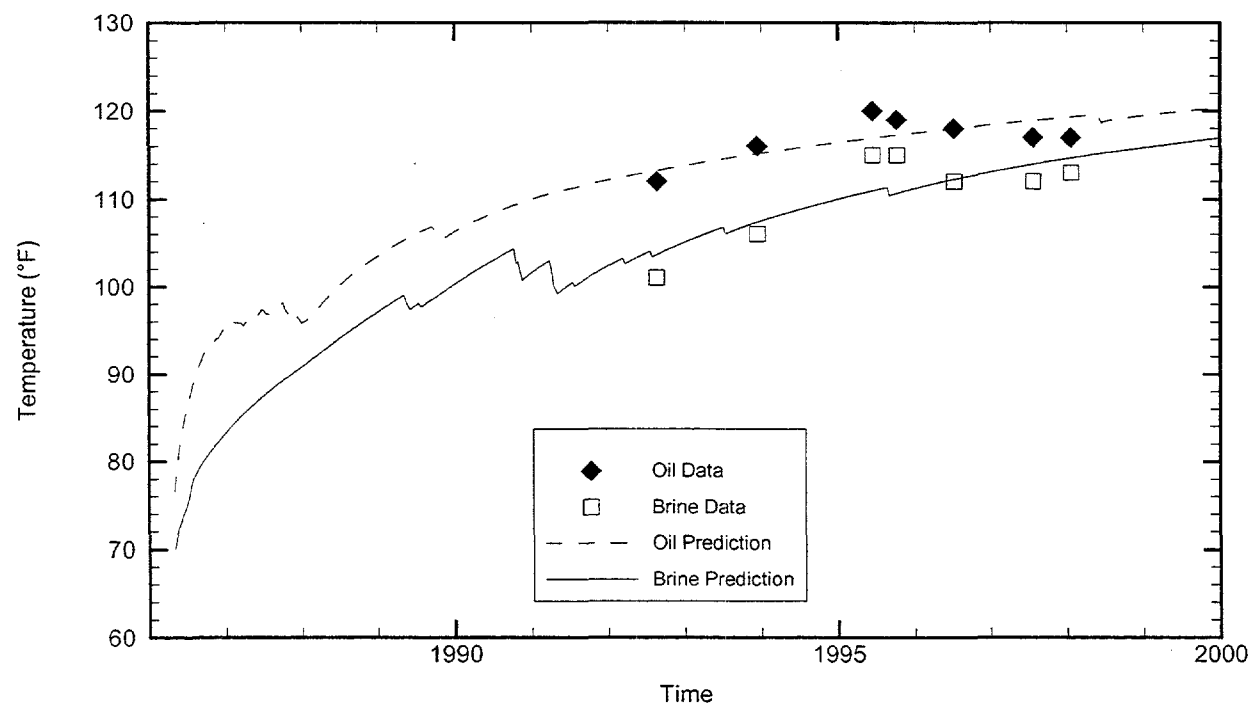
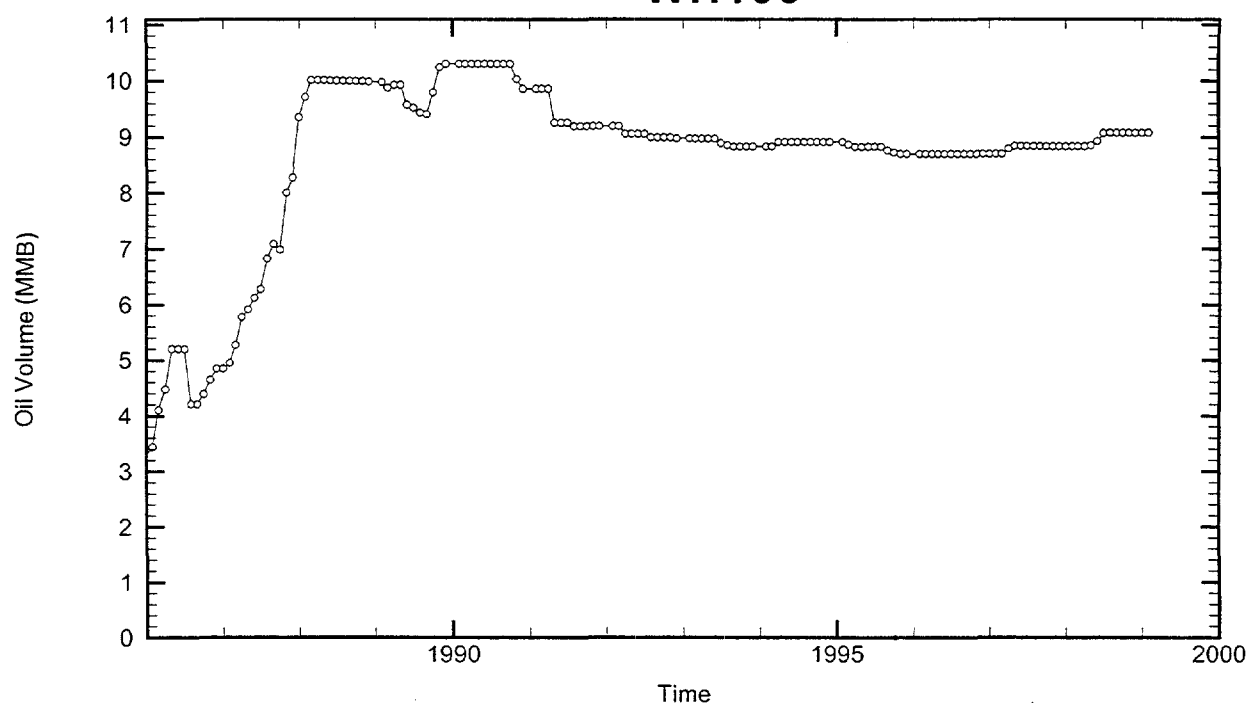
Cavern: WH105
End of Leaching: 01/18/1984
Duration of Leaching: 2.9897 months
Leaching Temperature: 64.32 °F

Oil Injection Temperature: 79.14 °F
Brine Injection Temperature: 88.49 °F
Number of iterations: 432

WH105



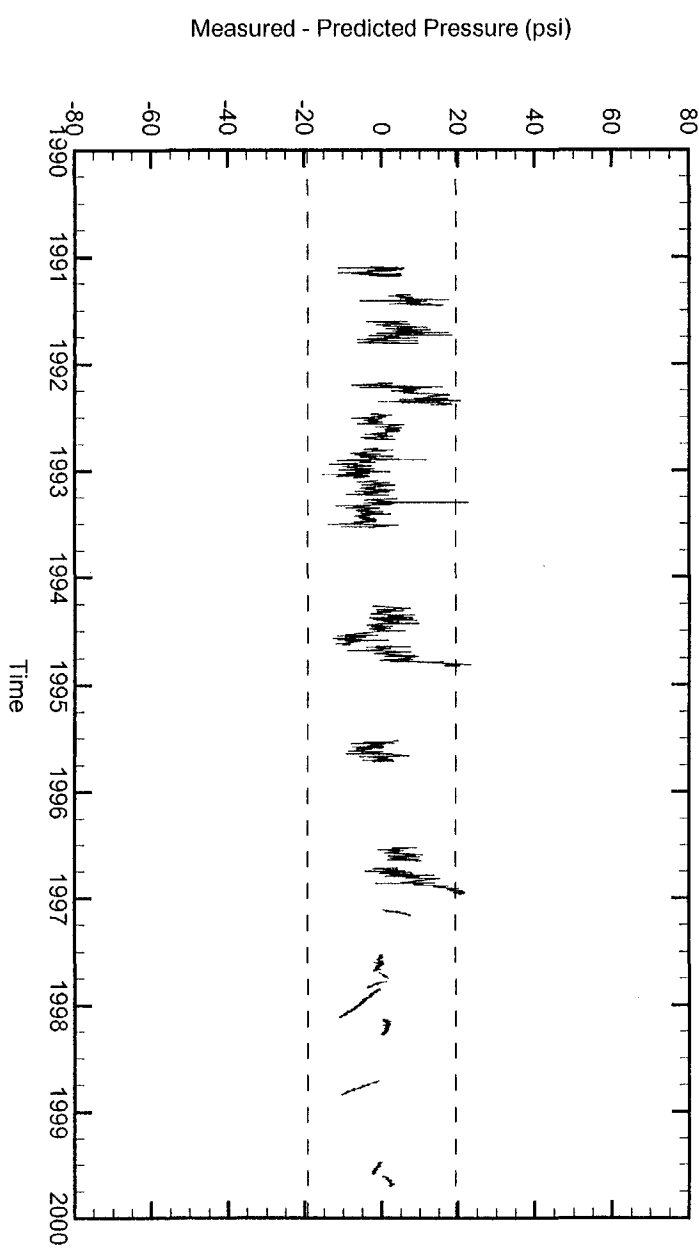
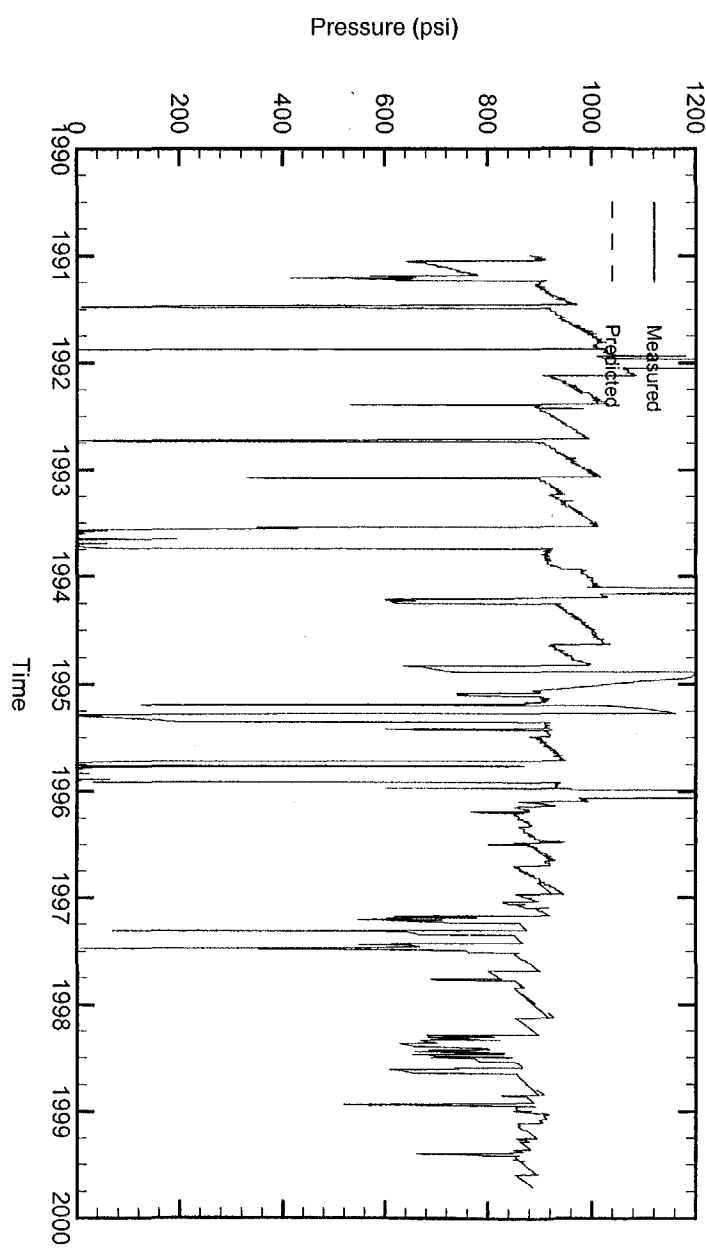
WH106



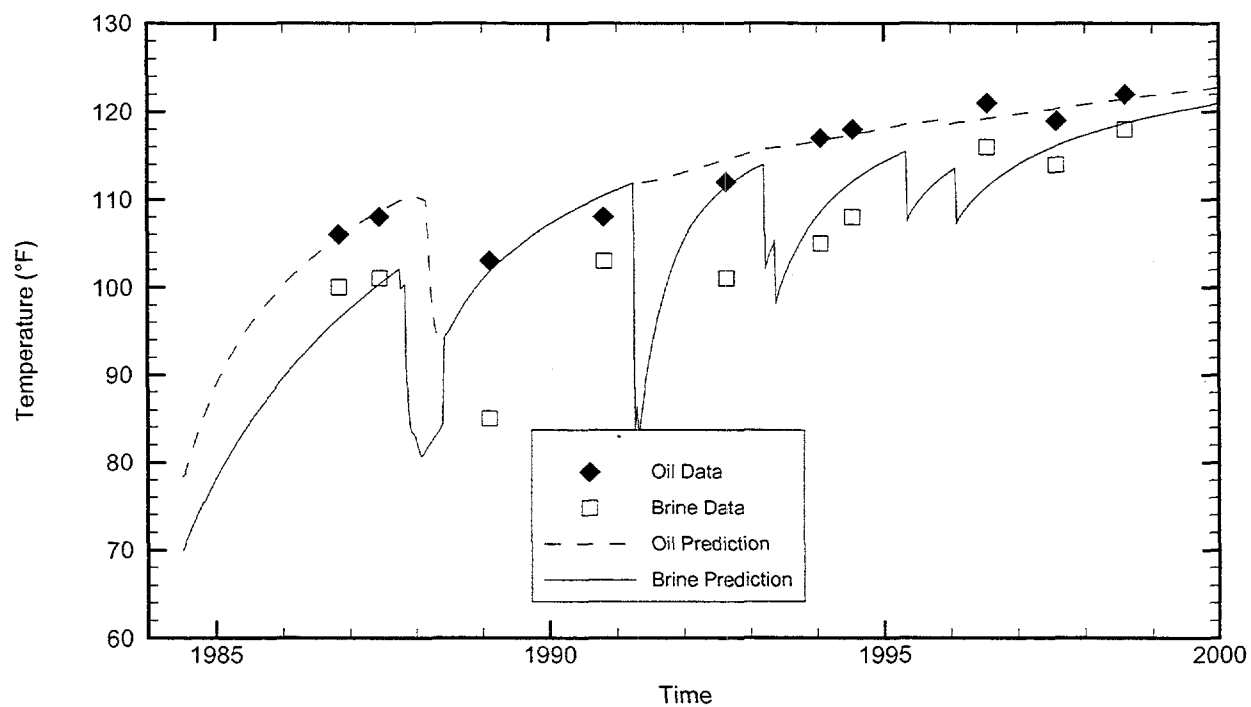
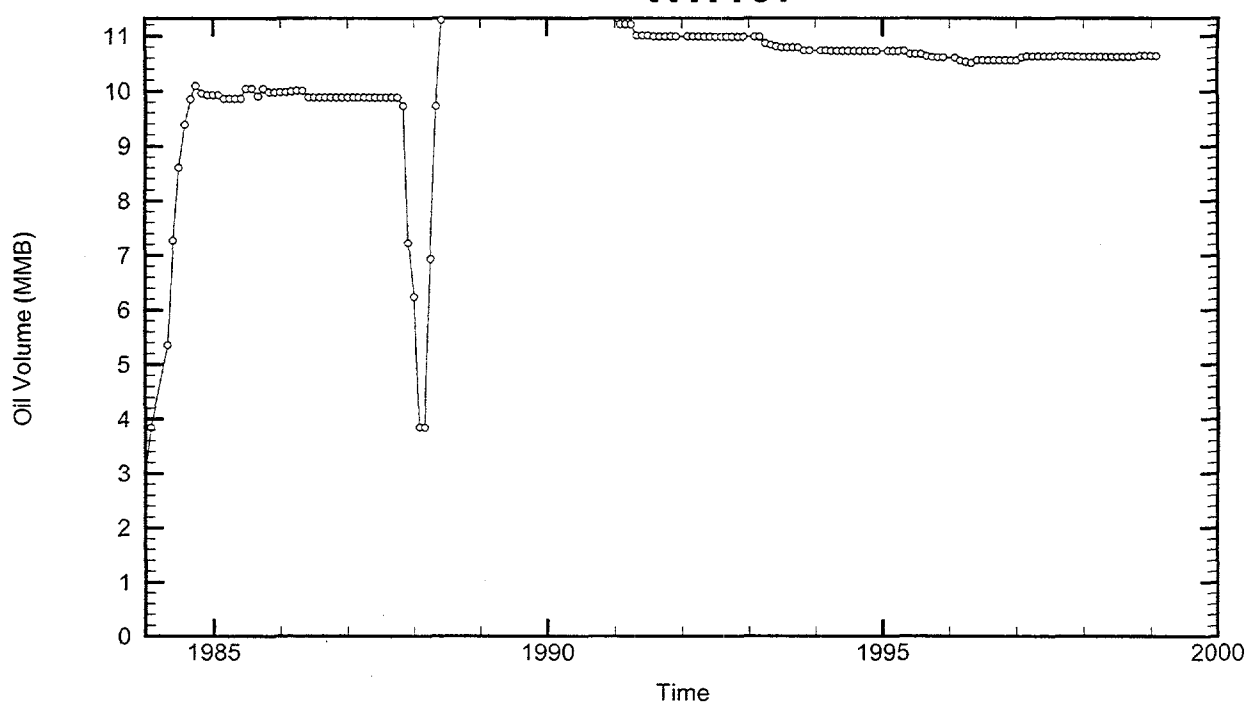
Cavern: WH106
End of Leaching: 05/01/1986
Duration of Leaching: 1.0833 years
Leaching Temperature: 70.00 °F

Oil Injection Temperature: 76.56 °F
Brine Injection Temperature: 89.84 °F
Number of iterations: 305

WH106



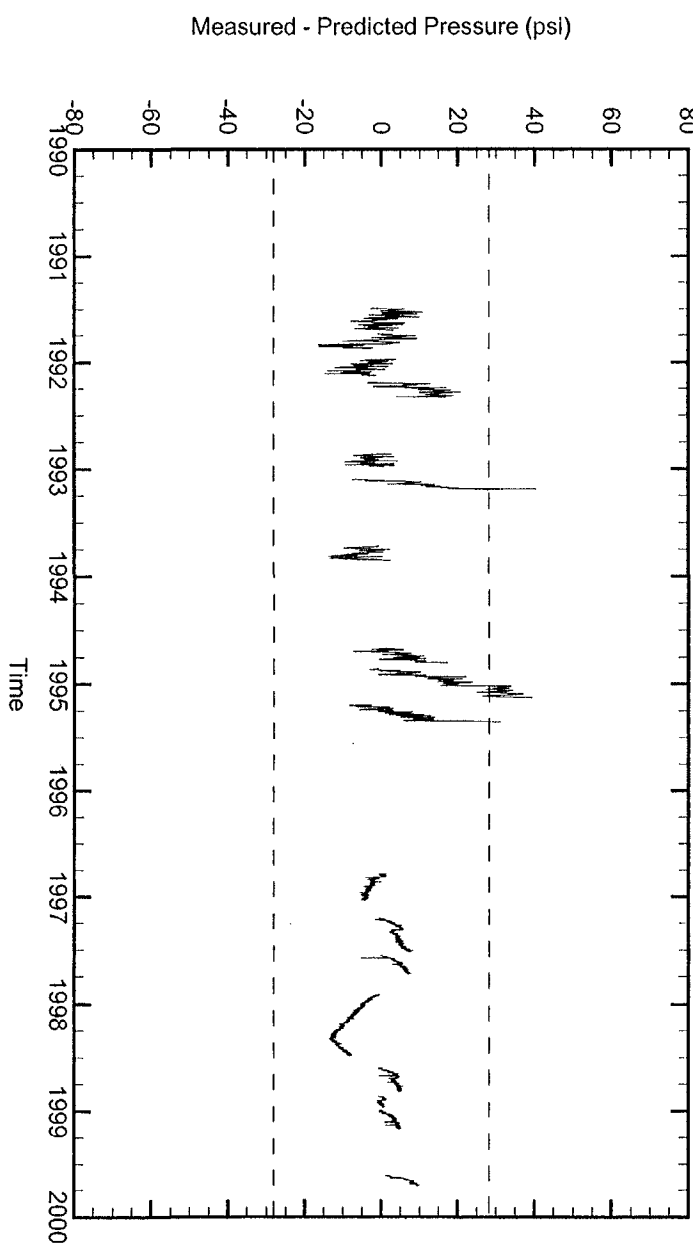
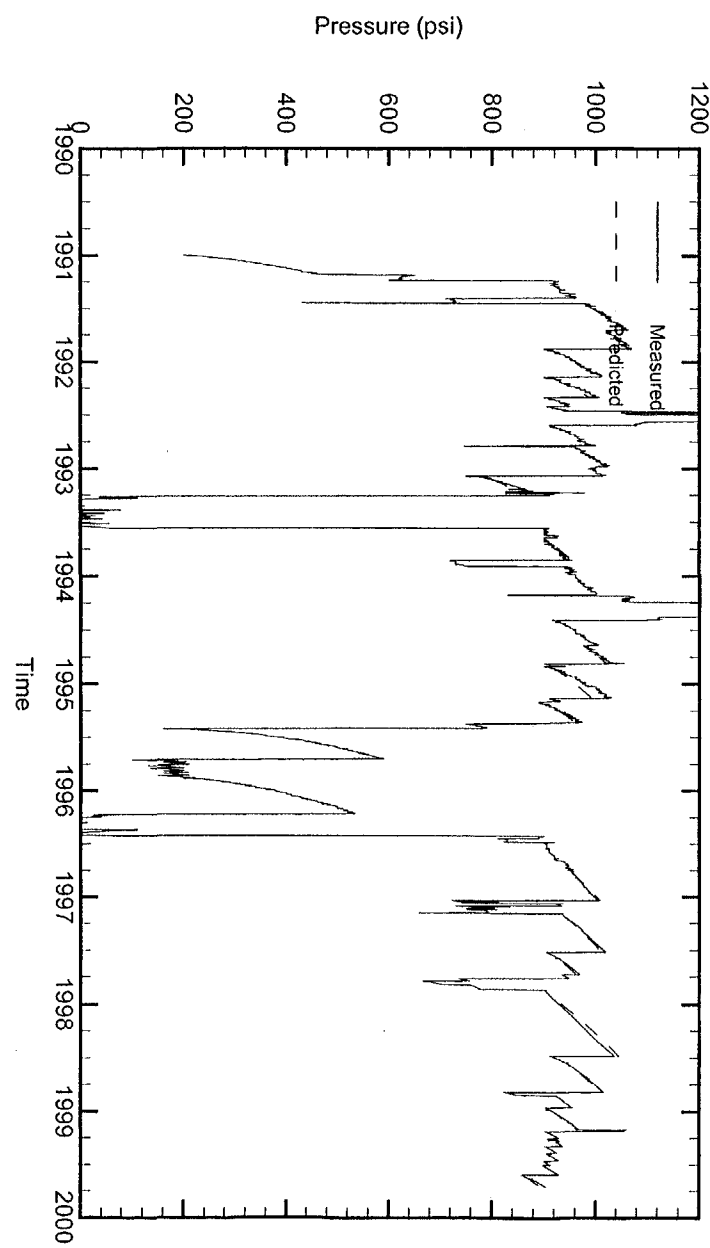
WH107



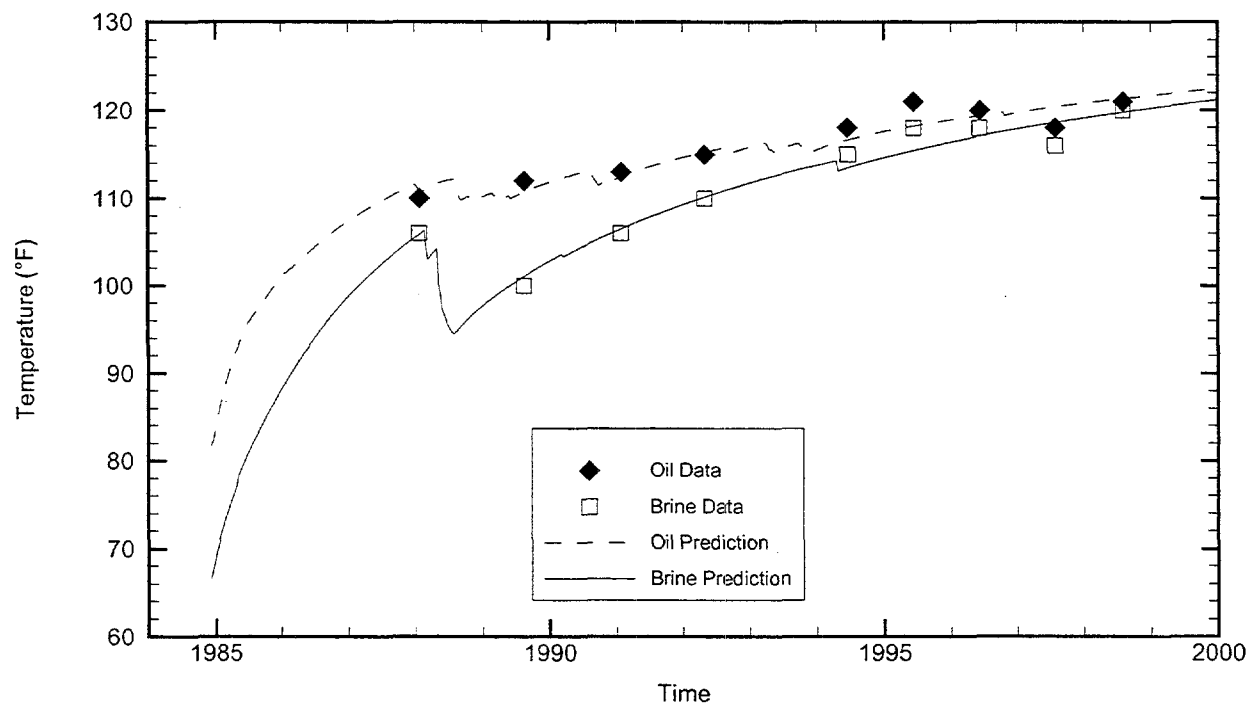
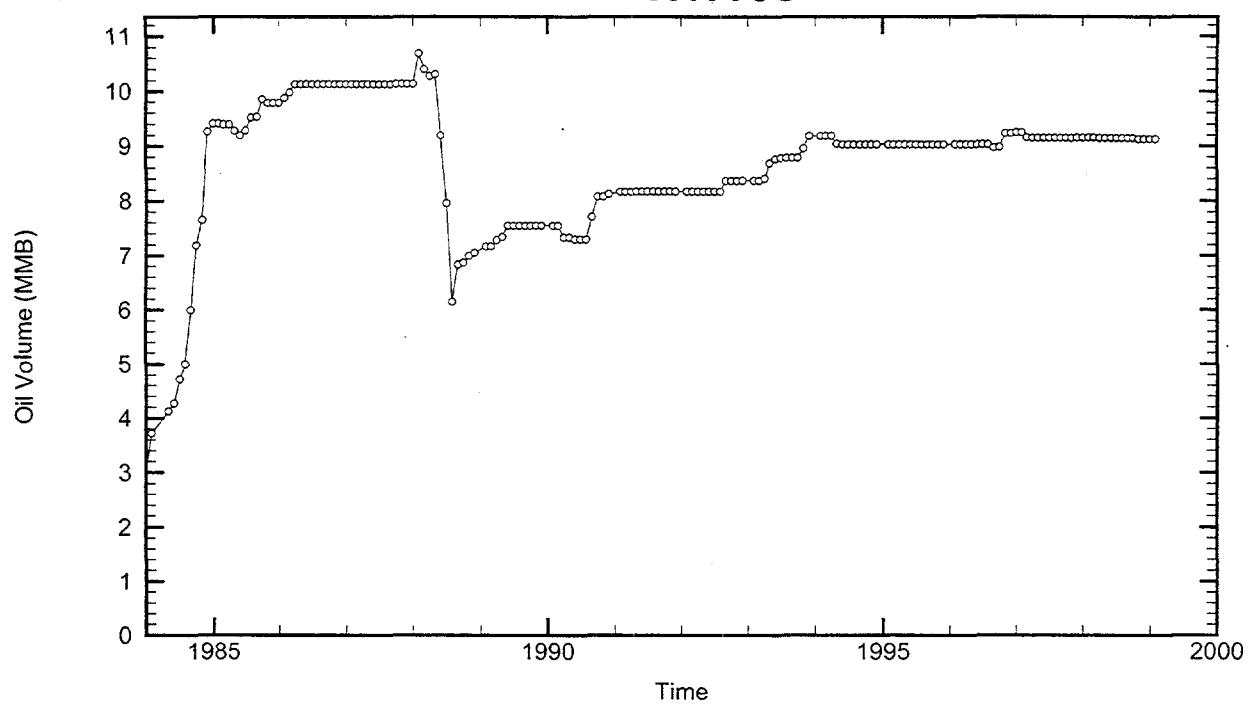
Cavern: WH107
 End of Leaching: 07/06/1984
 Duration of Leaching: 5.8152 months
 Leaching Temperature: 69.91 °F

Degas: 11/17/1995, 118.00 °F, 8.16 MMB
 Oil Injection Temperature: 78.27 °F
 Brine Injection Temperature: 72.32 °F
 Number of iterations: 181

WH107



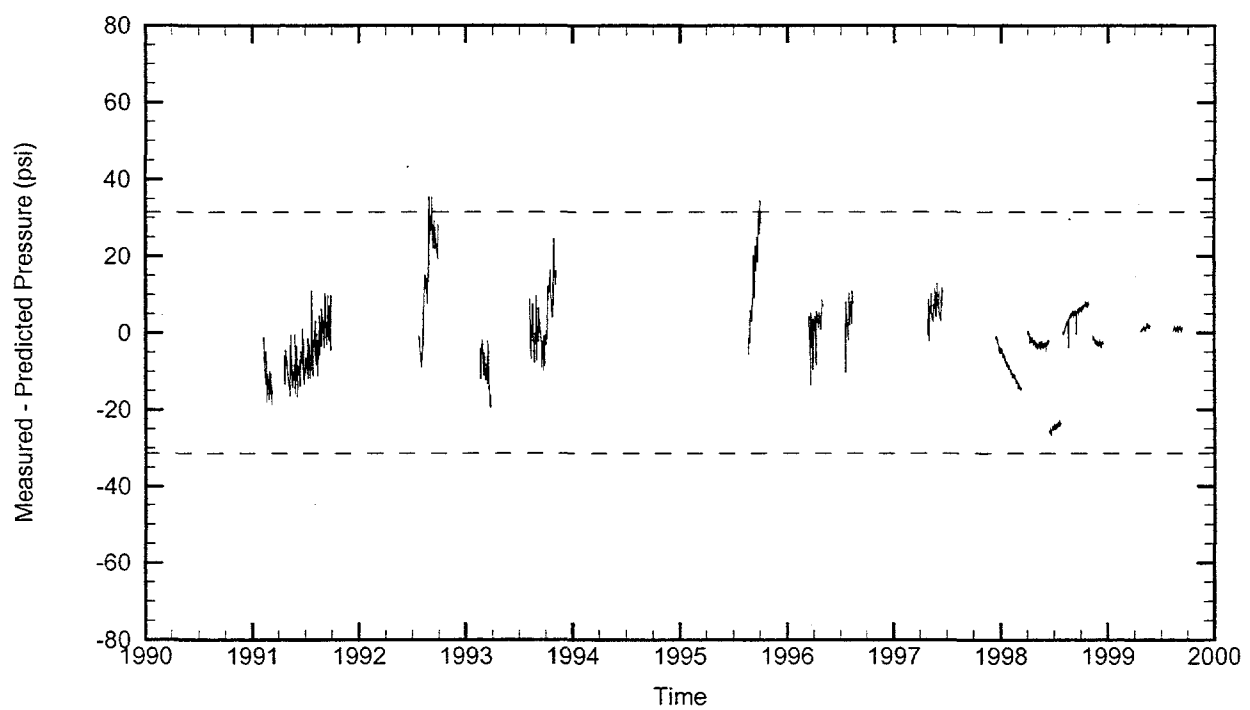
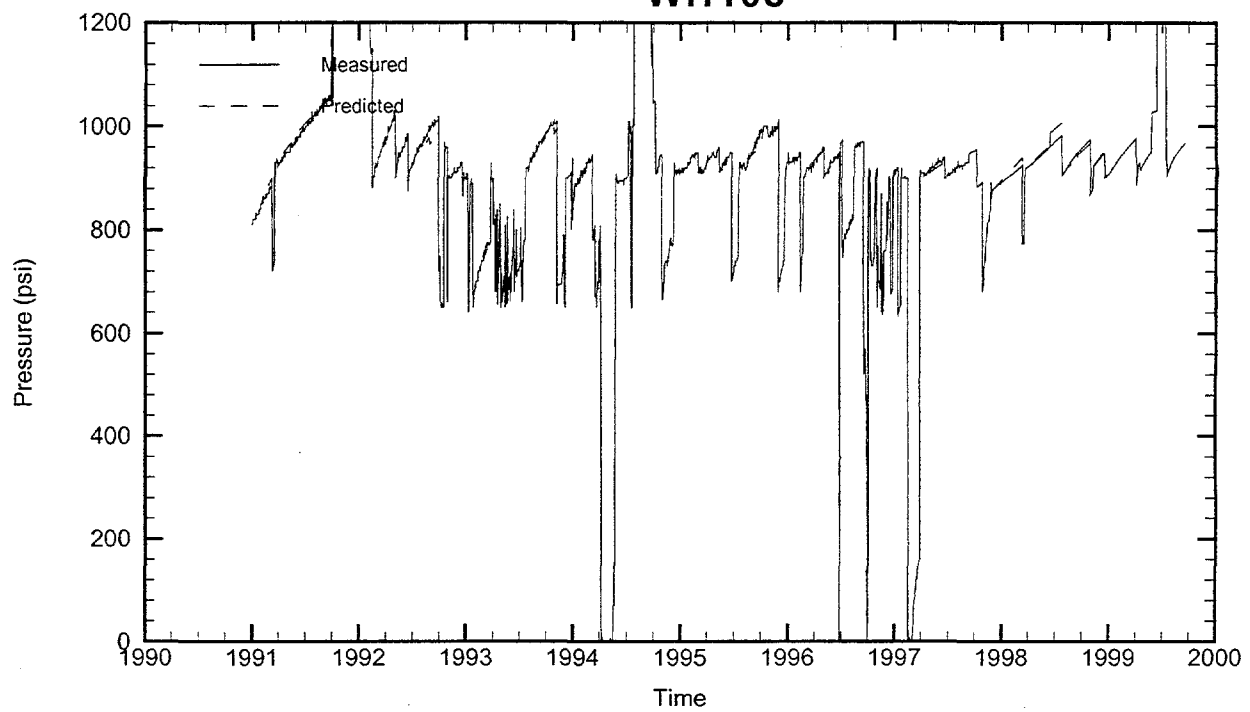
WH108



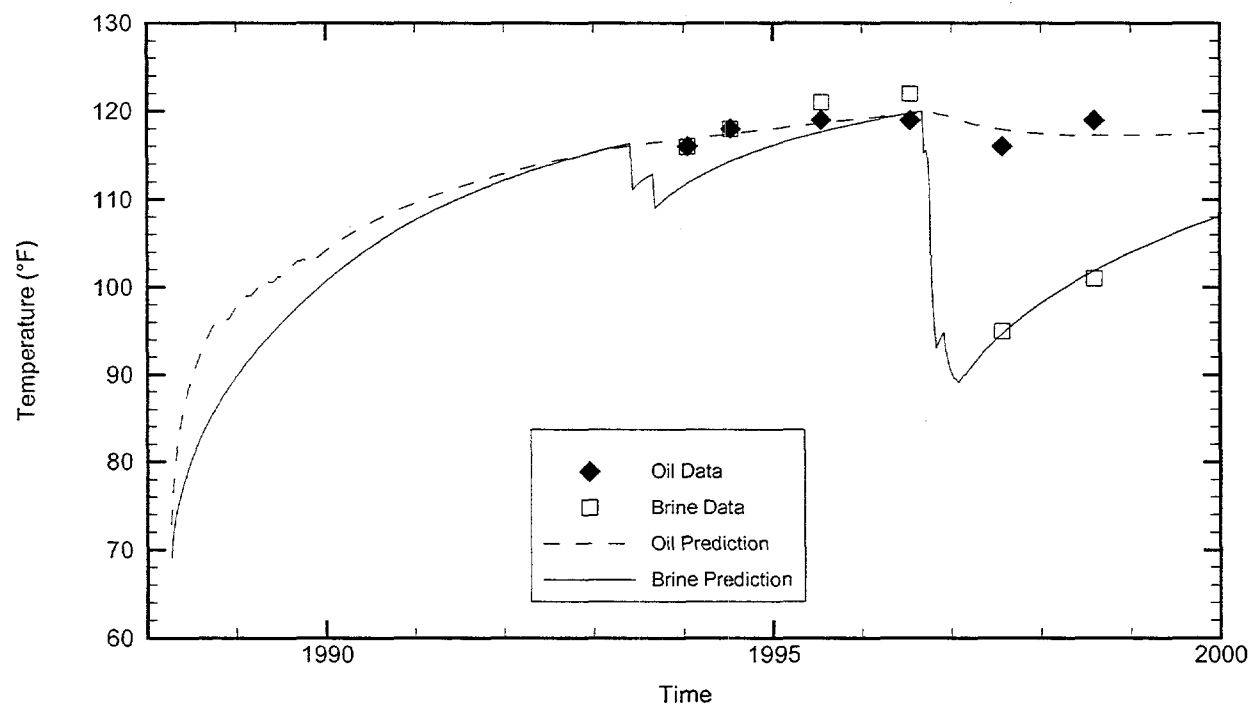
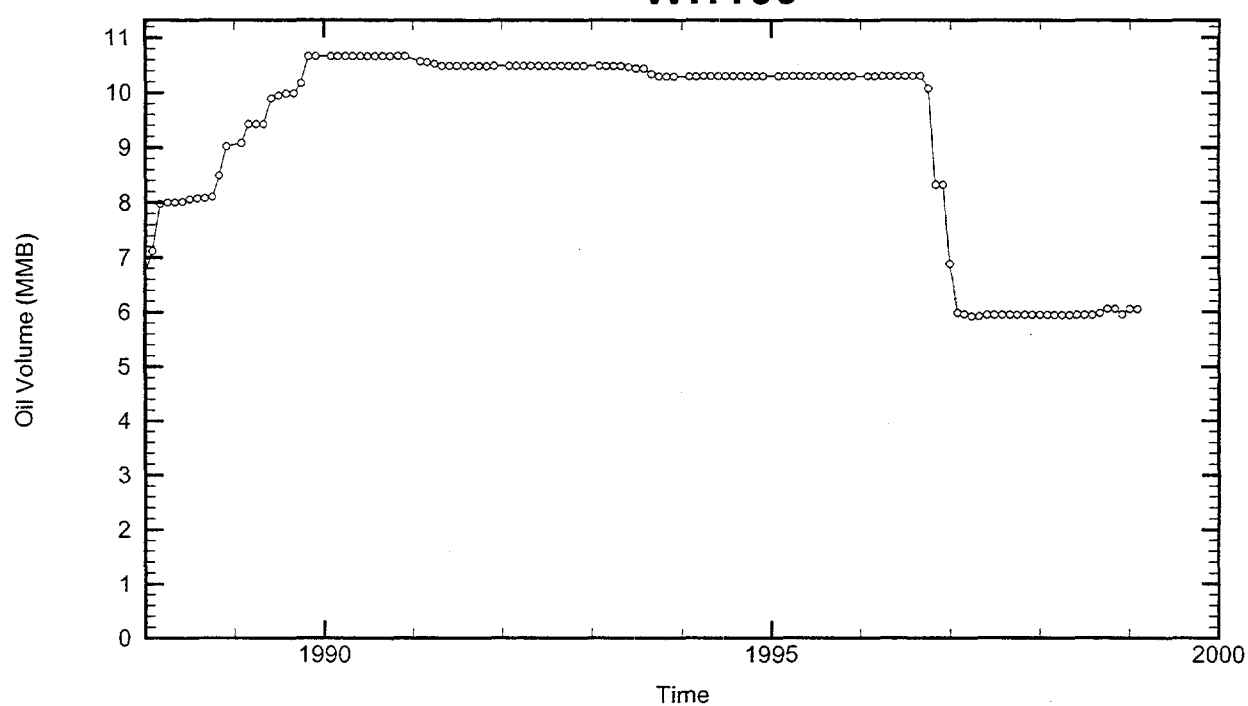
Cavern: WH108
 End of Leaching: 12/07/1984
 Duration of Leaching: 1.3799 months
 Leaching Temperature: 66.62 °F

Oil Injection Temperature: 81.71 °F
 Brine Injection Temperature: 90.00 °F
 Number of iterations: 443

WH108



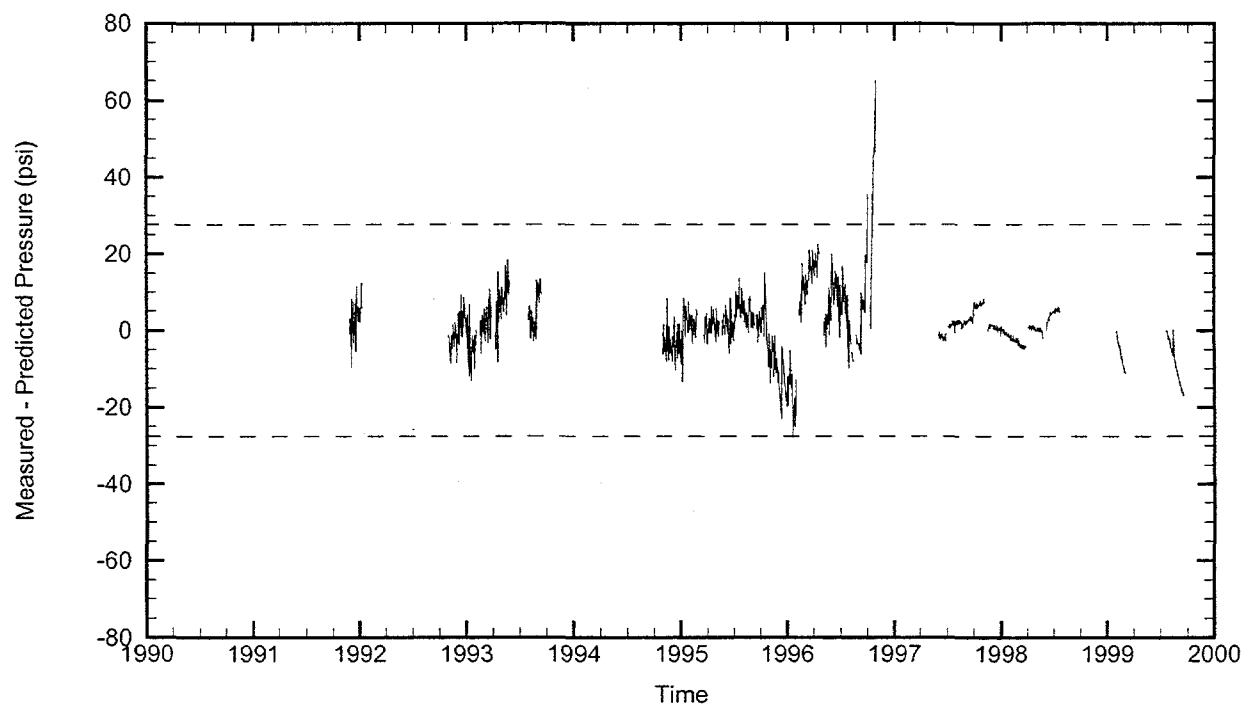
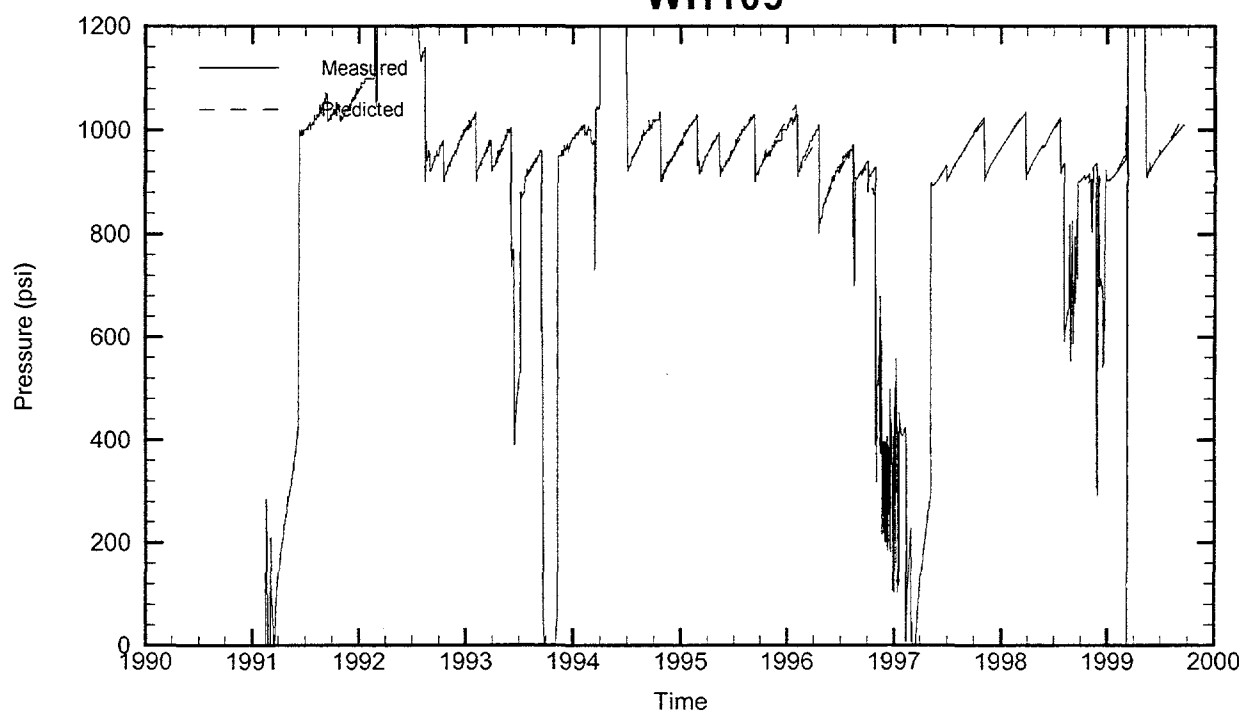
WH109



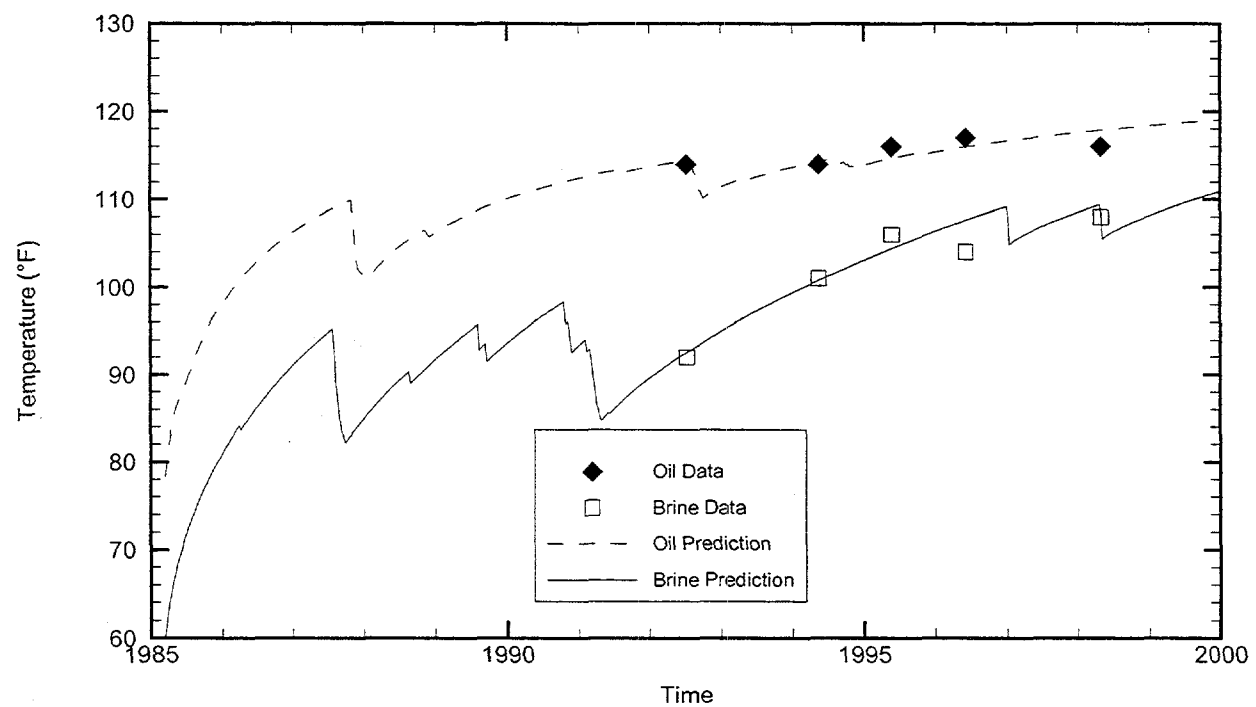
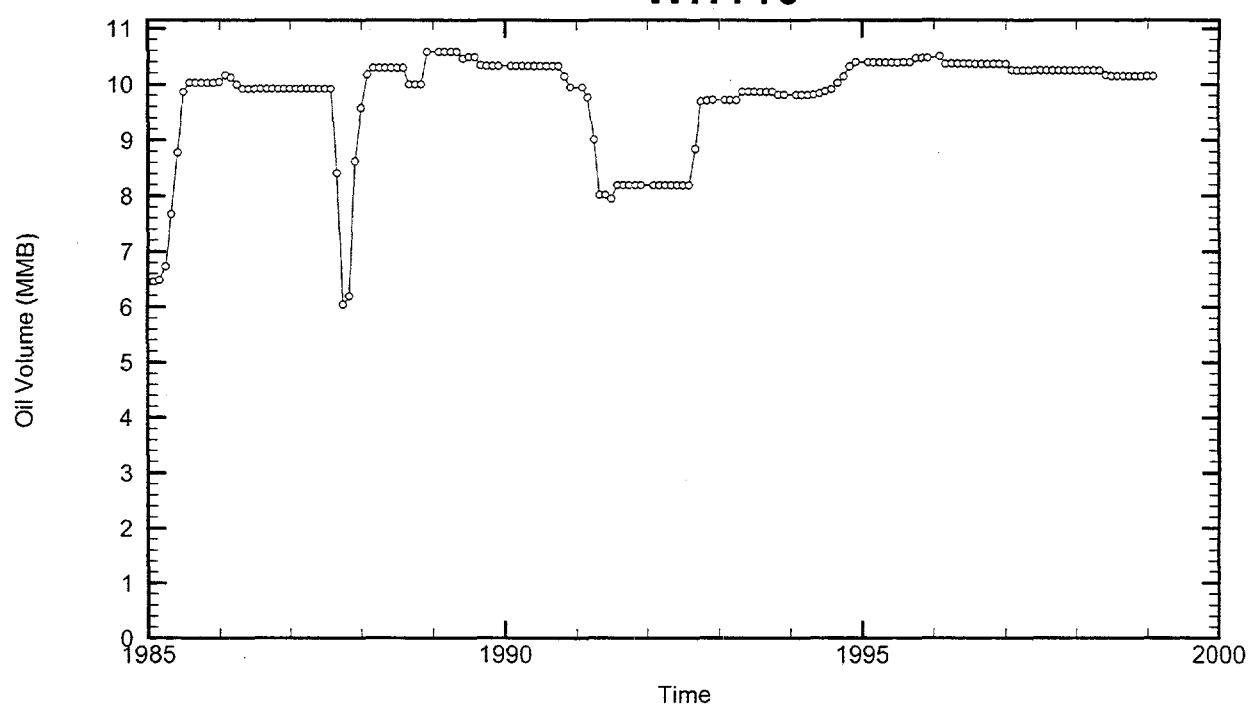
Cavern: WH109
End of Leaching: 04/06/1988
Duration of Leaching: 2.0000 days
Leaching Temperature: 69.08 °F

Oil Injection Temperature: 72.85 °F
Brine Injection Temperature: 76.23 °F
Number of iterations: 294

WH109



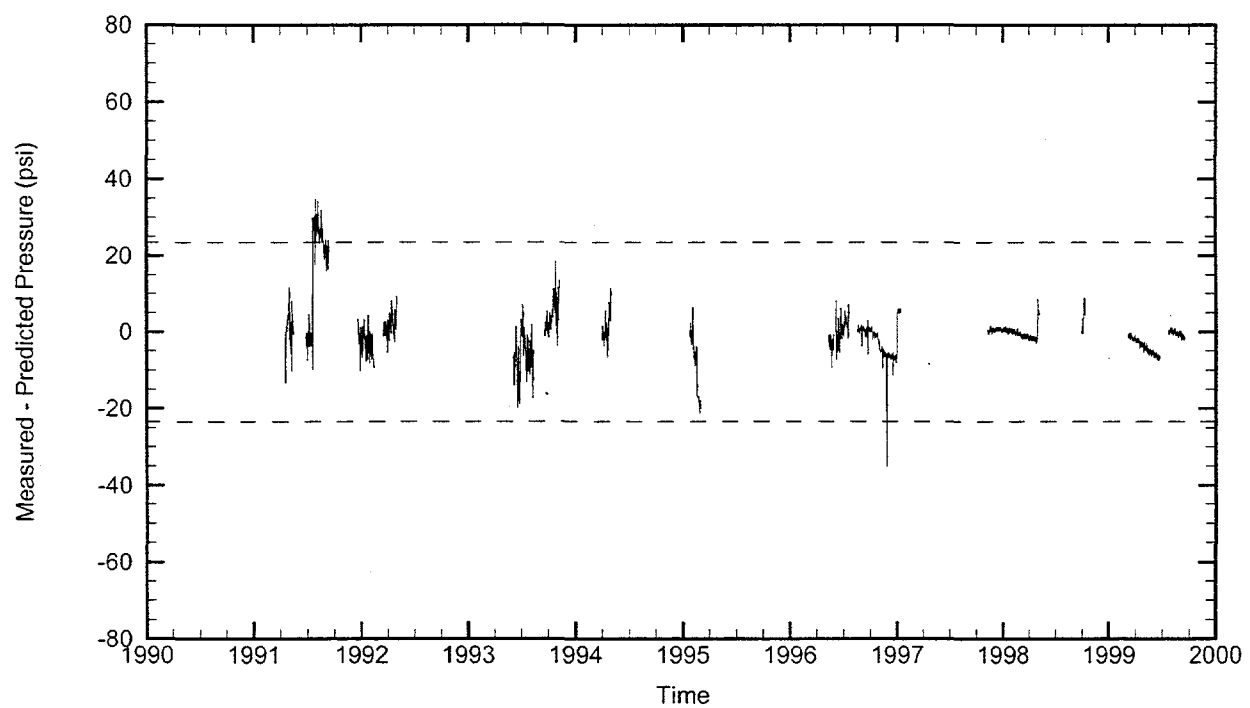
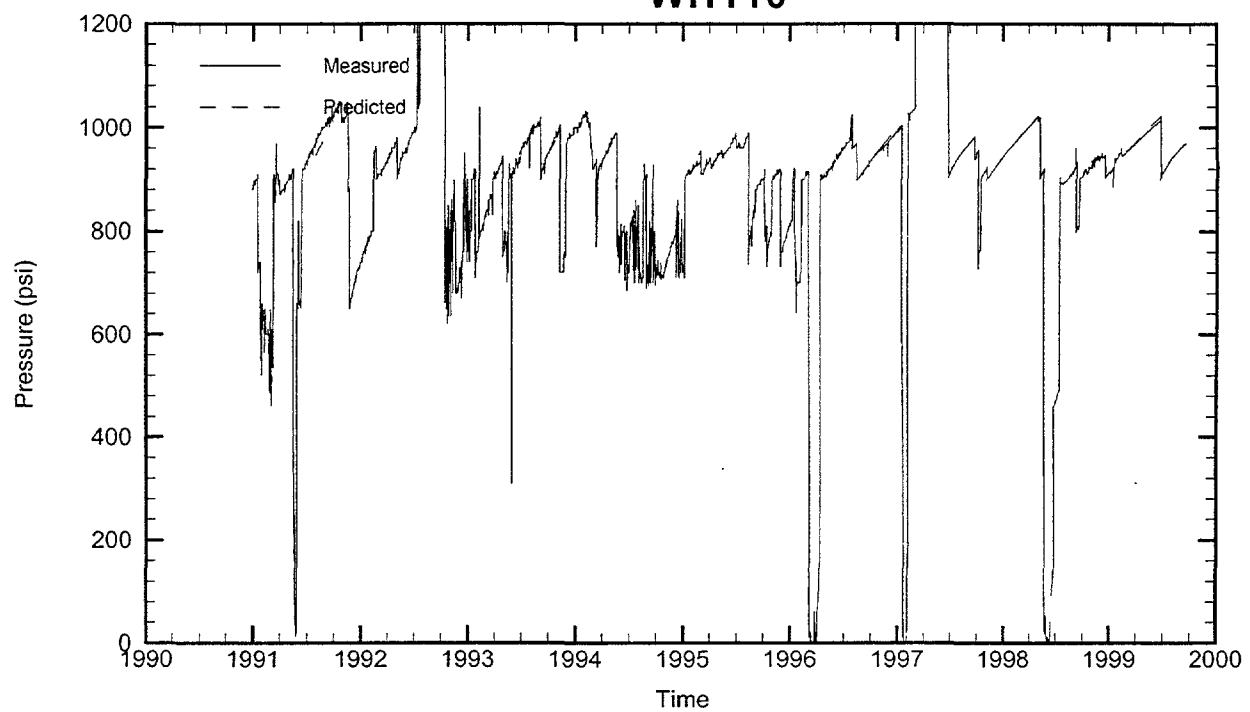
WH110



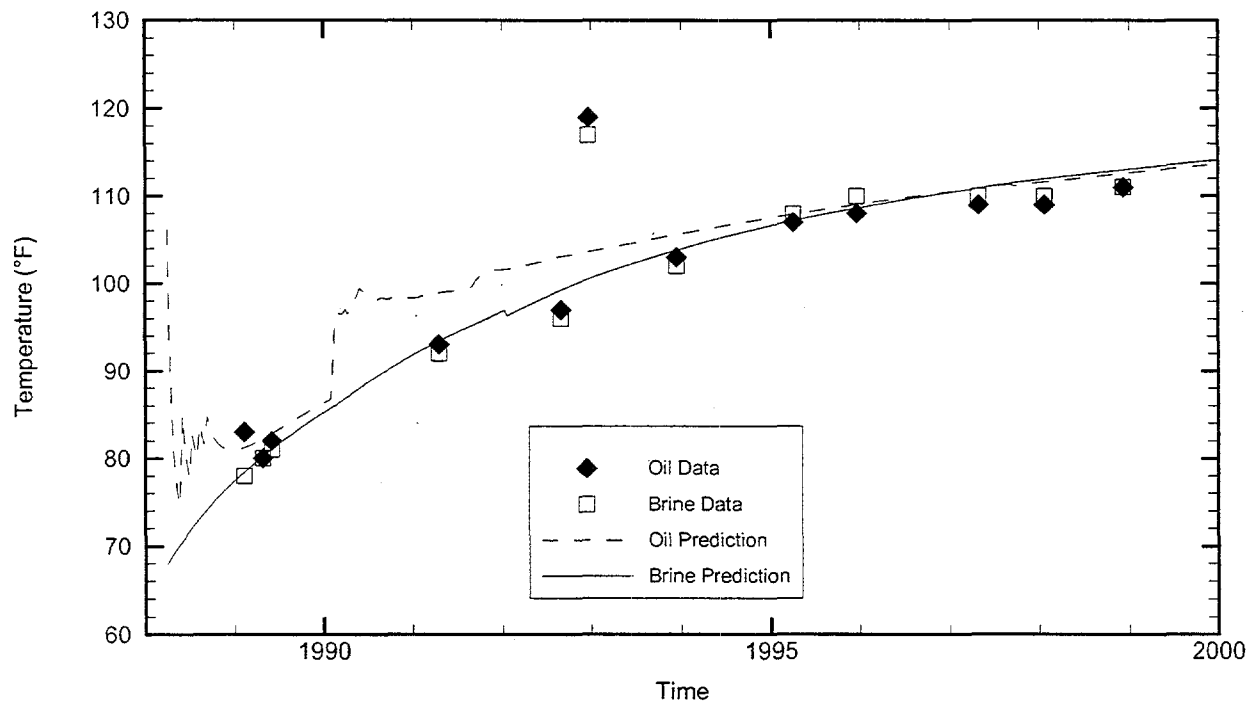
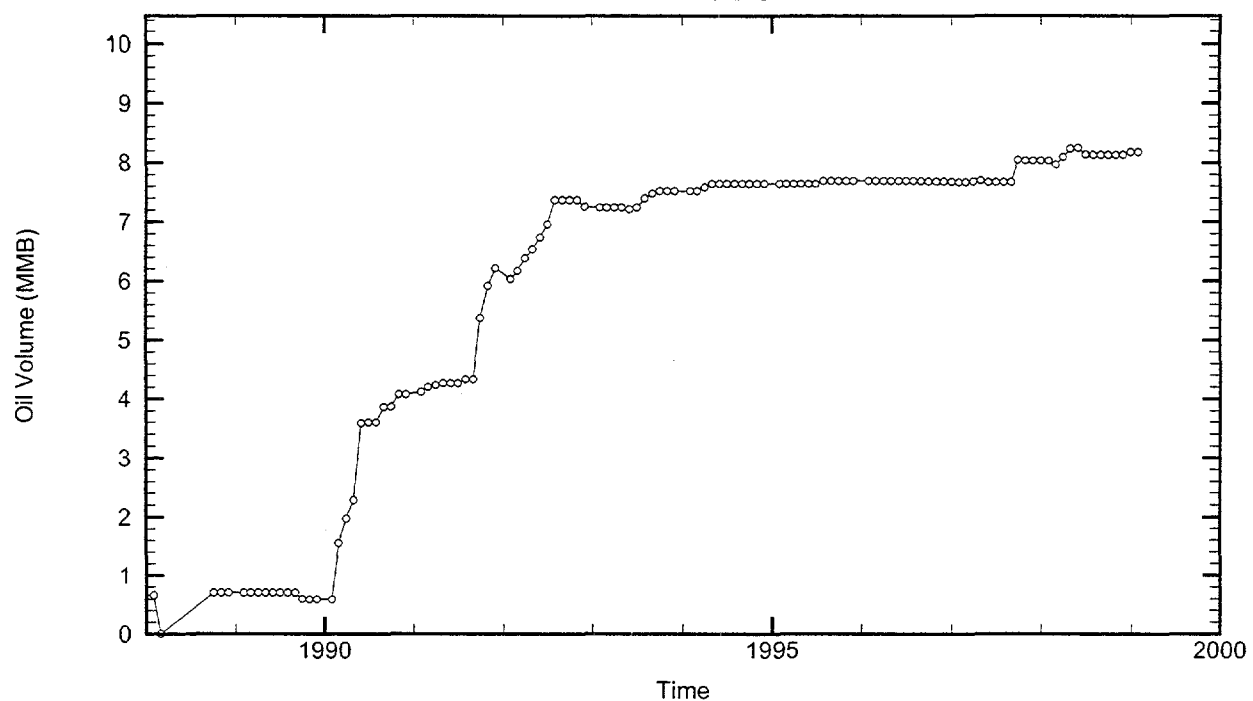
Cavern: WH110
End of Leaching: 03/15/1985
Duration of Leaching: 10.0000 days
Leaching Temperature: 60.21 °F

Oil Injection Temperature: 78.30 °F
Brine Injection Temperature: 76.13 °F
Number of iterations: 702

WH110



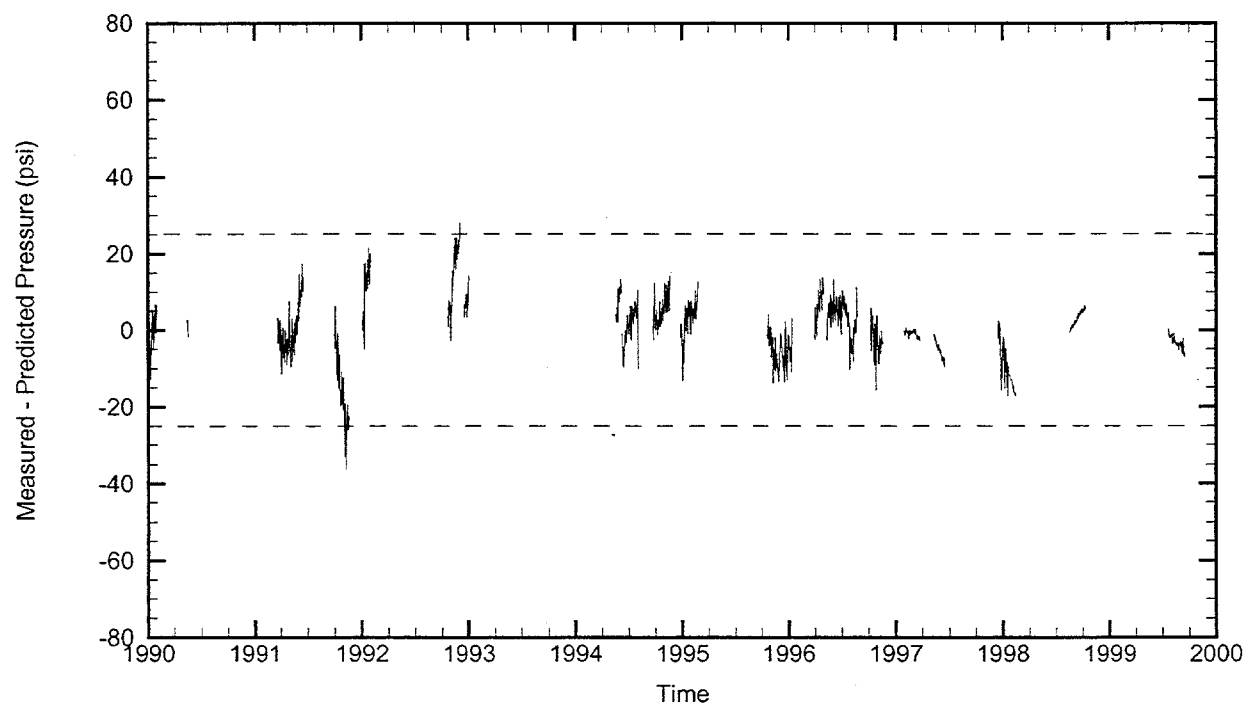
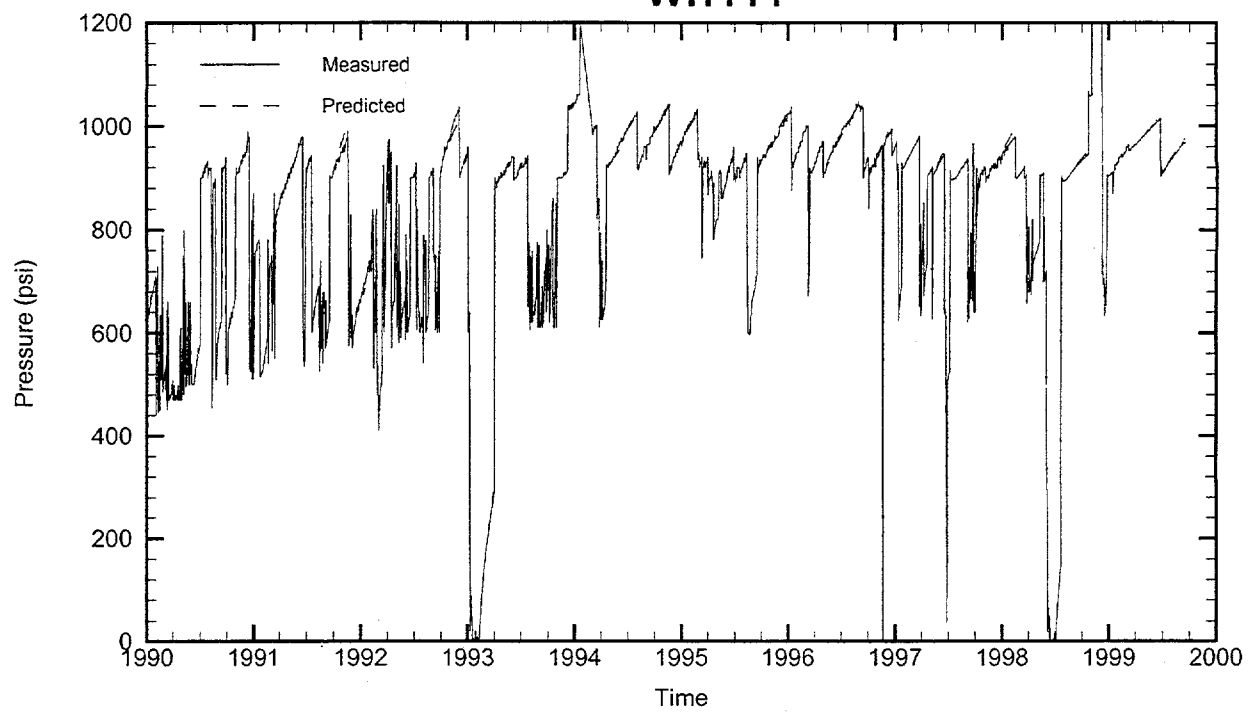
WH111



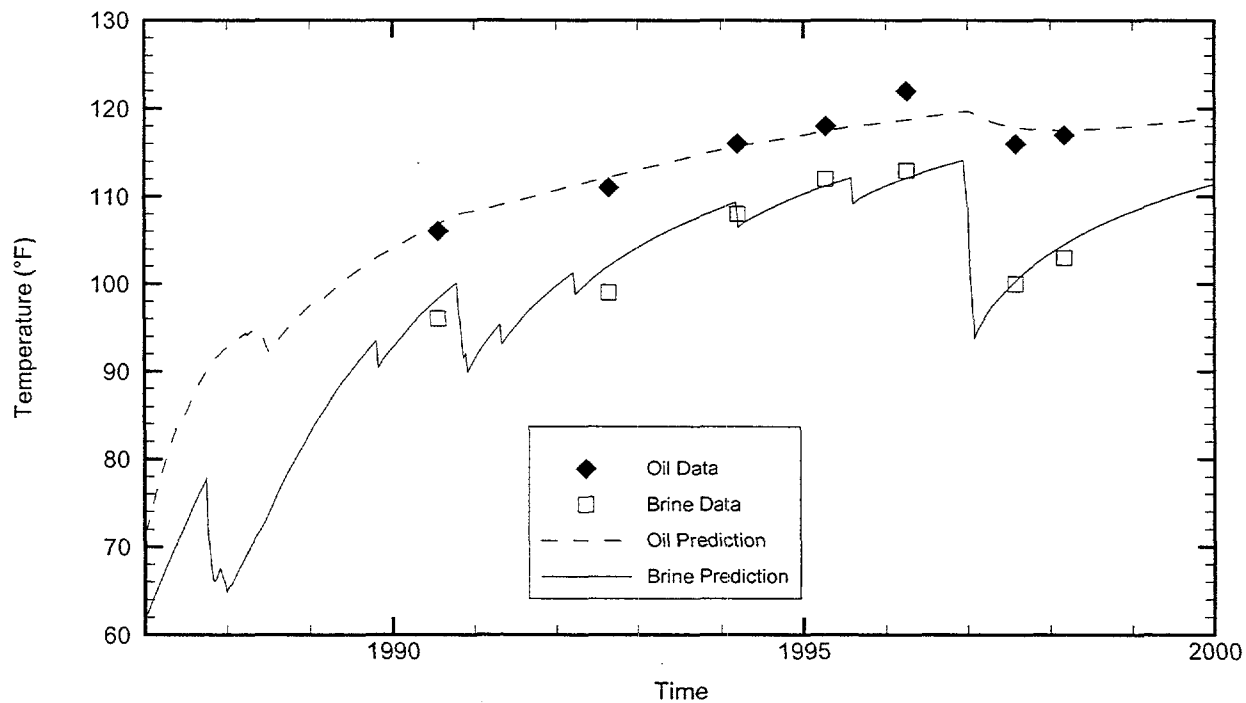
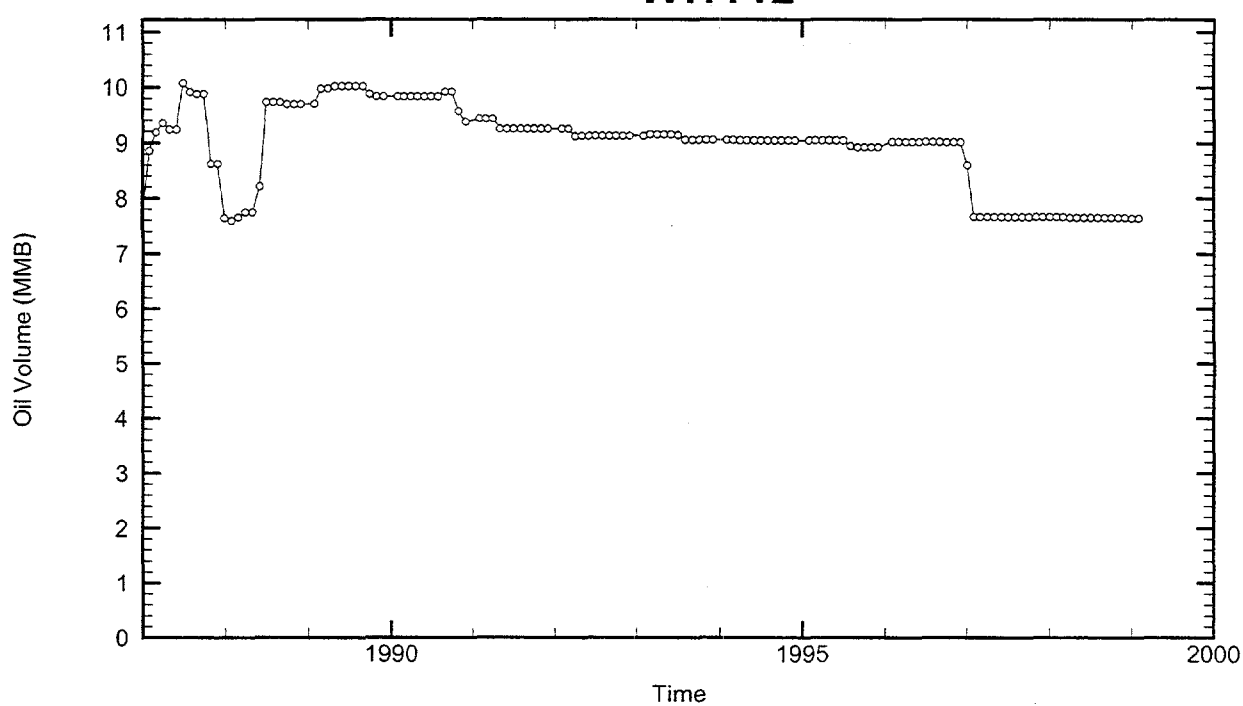
Cavern: WH111
End of Leaching: 04/01/1988
Duration of Leaching: 11.9589 months
Leaching Temperature: 67.95 °F

Oil Injection Temperature: 106.16 °F
Brine Injection Temperature: 64.36 °F
Number of iterations: 254

WH111



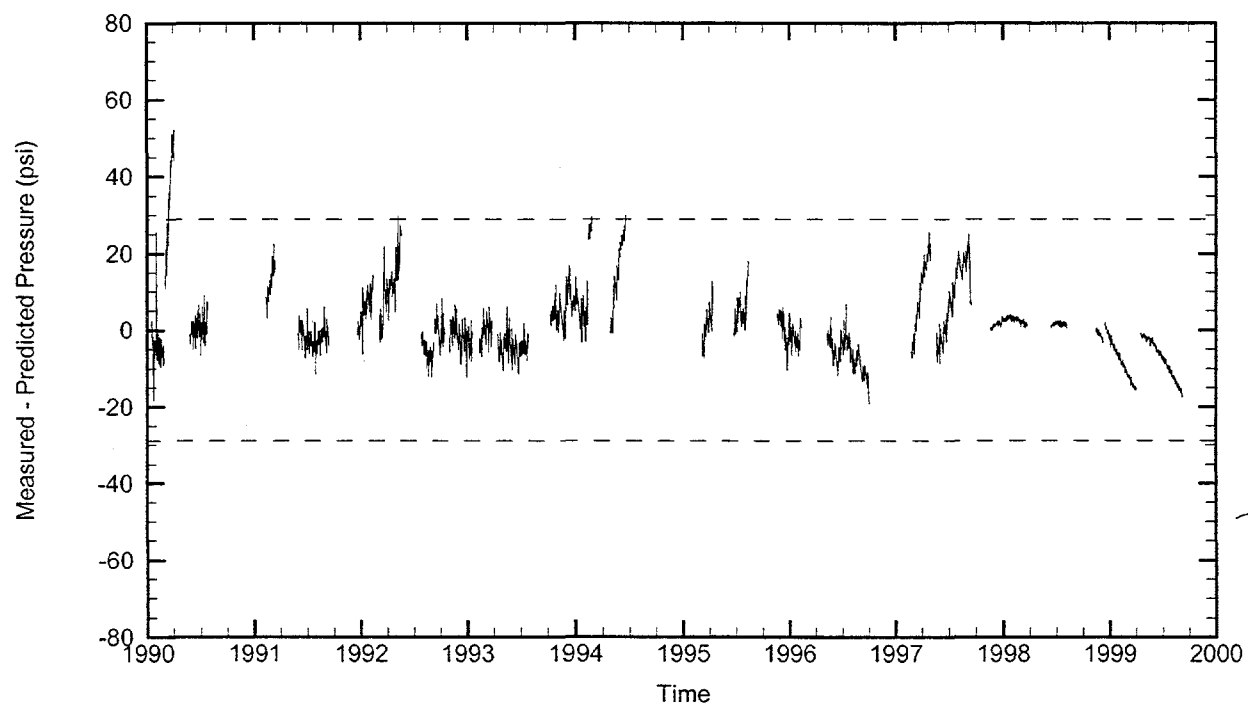
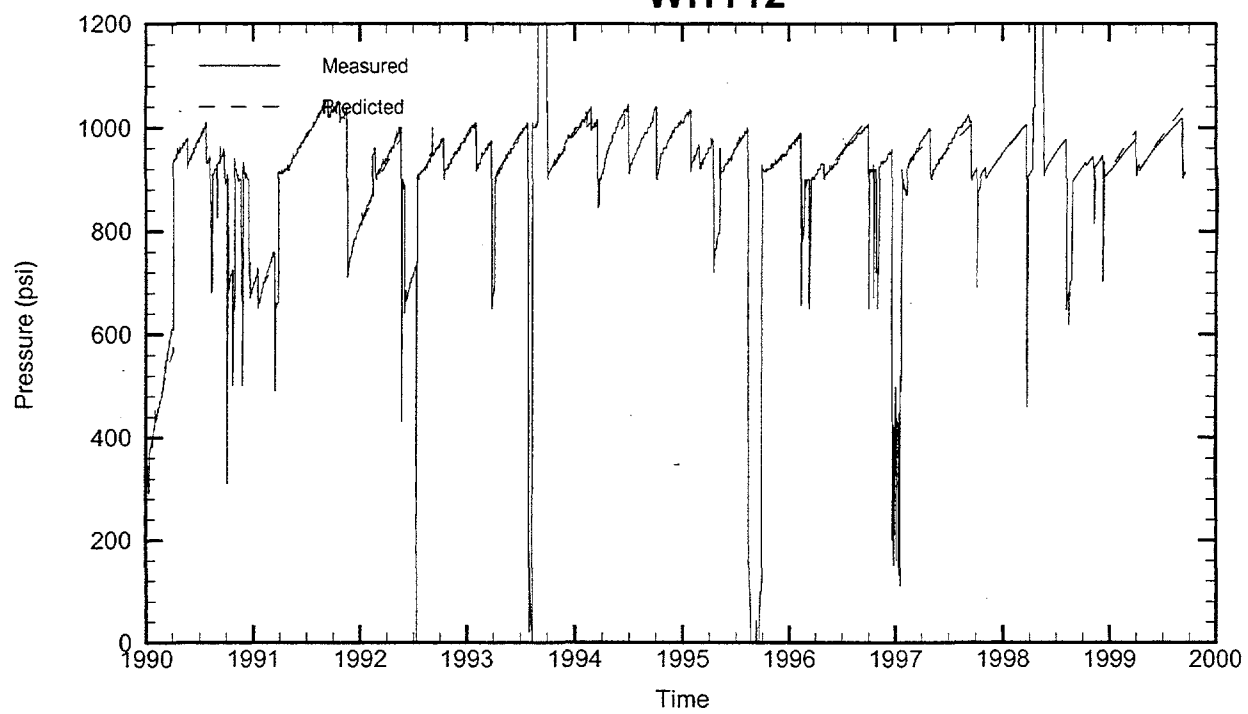
WH112



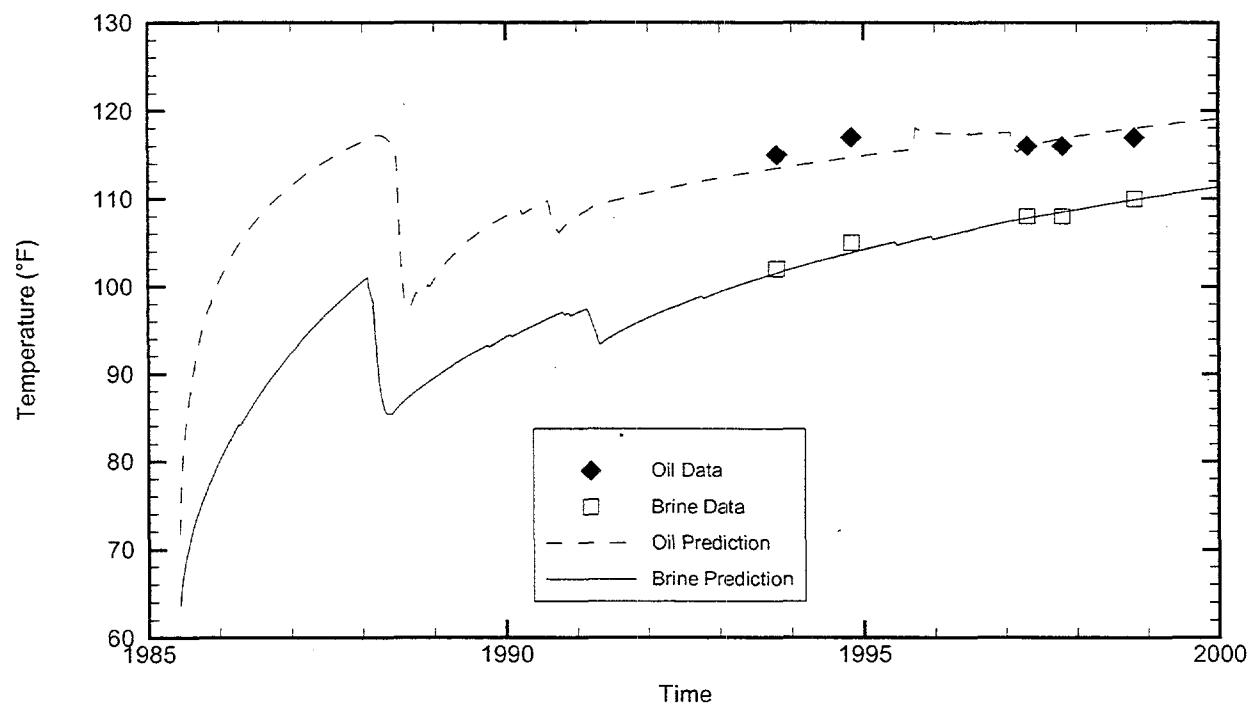
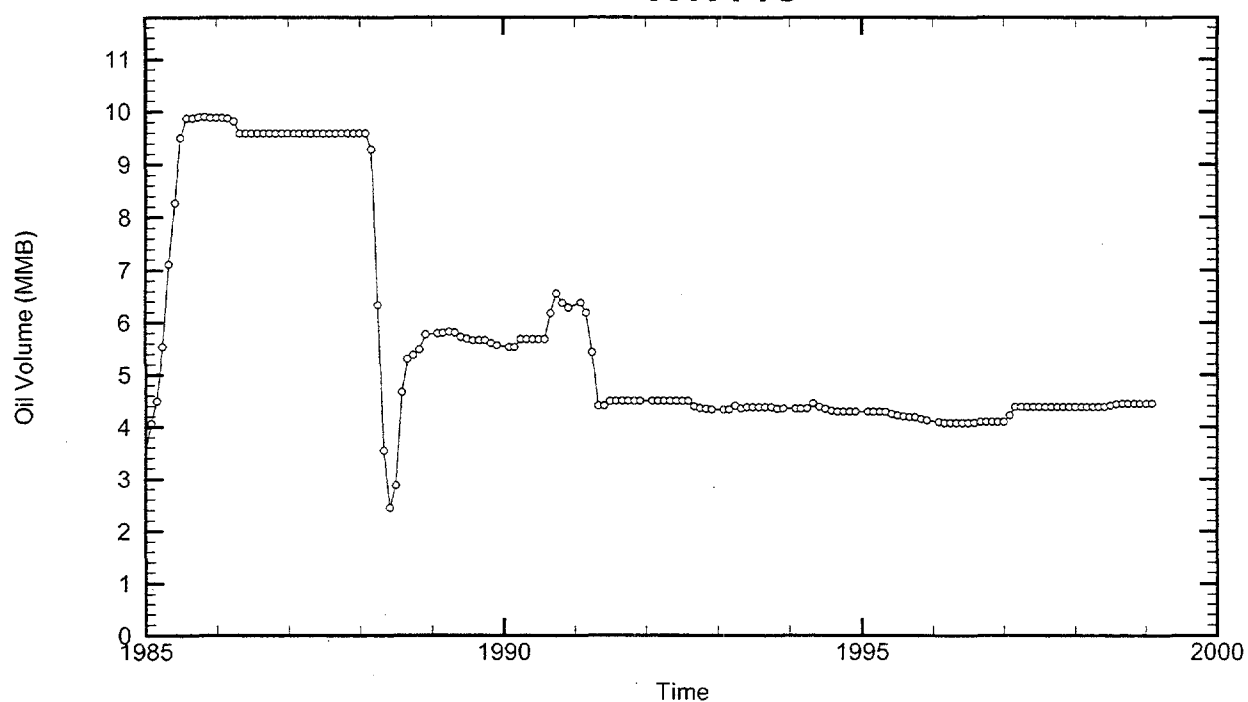
Cavern: WH112
End of Leaching: 01/03/1987
Duration of Leaching: 3.4825 months
Leaching Temperature: 61.67 °F

Oil Injection Temperature: 71.35 °F
Brine Injection Temperature: 50.01 °F
Number of iterations: 278

WH112



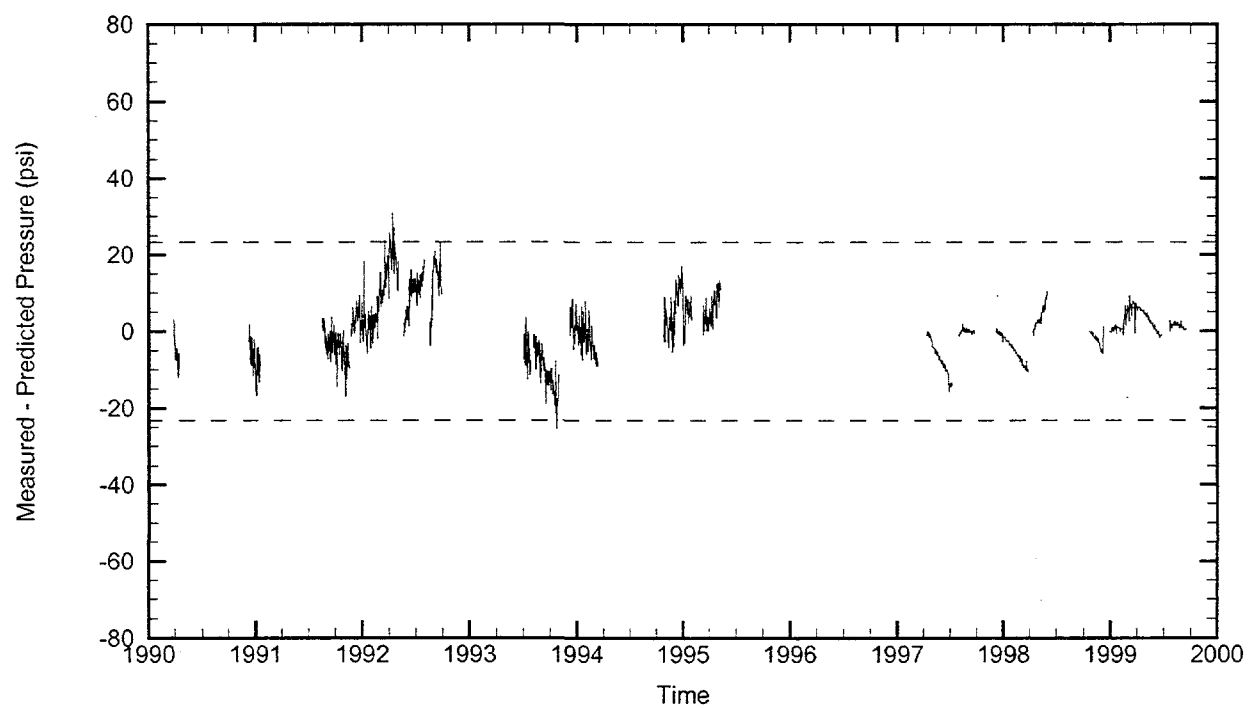
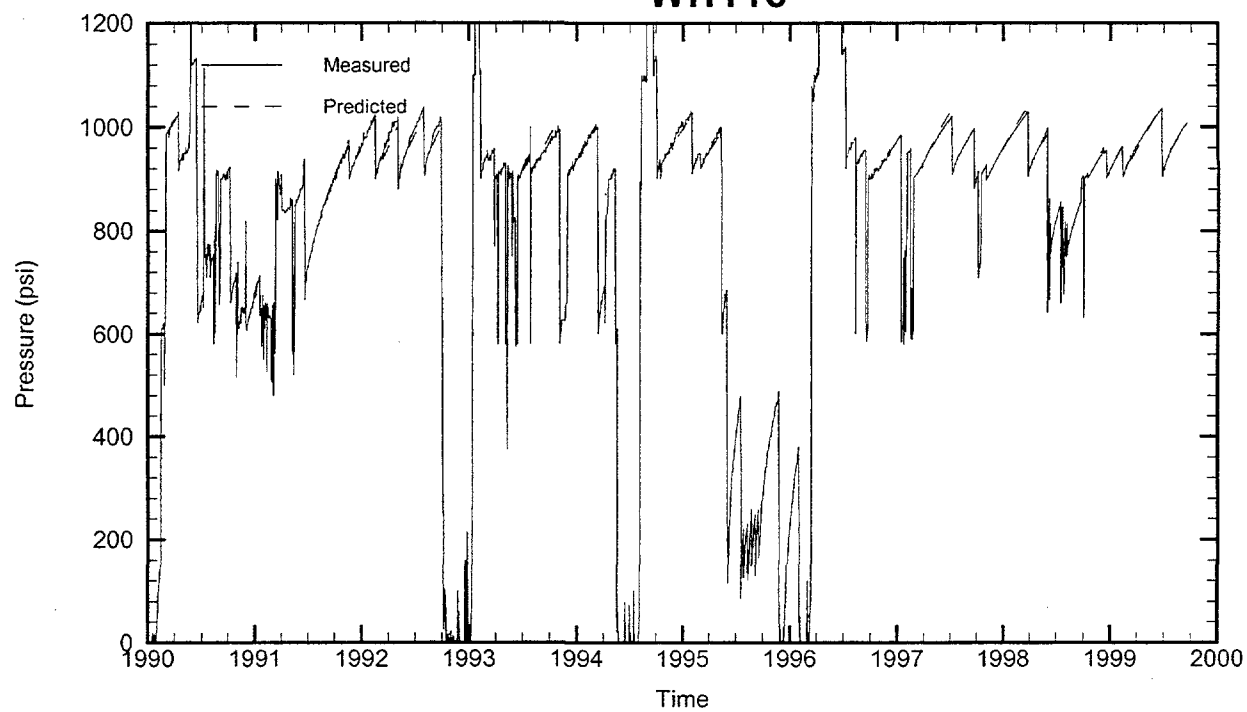
WH113



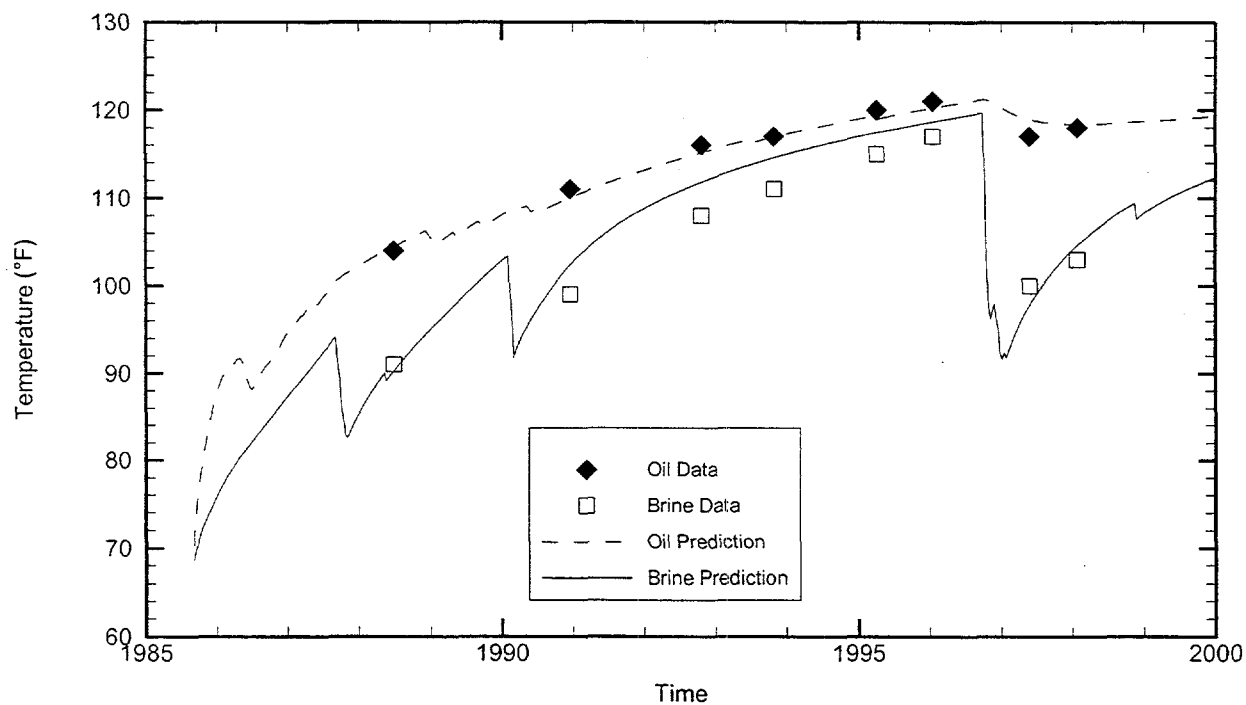
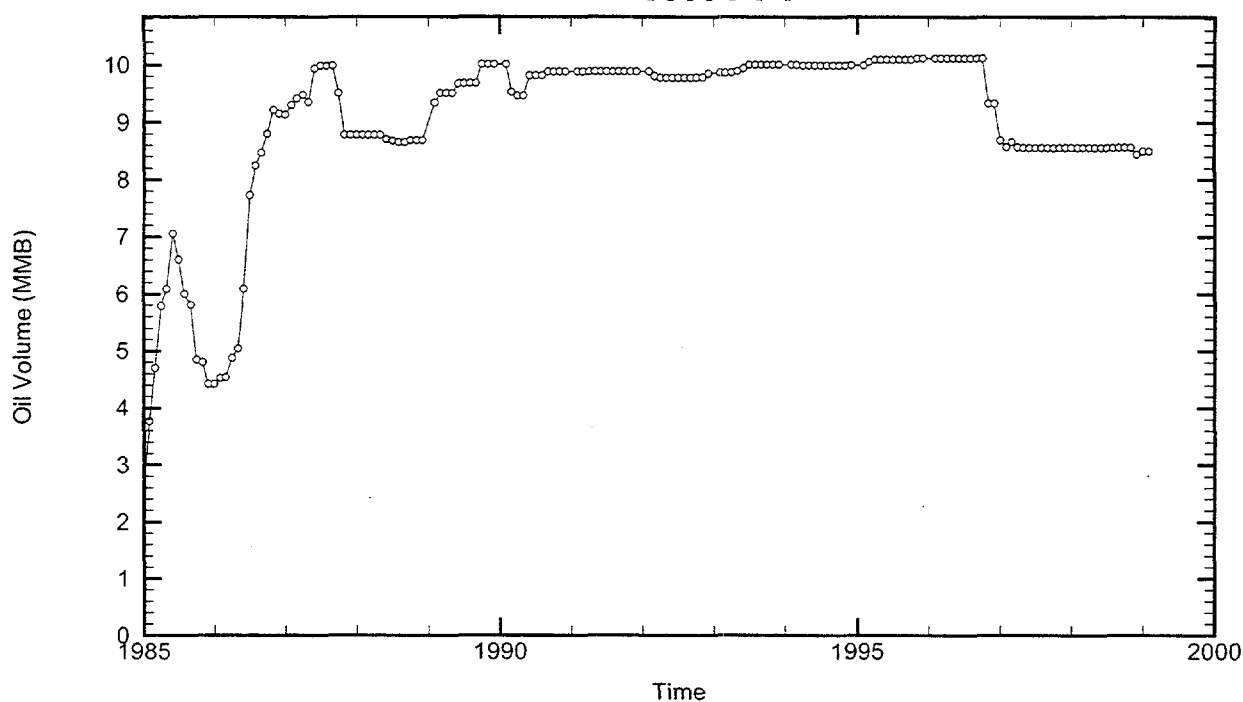
Cavern: WH113
End of Leaching: 06/10/1985
Duration of Leaching: 0.0000 days
Leaching Temperature: 63.60 °F

Degas: 09/22/1995, 118.00 °F, 4.66 MMB
Oil Injection Temperature: 71.69 °F
Brine Injection Temperature: 77.53 °F
Number of iterations: 239

WH113



WH114



Cavern: WH114

End of Leaching: 09/05/1985

Duration of Leaching: 1.6667 years

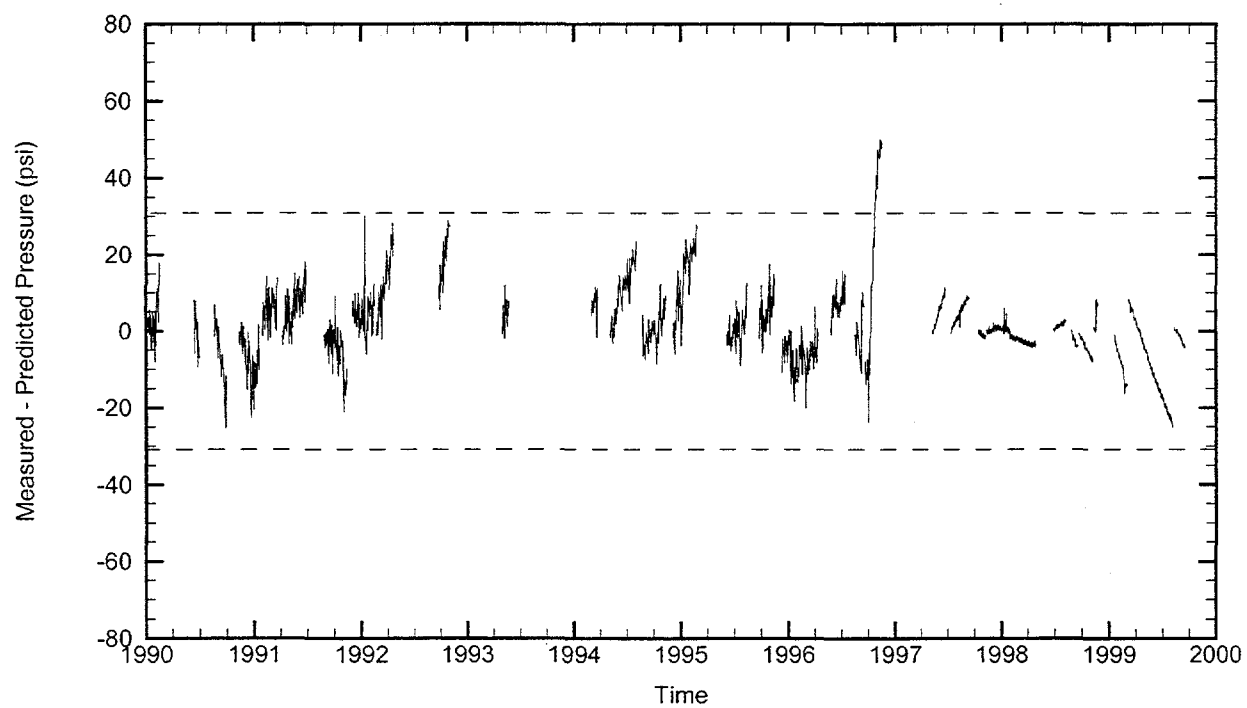
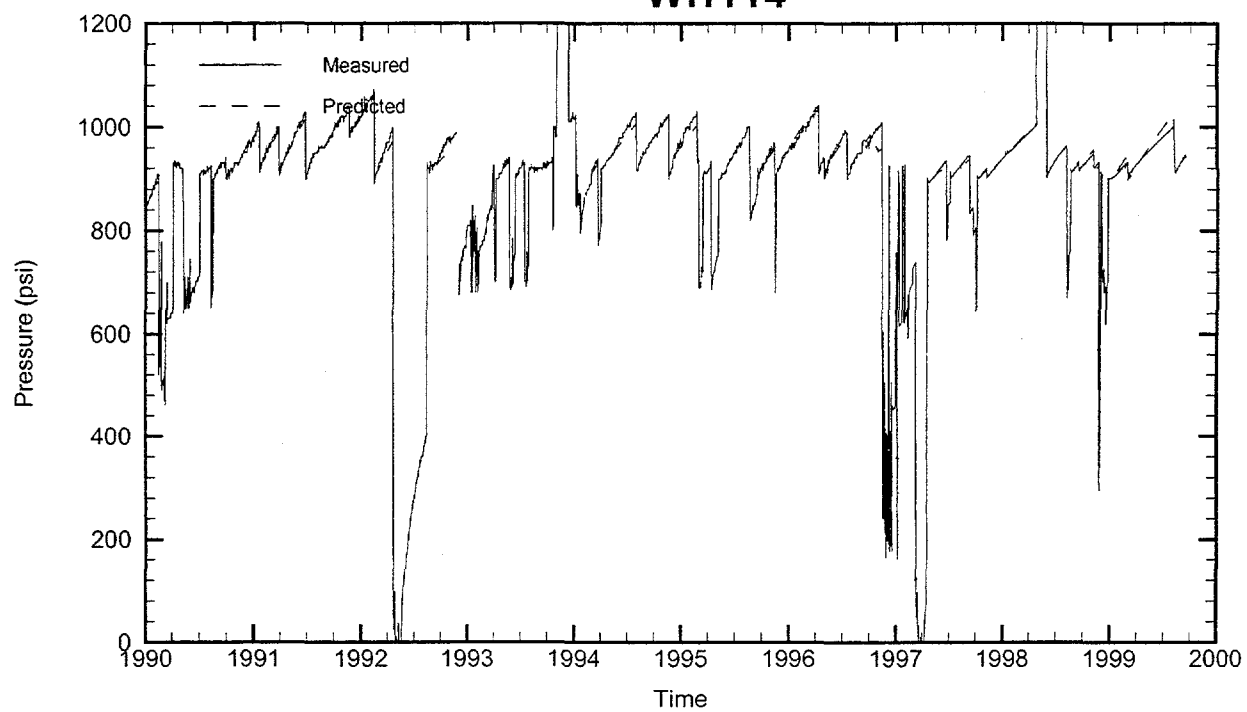
Leaching Temperature: 68.60 °F

Oil Injection Temperature: 70.27 °F

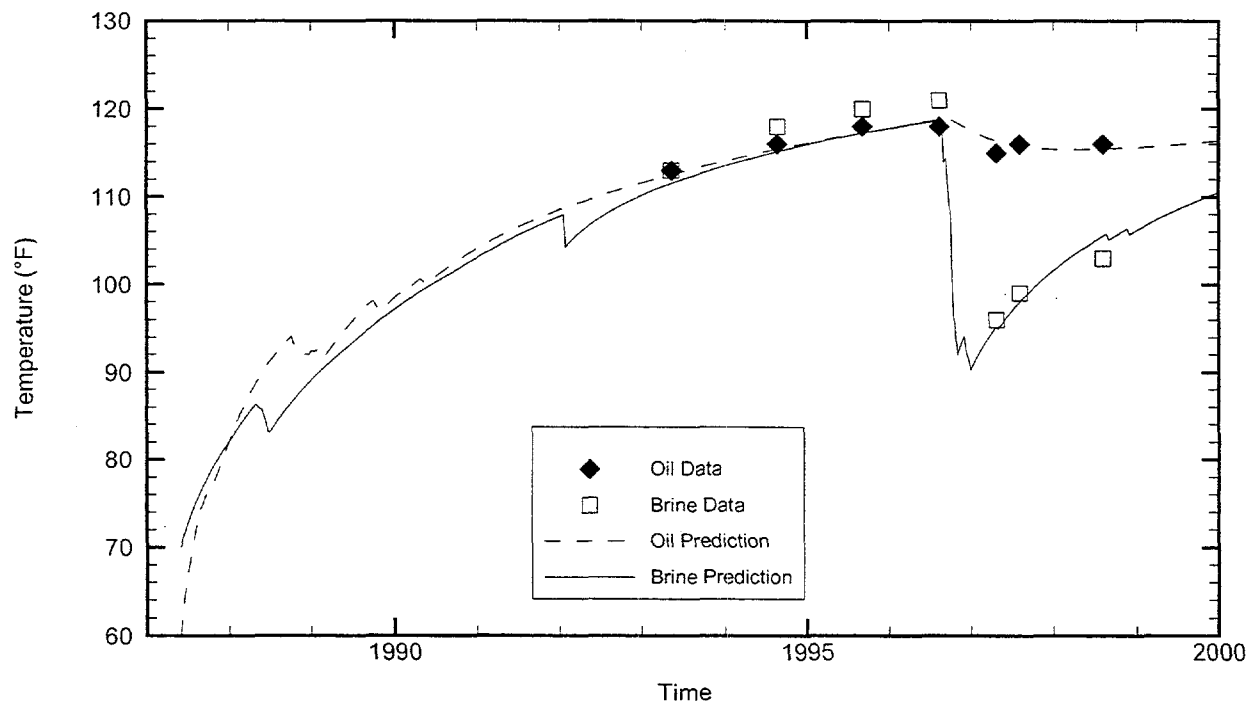
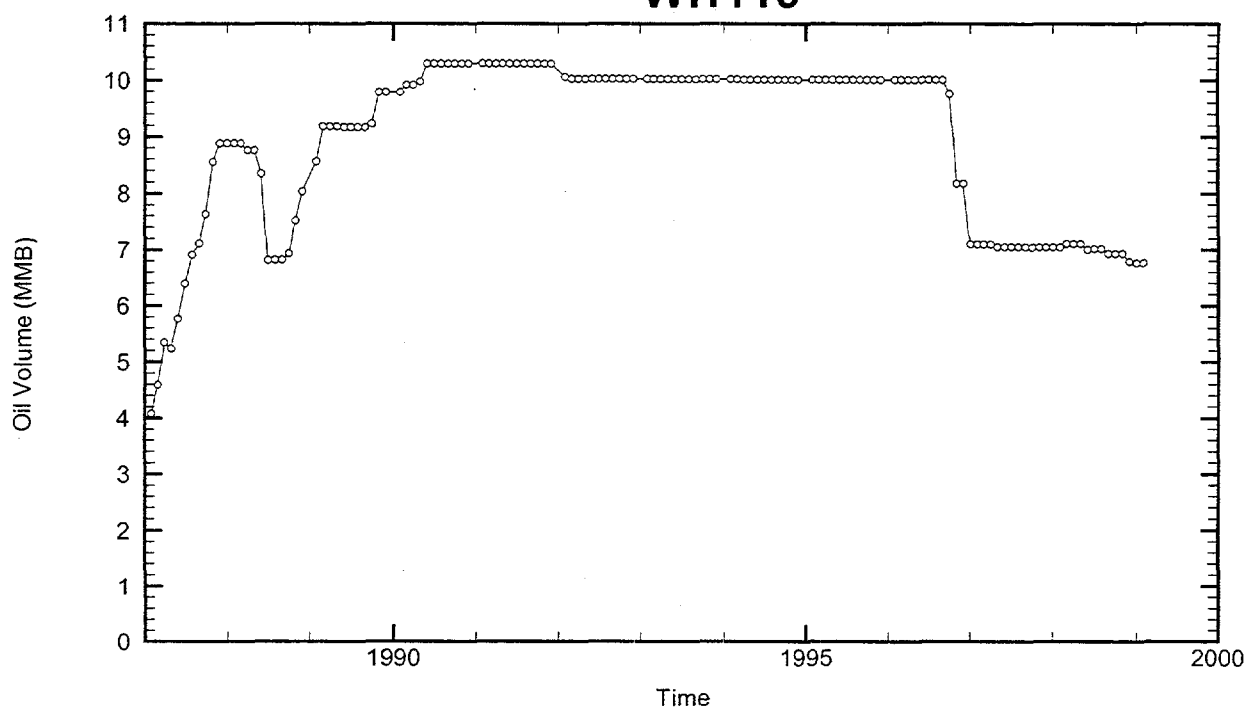
Brine Injection Temperature: 67.45 °F

Number of iterations: 513

WH114



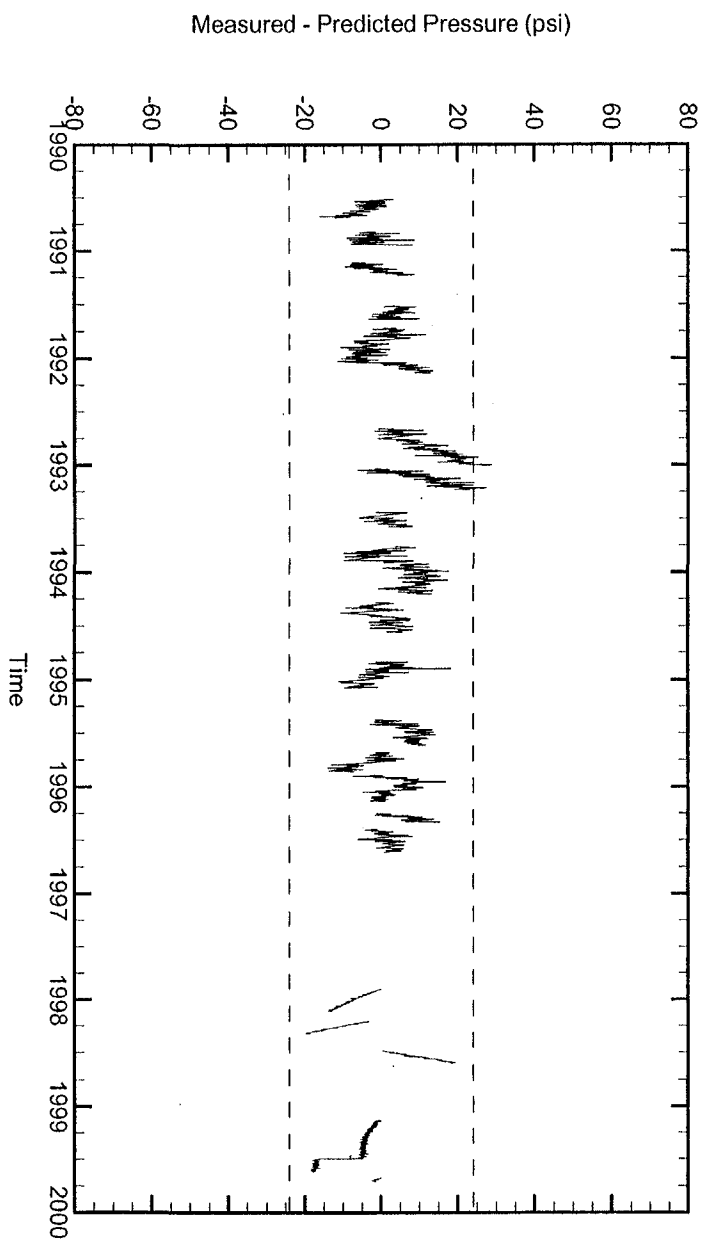
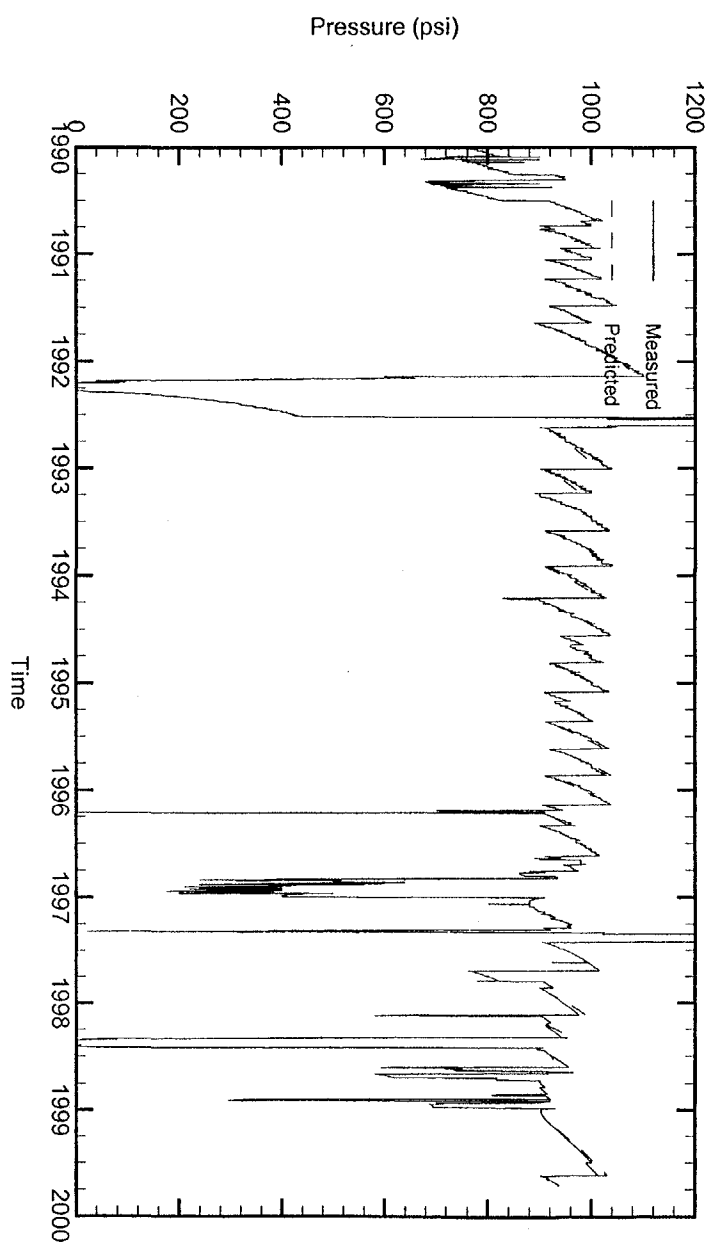
WH115



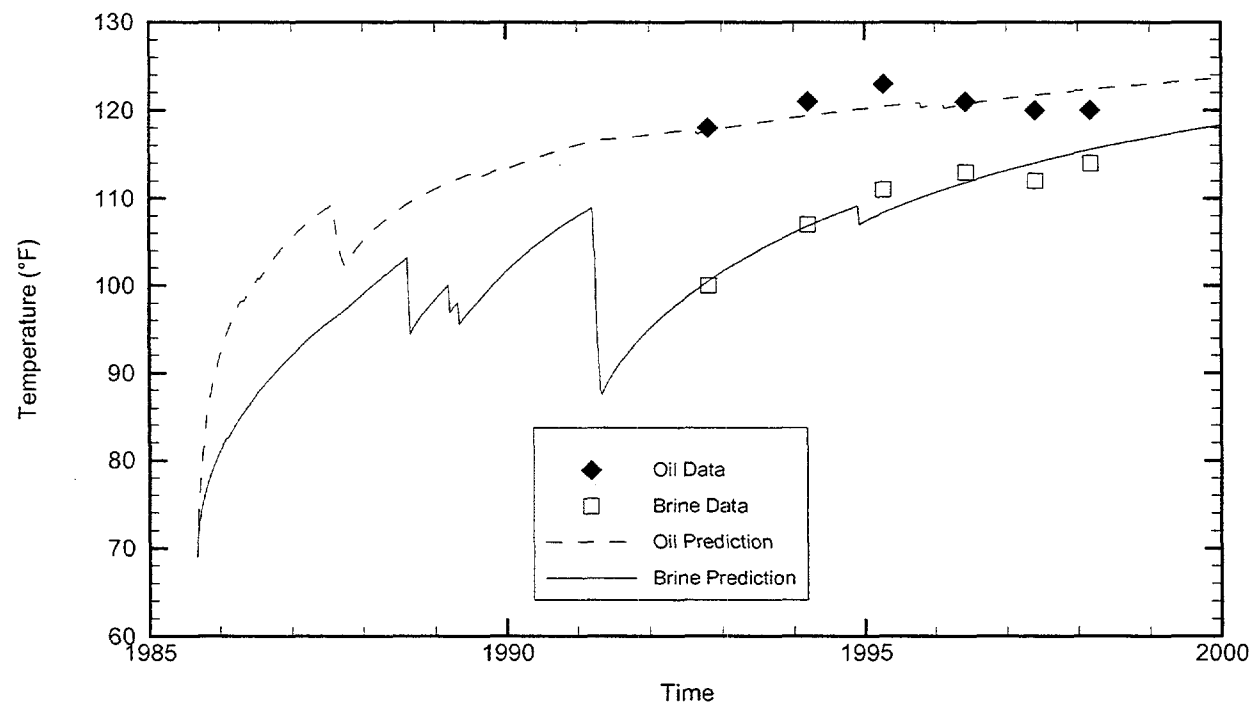
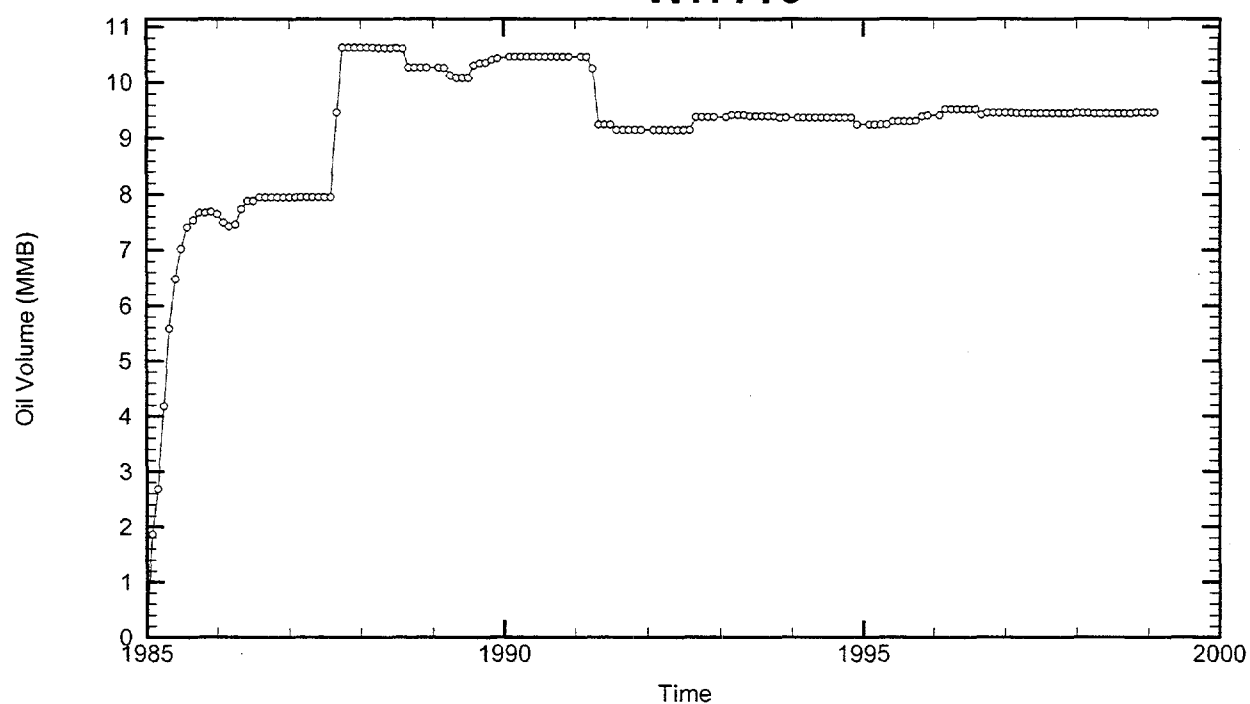
Cavern: WH115
End of Leaching: 06/01/1987
Duration of Leaching: 1.9713 months
Leaching Temperature: 69.98 °F

Oil Injection Temperature: 59.48 °F
Brine Injection Temperature: 75.11 °F
Number of iterations: 273

WH115



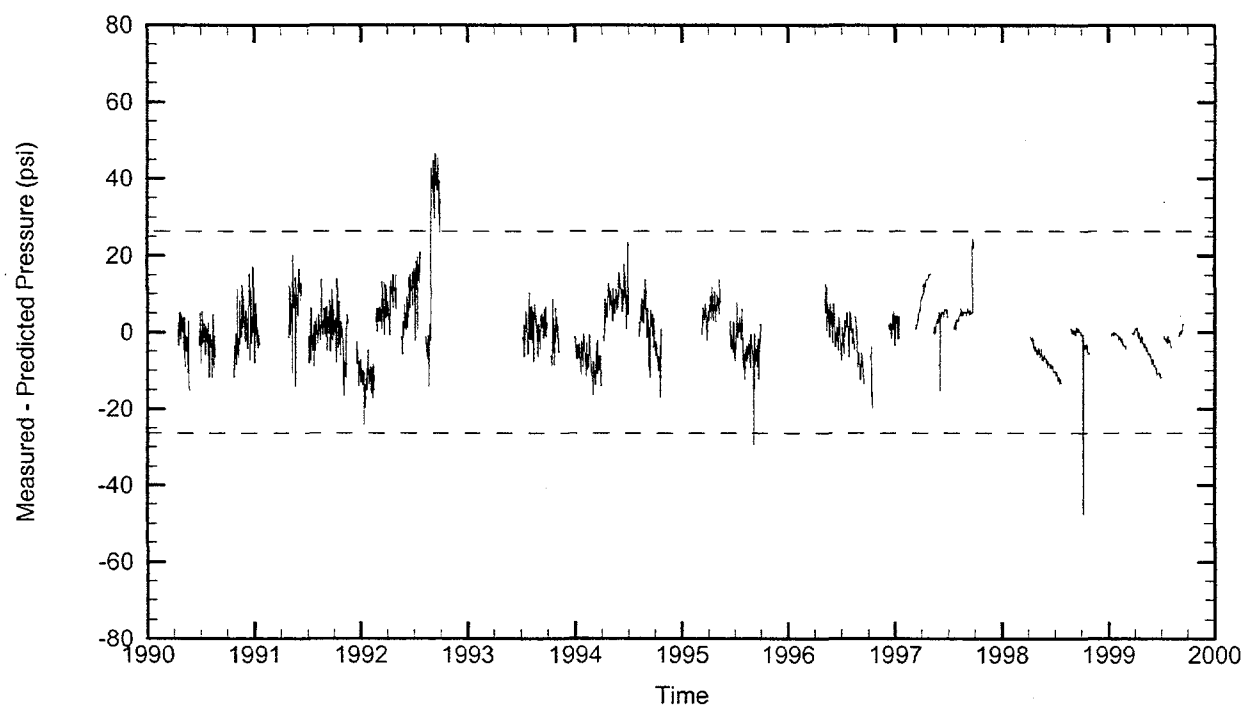
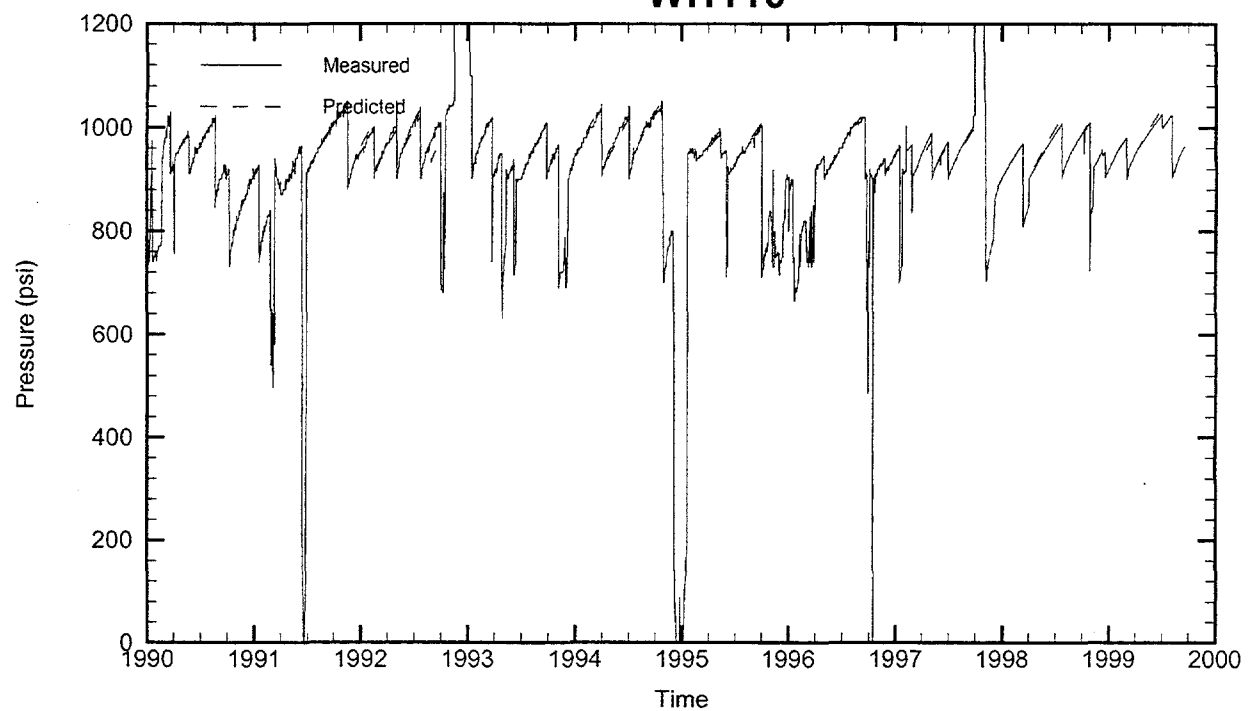
WH116



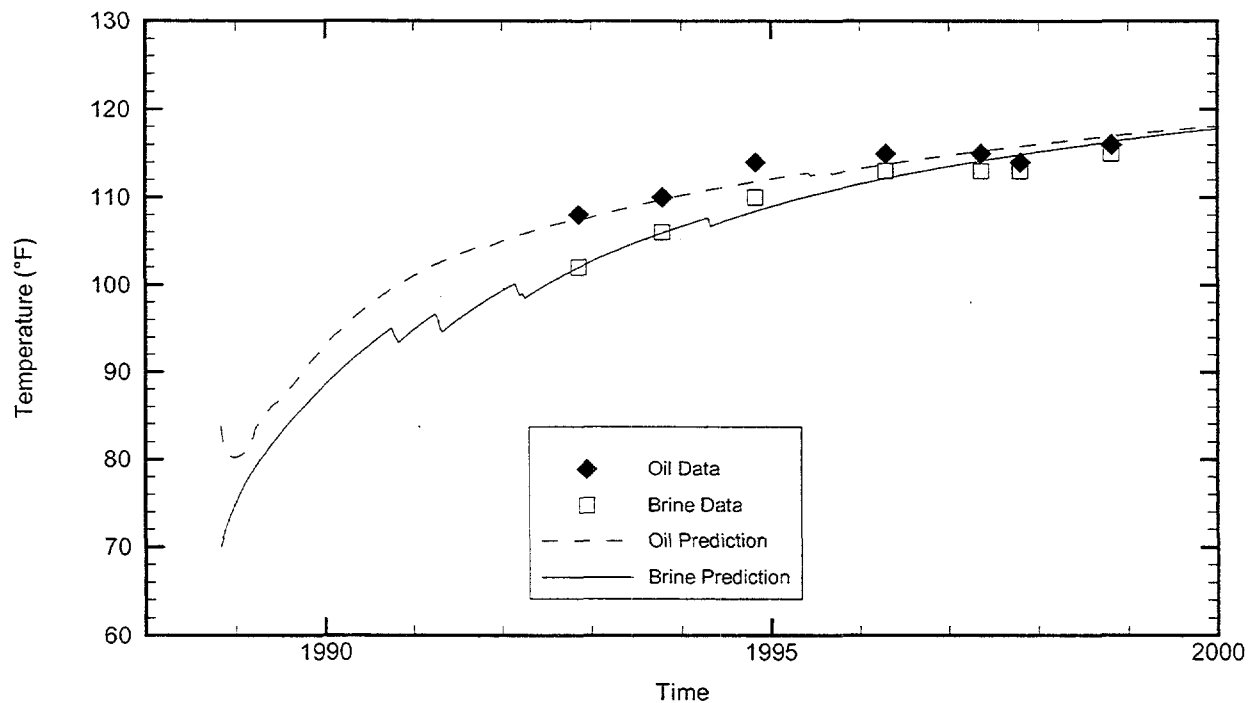
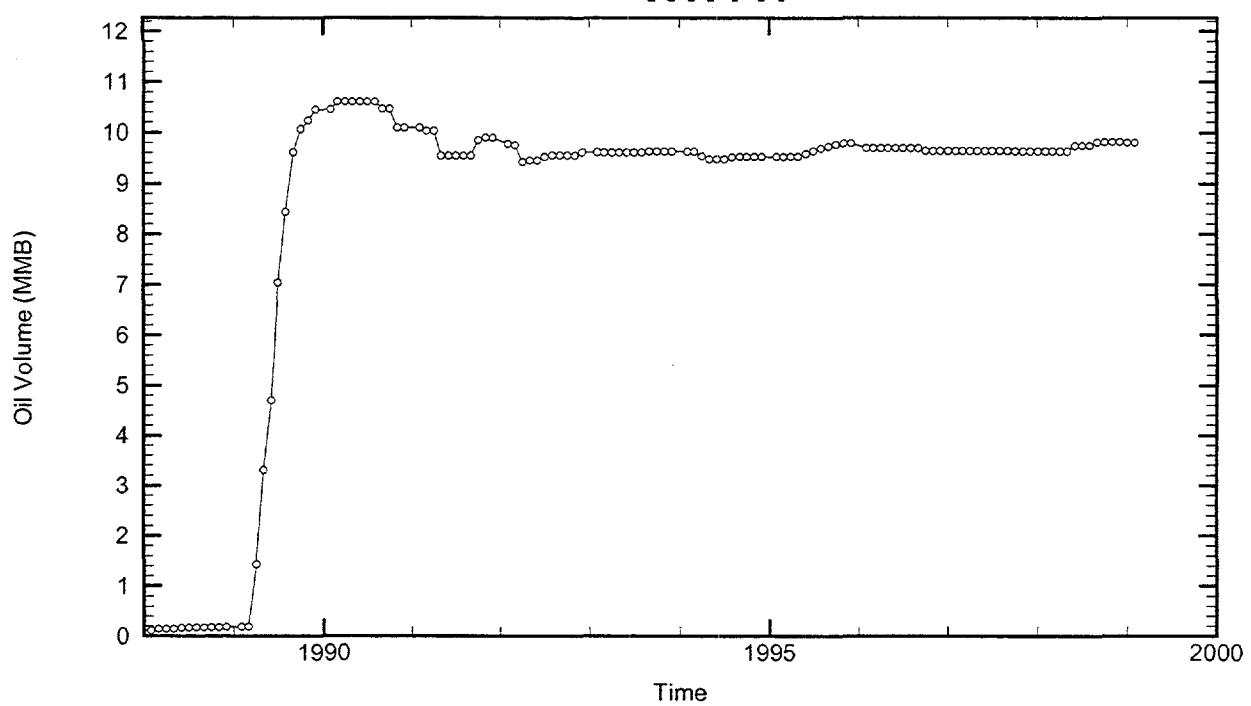
Cavern: WH116
 End of Leaching: 09/04/1985
 Duration of Leaching: 1.0000 days
 Leaching Temperature: 70.00 °F

Oil Injection Temperature: 69.01 °F
 Brine Injection Temperature: 71.06 °F
 Number of iterations: 402

WH116



WH117



Cavern: WH117

End of Leaching: 10/30/1988

Duration of Leaching: 1.0842 months

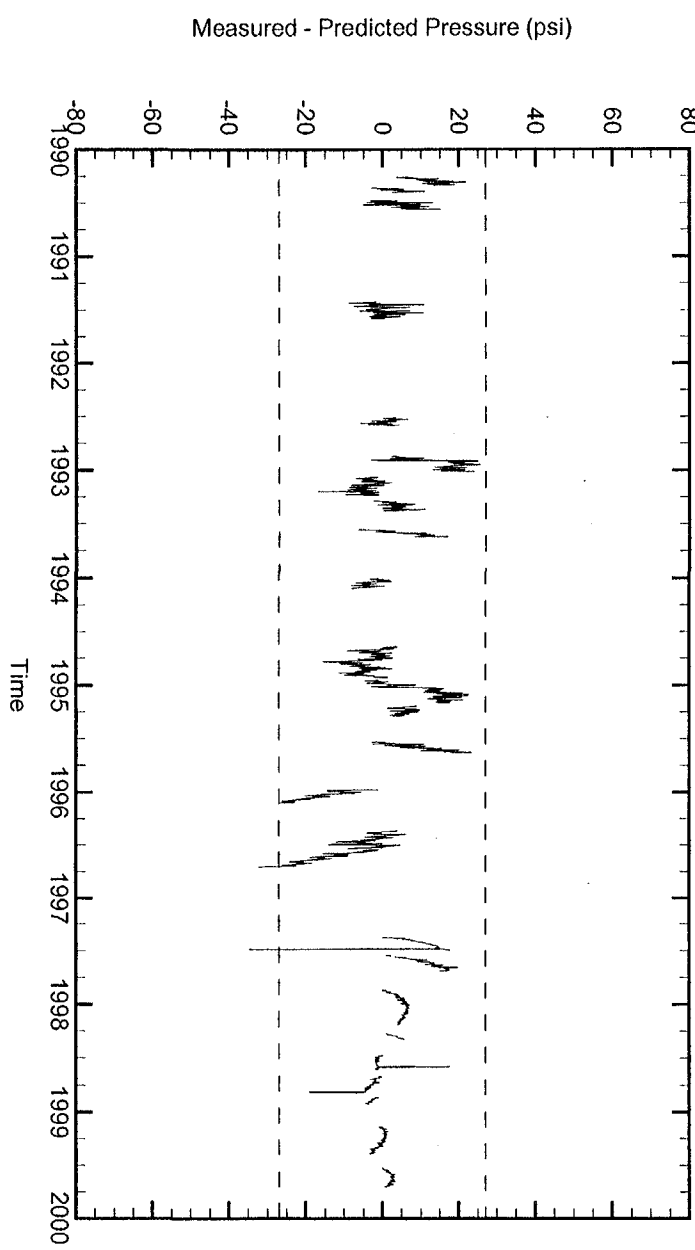
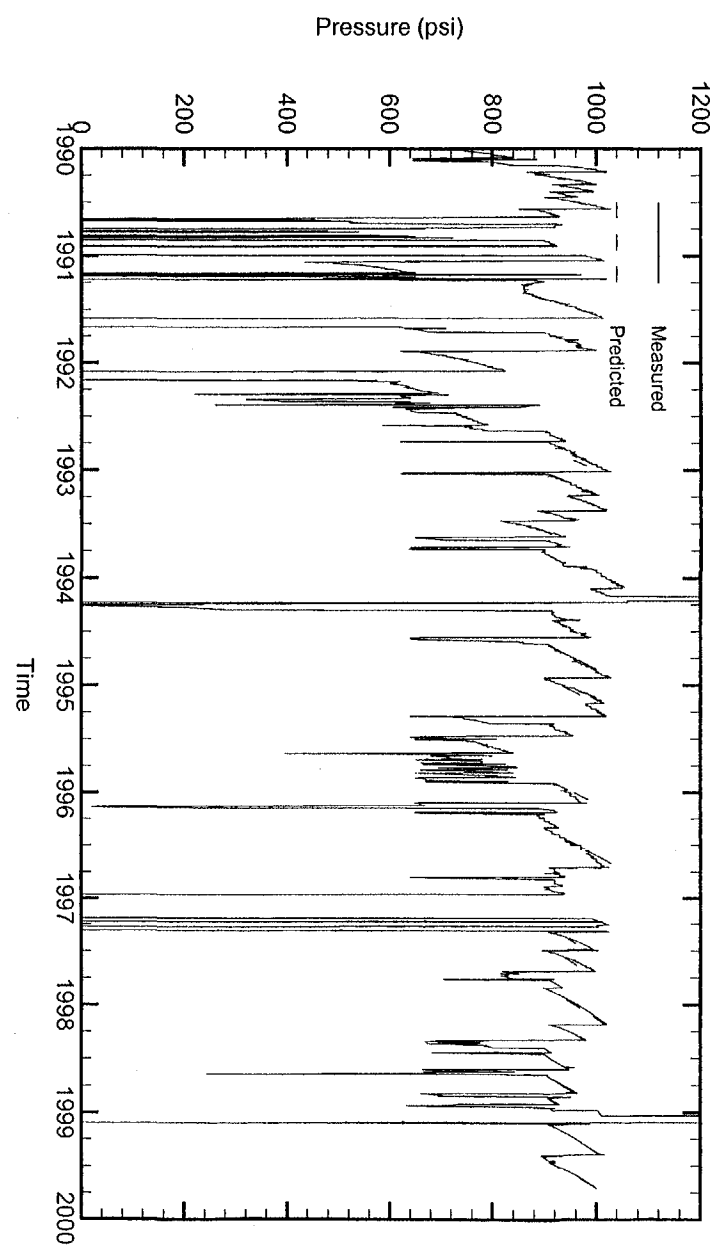
Leaching Temperature: 70.00 °F

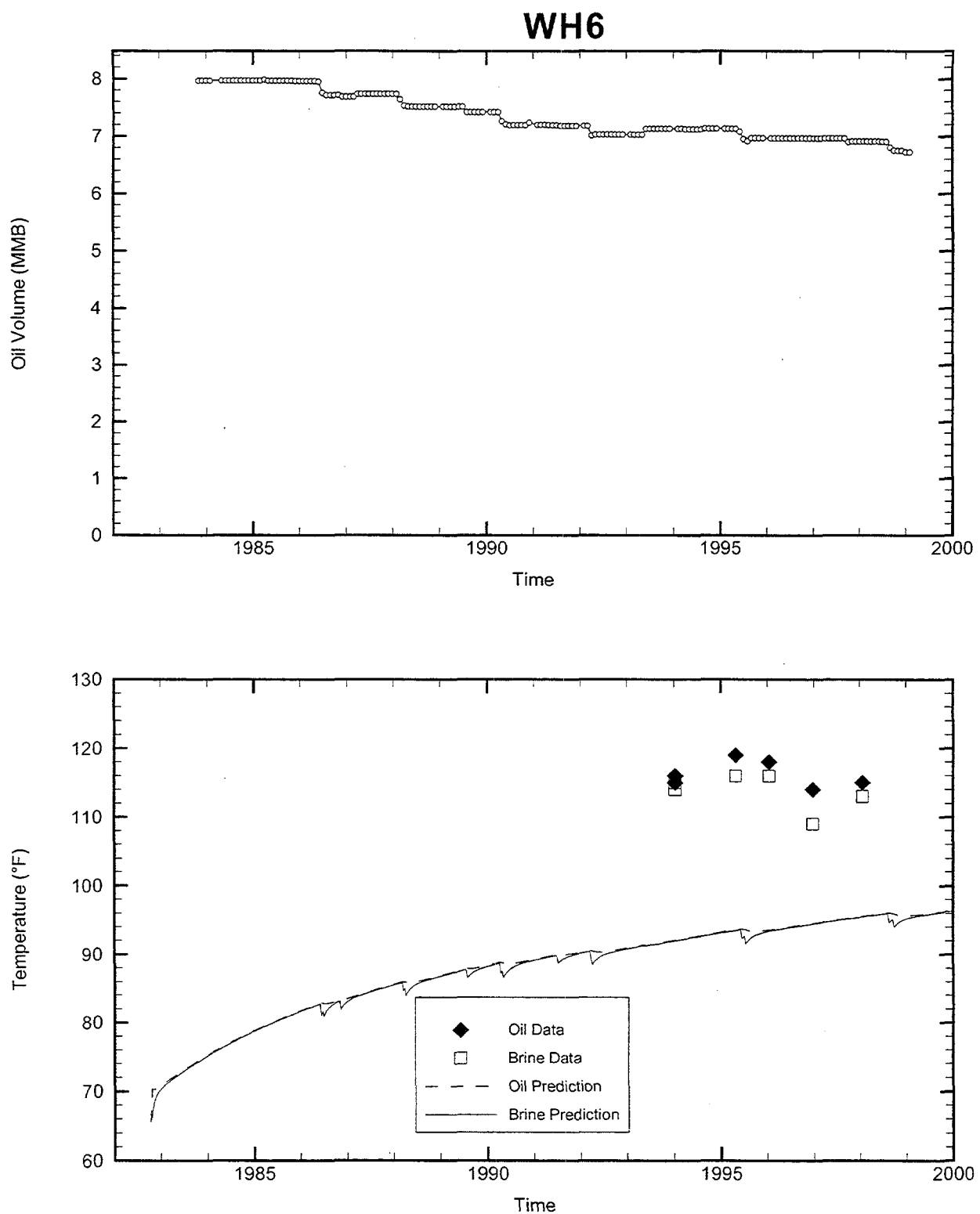
Oil Injection Temperature: 83.73 °F

Brine Injection Temperature: 82.76 °F

Number of iterations: 373

WH17

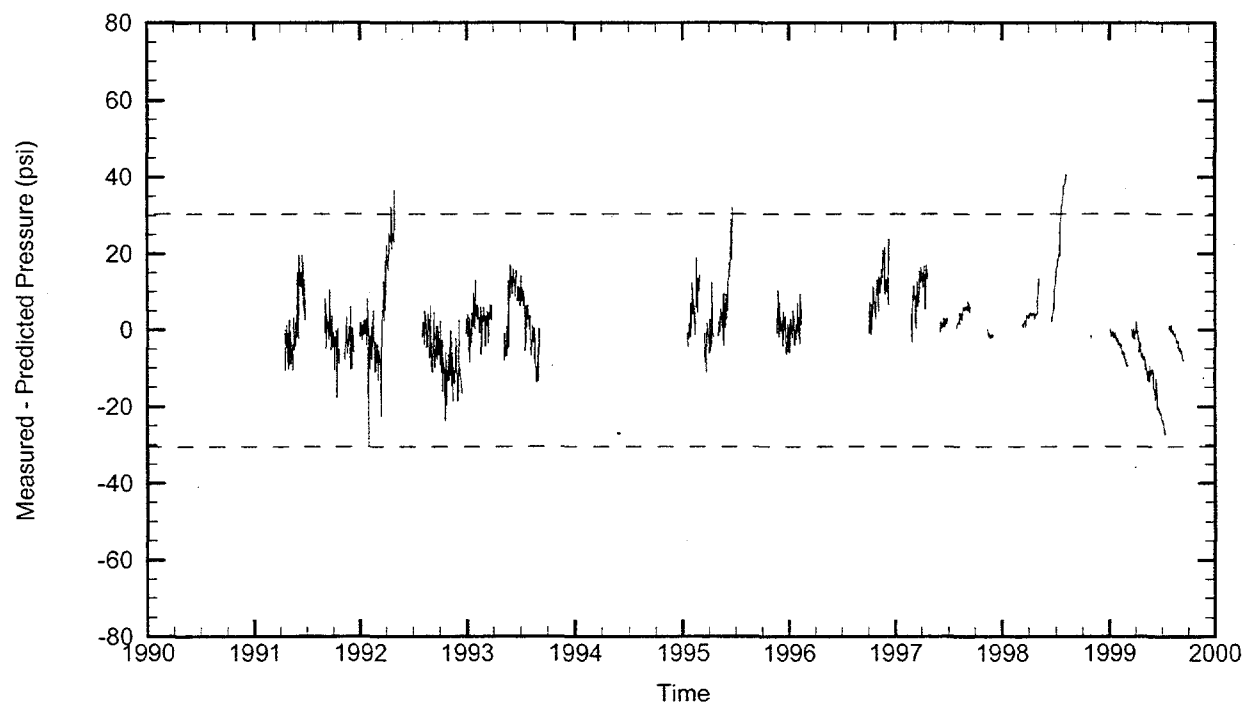
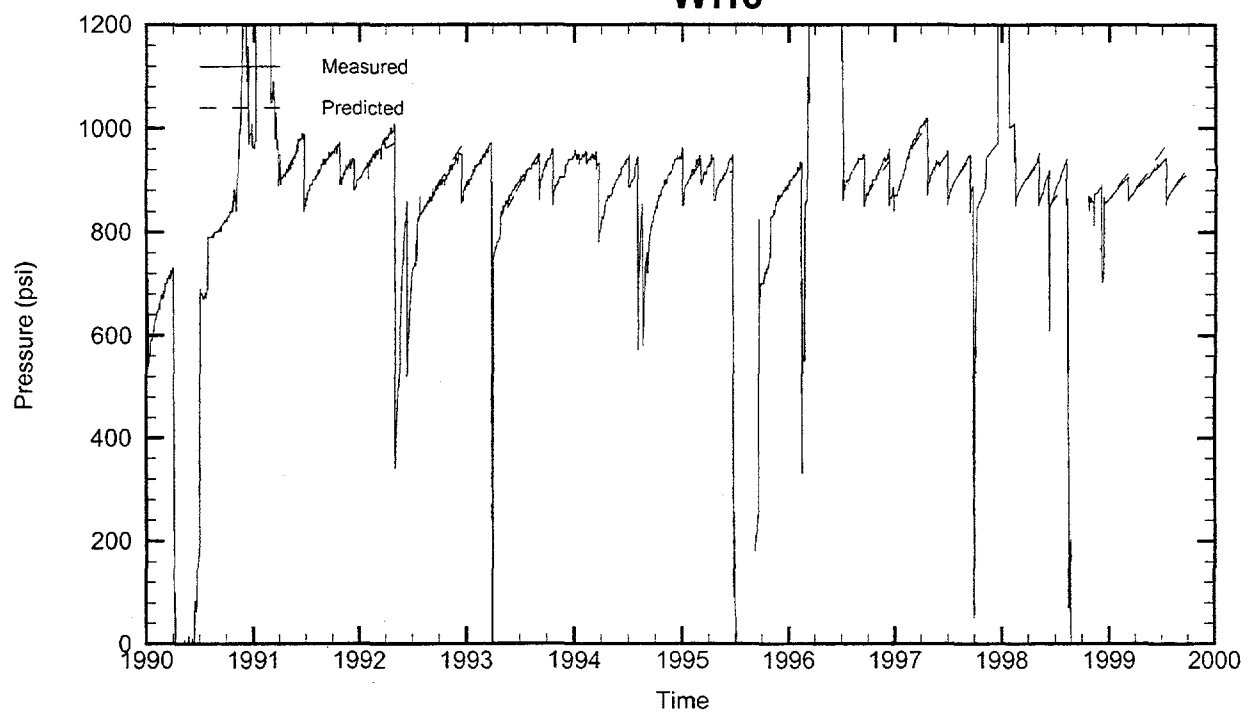


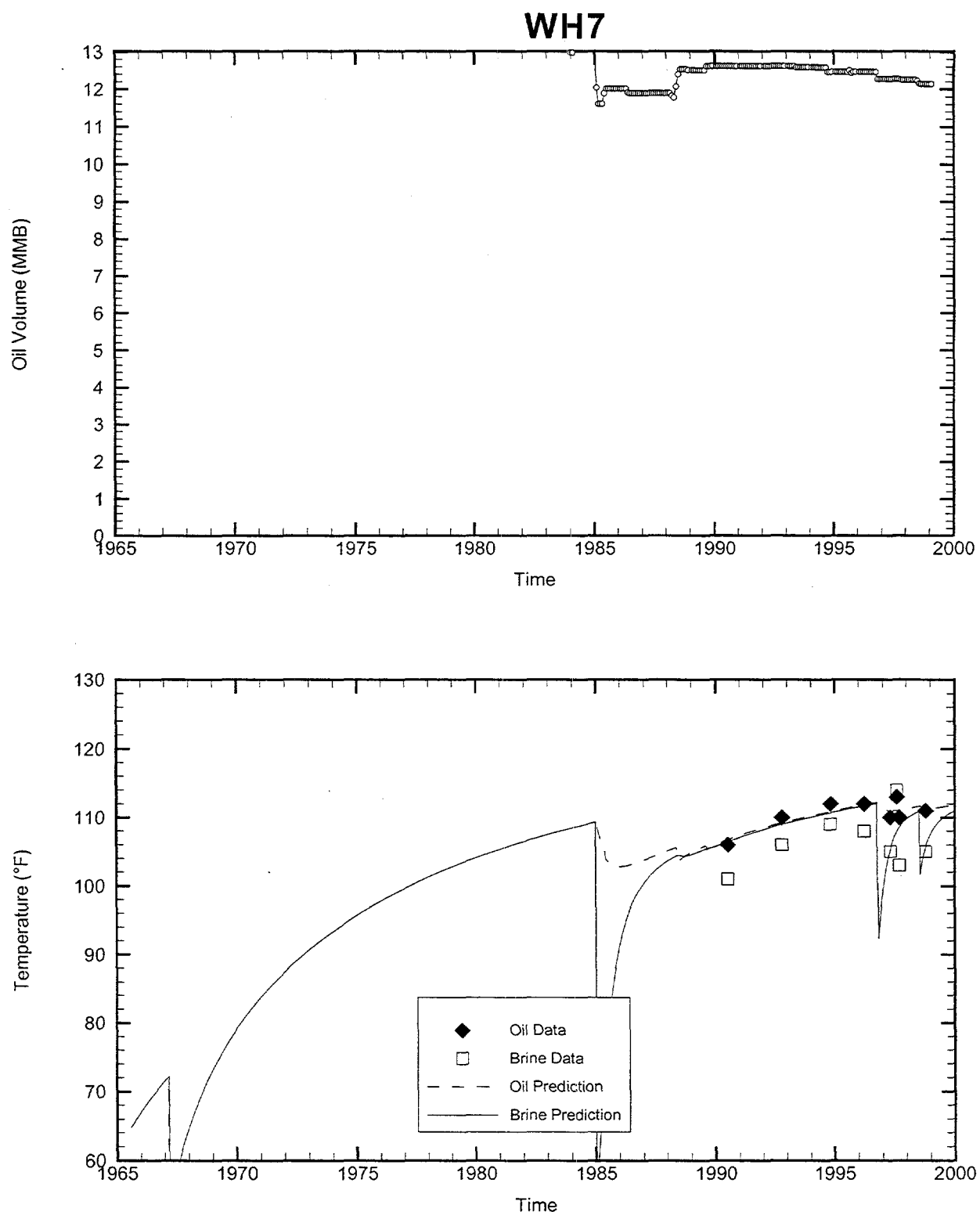


Cavern: WH6
 End of Leaching: 10/12/1982
 Duration of Leaching: 2.0041 years
 Leaching Temperature: 65.50 °F

Oil Injection Temperature: 70.50 °F
 Brine Injection Temperature: 70.50 °F
 Number of iterations: 800

WH6

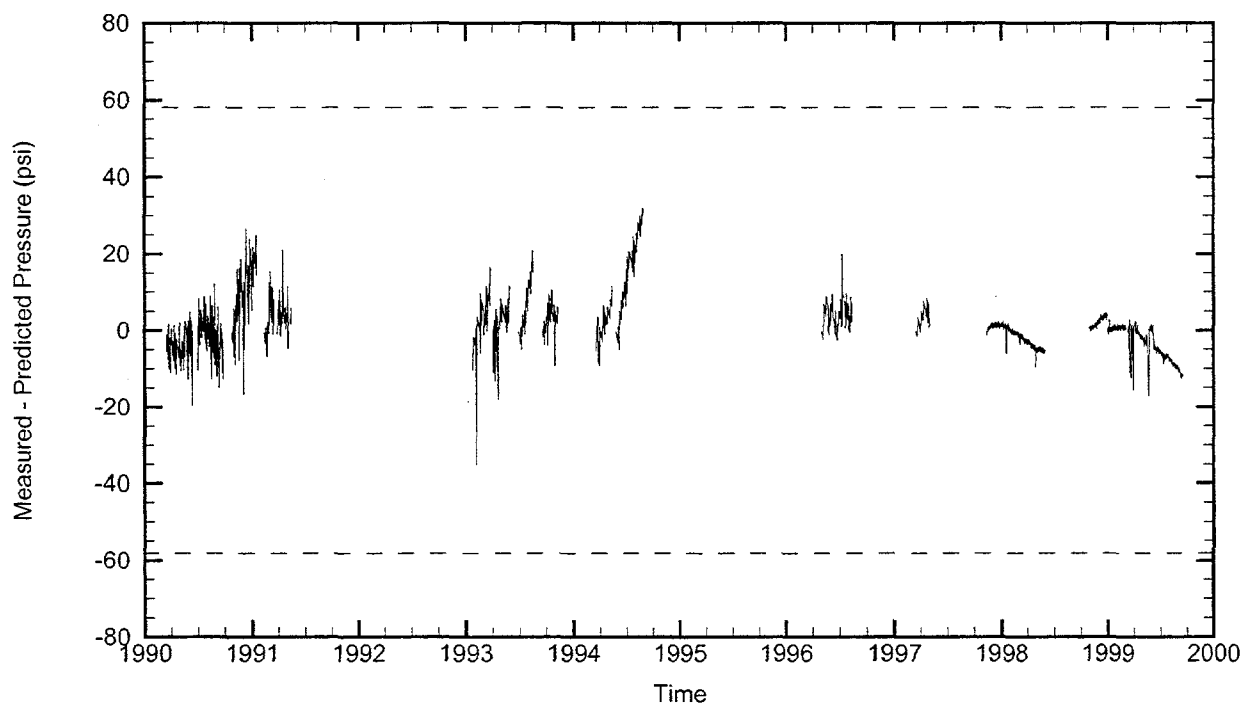
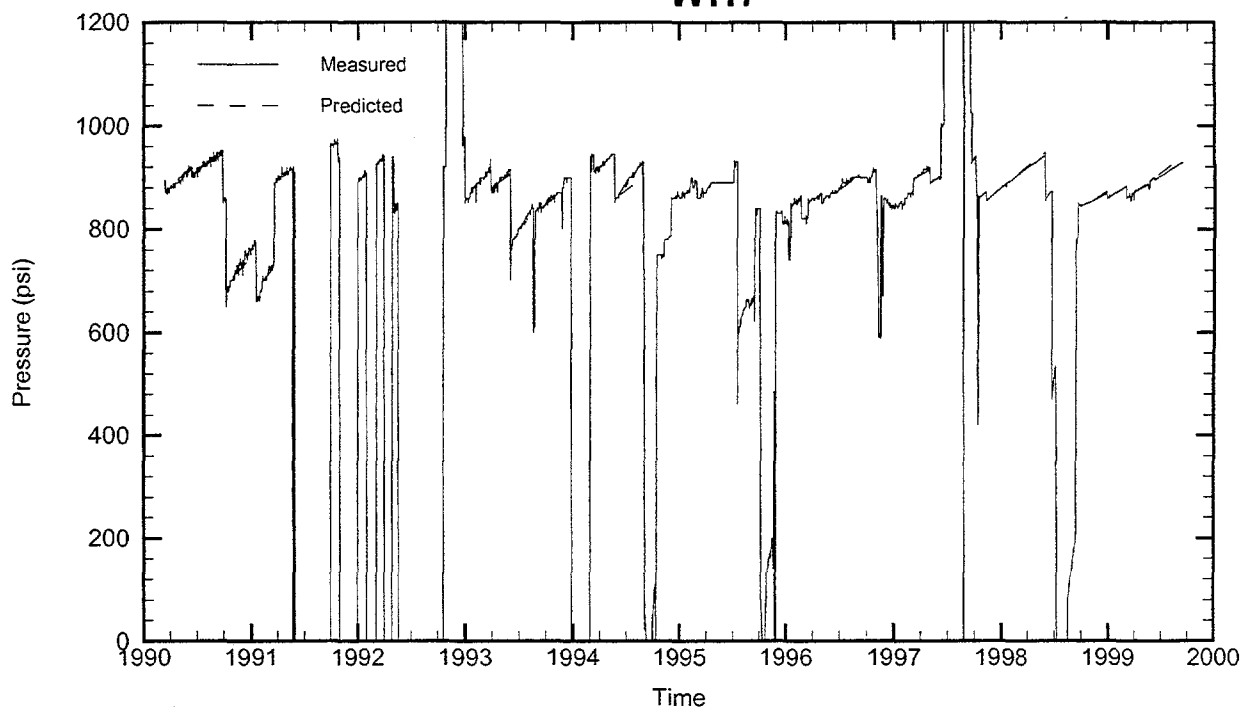




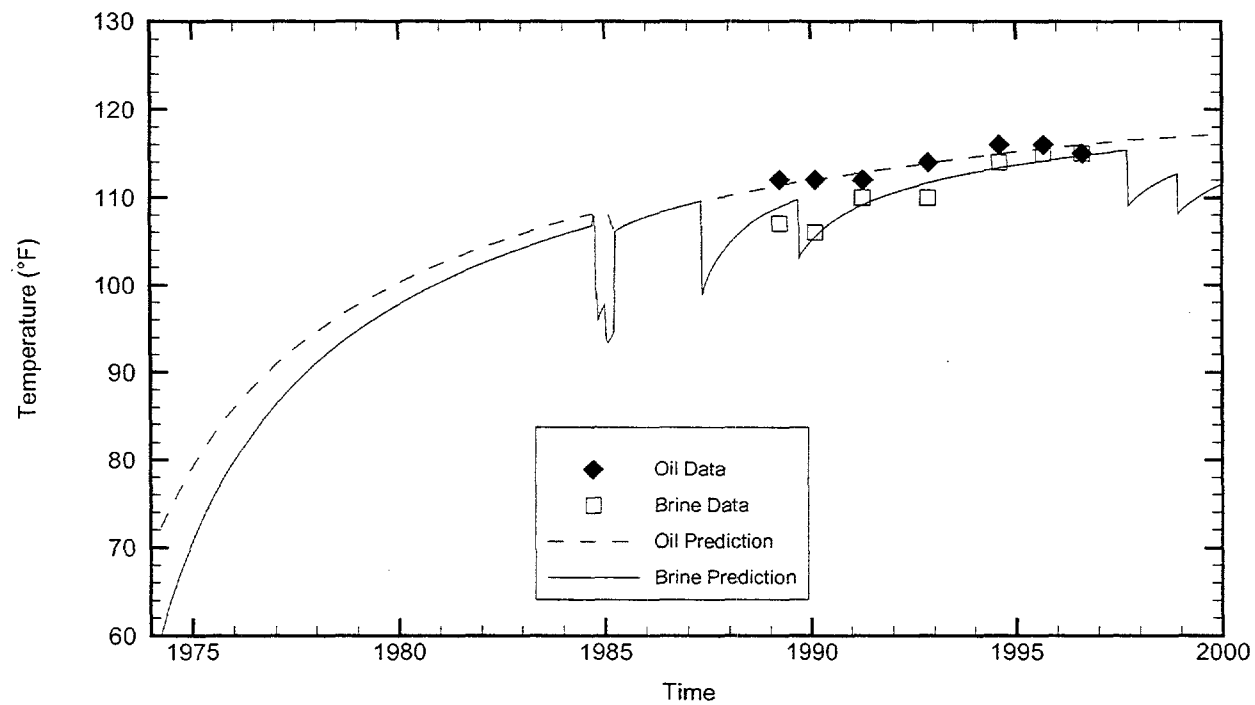
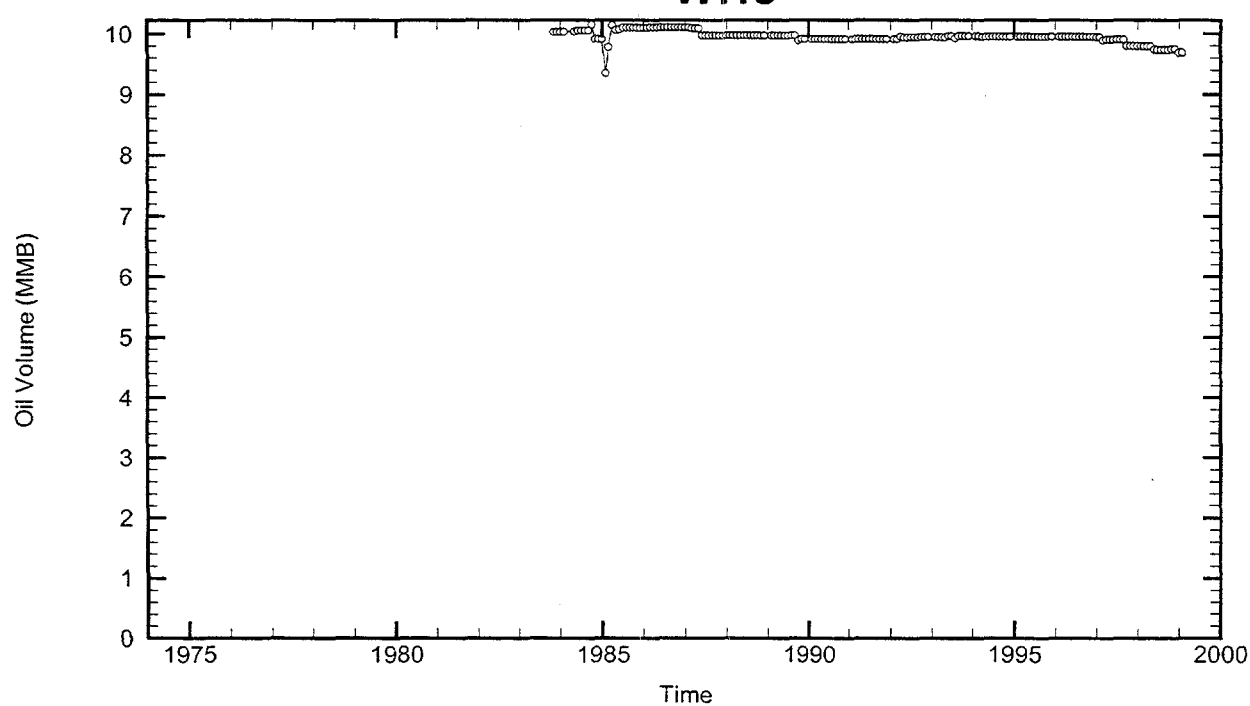
Cavern: WH7
 End of Leaching: 08/07/1965
 Duration of Leaching: 1.9986 years
 Leaching Temperature: 64.74 °F

Oil Injection Temperature: 50.00 °F
 Brine Injection Temperature: 50.09 °F
 Number of iterations: 406

WH7



WH8



Cavern: WH8

End of Leaching: 04/02/1974

Duration of Leaching: 1.9986 years

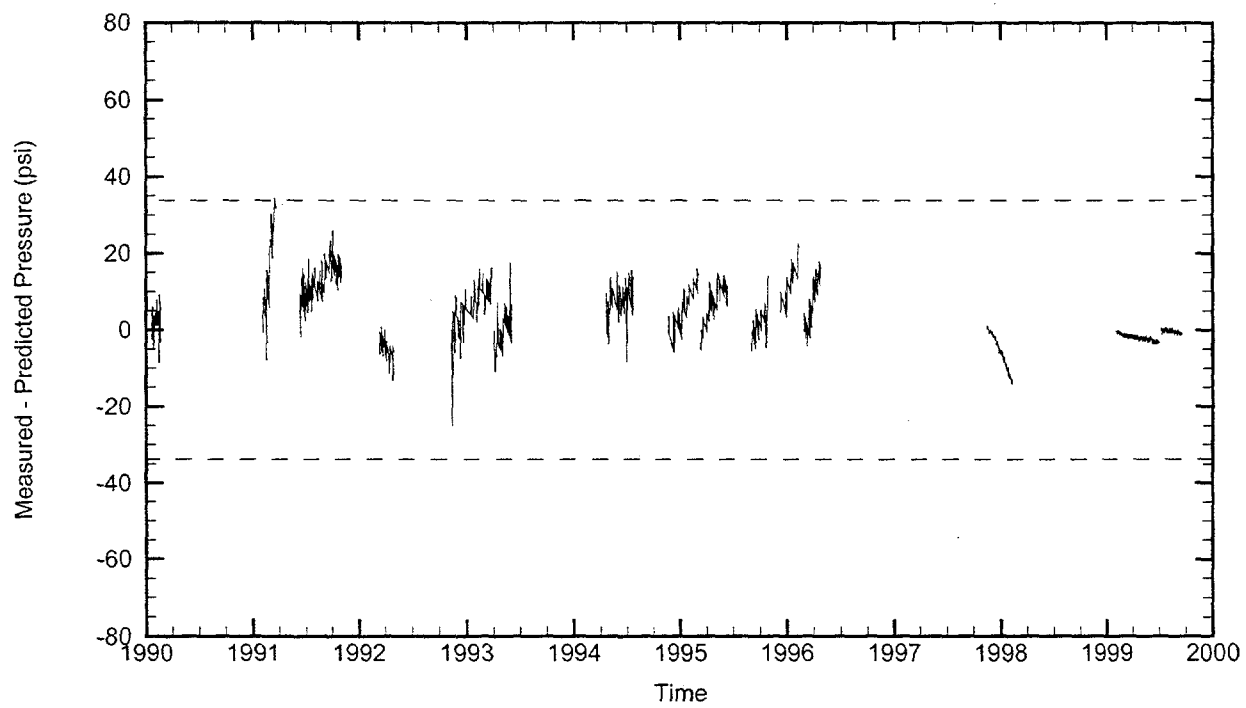
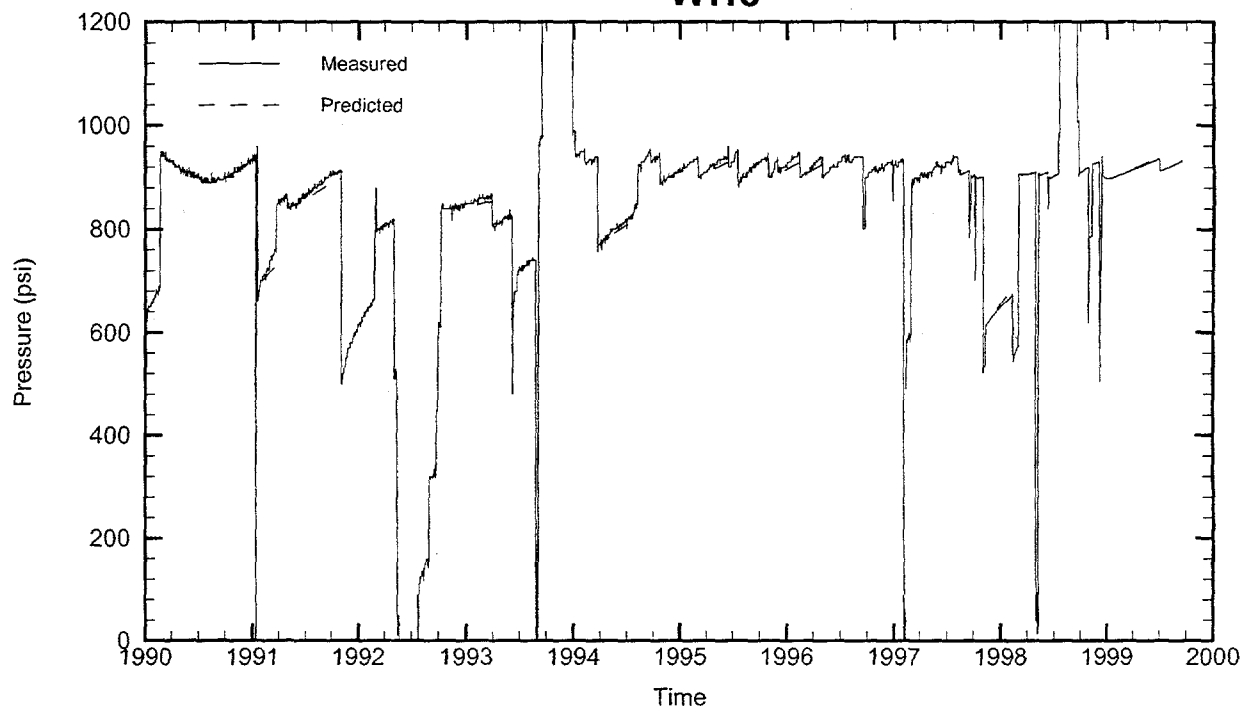
Leaching Temperature: 60.00 °F

Oil Injection Temperature: 72.28 °F

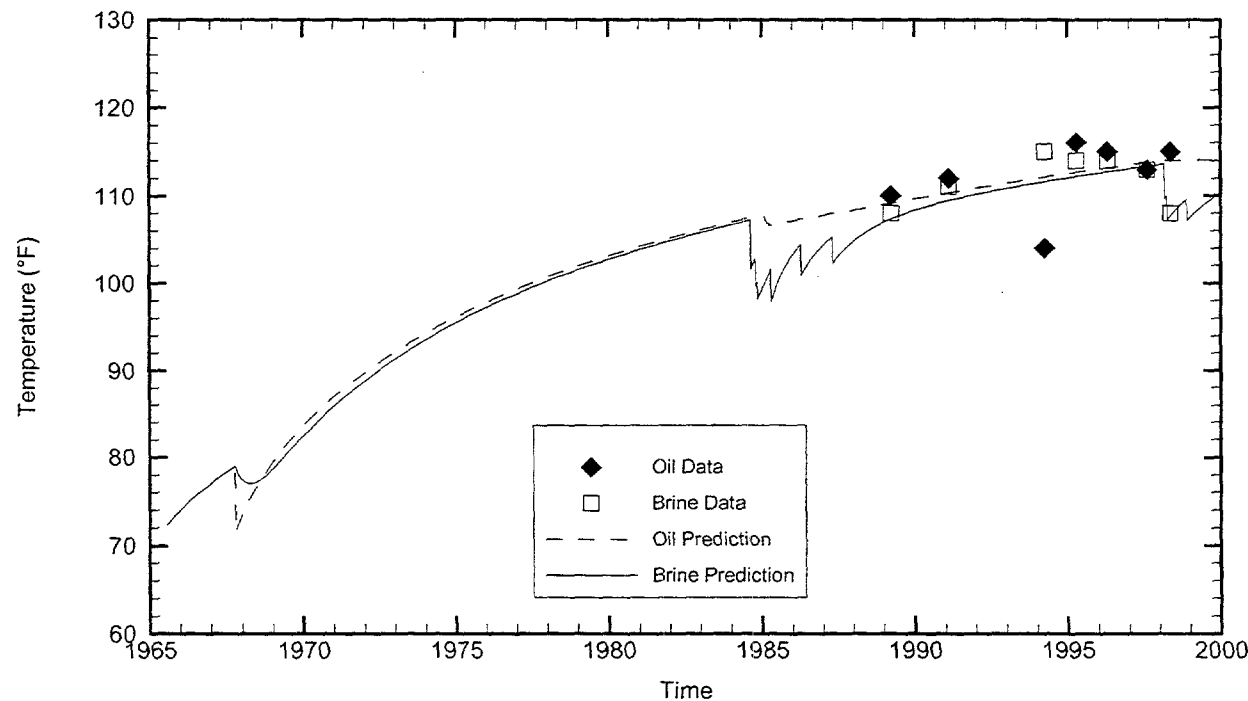
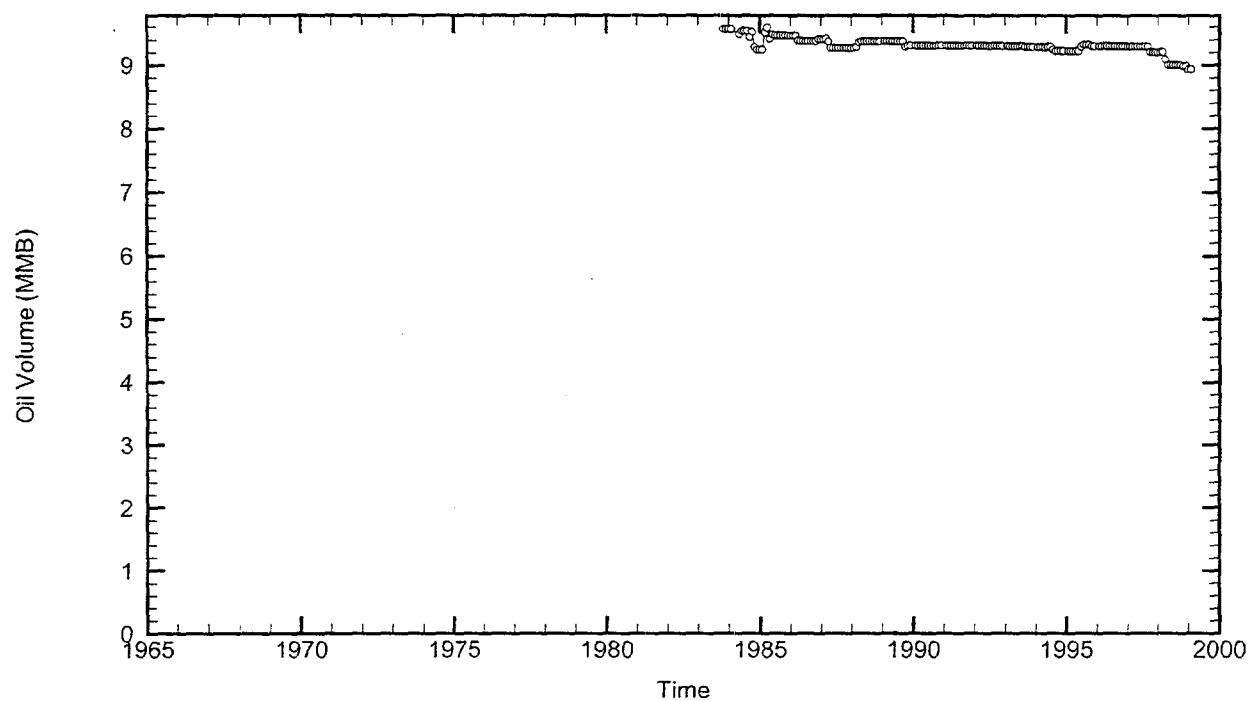
Brine Injection Temperature: 89.96 °F

Number of iterations: 800

WH8



WH9



Cavern: WH9

End of Leaching: 07/29/1965

Duration of Leaching: 1.9959 years

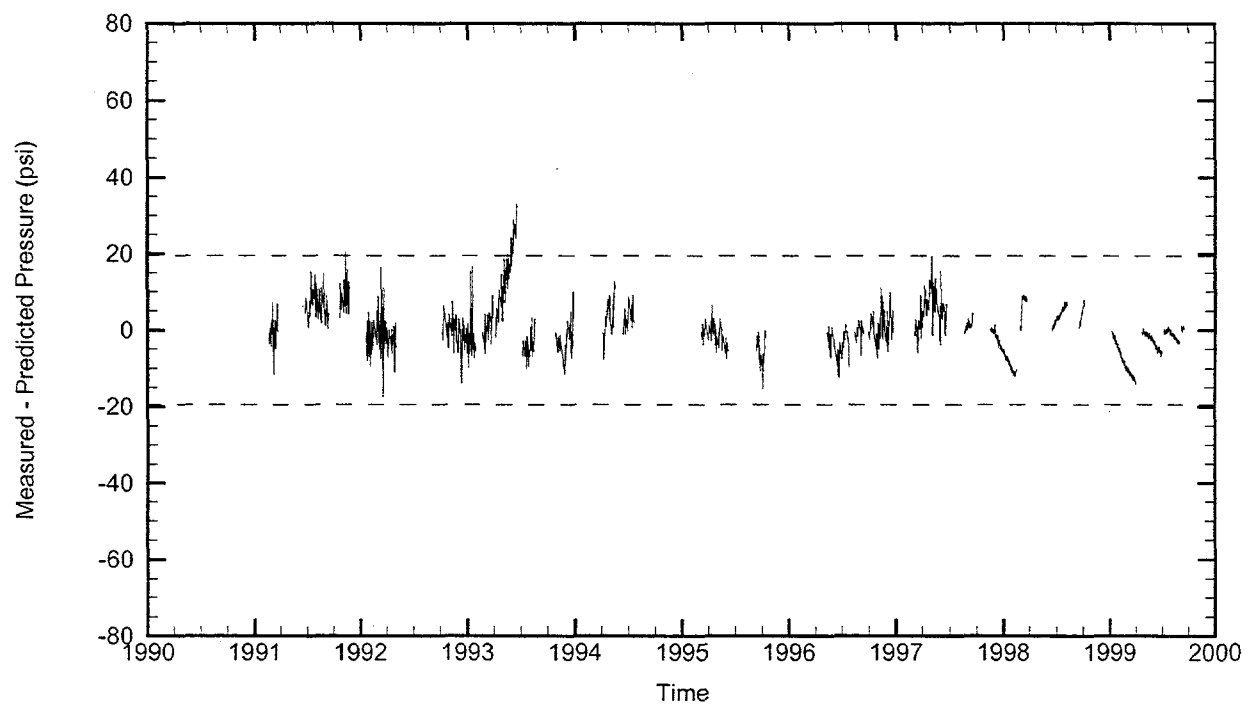
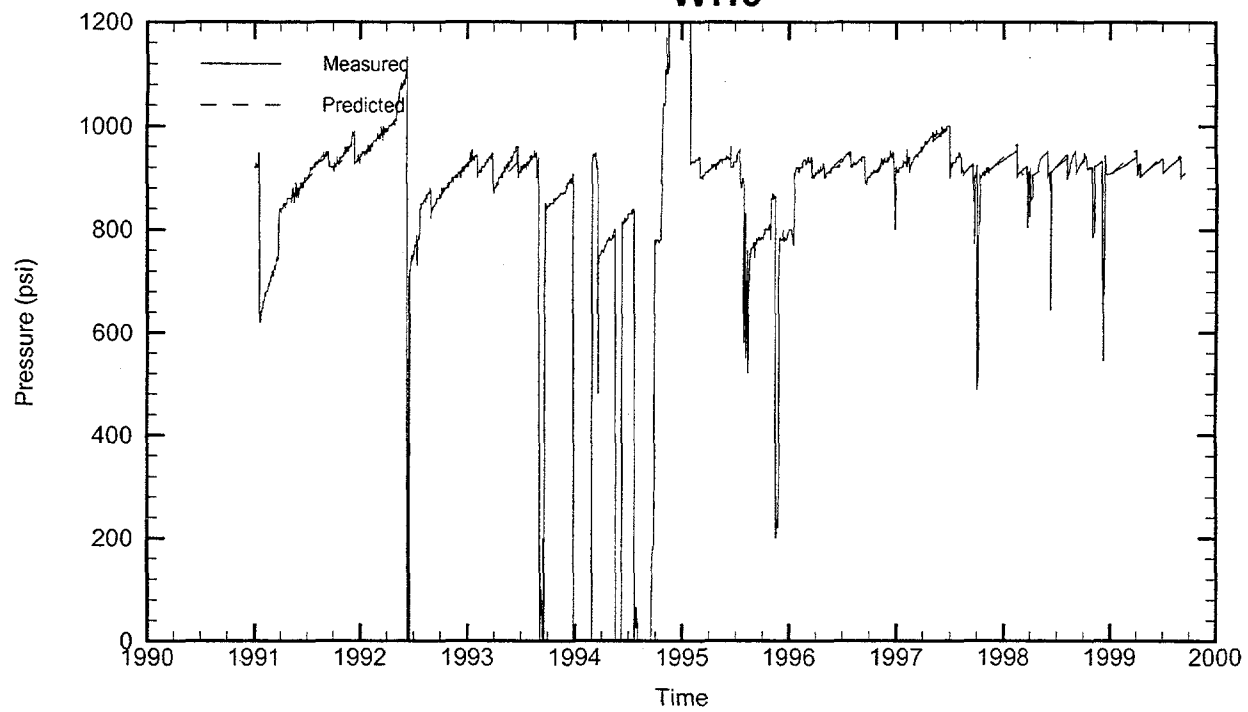
Leaching Temperature: 72.33 °F

Oil Injection Temperature: 70.94 °F

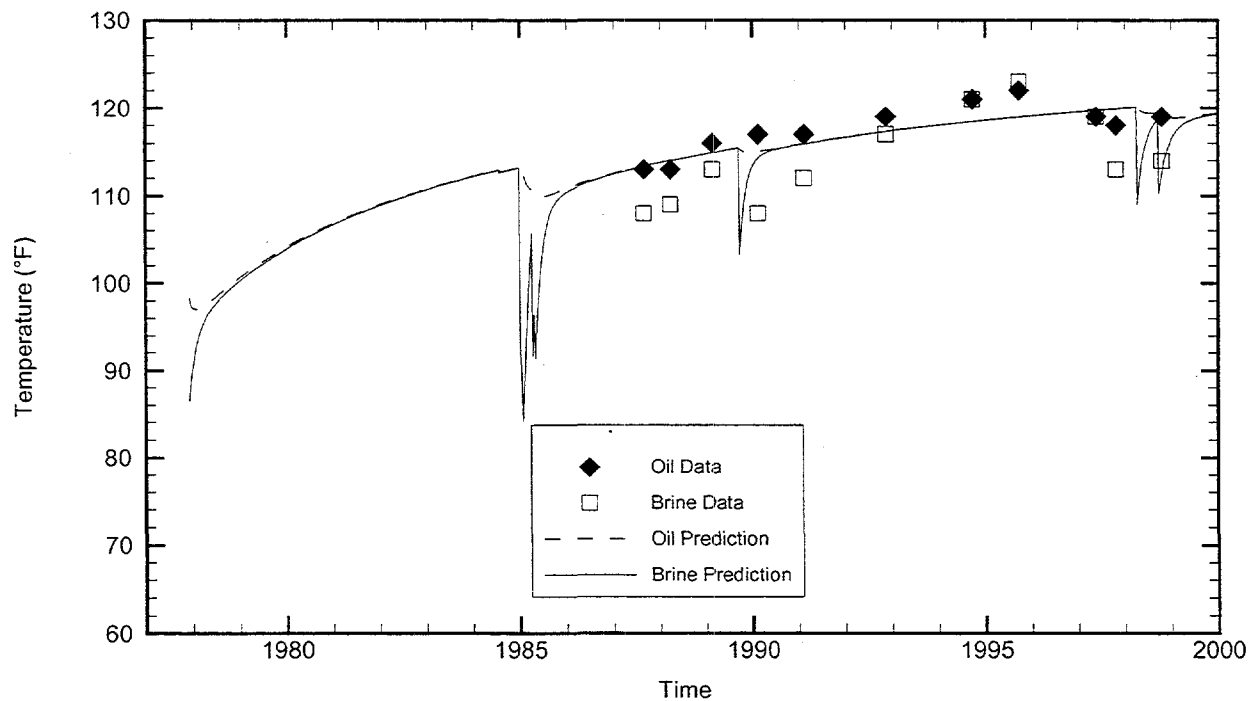
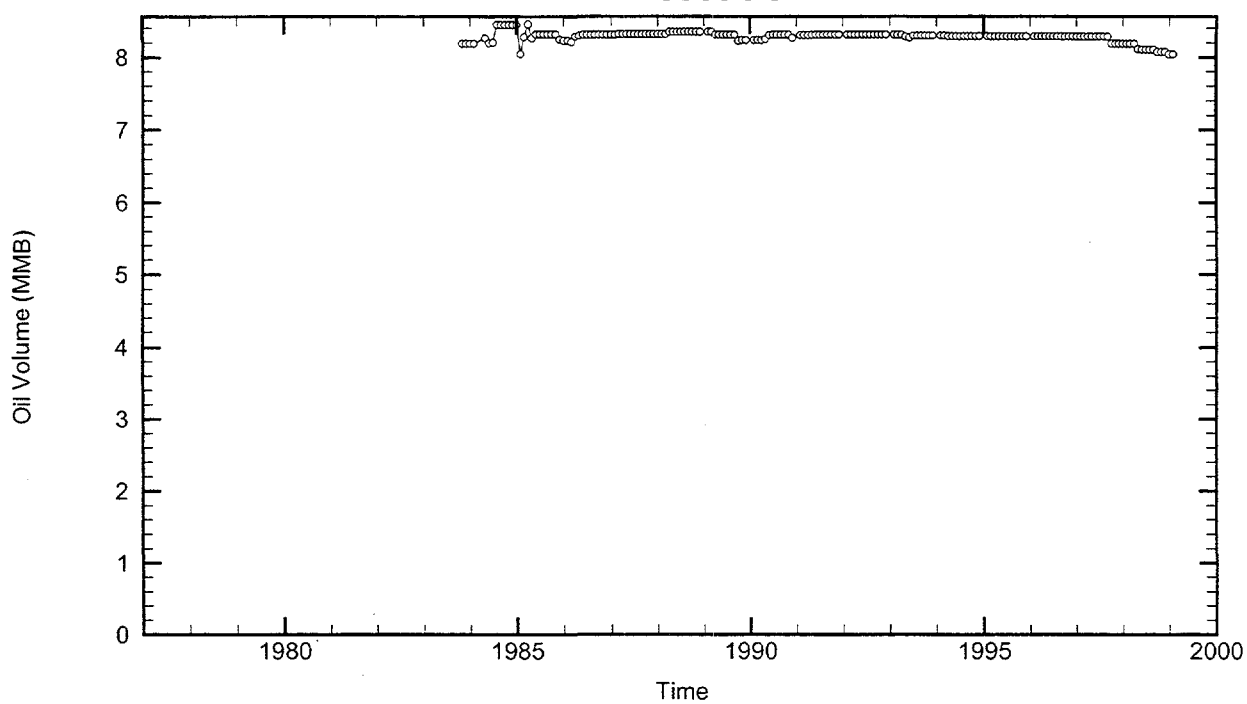
Brine Injection Temperature: 89.65 °F

Number of iterations: 522

WH9

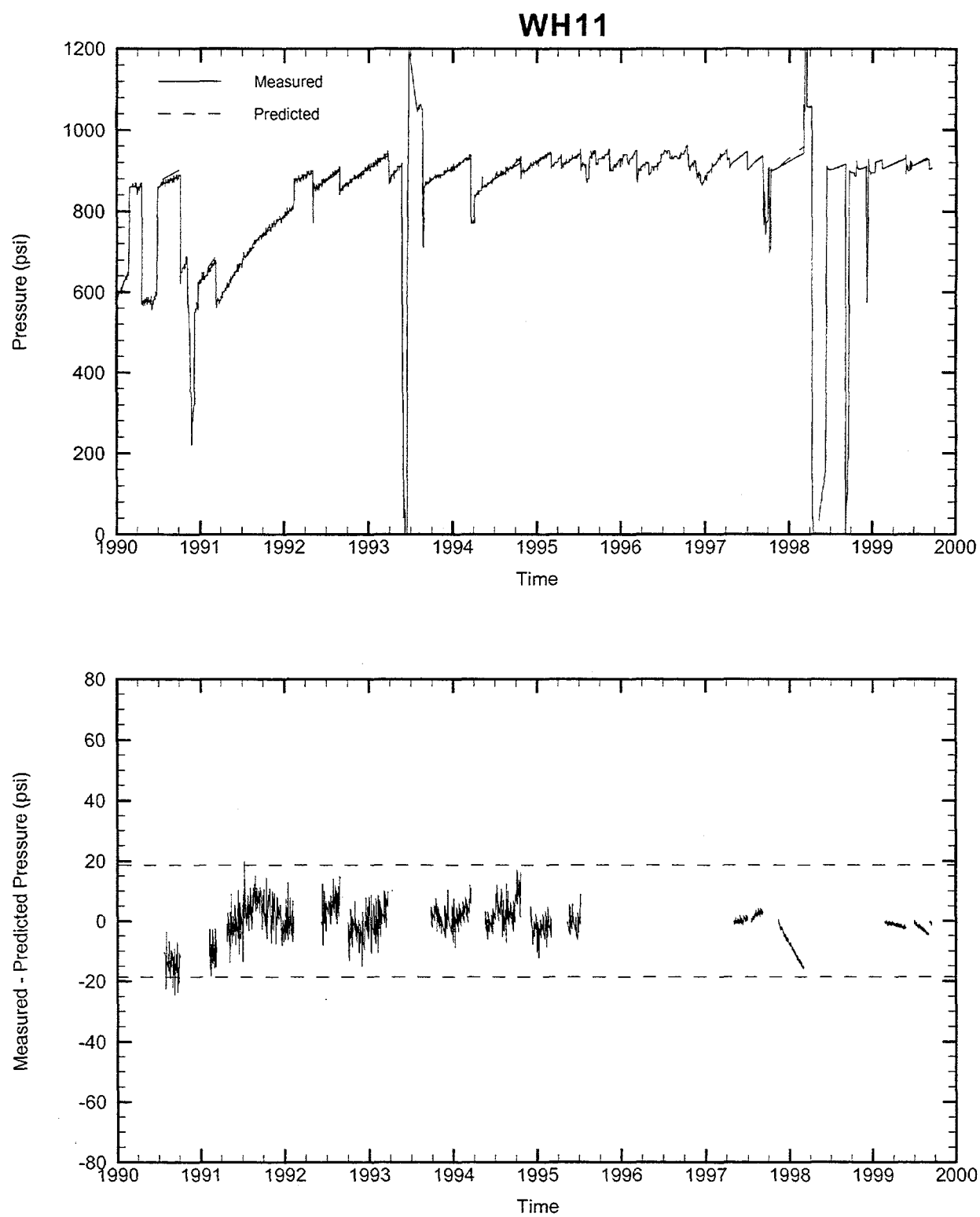


WH11



Cavern: WH11
End of Leaching: 12/06/1977
Duration of Leaching: 1.9986 years
Leaching Temperature: 86.46 °F

Oil Injection Temperature: 98.30 °F
Brine Injection Temperature: 66.48 °F
Number of iterations: 363



DISTRIBUTION

U.S. DOE SPR PMO (16)
900 Commerce Road East
New Orleans, LA 70123
Attn: W. C. Gibson, FE-44
 J. Aguinaga, FE-4421.1
 G. B. Berndsen, FE-443.1
 L. A. Boston, FE-4422
 J. Culbert, FE-443
 R. Francoeur, FE-4421.3
 A. Frugé, FE-4421.2
 J. C. Kilroy, FE-442
 R. E. Myers, FE-4421 (3)
 W. Poarch, FE-4421
 S. Sevak, FE-4421.5
 N. Shourbaji, FE-4422
 TDCS (2)

U.S. Department of Energy (3)
Strategic Petroleum Reserve
1000 Independence Avenue SW
Washington, D.C. 20585
Attn: D. Johnson, FE -42
 D. Buck, FE-42
 H. Giles, FE-43

DynMcDermott (8)
850 South Clearview Parkway
New Orleans, LA 70123
Attn: J. Barrington, DM-21
 G. K. Hughes, DM-22
 J. A. Farquhar, DM-21
 J. M. McHenry, DM-21
 J. Perry, DM-BH
 H. Bakhtiari, DM-BM
 F. Tablada, DM-BC
 I. Cormie, DM-WH

Sandia Internal:

MS 0701	P. B. Davies, 6100
MS 0706	R. E. Finley, 6113 (10)
MS 0706	B.L Ehgartner, 6113 (5)
MS 0706	T. E. Hinkebein, 6113
MS 0706	M. Molecke, 6113
MS 0706	D. Munson, 6113
MS 0750	S. Ballard, 6116 (5)
MS 0750	M. C. Walck, 6116
MS 9018	Central Tech. Files, 8940-2
MS 0899	Technical Library, 9616 (2)
MS 0612	Review & Approval Desk, 9612
	For DOE/OSTI